Nuclear Safety NEA/
CSNI/R(2015)2
May 2015
www.oecd-nea.org

Status Report on Spent Fuel Pools under Loss-of-Cooling and Loss-of-Coolant Accident Conditions

Final Report

OECD
BETTER POLICIES FOR BETTER LIVES

NEA
NUCLEAR ENERGY AGENCY

For Official Use **NEA/CSNI/R(2015)2**

Organisation de Coopération et de Développement Économiques
Organisation for Economic Co-operation and Development **04-May-2015**

English - Or. English

NUCLEAR ENERGY AGENCY
COMMITTEE ON THE SAFETY OF NUCLEAR INSTALLATIONS

Status Report on Spent Fuel Pools under Loss-of-Cooling and Loss-of-Coolant Accident Conditions

Final Report

JT03375526

Complete document available on OLIS in its original format

NEA/CSNI/R(2015)2
For Official Use

English - Or. English

ORGANISATION FOR ECONOMIC CO-OPERATION AND DEVELOPMENT

The OECD is a unique forum where the governments of 34 democracies work together to address the economic, social and environmental challenges of globalisation. The OECD is also at the forefront of efforts to understand and to help governments respond to new developments and concerns, such as corporate governance, the information economy and the challenges of an ageing population. The Organisation provides a setting where governments can compare policy experiences, seek answers to common problems, identify good practice and work to co-ordinate domestic and international policies.

The OECD member countries are: Australia, Austria, Belgium, Canada, Chile, the Czech Republic, Denmark, Estonia, Finland, France, Germany, Greece, Hungary, Iceland, Ireland, Israel, Italy, Japan, Luxembourg, Mexico, the Netherlands, New Zealand, Norway, Poland, Portugal, the Republic of Korea, the Slovak Republic, Slovenia, Spain, Sweden, Switzerland, Turkey, the United Kingdom and the United States. The European Commission takes part in the work of the OECD.

OECD Publishing disseminates widely the results of the Organisation's statistics gathering and research on economic, social and environmental issues, as well as the conventions, guidelines and standards agreed by its members.

NUCLEAR ENERGY AGENCY

The OECD Nuclear Energy Agency (NEA) was established on 1 February 1958. Current NEA membership consists of 31 countries: Australia, Austria, Belgium, Canada, the Czech Republic, Denmark, Finland, France, Germany, Greece, Hungary, Iceland, Ireland, Italy, Japan, Luxembourg, Mexico, the Netherlands, Norway, Poland, Portugal, the Republic of Korea, the Russian Federation, the Slovak Republic, Slovenia, Spain, Sweden, Switzerland, Turkey, the United Kingdom and the United States. The European Commission also takes part in the work of the Agency.

The mission of the NEA is:

- to assist its member countries in maintaining and further developing, through international co-operation, the scientific, technological and legal bases required for a safe, environmentally friendly and economical use of nuclear energy for peaceful purposes;
- to provide authoritative assessments and to forge common understandings on key issues, as input to government decisions on nuclear energy policy and to broader OECD policy analyses in areas such as energy and sustainable development.

Specific areas of competence of the NEA include the safety and regulation of nuclear activities, radioactive waste management, radiological protection, nuclear science, economic and technical analyses of the nuclear fuel cycle, nuclear law and liability, and public information.

The NEA Data Bank provides nuclear data and computer program services for participating countries. In these and related tasks, the NEA works in close collaboration with the International Atomic Energy Agency in Vienna, with which it has a Co-operation Agreement, as well as with other international organisations in the nuclear field.

THE COMMITTEE ON THE SAFETY OF NUCLEAR INSTALLATIONS

The NEA Committee on the Safety of Nuclear Installations (CSNI) is an international committee made up of senior scientists and engineers with broad responsibilities for safety technology and research programmes, as well as representatives from regulatory authorities. It was created in 1973 to develop and co-ordinate the activities of the NEA concerning the technical aspects of the design, construction and operation of nuclear installations insofar as they affect the safety of such installations.

The committee's purpose is to foster international co-operation in nuclear safety among NEA member countries. The main tasks of the CSNI are to exchange technical information and to promote collaboration between research, development, engineering and regulatory organisations; to review operating experience and the state of knowledge on selected topics of nuclear safety technology and safety assessment; to initiate and conduct programmes to overcome discrepancies, develop improvements and reach consensus on technical issues; and to promote the co-ordination of work that serves to maintain competence in nuclear safety matters, including the establishment of joint undertakings.

The priority of the committee is on the safety of nuclear installations and the design and construction of new reactors and installations. For advanced reactor designs, the committee provides a forum for improving safety-related knowledge and a vehicle for joint research.

In implementing its programme, the CSNI establishes co-operative mechanisms with the NEA's Committee on Nuclear Regulatory Activities (CNRA), which is responsible for the Agency's programme concerning the regulation, licensing and inspection of nuclear installations with regard to safety. It also co-operates with the other NEA Standing Technical Committees as well as with key international organisations such as the International Atomic Energy Agency (IAEA) on matters of common interest.

TABLE OF CONTENTS

LIST OF TABLES

LIST OF FIGURES

EXECUTIVE SUMMARY

Following the 2011 accident at the Fukushima Daiichi Nuclear Power Station, the Nuclear Energy Agency Committee on the Safety of Nuclear Installations decided to launch several high-priority activities to address certain technical issues. Among other things, it was decided to prepare a status report on spent fuel pools (SFPs) under loss of cooling accident conditions. This activity was proposed jointly by the CSNI Working Group on Analysis and Management of Accidents (WGAMA) and the Working Group on Fuel Safety (WGFS). The main objectives, as defined by these working groups, were to:

- Produce a brief summary of the status of SFP accident and mitigation strategies, to better contribute to the post-Fukushima accident decision making process;
- Provide a brief assessment of current experimental and analytical knowledge about loss of cooling accidents in SFPs and their associated mitigation strategies;
- Briefly describe the strengths and weaknesses of analytical methods used in codes to predict SFP accident evolution and assess the efficiency of different cooling mechanisms for mitigation of such accidents;
- Identify and list additional research activities required to address gaps in the understanding of relevant phenomenological processes, to identify where analytical tool deficiencies exist, and to reduce the uncertainties in this understanding.

The proposed activity was agreed and approved by CSNI in December 2012, and the first of four meetings of the appointed writing group was held in March 2013. The writing group consisted of members of the WGAMA and the WGFS, representing the European Commission and the following countries: Belgium, Canada, Czech Republic, France, Germany, Hungary, Italy, Japan, Korea, Spain, Sweden, Switzerland and the USA. This report mostly covers the information provided by these countries.

The report is organised into 8 Chapters and 4 Appendices and is summarized below chapter by chapter.

Chapter 1**: Introduction**

There are two main types of pools used for wet storage of spent nuclear fuel: At-reactor pools, used for temporary fuel storage, and away-from-reactor pools, which are larger facilities for interim storage of spent fuel awaiting reprocessing or final disposal. The fuel residing in at-reactor SFPs is usually characterized by higher decay power than fuel stored in away-from-reactor pools. Since the progression rate and severity of a cooling accident in the SFP relates with the power of the stored fuel assemblies, the most challenging accident scenarios are expected in at-reactor storage pools. For this reason, the report focuses on at-reactor SFPs in light water reactor (LWR) and Canada Deuterium Uranium (CANDU) reactor nuclear power plants.

Adequate cooling of the spent fuel stored in the SFP may principally be lost either by malfunction of the pool cooling system (loss of cooling accident) or by loss of the pool water inventory (loss of coolant

accidents). This report deals with both kinds of accidents. It summarizes operational experience on events and incidents with at-reactor SFPs, and provides a brief assessment of current experimental knowledge about phenomena involved in the aforementioned types of accidents. It also reviews state-of-the-art computer codes used for analyses of SFP cooling accidents, and discusses strengths and weaknesses of models and methods used in these codes. The report also aims to identify areas that need additional knowledge and to identify potential improvements in computational models and tools for better predictions of SFP accident progression and time margins to significant radiological releases.

Chapter 2: Spent fuel pools

Virtually all power reactors have some form of at-reactor pool with active cooling that allows storage of recently discharged spent fuel until its decay power is low enough for transport of the fuel to interim storage. The fuel residence time in the at-reactor pool depends, inter alia, on the applied strategy for spent fuel management and may range from a year up to several decades.

All SFPs are large robust monolithic structures. The pool walls are generally made of more than one metre thick steel lined concrete. Fuel assemblies are stored in racks that provide spacing for coolant flow and in some cases also for criticality control. The pools are filled with several additional metres of water above the spent fuel to provide biological shielding. An active cooling and purification system maintains optimal conditions for the stored fuel. Differences in pool design exist not only between reactor technologies, but also between technologies generations and often from site to site. Important design differences are the elevation of the pool with respect to grade and whether it is located inside or outside the primary containment of the reactor, the design of fuel transfer paths to the reactor, and the use of borated or demineralized water as coolant. In spite of these differences, the fundamental design parameters and safety provisions are consistent.

The possibility of loss of cooling or loss of coolant accidents is accounted for in the basic design of all SFPs. The cooling systems have built-in redundancies and are connected to emergency backup power to maintain their function. Pool penetrations are kept to a minimum. The cooling systems either have siphon breakers or the depth of the inlet and outlet pipes are limited to prevent draining of the pool. The large volume of water provides a significant thermal mass, which slows any accident progression and gives respite for operator intervention.

Following the Fukushima Daiichi accident, additional measures have been undertaken to improve SFP safety even further. These measures differ greatly due to the large variation on designs, but can be generally stated as improvements in accident response procedures, additional backup electricity or water supplies and instrumentation improvements.

Chapter 3: Possible accident scenarios, past accidents and precursor events

Evaluations of past events where SFP cooling has been lost show that malfunctions of the SFP cooling system are in most cases caused by inoperable cooling pumps. Inadvertent diversion of coolant flow and loss of ultimate heat sink are other causes. Likewise, the operational experience feedback on loss of coolant accidents shows that the SFP water inventory may be lost through improper line-up or breaks in connected pipes and systems, through leaking temporal gates or seals during refuelling or other activities, and exceptionally, through leaks in the pool liner.

The root cause to the reported events is in most cases human errors. None of the reported events has resulted in severe accidents. In fact, many of them were merely precursor events, with no or negligible consequences to the spent fuel. The events have escalated slowly, since the SFP water volume is large in comparison with the heat loads or leakage rates in the reported incidents, and there has always been

sufficient time for operator intervention. With regard to consequences, one may make reference to the 1983 Bruce-A Unit 4 incident in Canada and the 2003 Paks cleaning tank incident in Hungary. During the Bruce-A Unit 4 incident a CANDU 37-element fuel bundle was overheated in steam-air environment in the fuel transfer mechanism for an estimated time of 5 hours. During the Paks cleaning tank incident thirty spent fuel assemblies were being cleaned in a closed container that was submerged in the fuel manipulation pit of the SFP. After cleaning, the fuel was left in the container with insufficient cooling, which resulted in fuel damage and radioactive release to the SFP building. Although the Paks incident cannot be considered as a typical SFP accident, (in fact, the level of the SFP was maintained throughout the incident at its nominal value), it gave impetus to experimental as well as computational studies that have improved our understanding of fuel degradation phenomena related to loss of cooling of spent fuel with relatively low decay heat.

Chapter 4: Behaviour of spent fuel facilities during the Fukushima Daiichi accident

The Fukushima Daiichi Nuclear Power Station was hit by the Great East Japan Earthquake and the subsequent tsunami on March 11, 2011. The station had six at-reactor SFPs, one at each unit, a common pool and a dry cask storage facility. All AC power was lost at the SFPs for Unit 1 to 5, the common pool and the dry cask storage facility when emergency diesel generators (EDGs) stopped functioning as the seawater pumps and power panels were flooded by the tsunami, but the Unit 6 air-cooled EDG survived the tsunami. The cooling and water supply systems were lost for all SFPs following the loss of AC power (except Unit 6) and seawater cooling system. However, the cooling and water supply for the Unit 5 and Unit 6 SFPs were restored when the temporary residual heat removal system pumps started by using power from the Unit 6 air-cooled EDG. The air-cooling system for the common pool was restored when the off-site power supply was recovered. There were no cooling problems with the dry storage casks.

With no pool cooling to remove decay heat at the Unit 1 to Unit 4 SFPs, emergency water injection was conducted by using a helicopter, a concrete pump truck, a fire truck, and through various connected piping systems. The highest water temperatures and evaporation rates were reached in the Unit 4 SFP, which had the highest heat load (≈2.3 MW at time of the accident). The lowest water level in this pool, about 1.5 m above the fuel racks, was reached around April 20, 2011. There was no evidence of bulk boiling in any of the pools; measured peak water temperatures ranged from 62 to 92 °C. Eventually, pool water cooling by the alternative cooling system was started for all SFPs, and the water temperature has thereafter been maintained below 40 °C. Video inspections reveal that the fuel racks appear to be intact. These results, together with water analyses, suggest that, in all pools, almost no fuel is damaged. When conditions allowed, measures have been taken to ensure structural integrity of the SFPs, to investigate the impact of debris and dropped objects on the spent fuel assemblies and to purify the pool water.

Chapter 5: Accident phenomenology

Important phenomena involved in SFP accidents are fuel uncovery, heat-up and degradation of the fuel and storage racks, and the possibility of fission product release from damaged fuel. In addition, nuclear criticality is a concern for SFP accidents in light water reactors, where the margin to criticality in the pool may be lost by displacement of fuel assemblies and/or neutron absorbing material in the rack structure, and/or by loss of neutron absorption by an increase in coolant void fraction. Regarding criticality issues and large scale thermal-hydraulic and thermal-aeraulic phenomena in SFP accidents, our current understanding is based largely on computational analyses using codes commonly designed for reactor accidents. The criticality margin of LWR SFPs under different postulated accident scenarios has been computationally assessed, and thermal-hydraulic/aeraulic phenomena in the SFP and the pool building have been analysed with computational fluid dynamics (CFD) and system codes. Most of these studies have been done after the Fukushima Daiichi accident. Experimental campaigns have been conducted, and

more are planned, to assess and extend the applicability of the computational tools to various SFP accident scenarios.

As for phenomena related to high temperature fuel degradation and fission product release, there is a substantial database from separate effect tests and integral experiments, carried out in the past to study loss of reactor cooling accidents. The conditions expected in SFP accidents differ from those in reactor accidents by a more heterogeneous distribution of fuel assemblies, lower decay power, air-containing environment and lower pressure. However, the degradation and release phenomena are fundamentally the same. These differences have been identified and investigated in recent experiments. One of the major differences is that fuel degradation in SFP accidents may occur in environments containing air, which accelerates zirconium alloy oxidation by nitriding and oxide layer breakup. Air also speeds up UO_2 fuel degradation and volatilization by oxidation, and may increase the release of e.g. ruthenium and otherwise less volatile fission products

Chapter 6**: Experiments with relevance to SFP cooling accidents**

Separate and integral effect tests have been conducted since the 1980s to better understand the fuel behaviour and degradation under severe accident conditions. The main objective of these tests was to provide data for model development and validation of computer codes used for reactor safety analysis. Chapter 6 provides a review of relevant tests for SFP accident conditions. A number of the tests, while not originally developed for SFP accidents, provided valuable data and insights for application to SFP accident phenomenology. For example, the international Phébus Fission Product program, conducted in France, provided insights and data on the fission product release and late phase melt progression for LWRs. Most of the findings of these tests are directly applicable to accident progression in SFPs. Another set of integral tests, suitable for model validation and application to SFP accident conditions, are QUENCH-10 and QUENCH-16, conducted in Germany. These tests not only provided an improved understanding of the oxidation phenomena, but also examined the phenomena associated with recovery and quenching of overheated fuel rods. Also the experiments and tests carried out to investigate the 2003 Paks cleaning tank incident have provided useful data.

The only integral tests specifically targeted for SFP loss of cooling accidents were conducted at Sandia National Laboratories, USA, partly within the OECD/NEA Sandia Fuel Project. The main objective of the experimental work was to provide basic thermal-hydraulic data for completely uncovered and air cooled fuel assemblies for boiling and pressurized water reactors, and facilitate severe accident code validation and reduce modelling uncertainties. The accident conditions of interest for the SFP were simulated in a full-scale prototypic fashion.

A large number of separate effect tests have been done to characterize high temperature air oxidation of various cladding materials, and further tests are underway. These tests provide necessary data for modelling cladding degradation and zirconium fire initiation in SFP accidents. Most of the tests were done under isothermal conditions and studied the phenomena of oxidation kinetics in air and air/steam environments, oxidation breakaway, and nitriding. There have also been various separate effect tests to examine the fission product release characteristics of the fuel under air-rich conditions, where enhanced release of otherwise low-volatile species like ruthenium can become important. Major recent experiments of this kind include VERCORS and VERDON, conducted in France, and the VEGA programme in Japan, where both high burnup UO_2 fuel and $(U,Pu)O_2$ fuel were investigated. Finally, there were also some tests conducted in Korea that were designed for the evaluation of siphon breaker performance.

Chapter 7: Simulation tools

Simulation tools applied to SFP accidents include computer programs developed for analysis of thermal hydraulics, nuclear criticality, fuel rod behaviour and severe accidents. For the simulation of SFP thermal-hydraulics, CFD tools can be used in cases where 3D phenomena/regimes are important. They have the capacity to address problems at the local scale in 3D. However, SFP analyses are usually done at a larger scale, and the large simulation domain necessitates simplified modelling of the storage racks (porous medium approximation) and relatively coarse meshes in the CFD simulations. Thermal-hydraulics system codes are mostly applied for accident analysis at a large scale. System codes make use of 1D or 2D representations of the considered geometry, but they are being further developed to 3D.

Computational tools used for evaluation of the nuclear criticality safety of SFPs calculate the effective neutron multiplication factor of the SFP for any static configuration described in terms of geometry, material compositions, and extra information regarding cladding degradation, debris formation and physical state and level of the cooling water. These codes can in fact be used for both operational and accident conditions. Three types of calculation schemes are employed: a purely stochastic, a purely deterministic, and a hybrid scheme. A high level of accuracy in the results can typically be obtained by any of the schemes. The burnup dependent fuel composition can be provided by dedicated codes, which perform an in-core fuel depletion and fission products build-up analysis.

The fuel rod behaviour during the early phase of a loss of cooling incident or accident, up to the loss of rod-like geometry, can be simulated with transient fuel behaviour codes, which simulate the thermo-mechanical phenomena and the changes in fuel pellet and cladding in detail. However, they usually lack models for cladding high temperature oxidation in air-containing environments.

Severe accident codes have been developed for reactor applications by extending existing thermal-hydraulic codes with models for simulating phenomena in the reactor core during severe accidents. These codes are also used for analyses of SFP cooling accidents, because the major phenomena in severe reactor accidents are fundamentally the same as in severe SFP cooling accidents. However, the geometry and conditions expected in SFP accidents differ from those in reactor accidents, and the applicability of models in different severe accident codes is currently being verified for SFP conditions.

Chapter 8: Conclusions and recommendations

All SFPs are large robust monolithic structures. The cooling systems have built in redundancies and are connected to emergency backup power to maintain their function. The possibilities of loss of cooling and loss of coolant accidents are accounted for in the basic design of SFPs. The large water mass provides significant thermal inertia generally slowing transients. Following the Fukushima Daiichi accident, additional measures have been undertaken to improve SFP safety even further.

Although numerous events (mostly inoperable cooling pumps or coolant flow diversion) have occurred in the past, none led to fuel uncovery or fuel damage. Operational experience shows that reliable SFP instrumentation, accident management procedures and training are vital for responding to the events efficiently. During Fukushima Daiichi, station personnel had to take many extraordinary actions to ensure sufficient cooling; however, averting fuel uncovery at SFP Unit 4 was fortuitous.

Fuel-degradation and fission-product-release phenomenology are well known from severe accident studies, however expected SFP-accident conditions differ from these and SFP source-term estimation is a challenge. The relevant experiment database related to SFP loss-of-cooling and loss-of-coolant accidents consists largely of a number of integral LWR LOCA tests; only one integral test targeted a SFP accident (OECD/NEA Sandia Fuel Project) has been performed. Some integral tests dedicated specifically to SFP

accidents are planned; these experiments are important and should be supported. However, more dedicated experiments are needed. This is especially true for the CANDU technology, which has particular fuel assembly and storage rack designs. It is recommended that the Phenomena Identification and Ranking Technique (PIRT) is used to systematically identify phenomena that are both of high importance and high uncertainty, and thus, of primary interest for further studies.

Currently available computational tools are intended primarily for analyses of reactor accidents and more specific modelling for SFPs is desirable in these tools. Thermal-hydraulic system codes and severe accident codes are usually limited to 1 or 2D applications but SFP accidents are expected to be significantly influenced by 3D effects due to heterogeneous fuel arrangement and boundary conditions. CFD tools can address problems at local scale in 3D but SFPs involve a large simulation domain imposing simplified modelling. Regarding CANDU technology, there is currently no complete severe accident code that can be used: a code for CANDU SFP accident analysis should be developed. Another recommendation is that formal user guidelines are produced for the application of codes to SFP loss-of-cooling and loss-of-coolant accidents. This would ensure best practice in analyses and reduce user effects. The benchmarks carried out for the OECD SFP project helped identify code limitations: it is recommended that the NEA organize similar benchmarks for other SFP accident scenarios and codes.

The present report summarizes results of experiments and computational analyses carried out to date to gain understanding of phenomena with significance to SFP cooling accidents. Considering that some knowledge gaps currently exist and that ongoing and planned research projects are expected to produce results that will hopefully narrow these gaps within the foreseeable future, it is recommended that:

- a CSNI state-of-the-art report on SFP loss-of-cooling and loss-of-coolant accidents is written as the results of these research projects become available;
- a follow-on activity is launched on SFP combining probability of SFP accidents, which was beyond the scope of this document, and mitigation strategies.

LIST OF CONTRIBUTORS

Lead authors:

Name	Organization/Country	
M. Adorni	BEL V/Belgium	
H. Esmaili	US NRC/USA	
W. Grant	CNSC/Canada	
T. Hollands	GRS/Germany	
Z. Hózer	MTA EK/Hungary	
B. Jäckel	PSI/Switzerland	
M. Muñoz	CSN/Spain	
T. Nakajima	NRA/Japan	
F. Rocchi	ENEA/Italy	
M. Stručić	JRC/European Commission	
N. Trégourès	IRSN/France	(Chair)
P. Vokac	UJV REZ/Czech Republic	

Contributors who provided information for their country and review comments:

Name	Organization/Country
K.I. Ahn	KAERI/Korea
L. Bourgue	EDF/France
R. Dickson	CNL/Canada
P.A. Douxchamps	GDF-SUEZ/Belgium
L.E. Herranz	CIEMAT/Spain
L.O. Jernkvist	QT/Sweden

Secretariat:

Name	Organization/Country
A. Amri	NEA/OECD
L.O. Jernkvist	QT/Sweden
M. P. Kissane	NEA/OECD

LIST OF ABBREVIATIONS AND ACRONYMS

All abbreviations and acronyms are explained as they first appear in the text. To facilitate a non-linear reading of the report, the acronyms are also listed below.

AAC DG	Alternative AC Diesel Generators
ACRS	Advisory Committee on Reactor Safeguards (USA)
AFR	Away-From-Reactor (spent fuel pool)
AIC	Ag-In-Cd (control rod material)
ALWR	Advanced Light Water Reactor
AMAD	Activity Median Aerodynamic Diameter
ANL	Argonne National Laboratory (USA)
AOI	Abnormal Operating Instruction
AR	At-Reactor (spent fuel pool)
ASN	Autorité de Sûreté Nucléaire (France)
ATR	Advanced Thermal Reactor (Japan)
ATV	Azimuthal Temperature Variation
BDB	Beyond Design Basis
BEL V	Technical Safety Organization of the FANC (Belgian Nuclear Safety Authority)
BWR	Boiling-Water Reactor
CANDU	Canada Deuterium Uranium (Canadian type pressure tube heavy water reactor)
CCW(S)	Component Cooling Water (System)
CEA	Commissariat à l'Energie Atomique et aux Energies Alternatives (France)
CFD	Computational Fluid Dynamics
CIEMAT	Centro de Investigaciones Energéticas, Medioambientales y Tecnológicas (Spain)
CRL	Chalk River Laboratories (Canada)
CSN	Consejo de Seguridad Nuclear (Spain)
CNSC	Canadian Nuclear Safety Commission (Canada)
CSNI	Committee on the Safety of Nuclear Installations (OECD/NEA)
CVCS	Chemical and Volume Control System
DCH	Direct Containment Heating
DS	Dryer and Separator
EC	European Commission
ECCS	Emergency Core Cooling System
EDF	Electricité de France (France)

EDG	Emergency Diesel Generator
ENEA	Italian National Agency for New Technologies, Energy and Sustainable Economic Development (Italy)
ENSREG	European Nuclear Safety Regulatory Group
EPM	École Polytechnique de Montréal (Canada)
EPRI	Electric Power Research Institute (USA)
EPS	Emergency Power Supply
ESWS	Essential Service Water System
EU	European Union
FA	Fuel Assembly
FARN	Force d'Action Rapide Nucléaire (Nuclear Emergency Response Team, France)
FIMA	Fissions per Initial Metal Atom
FP	Fission Product
FPC(S)	Fuel Pool Cooling and Filtering (System)
GRS	Gesellschaft für Anlagen- und Reaktorsicherheit (Germany)
HBS	High-Burnup Structure
HPCS	High Pressure Core Spray
IAEA	International Atomic Energy Agency (Austria)
IC	Isolation Condenser
ICE	Inadvertent Criticality Event
ICM	In-Core Monitor
IFB	Irradiated Fuel Bay
IKE	Institut für Kernenergetik und Energiesysteme (Germany)
IRS	International Reporting System for Operating Experience (IAEA)
IRSN	Institut de Radioprotection et de Sûreté Nucléaire (France)
ISTP	International Source Term Programme
JAEA	Japan Atomic Energy Agency (Japan)
JNES	Japan Nuclear Energy Safety Organization (Part of NRA from March 1, 2014)
JRC	Joint Research Centre (European Commission)
KAERI	Korea Atomic Energy Research Institute (Republic of Korea)
KFKI AEKI	Central Research Institute for Physics, Atomic Energy Research Institute (Hungary)
KINS	Korea Institute of Nuclear Safety (Republic of Korea)
KIT	Karlsruhe Institute of Technology (Germany)
KWO	Kernkraftwerk Obrigheim (Nuclear power plant Obrigheim, Germany)
KWU	Kraftwerk Union
LANL	Los Alamos National Laboratory (USA)
LCO	Limiting Condition for Operation

LCS	Licensee Controlled Specification
LER	Licensee Event Report
LOCA	Loss of Coolant Accident
LOOP	Loss of Off-site Power
LUTCH	Scientific Industrial Association (Russia)
LWR	Light Water Reactor
L2PSA	Level 2 Probabilistic Safety Assessment
MCC	Motor Control Centre
MCCI	Molten Corium Concrete Interaction
MOC	Method of Characteristics
MOX	Mixed Oxide
MTA EK	Hungarian Academy of Sciences Centre for Energy Research (Hungary)
MUWC	Make-Up Water Condensate
MVDS	Modular Vault Dry Storage
NCA	Nuclear Critical Assembly (Toshiba, Japan)
NCS	Nuclear Criticality Safety
NEA	Nuclear Energy Agency (OECD, France)
NPP	Nuclear Power Plant
NPS	Nuclear Power Station
NRA	Nuclear Regulation Authority (Japan)
NRC	Nuclear Regulatory Commission (USA)
NSSC	Nuclear Safety and Security Commission (Republic of Korea)
NTTF	Near-Term Task Force (U.S. NRC)
OECD	Organization for Economic Co-operation and Development
OEF	Operational Experience Feedback
ORNL	Oak Ridge National Laboratory (USA)
PAR	Passive Autocatalytic Recombiner
pcm	per cent mille (one thousandth of a percent)
PHWR	Pressurized Heavy Water Reactor
PIRT	Phenomena Identification and Ranking Technique/Table
PNNL	Pacific Northwest National Laboratory (USA)
ppm	part per million
PSI	Paul Scherrer Institut (Switzerland)
PTR	Reactor Cavity and Spent Fuel Pit Cooling and Treatment System
PWR	Pressurized-Water Reactor
QT	Quantum Technologies AB (Sweden)
R/B	Reactor Building

RCIC	Reactor Core Isolation Cooling
RHR(S)	Residual Heat Removal (System)
RIA	Reactivity Initiated Accident
RPV	Reactor Pressure Vessel
RSK	Reaktor-Sicherheitskommission, Reactor Safety Commission (Germany)
RWST	Refuelling Water Storage Tank
SA	Severe Accident
SAFEST	Severe Accident Facilities for European Safety Targets
SAM	Severe Accident Management
SAMG	Severe Accident Management/Mitigation Guideline
SAT	Station Auxiliary Transformer
SBO	Station Blackout
SET	Separate Effect Test
SFP	Spent Fuel Pool
SFPCS	Spent Fuel Pool Cooling System
SFPS	Spent Fuel Pool Study (U.S. NRC)
SHC	Shutdown Cooling System
SONGS	San Onofre Nuclear Generating Station (USA)
SS	Stainless Steel
SÚJB	Státni Úřad pro Jadernou Bezpečnost, State Office for Nuclear Safety (Czech Republic)
SWC	Salt Water Cooling
TEPCO	Tokyo Electric Power Company (Japan)
UAT	Unit Auxiliary Transformer
UJV REZ	Nuclear Research Institute Rez pl (Czech Republic)
UKAEA	United Kingdom Atomic Energy Authority (UK)
VNIINM	Bochvar All-Russian Scientific Research Institute for Inorganic Materials (Russia)
VTT	Technical Research Centre of Finland (Finland)
VVER	Russian type pressurized-water reactor (Водо-водяной энергетический реактор)
WENRA	Western European Nuclear Regulators Association
WGAMA	Working Group on Analysis and Management of Accidents (OECD/NEA/CSNI)
WGFS	Working Group on Fuel Safety (OECD/NEA/CSNI)

1 INTRODUCTION

Spent fuel pools (SFPs) are large accident-hardened structures that are used to temporarily store irradiated nuclear fuel. Due to the robustness of the structures, SFP severe accidents have long been regarded as highly improbable events, where there would be more than adequate time for corrective operator action. The Fukushima Daiichi nuclear accident that followed after the Great East Japan Earthquake on March 11, 2011, has renewed international interest in the safety of spent nuclear fuel stored in SFPs under prolonged loss of cooling conditions

Following the accident, the Nuclear Energy Agency (NEA) Committee on the Safety of Nuclear Installations (CSNI) launched several activities to help contributing to the post-Fukushima accident decision making process. Within this framework, it was decided to write a "Status report on SFPs under loss of cooling accident conditions", to summarize the current state of design and knowledge.

1.1 Spent fuel pools and accident scenarios

There are two main types of pools used for wet storage of spent nuclear fuel: at-reactor (AR) pools and away-from-reactor (AFR) pools [1]. Virtually all power reactors have some form of AR pool that allows storage of spent fuel after core off-load until the residual power is sufficiently low to allow transport of the fuel to intermediate storage. The pool is also used during reactor refuelling operations, for temporary storage of fresh and spent fuel assemblies. Away-from-reactor pools are usually large facilities for interim storage of spent fuel awaiting reprocessing or final disposal. The AFR pools may be located at reactor sites, as in Fukushima Daiichi, or at independent, off-site places

At-reactor SFPs are designed to store several times the number of fuel assemblies present in the reactor core. They are in most nuclear power plants located outside the primary containment of the reactor. The design and size of AR SFPs depend on the reactor type, but the pools have many common features: they are large monolithically constructed water-retaining structures. The fuel assemblies are stored in storage racks, which are covered by 5 to 8 metres of water that provides cooling as well as biological protection. The typical depth of an AR SFP is 8 to 15 metres. The water is cooled by a dedicated cooling system with pumps and heat exchangers. SFPs are also equipped with instrumentation to monitor the water level, temperature and pressure and flow of circulating systems. The maximum heat load in an AR SFPs is obtained just after full core off-load. At this instant, the maximum thermal power released from all spent fuel in the pool is typically about 0.3 % of the reactor thermal power (e.g. 10 MW for a 900 MWe reactor). The thermal power decreases with fuel storage time

Adequate cooling of the spent fuel in the SFP can principally be lost either by malfunction of the pool cooling system (loss of cooling accidents) or by loss of the pool water inventory (loss of coolant accidents, LOCAs). It is important to point out that, while there are many similarities between the phenomena involved in reactor LOCAs and SFP loss of cooling/coolant accidents, the latter tend to be slower, due to the relatively low power of the fuel and the large water volume in the pool. Another important difference is that there are three physical barriers between the nuclear fuel and the environment when the fuel is in the reactor (the fuel cladding, the envelope of the primary circuit and the containment building), whereas there is usually only one physical barrier (the fuel cladding) when the fuel is stored in SFPs.

1.2 Objectives, scope and outline of the report

This report is intended to summarize current understanding of the behaviour of SFPs in loss of cooling and loss of coolant accident conditions. Past accidents and precursor events are reviewed, in particular the behaviour of the spent fuel facilities during the Fukushima Daiichi accident. Important aspects of the accidents and involved phenomena are addressed, such as the thermal-hydraulic behaviour of the pool, the issue of criticality, the accident progression under partial or complete loss of coolant, the hydrogen risk, the fission product release, etc. The report provides a brief assessment of current experimental knowledge about loss of cooling and loss of coolant accidents. It also presents state-of-the-art computer codes used for analyses of SFP accidents, and discusses strengths and weaknesses of models and methods used in these codes. The probability of SFP accidents and assessments of off-site health effects and contamination consequences of SFP accidents are, however, beyond the scope of this document

The fuel residing in AR SFPs is usually characterized by higher decay power than fuel stored in AFR pools. Since the progression rate and severity of a loss of cooling/coolant accident correlates with the power of the stored fuel assemblies (FAs), the most challenging accident scenarios are expected in AR storage pools. For this reason, the report focuses on AR SFPs in light-water reactor (LWR) and Canada Deuterium Uranium (CANDU) reactor nuclear power plants. The presentation is based on experimental data and results from computational analyses, published in open literature up to 2014.

The report is also aimed to identify areas that need additional knowledge and to identify potential improvements in computational models and tools for better predictions of SFP accident progression and time margins to significant radiological releases. An improved understanding of the phenomenology of SFP accidents and coolability mechanisms, along with a consensual view of the extent of remaining uncertainties, are indispensable for reliable estimates of accident progression and radiological consequence

Past studies that have been performed to look at various aspects of spent fuel and SFP safety, security and risk (including the major regulatory activities specifically in the USA) are summarized in [2]. The SFP research spans a period of more than three decades, from using early analytical tools to more recent state-of-the-art computational tools that rely on dedicated experimental work for validation of the models.

The outline of the report is as follows:

- Chapter 2 provides a description of AR SFPs for light water and CANDU reactors. The design of spent fuel racks, the pool cooling system, the instrumentation and measures for safety, accident prevention and mitigation are presented. The current situation in OECD member countries regarding spent fuel storage in general, and AR SFPs in particular, is summarized in Appendix A. The improvements made after the Fukushima Daiichi accident are also summarized. Appendix B details, country by country, the different measures taken after the accident.
- Chapter 3 deals with possible accident scenarios. It provides an overview of the operational experience feedback from AR SFPs and a representative selection of events that have occurred. The Paks cleaning tank incident is described in particular detail. Appendix C presents some significant precursor events and accidents that have happened with SFPs, and it also summarizes the results of two past assessments of events with loss of SFP cooling or water inventory.
- Chapter 4 is entirely dedicated to the behaviour of the SFPs and the dry cask storage at the Fukushima Daiichi nuclear power station during and after the 2011 accident.
- Chapter 5 describes the phenomenology of SFP loss of cooling and loss of coolant accidents. It covers the criticality issue and the thermal-hydraulic behaviour of a SFP under different stages of an accident. The fuel behaviour and fuel assembly and rack degradation, as well as the fission product release and transport during loss of cooling or loss of coolant accidents are addressed.

- Chapter 6 is a review of integral tests and separate effect tests with relevance to SFP accidents. Among the integral tests, the experiments recently conducted in the OECD/NEA Sandia Fuel Project are given particular attention. The separate effect tests covered by the review are mainly on cladding air oxidation and fission product release in air-rich environments.
- Chapter 7 deals with computer programs used for analysis of SFP accidents. The presentation is intended to give an overview of the different tools used for nuclear criticality, thermal-hydraulics and severe accident simulations. Details on some widely used severe accident codes are given in Appendix D.
- Chapter 8 presents the conclusions of the report and some recommendations for future research and activities are given.

2 SPENT FUEL POOLS

Spent nuclear fuel generated from the operation of nuclear reactors needs safe management following its removal from the reactor core. The spent fuel contains large amounts of radioactive isotopes and its fissionable material content is also significant. Furthermore, radioactive decay generates high power and radiation in the fuel at the beginning of the storage period in the AR SFP. In order to provide safe storage conditions, the SFP design and its operation must take into account criticality safety, heat removal and radiation shielding [3].

After a period of cooling, the decay heat will be low enough to move the spent fuel from the AR SFP into AFR interim storage facilities with less intense heat removal. Both wet and dry spent fuel facilities can be used for interim storage [1]. A summary of spent fuel management strategies in OECD member countries is given in Appendix A.

2.1 Spent fuel pools for light water reactors

Refuelling of light water reactors is carried out after reactor shutdown with open reactor vessel. The refuelling pool above the reactor vessel is filled up with water, and the replacement of spent FAs with fresh ones is carried out under deep water level by use of a refuelling machine. The nearly 4 m long LWR fuel assemblies are stored vertically in special rack systems. Appendix A contains a review of the SFP designs and storage rack types currently used in LWRs by some OECD member countries.

2.1.1 Pool design

A typical design of the SFP in pressurized water reactors (PWRs) is shown in Figure 1, whereas Figure 2 shows a typical pool design for boiling water reactors (BWRs). The pools are constructed of reinforced concrete with a stainless steel liner to prevent leakage and maintain water quality. The pools are envisaged to withstand design-basis seismic events. The cooling systems associated were not, in some cases, designed for such accidents at the early stages of operation, but they have been re-qualified afterwards.

For BWRs, the SFP is generally located within the reactor building, but outside of the primary containment. Also for PWRs, the SFP is usually located outside the containment, but adjacent to it in a separate fuel handling building or within the auxiliary building. Exceptions are the Russian VVER-1000 design, the German Kraftwerk Union (KWU) KONVOI or pre-KONVOI PWR design, and the AREVA EPR design, where the SFP is located inside the containment.

Typically, SFPs in light water reactors are about 12 m deep and vary in width and length; see Appendix A. The fuel is stored in stainless steel (SS) racks that are submerged with approximately 7 m of water above the top of the stored fuel. The water in the SFP of a BWR is demineralized water, whereas PWRs and VVERs (Russian design PWRs) use borated water. In addition to cooling, the SFP water inventory provides radiological shielding for personnel in the fuel pool area and adjacent areas. Shielding is also provided by the thick concrete walls of the SFP. Each plant generally has technical specification requirements for water temperature and level, and for the margin to criticality for the fuel stored in the SFP.

Each plant has a source of high purity water to fill the SFP, referred to in nuclear power plants as make-up. The preferred sources are usually the refuelling water storage tank for PWRs and the condensate storage tank for BWRs. The normal make-up is through a connection from the water source to the suction of the SFP cooling system pumps, and local valve operations are needed to initiate SFP make-up. The make-up rates among plants have a wide range. Plants also have alternate methods to provide make-up, if normal make-up is unavailable, and may include the service water system and the fire water system.

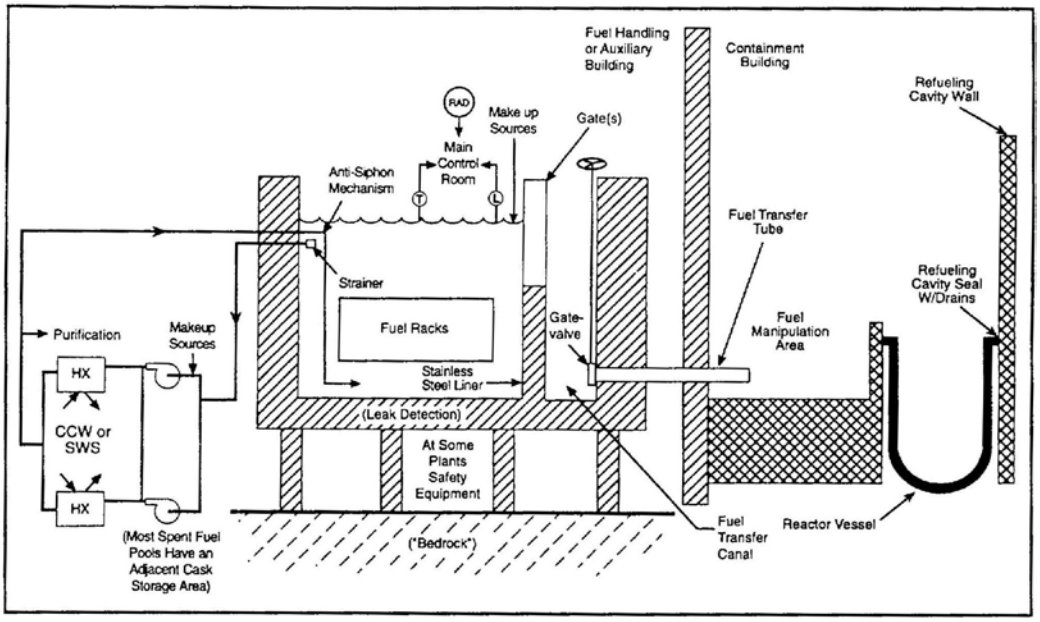

Figure 1: Generic SFP design for PWRs [4].

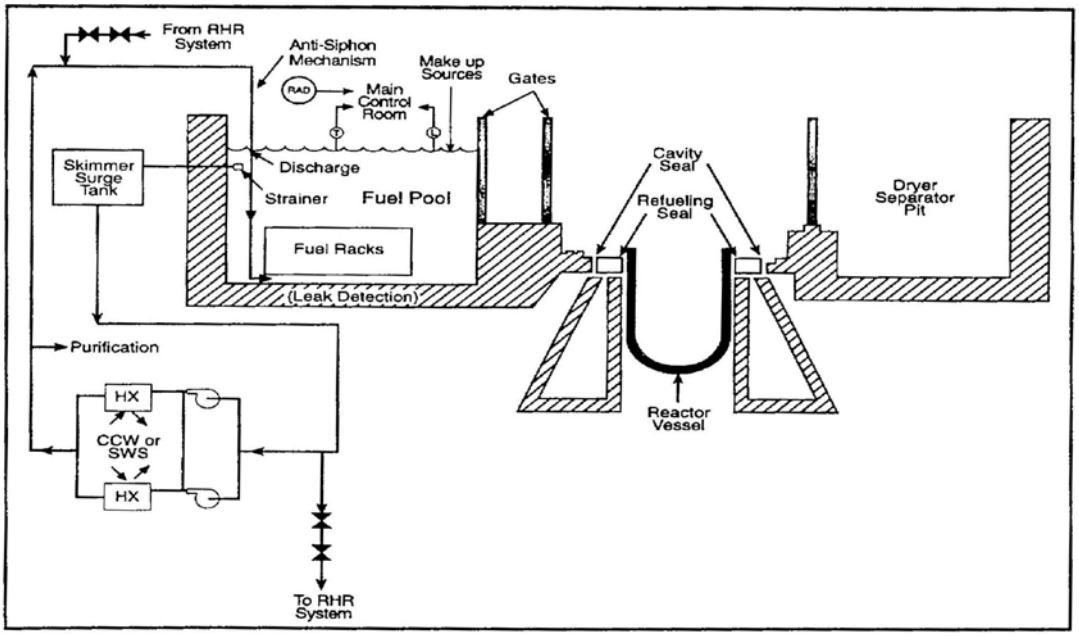

Figure 2: Generic SFP design for BWRs [4].

Finally, it is worth noting that, besides spent and fresh fuel, many other components and in-reactor equipment (e.g. control rods, fuel channels, flow restrictors, in-core instrumentation, primary and secondary neutron sources, etc.), may be stored in the SFP. Some VVER plants also have special containers in the SFP for the storage of damaged or leaking FAs, or individual leaking fuel rods removed from the assemblies; see section 2.1.2.3.

2.1.2 Spent fuel rack design

The design of storage racks and fuel assembly holder configurations within the SFPs of light water reactors varies considerably, not only depending on fuel/reactor type, but also from facility to facility.

2.1.2.1 PWRs

Examples of spent fuel storage racks used in SFPs of PWRs are shown in Figure 3, and details are given in Table 1. An early storage rack design for PWR spent fuel consists of an open frame arrangement with a 41 to 53 cm centre-to-centre spacing; Figure 3a). The racks are made of stainless steel and are approximately 4.3 m high. Criticality control is provided by the relatively large fuel assembly spacing together with borating of the SFP water. Subsequent PWR rack designs employ solid stainless steel holder walls to provide the neutron shielding required for a higher density storage configuration; see Figure 3b) through Figure 3d). The cylindrical "baskets" shown in Figure 3b), for example, provide a 32 cm centre-to-centre FA spacing. The inlet for water circulation through these elements is provided by a 4 cm diameter hole, drilled through each basket near the base plate. Figure 3c) shows an example of a square-shaped rack configuration. These racks include a 33 to 36 cm centre-to-centre FA spacing and provide for water flow through a base plate hole of varying diameter (e.g. 7.6 cm).

Figure 3d) shows high density[1] storage racks, which can reach a 26 cm centre-to-centre spacing. Neutron absorption is accomplished by holder walls, which in this particular design consist of two 3 mm stainless steel plates sandwiched around a 6 mm absorber plate made of 50 vol% boron carbide in a carbon matrix. Other typical neutron absorber materials comprise, e.g. Boraflex (including boron carbide and silica; nowadays no more used due to degradation issues), Boral (an aluminium alloy), Bocarsil (silicone rubber bearing boron carbide), or borated stainless steel, whether as structure material or as additional sheaths or sheets within the structure.

In most cases, a 20 to 40 cm open space is maintained between the base plate and the bottom of the pool and between the sidewalls and the outermost basket or holder. The high-density storage configuration in Figure 3d), however, is an exception in that the design allows racks to be placed within 1.3 cm of the walls of the pool. Many spent fuel holder designs provide only a single inlet hole for convective flow through each FA, located in the base plate or near the bottom of the holder. Except for the open frame design in Figure 3a), the racks do not allow cross flow between different FAs.

[1]. High-density storage means that rack FA spacing alone is inadequate to provide required margin to criticality.

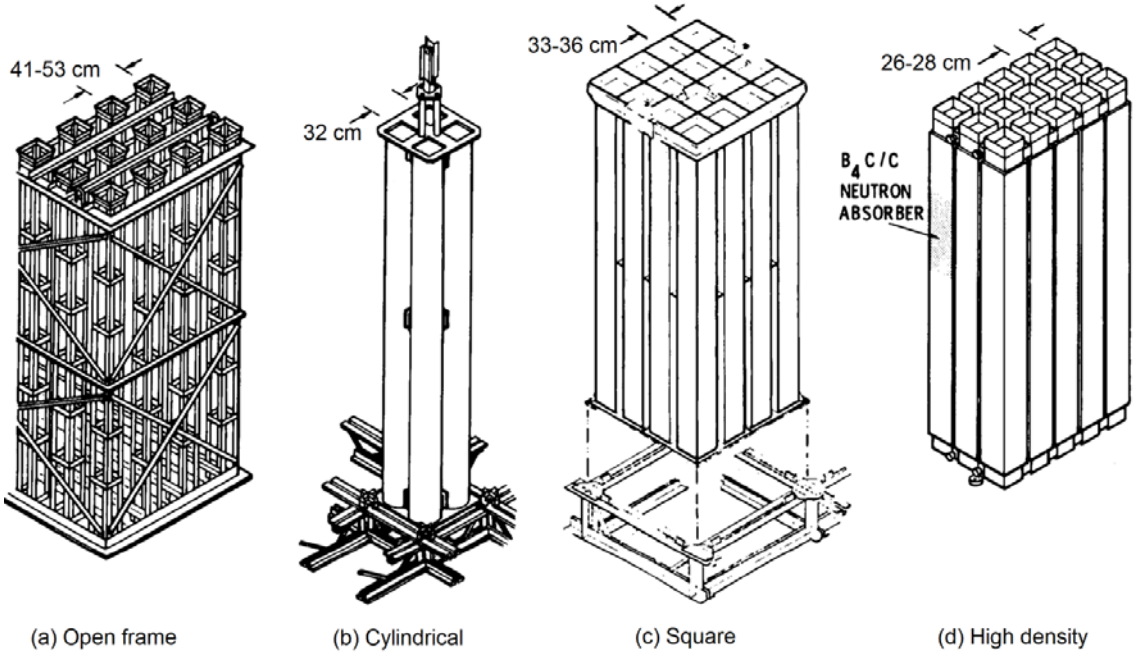

Figure 3: Spent fuel storage racks used in PWRs [5].

Table 1: Typical designs of PWR spent fuel storage racks.

	(a) Open frame	(b) Cylindrical	(c) Square	(d) High density
Height (m)	4.3	4.3	4.3	4.3 – 5.0
Centre-to-centre FA spacing (cm)	41 - 53	32	33 - 36	26 - 28
Inlet hole diameter (cm)	-	4	7.6	12.7
Cross flow between racks	Y	N	N	N
Neutron absorber	N	N	N	Y

2.1.2.2 BWRs

Examples of spent fuel storage racks used in SFPs of BWRs are shown in Figure 4, and their main specifications are given in

Table 2. The early low density BWR storage rack designs employ H-shaped partition walls made of aluminium that provide open spaces for water cross-flow to each fuel assembly; see Figure 4a). Sub-criticality is ensured by neutronic decoupling, provided by the water in the large open spaces between FA rows for this low density storage configuration; see Figure 4a)

Subsequent BWR rack designs employ square-shaped rack tubes made of stainless steel; see Figure 4b). The stainless steel holder walls provide the neutron shielding required for a higher density storage configuration. The racks provide water cross-flow between rows; see Figure 4b)

An example of a high density rack is shown in Figure 4c). The rack design employs square-shaped rack tubes made of boron-borated stainless steel, a material that provides additional neutron absorption. The rack tubes are placed in a checkerboard pattern, as shown in Figure 4c). This rack design does not allow lateral flow of water. An open space is provided between the base plate and the bottom of the pool for convective axial flow in each rack tube.

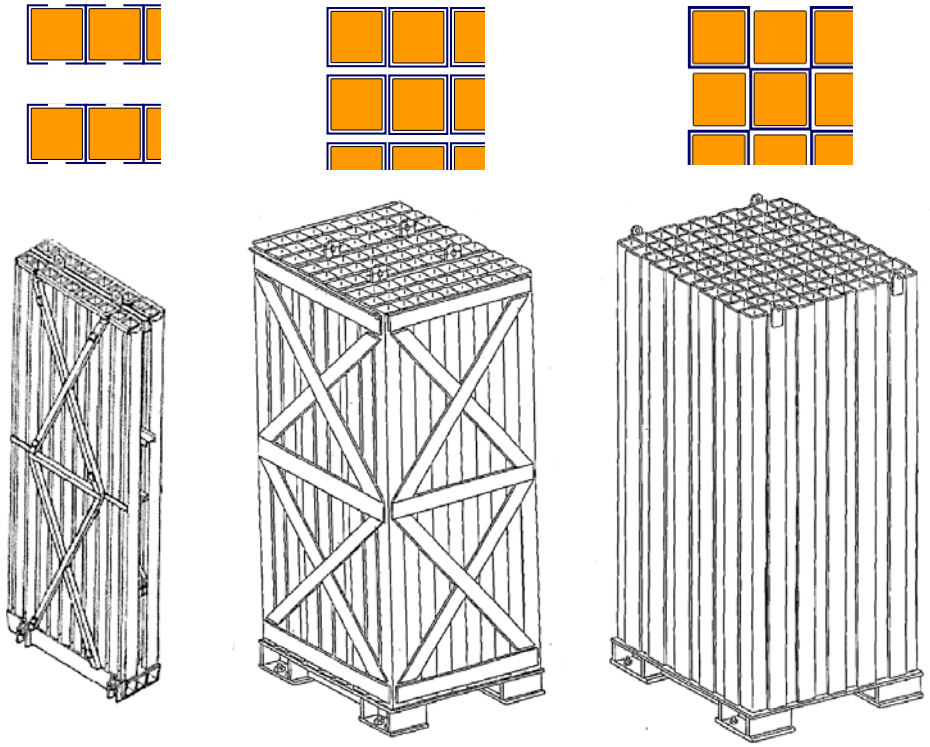

a) Low density rack (Aluminium rack) b) Higher density rack (Stainless steel rack) c) High density rack (Boron-borated SS rack)

Figure 4: Spent fuel storage racks used in BWRs [6, 7].

Table 2: Typical designs of BWR spent fuel storage racks [8].

	(a) Low density	(b) Higher density	(c) High density
Rack material	Aluminium	Stainless steel	Boron-borated stainless steel
Rack module configuration	2×10	9×10	11×11
Centre-to-centre FA spacing (cm)	-	About 17×20	About 16×16
Wall thickness (mm)	-	About 6	About 5
Cross flow between racks	Y	Y	N
Neutron absorber	N	N	Y

2.1.2.3 VVERs

The design of SFPs in Russian designed pressurized water reactors (VVERs) depends on the reactor type; see Appendix A. For VVER-440/213, the SFP is located close to the reactor in the reactor hall, but outside of the containment hermetic boundary. The reactor hall is an airtight room in the upper part of the reactor building. It is a large room, common for twin units. When the fuel pool is not used for refuelling operations, it is covered by panels. For VVER-1000, the SFP is located close to the reactor in the reactor building, inside of the containment hermetic boundary. The SFP is composed of three sections, separated by walls. One section is used for temporary full core off-loading only, whereas the other sections are used for longer term storage [9]. When the fuel pool is not used for refuelling operations, it is covered by panels.

Two types of fuel racks are used at VVER-440/213 plants [10]: i) stationary high density racks are used to store spent FAs and for refuelling during normal outage; ii) removable low density racks are used for whole core off-load during outage with reactor vessel inspection. The frequency of whole core off-loads is low (originally it was once in four years, now it can be different at each plant).

Mechanical support to FAs in the high density rack is provided by two stainless steel plates, joined by four tubes[2]. The lower support plate sits on adjustable legs, and holes in the plates provide positions for fuel assemblies; see Figure 5a). Positions for spent FAs are made from 3 m long hexagonal tubes of 3 mm thick stainless steel with 1 % boron, welded to both plates. The free space between two adjacent hexagonal tubes is about 4 mm. There are three stationary high-density racks in the VVER-440/213 SFP with a total capacity of 682 assemblies and 17 additional positions for cylindrical hermetic capsules to store assemblies with leaky fuel rods. A removable low density rack is temporarily inserted in the SFP and placed on top of the stationary high density racks when needed for full core off-loads. The low density rack is composed of three stainless steel plates joined by tubes, as shown in Figure 5b). During normal plant operation, this removable low density storage rack is stored empty in the reactor hall. Only one removable rack can be used for twin units.

[2]. High density fuel storage racks in VVERs may be slightly different from unit to unit. The design presented here is for racks currently produced at ŠKODA JS a.s.

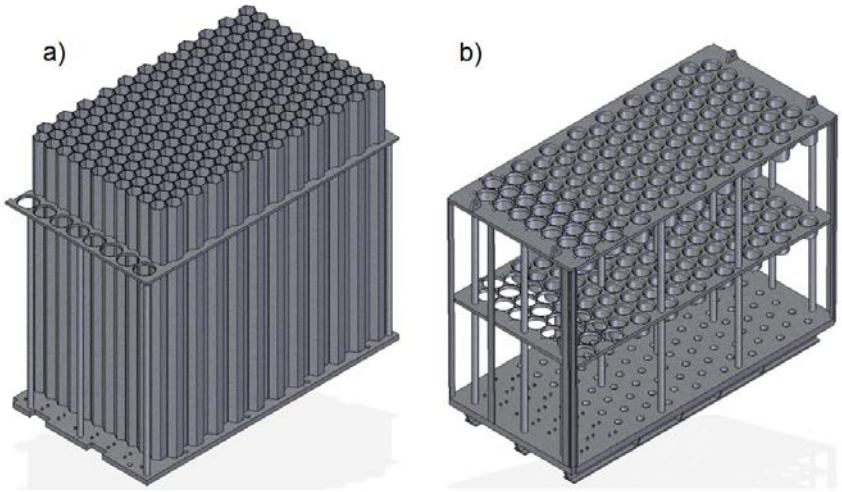

Figure 5: Spent fuel storage racks used in VVER-440/213.
a) High density rack. b) Low density rack used for full core off-loads.

As for VVER-1000, the three sections of the SFP contain only high density storage racks [11]. The first section has a single rack with 127 FA positions, and is used only for full core off-loads. The second section has two racks to store 312 spent FAs, and the third section has two racks to store 241 spent FAs and 25 additional positions for cylindrical hermetic capsules to store assemblies with leaky fuel rods. The total storage capacity of the VVER-1000 SFP is thus 680 FAs in high density racks and 25 FAs in hermetic capsules. The mechanical base of the high-density storage rack is provided by a stainless steel support plate, which sits on adjustable legs. Five tubes welded to the lower support plate fix the absorption section of the rack. The removable absorption section is composed of hexagonal absorption tubes and two plates with hexagonal holes. The ends of absorption tubes are welded to holes in the plates. The absorption tubes are made from 4.2 mm thick sheets of stainless steel with 1 % boron and 3.59 m long. The free space between two adjacent hexagonal tubes is about 4 cm. Adjusting cones are placed in the gaps between adjacent hexagonal tubes.

2.1.3 Fuel arrangement

Generally, the fuel assemblies are arranged in the storage racks in such a way as to ensure deep subcriticality of the SFP. In the USA, the licensees are expected to put spent FAs into the storage racks in a 1×4 repeating pattern (i.e., each assembly discharged during the most recent outage being surrounded by assemblies from previous outages) or equivalent. If direct placement of assemblies into this pattern is not achievable, licensees have a required time by which they must achieve this pattern. The purpose of requiring this fuel configuration is to take advantage of passive (radiative and convective) cooling mechanisms in the event of a loss-of-coolant inventory accident associated with a severe accident.

Figure 6 shows an illustration of different fuel loading patterns in the pool [2]. The uniform configuration, where the hot fuel assemblies are placed next to each other (allowed for some time after discharge), is the least favourable, while 1×4 and 1×8 patterns show increasing improvement in thermal management of the fuel. The advantages of the 1×4 pattern over the uniform pattern are well documented in both experimental [12] and analytical studies [2]. In [2], the reference plant assumed a preconfigured SFP with 1×4 pattern, even though the plant studied actually uses a 1×8 pattern. The analysis showed the potential for achieving coolability conditions under a broader range of conditions, as well as reductions in radioactive releases, with fuel stored in the more favourable configurations.

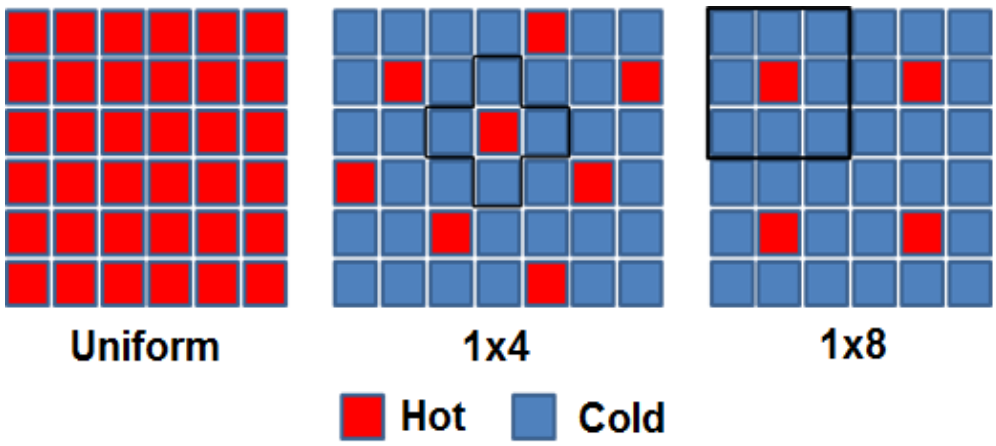

Figure 6: Various spent fuel patterns in the SFP storage racks [2].

2.1.4 Operational fuel handling

During refuelling operations, the refuelling cavity above the reactor is filled with water to equal the water level in the SFP. Fuel is moved between the SFP and the reactor via transfer canals in BWRs, VVERs and German PWRs, or via transfer tubes in other PWRs. For BWRs, VVERs and German PWRs, the movable gates that separate the SFP and the transfer canal from the reactor cavity provide an opening for fuel to be moved in a vertical position. Removal and replacement of the gates requires use of the plant travelling crane because of their size and weight. Thus, during refuelling, a loss of water from the refuelling cavity resulting in a drop in water level would also lower the water level in the SFP. Replacement of the gates to isolate the leak would be a major time-consuming operation.

For PWRs (other than the German design), the transfer tube provides for movement of the fuel in a horizontal position. The opening provides a much smaller flow path from the SFP to the reactor cavity than the movable gates in BWRs, VVERs or German PWRs. Also, a gate valve at the SFP end of the transfer tube can be closed to stop the flow path from the SFP to the reactor cavity.

2.1.5 Pool cooling systems

A study of SFP cooling systems (SFPCS) [4] in PWRs and BWRs indicates that a wide variety of configurations exists. This section provides simplified general descriptions of SFPCS configurations in LWRs.

The SFP coolant inventory is cooled by a dedicated cooling system. As shown in Figure 1 and Figure 2, the SFP coolant is pumped through heat exchangers, where sensible heat is transferred to an intermediate cooling system, which finally rejects heat to the plant's ultimate heat sink. The SFPCS takes suction from the SFP through a skimmer or strainer at such an elevation that a water level change in the SFP would cause the pumps to lose suction and prevent further SFP coolant inventory loss through a break in the SFP cooling system piping. The SFP cooling return lines either discharge near the top of the SFP or are arranged to distribute coolant flow around the bottom of the fuel in the SFP. The penetrations of SFPCS piping through the pool wall are located at high elevation, in order to prevent total loss of water from the pool in case of pipe rupture.

With a few exceptions, SFP cooling piping that extends deep into the SFP is equipped with antisiphon devices to prevent loss of SFP coolant inventory, should a system misalignment or pipe break create an

inadvertent siphon flow path. These are passive devices, designed to let air into the line as soon as they are uncovered by the lowering water, thereby breaking the siphon. They consist of a hole in the pipe or a line going upward; the latter design has the advantage of being easily closed if deemed necessary, e.g. for pool emptying. Depending on the configuration of the pool and on the initiating event, the siphoning effect can last a certain period before the siphoning breaks. The distance between the siphon breaker elevation and the pool level at which siphoning actually breaks is called the undershooting height. The latter is a function of the siphoning flow rate and the size of the siphon breaker air inlet; inlets that are 10 mm in size are effective up to drainage rates of 500 m^3/h [13]. Experimental results show that the leading effect of siphon breaking is the flow stratification in the upper part of the line [14]. This stratification is directly linked to the ratio between the air and water flow rates.

There are different degrees of redundancy for SFP pumps, heat exchangers, and intermediate cooling systems. BWR plants have the capability to align the residual heat removal (RHR) system to remove heat from the SFP, in the event that the normal SFP cooling system is unavailable or its capacity is lower than the heat rate to be removed. Each plant has a non safety-related system that is used to purify and clarify the SFP water. This system, which is often integrated with the normal SFP cooling system, is typically made up of filters, ion exchangers, and other supporting equipment.

2.1.6 Instrumentation

Light water reactors have instrumentation to monitor the performance of the SFP, although the type and extent of instrumentation vary significantly among plants. The parameters monitored include SFP level, temperature, liner leakage, pump discharge pressure, and system flow. Indication, recording, or alarm functions of these parameters are provided either in the main control room or on a local panel. Typically, most instrumentation is on a local panel, and only important parameters are monitored in the control room. The design features of instrumentation vary among different plant types and vendors, and sometimes even among plants designed by the same vendor.

The SFP water level is monitored, and in some designs, an abnormal level is alarmed in the control room. The water level sensor typically has a narrow range, about 2 metres, covering high and low alarm set points and the minimum technical specification level. Therefore, the control room indicator cannot monitor a level below this range and becomes useless for lower level conditions expected in case of a gross loss of SFP coolant inventory event.

In some plants, the pool water temperature is indicated or recorded in the control room; in others, the temperature is on a local panel. For most plants, an abnormal temperature is individually alarmed in the control room; for other plants, the alarm is on the local panel that initiates a common trouble alarm in the control room. The typical maximum temperature is 60 ºC in normal operation and refuelling outages.

Most plants have leak detection systems to determine if leakage is occurring from the SFP liner, spent fuel shipping cask pool, or from other portions of the fuel pool or reactor cavity structure. The leak detection system is usually made up of several channels that can be monitored individually, or are designed in such a way that leakage empties into drains that can be monitored and returned to sumps, liquid radioactive waste, or other cleanup or collection systems. The SFP leak detection system can usually be isolated if necessary to attempt to reduce SFP leakage.

Some plants have safety-related power to the SFP instrumentation, but the instruments themselves are in most cases not safety related. Other plants have neither safety-related power supplies for the instrumentation, nor instruments that are safety-related. In general, the plants have no redundancy for the SFP instrumentation.

In PWR SFPs with partial reliance on the presence of soluble boron for subcriticality, permanent boron concentration monitoring is typically implemented. In plants that do not rely on the presence of soluble boron, periodic single boron concentration measurements are typically made. Also, the activity concentrations of fission products and corrosion products are regularly measured in the SFP coolant

together with water chemistry parameters. An important part of the SFP instrumentation is the radiation dosimetry equipment.

2.1.7 Safety systems, prevention and mitigation

The cooling system of the SFP should be available whenever there is spent fuel stored. The system must operate in both normal operation and in the event of an accident. Therefore, the cooling system of the pool is a safety-related system. The safety systems of SFPs are much simpler compared to Emergency Core Cooling Systems (ECCS). For example, manual operator actions are needed to cope with SFP accidents, and the systems typically have less redundancy. Emergency water for SFP cooling can be taken from different sources.

In case of a loss of cooling accident or loss of external power, the SFP cooling system pumps are connected to the Emergency Diesel Generators (EDGs). Component cooling water supplying valves to the heat exchangers may be opened manually, so those exchangers can be cooled in any operating mode. The major flaw in this system would be a significant loss of water from the SFP. To protect against this possibility, the configuration of the suction and discharge pipes and the availability of anti-siphon devices guarantee a column of water above the FAs higher than the required minimum of 3 m for the purpose of shielding against radiation [15].

The demineralized water system provides makeup water to compensate for losses from the pool. The reactor makeup water system is a Seismic Category I system, and supplies water in case that the demineralized water system is unavailable. The emergency supply of water to the pool would be taken from the Essential Service Water System (ESWS) (Seismic Category I). There is also an alternative supply of water from the hose connections located in the fuel building in the area near the pool, with water from the fire protection system distribution ring. In PWR and VVER reactors, only borated water can be used in the SFP.

Periodic maintenance and visual inspections are performed according to current standards. As for safety related equipment for surveillance and monitoring of the SFP, a description of the available instrumentation is given in Section 2.1.6.

2.2 Spent fuel pools for CANDUs

CANDU pressurized heavy water reactor (PHWR) plants are capable of and routinely refuel on power. This necessitates a fuel handling and storage system that is capable of handling a steady stream of spent fuel being placed into wet storage. The fuel is irradiated natural uranium fuel, stored in demineralized light water.

CANDU fuel bundles are roughly half a metre long and 10 centimetres in diameter. Fuelling operations typically fuel four or eight bundles in a channel, with 12 to 16 bundles being fuelled each day on a given reactor. The fuel resides in horizontal pressure tubes inside a large heavy water filled calandria vessel. Fuelling is performed by a pair of fuelling machines, one which loads new fuel into the channel and a second identical machine that accepts the spent irradiated fuel. The fuelling machine containing the spent irradiated fuel then travels to the irradiated fuel port and transfers the fuel via the irradiated fuel port to a basket located in the reception bay. Representative data for CANDU SFP and storage rack designs are provided in Appendix A, together with a brief summary of national requirements/criteria for CANDU SFPs.

2.2.1 Pool design

The SFP at CANDU plants, also known as the primary irradiated fuel bay (IFB), is divided into three sections [16, 17]. The reception bay is a smaller section, with an independent cooling system, where the

fuel is first moved into from the fuelling machine. Fuel is typically stored here for one to two weeks before it is transferred to the main storage bay.

The storage bay is the largest section and can be sealed off from the reception bay if needed. Fuel is stored here in low density open racks. Depending on the design, fuel is either stored here for a short period, 6 months to 4 years, and then moved on to a larger long term wet storage bay (secondary irradiated fuel bay) or is stored until (7 to 10 years) it is cool enough to be placed directly into dry storage. The storage bay also typically has a fuel inspection station, where underwater remote inspection of spent fuel is performed to monitor and assess fuel performance.

The third section is the wet cask handling bay, also known as the transfer bay, where transfer casks and dry storage casks are loaded under water. This bay is removed from the storage section of the bay as to prevent the possibility of a cask dropping on a rack of spent fuel. The transfer bay can also be isolated from the storage bay. In plant designs with a secondary irradiated fuel bay, this bay can also contain an underwater transfer duct to the secondary bay.

Defected fuel is normally stored in racks adjacent to the fuel inspection station. Severely damaged fuel is placed in sealed canisters. Some CANDU reactors produce medical isotopes (^{60}Co), which are placed in the storage bay prior to shipping.

The SFPs are large monolithically constructed, reinforced concrete, water-retaining double-walled structures, located at or slightly above ground level; see Figure 7. The walls and floor are typically 1.5 to 2 m thick with a steel floor liner, which runs 0.5 m up the walls. The walls of the fuel pool are then typically either lined with a fibreglass reinforced epoxy coating up the remainder of the wall or a steel liner. This structure is encased in a second set of walls with a small interspace between the walls. The walls are seismically qualified and the interspace is instrumented to detect leakage. Should leakage occur, there is a sump to collect the water, which can then be pumped back into the pool. If the worst case failure of the inner wall occurs, the outer wall will ensure pool integrity and the resulting water level drop will not be significant enough to jeopardize fuel cooling or biological shielding.

The size and shape of the pools varies greatly from station to station. The variation is due in great part to the different philosophies for long-term storage (dry storage vs. longer term wet storage) and whether or not it is a single or multi-unit station. As a general rule of thumb, receptions bays are half the size of the main fuel pool. The main fuel pools can be as small as 20×12 m, or as large as 34×17 m. All spent fuel storage pools are at least 8 m deep.

2.2.2 Spent fuel rack design

The fuel discharged into the reception bay is loaded into baskets or directly into trays, and then, after a few days, transferred into the storage bay. The bundles in baskets are then loaded into trays or modules. Bundle spacing is not a concern, as there are no criticality issues with natural uranium fuel in light water or air. Trays are placed into racks, with 2 trays per racking level; see Figure 8. The racks are low density and open to both horizontal and vertical flow, seismically qualified and bolted to the floor.

Figure 7: CANDU storage bay with fuel racks.

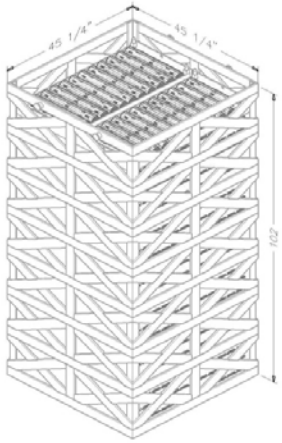

Figure 8: CANDU spent fuel racks.

2.2.3 Fuel arrangement

CANDU fuel cannot go critical in light water or air, nor are there currently any concerns with the ability of fuel to be passively cooled in a severe accident, as the CANDU racks are open. As such, the fuel arrangement is optimized for operational expediency. The fuel arrangement in a tray normally matches the order the fuel is discharged from the channel and fuelling machine.

2.2.4 Operational fuel handling

Fuelling is performed by a pair of fuelling machines, one which loads new fuel into the channel and a second identical machine that accepts the spent irradiated fuel [18]. The fuelling machine consists of a trolley and a head: The trolley component is used to move the machine from the unit to the new fuel loading or irradiated fuel unloading transfer ports. The head consists of a fuel magazine, which looks and acts much like the cylinder from a revolver hand gun, and a sophisticated ram assembly. The magazine typically has 8 chambers for fuel in the cylinder, each holding 2 fuel bundles; other chambers hold tools or spare parts. The chamber is submerged in actively cooled heavy water.

The ram is used to push fuel out of the magazine chambers and coolant flow pressure is normally used to wash bundles into the magazine chambers, with the ram slowly being retracted to control the speed of this operation.

The fuelling machine containing the spent irradiated fuel then travels to the irradiated fuel port and locks onto it. As transfer of heavy water to the bay is undesirable, the magazine is partially drained of water such that the top chamber is fully in air. The magazine is then rotated such that a chamber with irradiated fuel occupies the top position and then the ram moves the two fuel bundles in that chamber into the irradiated fuel port. The transfer mechanism then inserts a ladle into the port, picking up the two bundles and transferring them into a basket that is then transferred into the reception bay light water. The entire process is automated and normally takes less than 4 minutes. A “bundle in air” alarm annunciates, should the process exceed 7 minutes. Plant-specific safety analyses determine the maximum duration in air, based upon licensing bundle power limits. Emergency cooling via flooding of the port or spray cooling is available, should the need arise. The fuel is left to cool in the reception bay for roughly one to two weeks before being transferred underwater to the storage bay.

A CANDU fuel bundle weighs roughly 24 kg, such that movement of fuel bundles can be performed by lift assisted hand tools, whereas basket and trays require craning to move. In the storage bay, fuel bundles are stored in trays or modules of 24 bundles. Trays are placed into a racking or framing system.

Racks/frames are stacked on top of each other to form towers. The towers are bolted to the floor of the pool and are seismically qualified.

Movement of fuel can result in mishandling. Several incidents have occurred, where bundles or trays of bundles have been dropped. To date, the events have proven benign, as CANDU fuel upon impact disassembles into its component pencils (rods). These short rods, though safety analysis assumes some will fail and release fission gases, have remained intact.

2.2.5 Pool cooling systems

The reception bay and the storage bay of the SFP have independent cooling and purification systems. The wet cask handling bay typically has a purification system, but not an independent cooling system, as it relies on the storage bay for cooling, due to the bay not being intended for storage of bundles.

The cooling systems are a pump and heat sink design, with the heat being transferred to the service water system and then directly to the ultimate heat sink. There is redundancy in the system with either a 2×100 % or 3×50 % pump/heat exchanger capacity design. The purification system employs ion exchangers and resin traps to remove radionuclides and general contaminants. Penetrations into the pool for the purification and cooling systems are typically located 1 m below the water level. This limits the maximum water loss, should there be a failure of the associated piping. Some designs extend piping down into the water to deliver water to the bottom of the pool. Siphon breakers are employed in these designs to ensure safety.

2.2.6 Instrumentation

The instrumentation of SFPs in CANDUs can be grouped into five high level groups:

- temperature;
- pressure and flow of circulating systems;
- water level;
- radiation monitoring; and
- pump and valve position/operation indications.

All instrumentation annunciates to the local control panel, with a subsequent general IFB trouble annunciating to the main control room.

Temperature is measured at the inlet and outlet of cooling and purification system into the bay, as well as the inlet and outlet temperatures of the heat exchangers. The instrumentation used is resistance temperature detectors placed in thermal wells. High and low temperature alarms, typically $\pm 3\ ^{\circ}C$, are announced at the local control panel.

The purification and cooling system is instrumented for both pressure and flow rates. Flow rates for the cooling system use orifice plate and differential pressure cells, whereas the lower flow rate purification system uses rotameters. Flow alarm set points are set to roughly 50 % of normal flow. Pressure measurements are made at all pump discharges, as well as ΔP measurements across the purification system ion exchange columns.

Fixed area radiation monitors are located at strategic points around the fuel pool. As the fuel pools are not radioactive work areas, alarms are set at the corresponding regulatory limits. These alarms are to protect workers during fuel handling, but also would sound in the case of a water level drop significant enough to impair the biological shielding of the bay. The chemistry of the pool water is monitored by regular grab samples.

Water level measurements in the bays are performed currently either by dual float type level switches, indicating either high or low water level to the local control panel, or an air bubbler system that is capable of indicating the actual water level over its range to the local control panel. The sumps also use a dual float switch, but one switch controls the pump and the other is a high level alarm.

2.2.7 Safety systems, prevention and mitigation

CANDU SFPs are monolithic structures with a double-wall design that is intended to make a water inventory loss, significant enough to lose fuel cooling or biological shielding, extremely unlikely. The most credible events are limited loss of water inventory and a subsequent loss of cooling. In this case, the prime concern is providing adequate makeup water to ensure fuel is maintained wet. Although not originally designed to accommodate 100 °C bay water, the SFP integrity has been assessed and found to preclude structural failure in the event of boiling in the pool. Minor wall cracking may occur, but will be within make-up capacity.

The bays and associated systems are seismically qualified to maintain their structural integrity. Instrumentation and cooling pumps are typically connected to emergency standby generators, which are further backed up by an emergency power supply that is seismically qualified. Standby generators and emergency power supply (EPS) are located at ground level and geographically dispersed. Portable diesel generators have also been acquired, in light of the Fukushima Daiichi accident, to add an additional layer of defence in depth; see Appendix B.

CANDU plants have multiple tie-ins between plant systems to ensure that adequate cooling water can be rerouted as needed in the event of a malfunction or accident. The SFPs are no different. Station makeup water would be the primary source, with firewater and then emergency water as the alternate options. Though there is redundancy in the purification and cooling systems, stations also have portable skid pumps that can be temporarily installed.

There are no criticality design considerations, as fresh and irradiated natural uranium fuel cannot go critical in light water or air. While the use of lake water, should that be needed in an extreme accident situation, would present some long term corrosion issues to the stored fuel and bay, it would not pose a criticality safety risk.

2.3 Measures undertaken after the Fukushima Daiichi accident

The Fukushima Daiichi accident was a reminder of the importance of maintaining at all times the water inventory in the SFP and of keeping the stored fuel elements cooled. It also revealed the need for providing reliable instrumentation during the development of an accident to alert the operators about the existing situation before they should start the required recovery actions. For these reasons, nuclear power plants (NPPs) have made a series of improvements in both systems, emergency water supply to the pool and monitoring instrumentation. These improvements are currently being implemented and include different alternatives, depending on the technology and the country.

As a consequence of the Fukushima Daiichi accident, the European Commission and national nuclear safety regulators in the European Union (EU) launched a process to carry out EU-wide risk and safety assessments of existing and planned nuclear power plants; the so called EU stress tests [19]. The stress tests programme was designed to re-evaluate (based on technical studies, calculations and engineering judgment) the safety margins of the European nuclear power plants when faced with extreme natural events, and to take relevant action wherever needed. The scope covered all reactor units in Europe, including the associated AR SFPs, and dedicated spent fuel storage facilities.

The EU stress test programme has identified a number of improvement opportunities that could reinforce the robustness of the facilities and increase the licensee's and national authorities' emergency preparedness. The adequate provisions have been arranged by the licensees in order to fulfil their own

commitments towards safety improvement, as well as the additional requirements from the regulatory bodies and the complementary recommendations from the European peer review teams.

Regarding the SFP, licensees have analysed the cooling systems of the SFPs and the strategies in place to face up to a loss thereof, as well as aspects relating to the loss of radiation shielding that a decrease in the water level of the pools would entail. Licensees and regulatory bodies propose the following general improvements so as to strengthen the response of the plants when faced with prolonged scenarios of loss of safety functions in combination with external events:

- Provide alternative fixed and portable means to feed water to the SFP with adequate boron concentration, if required;
- Improve the instrumentation for measuring the level, temperature and area radiation of the SFP;
- Provide additional electrical power supply;
- Manage hydrogen risk in the SFP building;
- Arrange stored fuel to improve cooling in the event of a loss of coolant inventory accident associated with a severe accident;
- Avoid inadvertent draining of the pools: provide anti-siphon devices and periodic checking of their availability;
- Create protected equipment zones, in-site and out-of-site;
- Develop severe accident mitigation guidelines (SAMGs) for SFPs ;
- Assure structural integrity of SFPs and structures under beyond design basis (BDB) seismic conditions.

The measures undertaken for SFPs in some OECD member countries are presented in Appendix B.

3 POSSIBLE ACCIDENT SCENARIOS, PAST ACCIDENTS AND PRECURSOR EVENTS

3.1 Operational experience of spent fuel loss of cooling events

Adequate cooling of the spent fuel in the SFP can principally be lost either by malfunction of the pool cooling system or by loss of the pool water inventory. In the following, examples are given of past events for both types. The chosen events are not the most significant ones, but they present different possible scenarios that lead or could lead to loss of spent fuel cooling.

Operational experience feedback

The operational experience feedback (OEF) process is indispensable in prevention of accidents. The fundamental elements of the OEF process are investigation and cause analysis of events or near misses. By determination of causes of events, practically specific actions for preventing recurrence can be easily defined. These experiences, i.e. results of analyses, could be used in other plants too. Therefore, when looking to possible improvements in reducing the radiological impact triggered by undesirable events, it is always advisable to check experience from the past events from different sources.

Losing the cooling of the SFP in a nuclear power plant is an event mostly connected with inability of SFP cooling pumps to operate. This is often caused by loss of electrical supply to pumps. Usually, if the loss of off-site power occurs, manual action is needed to connect back-up electrical supply. If back-up electrical supply is unavailable, the pumps cannot operate and the temperature of the pool will consequentially start to increase. In evaluated recent events, electrical supply became available and cooling continued well before the SFP water reached the maximum allowed temperature.

Selection of events

In this section, examples of events where the cooling of pools or part of their water inventory is lost are described. We can say that no major events occurred, i.e., events with significant consequences related to SFP loss-of-cooling have not happened. However, the described events illustrate different scenarios in which SFP cooling or water level was affected, and in escalated scenarios, it could result in fuel damage. Therefore, the described events are selected such that difference in their nature is emphasized rather than level of significance.

The main sources of event reports used in this short study are the International Atomic Energy Agency (IAEA) International Reporting System for Operating Experience (IRS) [20], the U.S. Nuclear Regulatory Commission (NRC) Generic Communications [21] and Licensee Event Reports (LERs) [22], and the European Clearinghouse on NPP Operational Experience Feedback [23].

3.1.1 Analysis of fuel related events

In 2009, the European Clearinghouse on NPP Operational Experience Feedback [23] performed a study on events reported in the IAEA International Reporting System for Operating Experience [20] related to nuclear fuel. The study, which is presented in [24], found that the main causes of these events are human errors and, to a lesser extent, design deficiencies. Some of these deficiencies originated from the initial design of the SFP, but in some occasions, the design deficiencies derived from a change in the characteristics of the stored fuel (e.g. higher enrichment and burn-up, re-racking).

In the study [24], 28 events have been identified to be related to fuel integrity in storage facilities, mainly in the SFP. According to their nature, they have been classified in events related to Loss of cooling; Loss of margin to criticality; Fuel integrity, and Radiological impact. Figure 9 shows the distribution of the events in storage facilities.

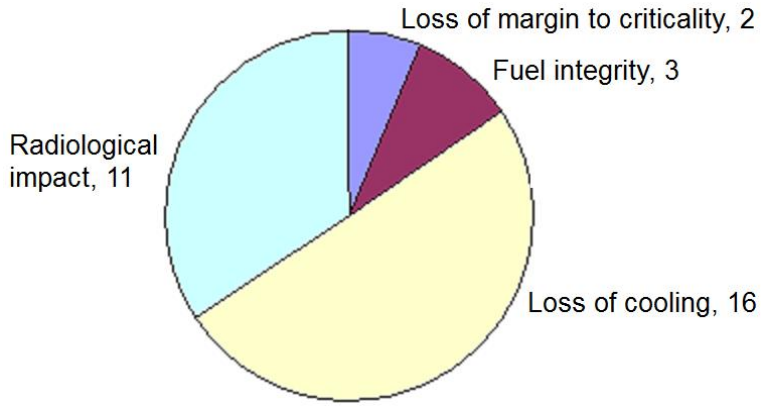

Figure 9: Distribution of IRS events in SFPs [24]. Since events with loss of SFP water level also have radiological impact, four of the 28 reported events are counted twice in the diagram.

Events with a reduction in the margin to criticality and events with fuel integrity concerns are scarce, and their specific causes are erroneous concentrations of boron, incidents with inadequate neutron absorbers in structures, errors in the calculation of the margin to criticality, or failure in the control and monitoring of the SFP water chemistry. Restoring the boron concentration, repairing the neutron absorber in the structures, and correcting the calculations are sufficient to recover the criticality margin.

Events with radiological impact are relatively more frequent, due to the numerous activities and circumstances that could lead to radiological exposure of the workers. It should be noted that radiological exposure in this context does not mean fuel overheating and radioactive release from damaged fuel. The main cause of these events is activities in the SFP building, not carefully planned and analysed to identify all possible sources of radiological exposure (risk analysis).

Events with loss of cooling (including SFP water level drops) are also relatively more frequent, and are caused by the characteristics of the SFP cooling system (interconnections and manual operation), by leakages in the liner, and the lack of monitoring systems so detection of the problem could be delayed. This group of events includes all the events that have originated from any kind of loss of cooling capacity, either cooling system equipment malfunction or loss of coolant (significant drop of the fuel pool water level). It should be remarked that these events are slow, and there is usually enough time to restore the cooling function.

3.1.1.1 Events related to cooling system inoperability

Loss of cooling can be caused by the loss of SFP cooling flow, or because the heat generated in the SFP is not fully transferred to the ultimate heat sink. In the first case, the loss of SFP coolant flow can be due to several reasons, such as loss of electrical power to the cooling pumps, pump failure, flow blockage, loss of suction caused by the loss of water level, or a diversion in the SFP cooling system.

In the second case, loss of heat sink can be due to the lack of enough cooling flow in the heat exchangers, or due to heat loads higher than the system design capacity. The current tend to perform full core off-load a short time after shutdown, as well as the higher fuel burnup, increase the heat loads on the SFP cooling system. Any degradation of the heat removal characteristics, such as heat exchanger fouling, insufficient coolant flow, etc. can result in increased water temperature in the SFP.

3.1.1.2 Events related to loss of SFP water inventory

During a loss-of-water inventory accident, there is considerable potential to uncover the fuel. This would result in radiation fields that would prevent access to the SFP and heat-up of the uncovered fuel assemblies.

The main pathways for loss of SFP coolant inventory are the connected systems, the leakage through temporary gates or seals during refuelling or other activities, and leakage through the SFP liner or structure. Loss of water inventory through connected systems can be caused by a leakage through pumps seals, heat exchanger cracks, failed welds and cracks or breaks in the piping. In general, the drain-down of the SFP would be limited by the actuation of siphon breakers, provided they are correctly designed and not plugged. Loss of water inventory can also occur through temporary gates or seals while the SPF is connected to the reactor cavity for refuelling. Failure of the seals allows a fast, but limited, loss of inventory, except when the configuration of the plant structure is unfavourable.

Loss of water inventory may also occur through failures or leakages of the SFP liner, due to liner defects, severe seismic events or accidents, such as dropping of heavy loads. Past studies in the USA (mainly [25, 26]) have suggested that a large seismic event (beyond the design-basis for the plant) is the largest contributor to SFP risk. Cracking of the SFP liner is highly unlikely: Generic seismically-induced SFP liner failure likelihoods of 2×10^{-6} to 6×10^{-6} per year were predicted in [26], while a range of 2×10^{-7} to 2×10^{-6} was found in [25]. The likelihood of liner failure, leading to fuel uncovery, as a result of a transport cask or heavy load drop into the SFP was estimated to be even lower [25, 26].

Losses of SFP coolant inventory may produce flooding or environmental problems in other areas of the plant, especially if the SFP is located at high elevation. Ventilation and drain systems can transport water and steam to other parts of the plant and affect emergency equipment. Prolonged operation at elevated SFP water temperatures may impair the cleaning capacity of the purification system, and may cause the atmosphere temperature in the storage area to be higher than the limiting temperature assumed in the design of the ventilation systems. If steam is generated, it could also damage the iodine filters in the fuel building or could prevent personnel from entering the SFP hall.

Preventive and corrective actions to avoid SFP loss of cooling or loss of inventory include the careful installation of gates and seals, the monitoring of the SFP water level by adequate and accurate instruments and alarms, adequate procedures and training. The available time to perform human actions is sufficient in events of this kind, except in the case of a full core off-load shortly after shutdown.

3.1.1.3 Causes of loss-of-cooling events

According to analyses reported through IRS for SFP events that happened before 2009, the causes for loss of SFP cooling could be summarised as follows:

- Corrosion of studs on valve;
- Line-up error;
- Insufficient attention to alarms signals;
- Inadequate alarm system design;
- Loss of electrical supply;

- Human error;
- Poor task programming;
- Lack of coordination;
- Alarm failure;
- Deficiencies in procedures;
- Equipment failure (anti-siphon device plugged);
- Deficient equipment design;
- Incorrect system operation;
- Failure of a freeze seal;
- Inadequate management control;
- Inadequate training;
- Inadequate procedures;
- Personnel was unaware of potential seal failure;
- Inadequate task performance;
- Inadequate maintenance;
- Inadequate SFP level monitoring;
- Loss of coolant circulation;
- Inadequate performance of the SFP cooling system;
- Inadequate instrumentation.

Beside the general lessons from these event analyses, some lessons on more specific issues should be emphasized:

- Consistency of planned core off-load evolutions and decay heat removal with the licensing basis must be assured;
- Appropriate reviewing of all relevant procedures associated with core off-loads must be assured;
- The decision making process with respect to responsibility for declaration of limiting conditions for operation (LCO) requires clarification;
- A generic fluid movement guide needs to be prepared to enable a more timely response to this type of incident;
- Sensors/transmitters need to be designed for all types of environment in which they are required to operate;
- Procedures need to be implemented for line-up changes to perform regular recirculation of tanks.

3.1.2 Examples of SFP loss-of-cooling events

Table 3 is a summary of events related to loss of SFP cooling, including incidents with partial loss of pool water inventory. It should be remarked that none of the events resulted in fuel uncovery, fuel damage or fission product release. The events are selected based on differences in their nature, which are not specifically dependent on reactor type. More detailed descriptions of these events, their causes and

consequences can be found in Appendix C. The same appendix also includes summaries of results from two past assessments of the risk for SFP accidents, carried out in the USA and in France.

Table 3: Some past events related to loss of SFP cooling. Details are given in Appendix C.

NPP, type	Event	Cause	Consequences
Kori 1, Korea, PWR	Loss of shutdown cooling due to station blackout during refuelling outage.	Loss of off-site power resulted in loss of SFP cooling.	SFP temperature increased slightly.
Catawba 1, USA, PWR	Dual unit loss of off-site power resulting from inadequate relay modification.	Loss of off-site power resulted in loss of SFP cooling.	Short loss of SFP cooling capability.
Forsmark 3, Sweden, BWR	Emergency diesel generators failed to start after undetected loss of two phases on 400 kV incoming off-site supply.	Loss of two phases on 400 kV off-site power resulted in loss of SFP cooling.	Loss of SFP cooling capability with no increase in SFP temperature.
Almaraz-2, Spain, PWR	Irradiated fuel, both in the vessel and the SFP, without forced cooling during refuelling outage.	Loss of component cooling water system capability.	SFP cooling was lost for 7 hours and temperature increased by 12 K.
Belleville 2, France, PWR	Disruption of the SFP cooling.	Fire in the pump room of one of the two SFP cooling system trains, while the other was out of order.	Simultaneous failure of SFP cooling trains, for 6 hours and then for 15 hours.
SONGS 2, USA, PWR	Inoperable SFP cooling pumps results in loss of safety function.	One SFP cooling pump out of service and the other tripped on overcurrent signal.	SFP temperature increased slightly.
SONGS 2, USA, PWR	Both trains of SFP cooling inoperable results in a loss of safety function.	Salt water cooling system low flow affected component cooling water system.	SFP temperature increased slightly.
Khmelnitski 1, Ukraine, VVER-1000	Drop in the level of the wet refuelling pool and flooding of reactor building areas.	Inappropriate valve maintenance activities caused leak through open joint on one SFP valve.	Significant drop in the level of the wet refuelling pool (1.9 m).
Borssele, The Netherlands, PWR	Insufficient testing of functionality of siphon breaker valve at spent fuel basin.	Lack in inspection program.	None.*
Cattenom 2 and 3, France, PWR	"Siphon breaker" missing on SFP cooling systems pipes.	Injection pipe could extract the water from the pool through a siphon effect.	None.*

* Design/inspection changes were implemented later to prevent uncontrolled drainage of the SFP.

3.1.3 Spent fuel loss-of-cooling events: conclusions

Understanding and analysing past events can significantly help to reduce the number of events with similar consequences in the future. Through the brief evaluation of specific events in Section 3.1.1, it could be concluded that recommendations from some major studies of SFP loss of cooling scenarios [4, 24, 27] remain applicable for all NPPs with spent fuel in wet storage. There are a lot of lessons that can be learned from events, and even if the majority of the plants have not experienced similar problems, it is worth to emphasize some major areas where improvements could be made.

Procedures and training

If any changes, improvements or developments in procedures are required and implemented, dissemination and adaption have to be provided to personnel in parallel. Training departments usually have a key role in this task, and specific training provisions are often necessary for broader scope of needs. Some recommendations regarding procedures and training, derived from lessons from events:

- Create accident procedures dedicated to loss of inventory accidents in refuelling cavity and SFP;
- Integrate operating prescriptions for reduction of the risk of safety injection accumulator tank discharge when reactor building and fuel building pools are full of water and interconnected;
- Assure that planned core off-load evolutions and decay heat removal are consistent with the licensing basis;
- Review SFP test and maintenance procedures in depth;
- Reinforce emergency action level declaration requirements and procedure;
- Procedures need to be implemented for line-up changes to perform regular recirculation of tanks;
- A generic fluid movement guide needs to be prepared to enable a more timely response to SFP loss of coolant events;
- Ensure that all relevant procedures associated with core off-loads have been appropriately reviewed;
- Along with procedural changes and reviews, training to detect and respond to SFP loss-of-inventory and loss-of-cooling events, including those caused by loss of off-site power, is needed and should address configuration controls that can prevent and/or mitigate such events.

Surveillance and maintenance

Many systems and equipment sets have to be available and operable to support safe SFP operation for different stages of SFP normal operation and in all stages during accident propagation, including fuel uncovery. The following surveillance and maintenance recommendations have some of greatest importance for affected plants as well as for other plants in providing the desirable level of reliability:

- Plant features, such as reactor cavity seals, gate seals, or anti-siphon devices need to be thoroughly examined where their failures could potentially cause loss of SFP coolant inventory;
- Reinforce the operating specifications and the preventive maintenance programme for the pool cooling function;
- A formal station process needs to be developed to direct diagnostic testing of medium voltage cable and connectors on a periodic basis and following identified issues with these components;
- Establish a maintenance strategy, which takes into account that, when there is only one train operable of the Chemical and Volume Control System (CVCS), Component Cooling Water System (CCWS) or ESWS, the common pump must be available;
- Improve/develop measures to eliminate shortcomings in the pre- and post-maintenance testing programme of SFP and its supporting equipment;
- Adequateness and quality of the test and maintenance programme of components that are relevant for the safe operation of the NPP should be periodically and thoroughly re-evaluated and enhanced;
- Lock in closed position the interconnections between the Fuel Pool Cooling and Filtering System (FPCS) and the Residual Heat Removal System (RHRS), except when the RHRS back-up by the

Reactor Cavity and Spent Fuel Pit Cooling and Treatment System (PTR) is required operable by the technical specifications;

- Control of the aging of the flexible sleeves should be improved.

Design changes

The following recommendations, to eliminate detected deficiencies, should be incorporated in modification processes of many NPPs:

- Processes associated with modification scope description, specification of critical design inputs, specification of vendor services and oversight, and checker responsibilities should be revised;
- Design change of the siphon breaking device (e.g. enlargement of the diameter of this device) is necessary for some plants to prevent siphon-effect drainage of SFP;
- The steam generator dam should be strengthened;
- Reliable instrumentation is necessary to monitor SFP temperature and level and SFP area radiation, including periods following a loss of off-site power, in order to detect SFP loss-of-inventory events and loss-of-cooling events in a timely manner;
- Accessibility and operability of the emergency means for making up the pool should be ensured in the event of fire or flooding in the rooms located in the fuel storage building;
- Sensors/transmitters must be designed for all types of environment in which they are required to operate;
- Design and modification processes should include systematic assessment of the reliability of the concerned safety related systems;
- Review and possible design changes may be necessary for key equipment for the case of earthquakes.

Human and organisational factors

Human and organisational factors seem more important in recent event evaluations than they were in the past. It became evident that improvements in these areas remarkably contribute to better safety indicators. Consequently, by improving human and organisational factors, efficiency of implementation of other recommendations can increase too. Some recommendations regarding SFP cooling reliability emphasize the importance of the human factors and man-machine interface; organization and implementation of plant modifications and corrective actions; communication and correct use of feedbacks; personnel workload evaluations, and shift team trainings. Furthermore, the need for some reinforcements is determined especially for:

- Regulatory oversight programme in addressing the safety culture;
- Reporting requirements and needs;
- The decision making process with respect to responsibility for declaration of limiting conditions for operation;
- Emergency diesel generator reliability requirements;
- Configuration control and risk management during refuelling outage.

3.2 The Bruce-A Unit 4 fuel transfer incident

On 1983 November, a CANDU 37-element fuel bundle was overheated in steam-air environment in the fuel transfer mechanism of Bruce-A Unit 4 reactor, Canada [28]. This event occurred as part of the fuel

transfer to the SFP, rather than in the SFP itself. This incident shows much of the same phenomenology as would be expected in a CANDU SFP. Its main differences from a CANDU SFP loss of coolant were that:

- it had no neighbouring fuel bundles,
- the temperatures at the end-plates were lower than the temperatures in the rest of the bundle, and
- the decay heat was higher than expected for a bundle in a CANDU SFP.

3.2.1 Description of the event

Bundle G70551W was a standard 37-element Bruce Nuclear Generating Station bundle irradiated to an average burnup of 5.9 MWd/kgU at an average outer element power of 41 kW/m. It was discharged from the reactor as part of normal scheduled fuelling. The bundle was kept in the fuelling machine under heavy water cooling for about 2 hours before discharge to the fuel transfer chamber. Because of problems with other equipment, the bundle was left on the cradle in the flooded fuel transfer chamber for many hours, with the scoop in the up position, covering the bundle. The vent valve was left closed, so injection of air from the instrumentation bubbler formed an air space in the top of the chamber, which slowly uncovered the bundle. After the bundle was uncovered, local boiling would also have occurred, which could have displaced further water from the chamber. The bundle was probably partly uncovered for a total of 5 hours; the vent valve was opened once during the incident, which would have re-flooded the bundle. The incident was terminated when the fuel port seal was opened, submerging the bundle and releasing airborne activity from the chamber.

Sheath oxidation was more rapid at the bearing pad braze heat affected zones. At the central bearing pad plane of the bundle, the sheaths of 22 of the 37 elements (in the upper and central parts of the bundle) were severely oxidized, and in many cases were ballooned and distorted. Hydriding was found in the unoxidized part of some sheaths. The inner elements had degraded into rubble. None of the sheath oxides had a columnar structure, so the bundle temperatures probably did not exceed 1050°C. Melting of a few of the beryllium brazes indicated temperatures above 970°C. Oxidation of the sheath inner walls and of the UO2 was minimal, so the air was probably rapidly deoxygenated by the Zircaloy oxidation. Also, fuel-sheath interaction was not observed.

3.2.2 Oxidation studies on irradiated defected CANDU fuel elements

Some studies were carried out, in which irradiated CANDU fuel elements with 0.8 mm drilled holes were subjected to air at temperatures between 175°C and 900°C. For tests up to 400°C, one hole was drilled near each end of the element, and a set of four holes was drilled near the centre of the element. The elements had reasonable dimensional stability up to 685 hours at 220°C and 230°C, but showed severe sheath splitting after 200 h at 250°C. A diametral increase of 4% was found to cause sheath splitting. A limit of 2% diametral increase was set to avoid sheath splitting. Observations on elements with single drilled holes showed very limited fission product release after 24 h at 400°C, 2 h at 600°C or 2.5 h at 900°C, despite local diametral increases between 5.7% and 50% and severe sheath splitting [29-31].

3.3 The Paks cleaning tank incident

On April 10, 2003, during refuelling outage in the Paks unit 2, Hungary, 30 spent fuel assemblies were being cleaned in a special container in the fuel manipulation pit of the SFP. After completing the cleaning process, the fuel was left in the container with reduced cooling, which resulted later in severe cladding oxidation and fuel damage [32, 33]. Although this incident cannot be considered as a typical SFP accident, it gave insights that can be useful for understanding phenomena related to SFP loss of cooling/coolant accidents. It also prompted research about such accidents. The incident was similar to an SFP loss of cooling/coolant accident with regard to the following:

- the event took place after refuelling;

- the spent fuel assemblies had low decay heat;
- the fuel rods were oxidised in steam atmosphere for several hours;
- ballooning and burst of cladding tubes took place during the heat-up of the fuel;
- the eventual reflooding of the FAs resulted in brittle failure.

On the other hand, the incident was different from an SFP loss of cooling/coolant accident, since:

- it happened inside of a closed tank under a deep water column;
- the hydrogen produced by oxidation accumulated inside of the cleaning tank;
- most of the released activity was absorbed by the SFP water;
- air could not enter the fuel assemblies even in the late phase of the accident.

3.3.1 Description of the event

Decontamination activities applied prior to replacement of steam generator feed water distributors in the Paks (VVER-400) NPP led to the generation of magnetite deposits on the internals and on FAs in reactors 1, 2 and 3. The increase of hydraulic resistance caused by these deposits resulted in hydraulic asymmetries. To reduce these problems, it was decided that every fuel assembly, returned after annual outage or refuelling outage into the reactor, should undergo a chemical cleaning.

The cleaning system consisted of a container installed in a pit for fuel manipulations connected via a lock to the SFP, interconnecting lines, heat exchangers and filter equipment; see Figure 10. This technical system formed an internal closed circuit almost completely submerged into water, except for the heat exchangers and filters that were located on the reactor desk or beside it. The container received 30 assemblies for cleaning at a time, and the cleaning process was performed by circulation for about 35-40 hours. During the annual outage of Paks unit 2, altogether 210 FAs, i.e. assemblies for 7 containers, were scheduled to be cleaned.

The cleaning programme for the sixth batch of FAs loaded into the cleaning tank was completed by 16:55 on April 10. The fuel was not removed from the cleaning tank immediately, since the crane was busy with other tasks. The coolant was circulated by a submergible pump with much lower mass flow rate than used in the cleaning process; see Figure 10. Contracted specialists continuously maintained the cooling of the cleaning tank at 37 °C. At 21:53, activity was detected by the krypton measurement system installed in the cleaning circuit, and at the same time, the 'alarm' level was reached by the noble gas activity concentration monitors in the reactor hall, and then the operational dosimetry systems installed in the ventilation stack indicated abrupt increase of noble gas activity (max. 0.2×10^{13} Bq/10 min). The plant supervisor ordered to terminate the work carried out in the reactor building and to leave the area. An extraordinary maintenance committee was called, in order to evaluate the event and to take necessary actions. As highest priority, it was decided to open the cleaning tank, to carry out visual inspection, and if possible, to separate the nonhermetic FA and also to analyse the water quality.

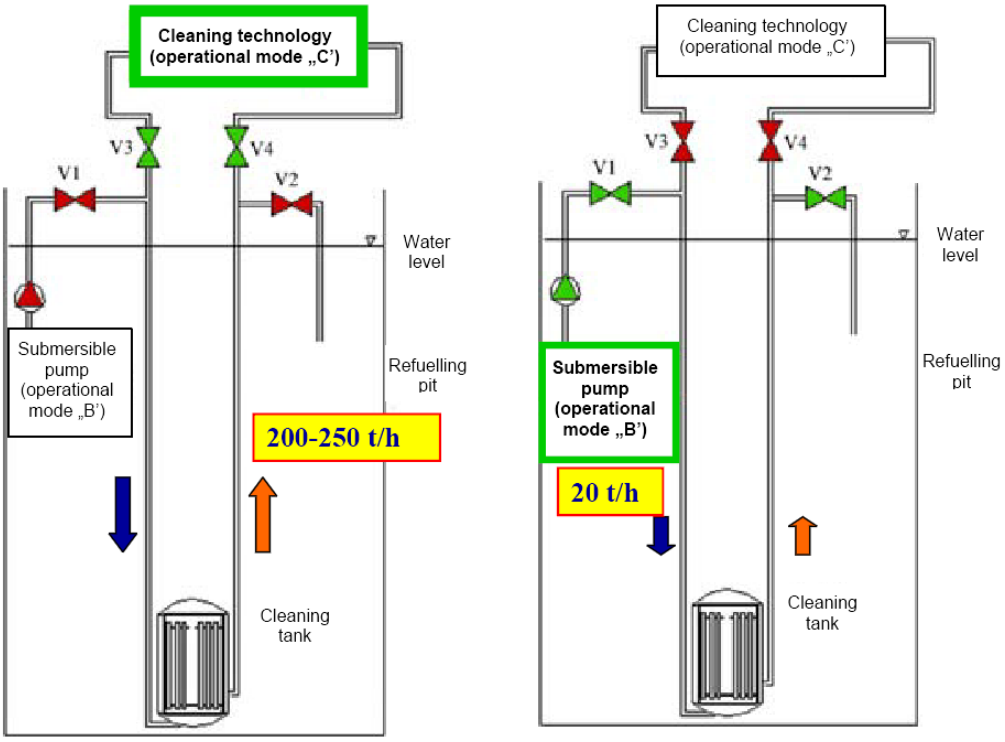

Figure 10: Arrangement of the cleaning tank cooling during cleaning (left) and post-cleaning (right) [32].

The cleaning tank head was unlocked by a contractor at 02:15, April 11. Immediately after this, an activity increase was observed in the dosimetry control and monitoring system (Figure 11) and, at the same time, the water level in the SFP lowered by approximately 7 cm. The first results of water chemistry analysis identified the fission products ^{134}Cs, ^{137}Cs, ^{131}I, ^{132}I, ^{133}Xe and ^{85}Kr in the samples at activity level of 10^4-10^7 Bq/kg. Activity of less volatile species was also detected in the water samples [34]. During the cleaning tank head removal operation, one of the three cables of the lifting tackle broke, thus the head removal failed. The head was lifted on April 16, 2003, and the inspection was performed with video camera. The damage of the fuel assemblies was seen to be more severe than assumed before.

Later inspection has revealed that, due to the special design of the cleaning tank and the characteristics of the fuel assemblies, the cooling by the submersible pump of lower mass flow was insufficient. The low flow rate pump was not capable of removing the decay heat (241 kW) due to a by-pass effect. The temperature stratification blocked the flow, and therefore, the coolant temperature reached saturation temperature in the upper part of the cleaning tank. Then, the steam-formation pushed the main volume of the coolant out of the cleaning tank vessel. This way, the FAs were left without proper cooling for hours and heated up to above 1000 °C, which resulted in severe damage and oxidation of the FAs. Oxidation in high temperature steam and hydrogen uptake resulted in embrittlement of the fuel assembly shrouds and the fuel rod cladding. When opening the cleaning tank, the injection of cold coolant caused the breaking up of the embrittled shrouds and fuel rod cladding.

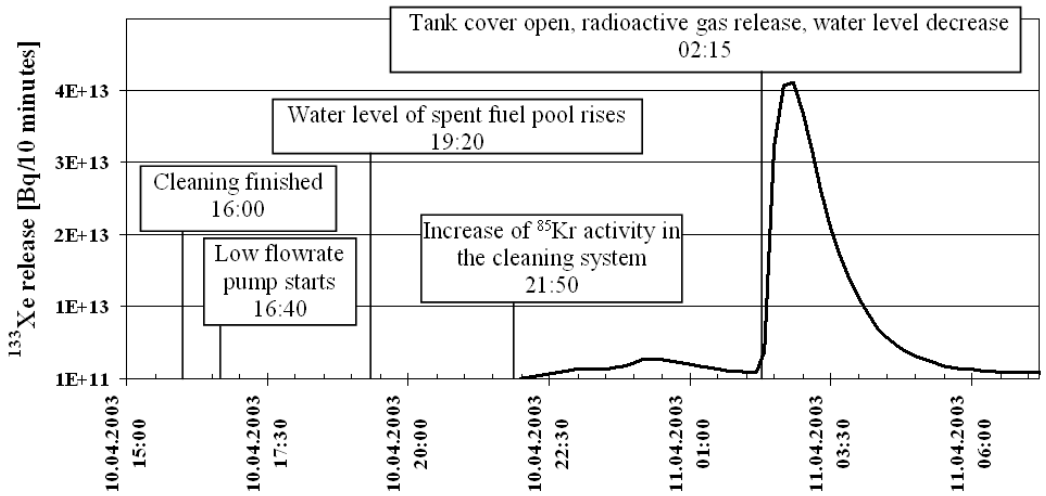

Figure 11: The course of the incident in time [35].

Video examination indicated that most of the fuel assemblies suffered damage. Brittle failure and fragmentation of FAs were observed. Above the upper plate, several assembly heads were broken, standing in inclined position. One assembly header was found far from its original place. Many FAs were broken and fragmented also below the upper plate, and some assemblies were fractured in their entirety. Fuel rod fragments and shroud pieces accumulated on the lower plate between the FAs. Many fuel rod pieces and fragments of assembly shroud were dispersed within the tank. Some fuel pellets fell out of fuel rods, their form remained mainly intact. Heavy oxidation of the zirconium components was identified. Less oxidation was found in the periphery than in the centre, and the bottom part of the fuel remain intact. The radioactive noble gases that escaped from the damaged FAs were released into the environment through the reactor hall stack with negligible impact on the environment. Most of the non-gaseous fission products were trapped by the large water mass of the pool, and removed by the water purification system [34]. The personal exposure doses were not higher than the internal or regulatory limits. After the incident, the damaged fuel was removed from the cleaning tank and encapsulated in containers, which are stored in special positions of the SFP. The damaged fuel will be reprocessed.

3.3.2 The IAEA mission

In June 2003, a group of examiners mandated by the IAEA visited the Paks NPP in accordance with the Hungarian government's wish, in order to help reveal objectively the causes of the incident. The investigation of the group pointed out that the main reason for the incident was the insufficiency of the cleaning tank cooling system and, among others, revealed several cleaning system design deficiencies [36, 37].

The group recommended several correcting measures for both the power plant and the Hungarian regulator. Among other things, they made suggestions connected with licensing of new technologies and methods, improvement of the safety culture, education of the staff, development of emergency plans and feedback of operational experiences. A strong recommendation was that the safety of an important operating activity should not be given to a contractor without the supervision of the operator. The international examiner group also proposed to strengthen the communication between the operator and the regulator [37].

3.3.3 The OECD-IAEA Paks Fuel Project

The OECD-IAEA Paks Fuel Project aimed to support the understanding of fuel behaviour in accident conditions on the basis of analyses of the Paks incident. Computer simulations of the most relevant aspects of the event and comparisons of the calculated results with the available information were carried out between 2006 and 2007. A database was collected to provide input data for the calculations. The activities of the project covered analyses of thermal-hydraulics, fuel behaviour and the release of fission products [32]:

- The thermal-hydraulic calculations described the cooling conditions possibly established during the incident (applied computer codes: MELCOR, RELAP5, ATHLET, APROS, CFX, ATHLET-CD, ICARE/CATHARE and ASTEC);
- The simulations of fuel behaviour described the oxidation and degradation mechanisms of FAs (applied codes: MELCOR, ATHLET-CD, ASTEC, FRAPTRAN, FRAPT6, TRANSURANUS and FRAPCON);
- The release of fission products from the failed fuel rods was estimated and compared to available measured data (application of MELCOR, ATHLET-CD and hand calculations with simple models).

Despite the use of the common input database and harmonization of some important input parameters, significant differences were observed between results obtained by different codes and different users. This can be explained, on one hand, by differences in the computational models available in the different codes and, on the other hand, by variance of modelling approaches used by the participants for the description of the cleaning tank (e.g. nodalization scheme) and the boundary conditions of the incident (e.g. heat losses to the surrounding water pool). The applied computer codes could not reproduce all the phenomena of the Paks incident. Probably the most important effect not considered by the codes was the hydrogen uptake by zirconium and its effect on the degradation of mechanical properties and loss of fuel integrity.

Nevertheless, important phenomena that were predicted well in the computer simulations included: the water level in the cleaning tank and surrounding pools; the timing of fuel failures, and the rate of released activity from the fuel. The activity release calculations were limited to the release from fuel and did not include transport of radioactive isotopes in the spent fuel storage pool or in the reactor hall. The two main computer codes for activity release calculations were MELCOR and ATHLET-CD; see Appendix D. For the volatile fission product groups, iodine releases were slightly underestimated, while caesium was slightly overestimated. Tellurium release was predicted well, and even for the less volatile fission products, such as cerium, the calculated results showed reasonable agreement with the measured data.

The numerical analyses improved the understanding of the Paks incident and helped to make more precise some parameters of the incident, such as:

- the by-pass flow at low flow rate amounted to 75-90 % of the inlet flow rate, which led to the formation of a steam volume;
- the maximum temperature in the tank was between 1200 and 1400 ºC;
- the degree of zirconium oxidation reached 4-12 %;
- the mass of produced hydrogen was between 3 and 13 kg.

The OECD-IAEA Paks Fuel Project improved the current knowledge on fuel behaviour under accident conditions, and led to recommendations for some further actions for research in this area.

4 BEHAVIOUR OF SPENT FUEL FACILITIES DURING THE FUKUSHIMA DAIICHI ACCIDENT

The Great East Japan Earthquake took place on 11 March 2011, and the resulting tsunami caused loss of emergency diesel powered AC generators and produced conditions known as station blackout (SBO) at the Fukushima Daiichi Nuclear Power Station (NPS). As results of the SBO, the emergency cooling systems and water supply systems failed and the three Units 1 to 3 subsequently suffered severe core damage.

Following the loss of all AC power at Units 1 to 5, the SFP cooling flow was lost in the Unit 1 to Unit 4 SFPs, while the Unit 6 air-cooled emergency diesel generator survived the tsunami and was used to maintain cooling and water supply for the Unit 5 and Unit 6 SFPs [38]. With no pool cooling to remove decay heat at the Unit 1 to Unit 4 SFPs, emergency water injection was conducted by using a helicopter, a concrete pump truck, a fire truck, and the make-up water condensate (MUWC) or SFP cooling and clean-up system line. Eventually, pool water cooling by the alternative cooling system was started at Unit 1 to Unit 6 SFPs, and the water temperature has then been maintained below 40 °C, which is a typical SFP temperature. Video inspections reveal that the fuel racks appear to be intact, and water analyses indicate that fuel damage in the pools is unlikely. Hence, there is no evidence that the fuel in the pools was damaged.

In this section, an overview of the Fukushima Daiichi accident, as well as a chronology of the situation at the SFPs are presented, based on information provided by the licensee Tokyo Electric Power Company (TEPCO).

4.1 Outline of the Fukushima Daiichi nuclear power station

4.1.1 Units 1 to 6

The Fukushima Daiichi Nuclear Power Station has six boiling-water reactors of General Electric design. Units 1 to 4 are located at the southern part of the station, and Units 5 and 6 are located at the northern part of the station, as shown in Figure 12 [39]. The common pool is located behind Units 3 and 4, and the dry cask storage facility is located between Units 1 and 5 along the coast. Units 1 to 5 employ Mark-I containment and Unit 6 employs Mark-II. A generic cross-section of a BWR/4 with a Mark-I containment is shown in Figure 13 [40]. When the disaster occurred on 11 March 2011, Units 1 to 3 were in operation, Unit 4 was defueled for maintenance, and Units 5 and 6 were in a state of cold shutdown for maintenance. Table 4 summarizes the status of the Fukushima Daiichi NPS as of March 11, 2011 [38].

Table 4: Status of the Fukushima Daiichi NPS as of March 11, 2011 [38].

		Unit 1	Unit 2	Unit 3	Unit 4	Unit 5	Unit 6
Status of Units		*Operated at rated ouput*			*Shutdown for maintenance*		
Electric output (10,000kW)		*46.0*	*78.4*				*110.0*
Reactor type		*BWR3*	*BWR4*				*BWR5*
Containment vessel type		*Mark-I*					*Mark-II*
Commissioning		*1971*	*1974*	*1976*	*1978*	*1978*	*1979*
Number of FAs in a core	*UO_2 fuel*	*400*	*548*	*516*	*0*	*548*	*764*
	MOX fuel	*0*	*0*	*32*	*0*	*0*	*0*

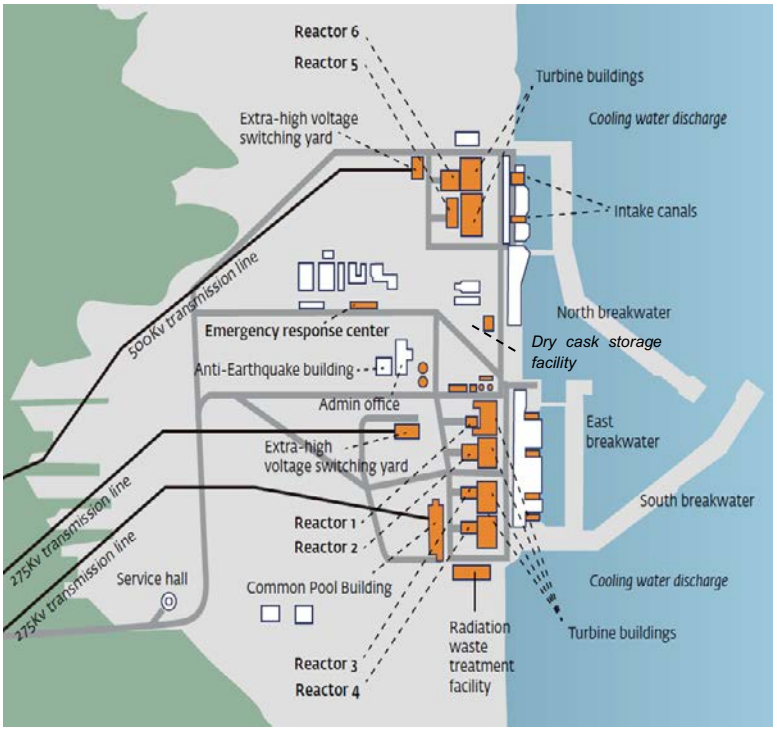

Figure 12: Layout of the Fukushima Daiichi NPS [39].

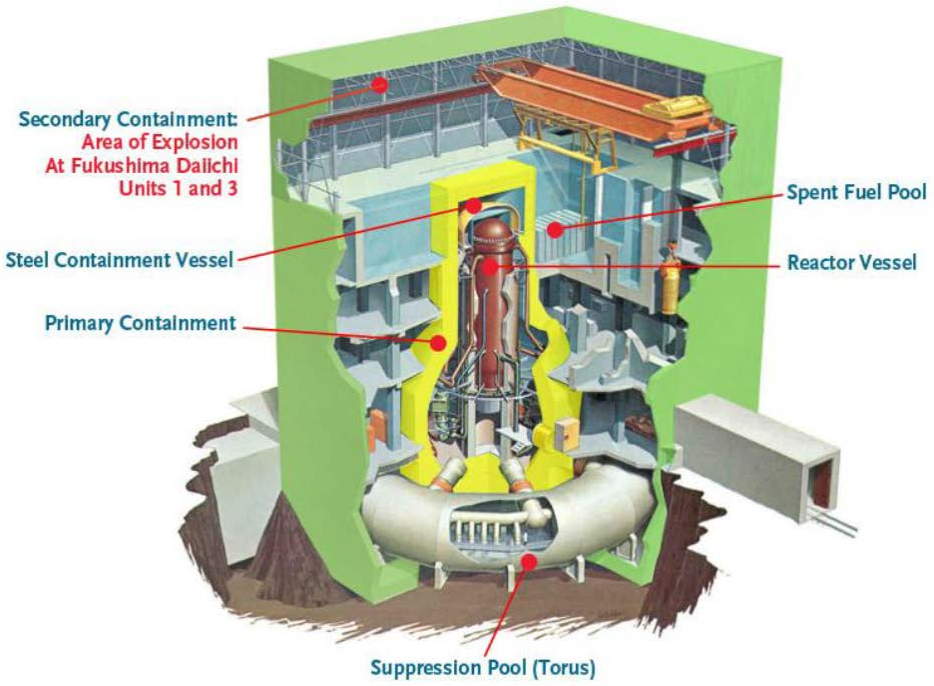

Figure 13: Generic cross-section of a BWR/4 with a Mark-I containment [40].

4.1.2 Spent fuel pools

The SFP at each unit is located in the secondary containment, as shown in Figure 13. A typical BWR SFP is rectangular in cross section and about 12 m deep; see Appendix A. The pool walls are constructed of reinforced concrete, and a stainless steel liner is attached to the inside walls with studs embedded in the concrete. The inside geometric dimensions of the Fukushima Daiichi SFPs are shown in Table 5. The fuel assemblies are stored in SFPs at each unit, in a common SFP, and in on-site dry cask storage. The storage status of fuel assemblies as of March 11 is summarized in Table 5 [38]. The predicted decay heats from fuel stored in the SFPs of Unit 1 to Unit 4 are shown versus elapsed time from the accident in Figure 14.

Unit 1 to Unit 6 SFPs have the fuel pool cooling and clean-up system. As an auxiliary cooling system, Unit 1 SFP has the shutdown cooling system (SHC), and Unit 2 to Unit 6 SFPs have the residual heat removal system. For accident management, the make-up water condensate system, which has a make-up water storage tank, is connected to the SHC line in the Unit 1 SFP and to the RHR line in Unit 2 to Unit 6 SFPs. The common pool has an FPCS with air cooling. The cooling system diagrams of SFPs are shown in Figure 15 [41].

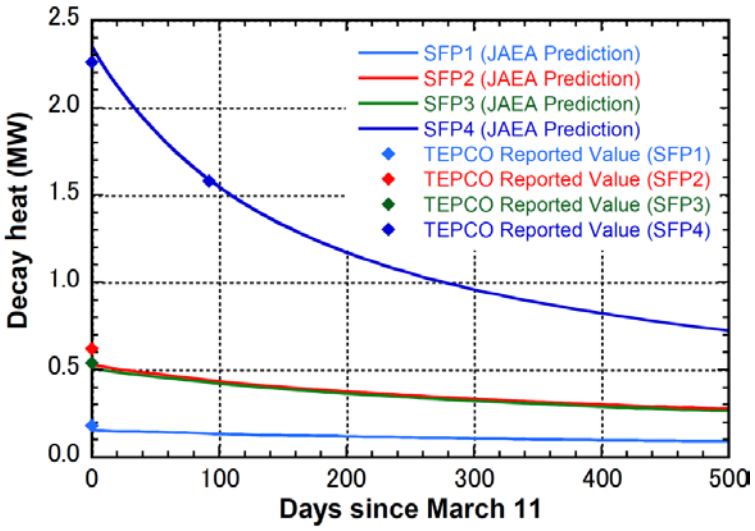

Figure 14: Predicted decay heats in SFPs of Unit 1 to Unit 4 [42, 43].

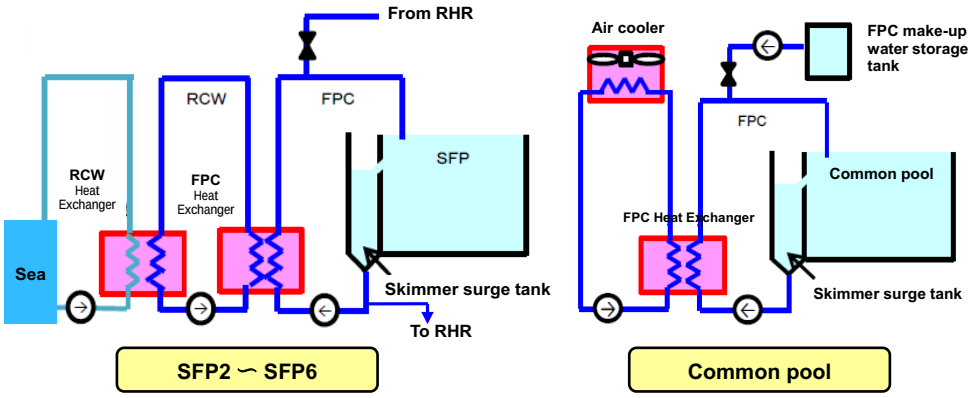

Figure 15: Cooling system diagrams of SFPs [41].

Table 5: Storage status of fuel assemblies at the Fukushima Daiichi NPS as of March 11, 2011 [38].

		SFP 1 (Unit 1)	SFP 2 (Unit 2)	SFP 3 (Unit 3)	SFP 4 (Unit 4)	SFP 5 (Unit 5)	SFP 6 (Unit 6)	Common pool	Dry cask storage
Reactor type		BWR3	BWR4				BWR5		
Containment vessel type		Mark-I					Mark-II		
Number of fuel assemblies in SFP and at dry cask facility	Spent Fuel	292	587	514	1331	946	876	6375	408
	Fresh fuel	100	28	52	204	48	64	0	0
	Total number	392	615	566	1535	994	940	6375	408
	Storage capacity	900	1240	1220	1590	1590	1770	6840	–
Storage rack type	Aluminum	○	○	○	–	–	–	–	
	Boron-borated aluminum	○	○	○	–	–	–	–	
	Stainless steel	–	–	–	○	○	○	○	
Decay heat (MW) as of March 11, 2011		0.18	0.62	0.54	2.26	1.01	0.87	1.03	–
Geometric dimension of pool	Length (m)	7.16	9.906			9.91	10.368	12.2	
	Width (m)	12.04	12.192			12.2	12.192	29	
	Depth (m)	11.8	11.912			11.81	11.811	11.5	
	Volume (m^3)	1017	1439			1428	1493	4069	
	Water volume (m^3)	990	1390				ca. 1450	ca. 4000	

4.2 Overview of the Fukushima Daiichi accident

On March 11, 2011, Units 1 to 3 were in operation and Units 4 to 6 were shut down for maintenance at the Fukushima Daiichi NPS. At 14:46, due to the earthquake, the operating reactors were automatically shut down. Also, all the off-site power supply was lost due to the earthquake. However, electric power necessary to maintain reactor cooling was kept with the emergency diesel generators.

The first of a series of tsunamis produced by the earthquake arrived at the site at 15:27. Around 15:35, a peak of wave exceeding 14 metres caused flooding of many cooling seawater pumps, EDGs and power panels. It caused station blackout of Units 1 to 5, and all of the cooling functions using AC power were lost in these units. All DC power was lost at Units 1, 2 and 4, while some DC power from batteries remained available at Unit 3, but it eventually exhausted. Two of the three EDGs at Unit 6 were inoperable after the tsunami. One air-cooled EDG at Unit 6 continued to function and supplied electric power to Unit 6, and later Unit 5, to maintain cooling to the reactor and SFP. Table 6 summarizes the damage situation of power supply and SFP cooling system caused by the earthquake and resulting tsunami [38, 40].

With no core cooling to remove decay heat, core damage began at Unit 1 on the day of the event. Steam-driven injection pumps were used to provide cooling water to the reactors at Units 2 and 3, but these pumps eventually stopped working, and all cooling water to the reactors was lost. As a result of inadequate core cooling, fuel damage also occurred in Units 2 and 3.

Hydrogen generated from the damaged fuel in the reactors accumulated in the reactor buildings, either during venting operations or from other leaks, and ignited, producing explosions in the Unit 1 and Unit 3 reactor buildings. The hydrogen generated in Unit 3 may have migrated into the Unit 4 reactor building, resulting in a subsequent explosion and damage. The loss of primary and secondary containment integrity resulted in ground-level releases of radioactive material. Figure 16 shows the view of the reactor buildings following the explosions [38].

Table 6: Damage situation of power supply and SFP cooling systems after the earthquake (upper part) and after the resulting tsunami (lower part) [38, 40].

			Unit 1	Unit 2	Unit 3	Unit 4	Unit 5	Unit 6
Before the Earthquake	Status of Units		Operated at rated output			Shutdown for maintenance		
After the Earthquake	Scram		Succeed	Succeed	Succeed	—		
	Power	DC power	◎	◎	◎	◎	◎	◎
		EDG A	◎	◎	◎	◎	◎	◎
		EDG B	◎	◎	◎	◎	◎	◎
		HPCS EDG			—			◎
	Cooling system	RHR(A)	—	○ → ◎	○	—	○	○
		RHR(B)		○	○	○	○	○
		IC	○ → ◎			—		
		RCIC	—	○ → ◎	○	—	—	—
		MUWC	◎	◎	◎	◎	◎	◎
		SFP cooling (FPC)	◎ → △	◎ → △	◎ → △	◎ → △	◎ → △	◎ → △
		SFP cooling (RHR)	—	○	○	◎ → ○	○	○
		SFP cooling (SHC)	○			—		
After the Tsunami	Power	DC power	×	×	◎ → ×	×	◎	◎
		EDG A	×	×	×	×	×	×
		EDG B	×	×	×	×	×	◎
		HPCS EDG			—			×
	Cooling system	RHR(A)	—	×	×	—	×	×
		RHR(B)		×	×	×	×	× → ◎
		IC	×			—		
		RCIC	—	◎ → ×	◎ → ×	—	—	—
		MUWC	×	×	×	×	× → ◎	◎
		SFP cooling (FPC)	×	×	×	×	×	×
		SFP cooling (RHR)	—	×	×	×	× → ◎	× → ◎
		SFP cooling (SHC)	×			—		

Power supply

◎ : Operated or In operation ○ : Standby △ : Stopped due to loss of off-site power supply × : Failed — : No application or Under inspection

Figure 16: View of the reactor buildings following the explosions [38].

Following the loss of all AC power at Units 1 to 5, the SFP cooling flow was lost in the Unit 1 to Unit 4 SFPs, while the Unit 6 air-cooled EDG survived the tsunami and was used to maintain cooling and water supply for the Unit 5 and Unit 6 SFPs. With no pool cooling to remove decay heat at the Unit 1 to Unit 4 SFPs, emergency water injection was conducted by using a helicopter, a concrete pump truck, a fire truck,

and the FPC line. Eventually, pool water cooling by the alternative cooling system was started at the Unit 1 to Unit 6 SFPs, and the water temperature stabilized between 30 and 40 °C. A typical alternative cooling system of Unit 3 SFP is shown in Figure 17 [38]. Video inspections of the Unit 3 and Unit 4 SFPs show that the fuel racks appear to be intact, and water analyses of SFP 1 to 4 indicate that fuel damage in the pools is unlikely. Hence, there is no evidence that the fuel in the pools was damaged.

The general sequence of events (with the timelines for the units ordered by time of major events) is shown graphically in Figure 18 [38, 39, 44]. It illustrates the coincidence of parallel accident progressions, including emergency actions taken in the SFPs, such as water supply from MUWC or FPC line, water spray via helicopter, fire truck, and concrete pump truck, and eventual pool cooling using alternative cooling system.

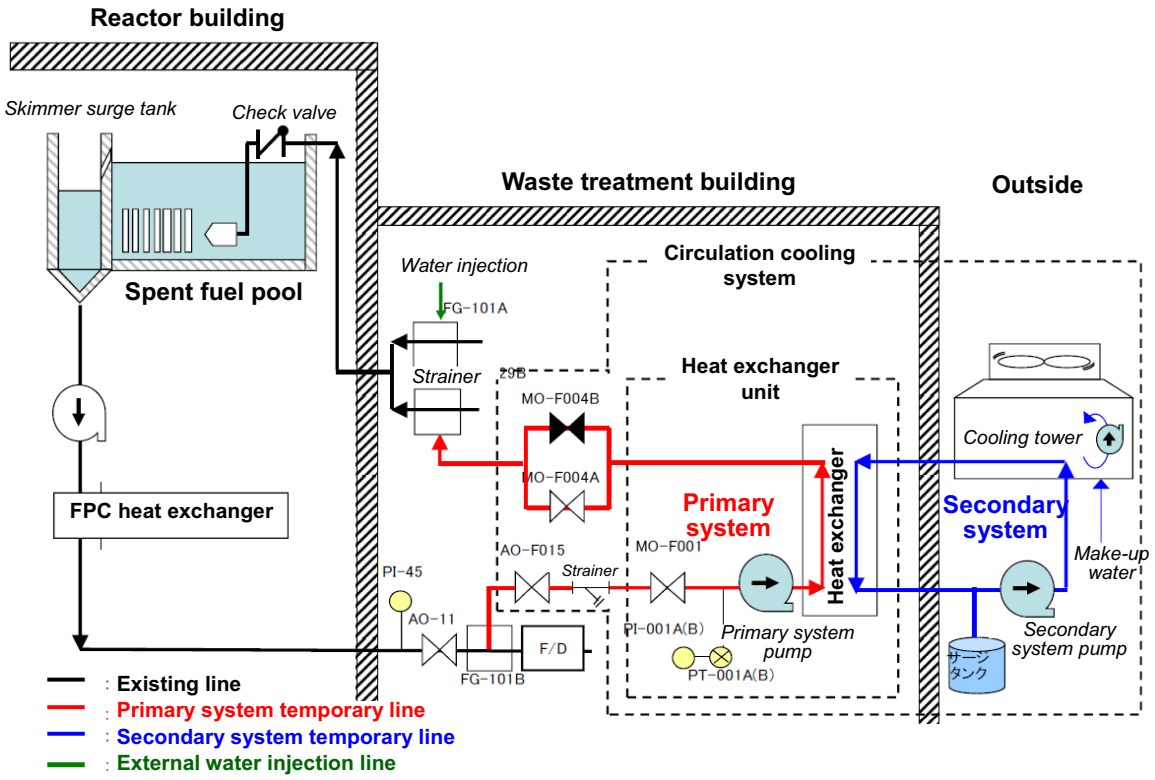

Figure 17: Alternative cooling system diagram of the Unit 3 SFP [38].

Figure 18: Major event sequences at the Fukushima Daiichi NPS and SFPs (continued on next page) [38, 39, 44].

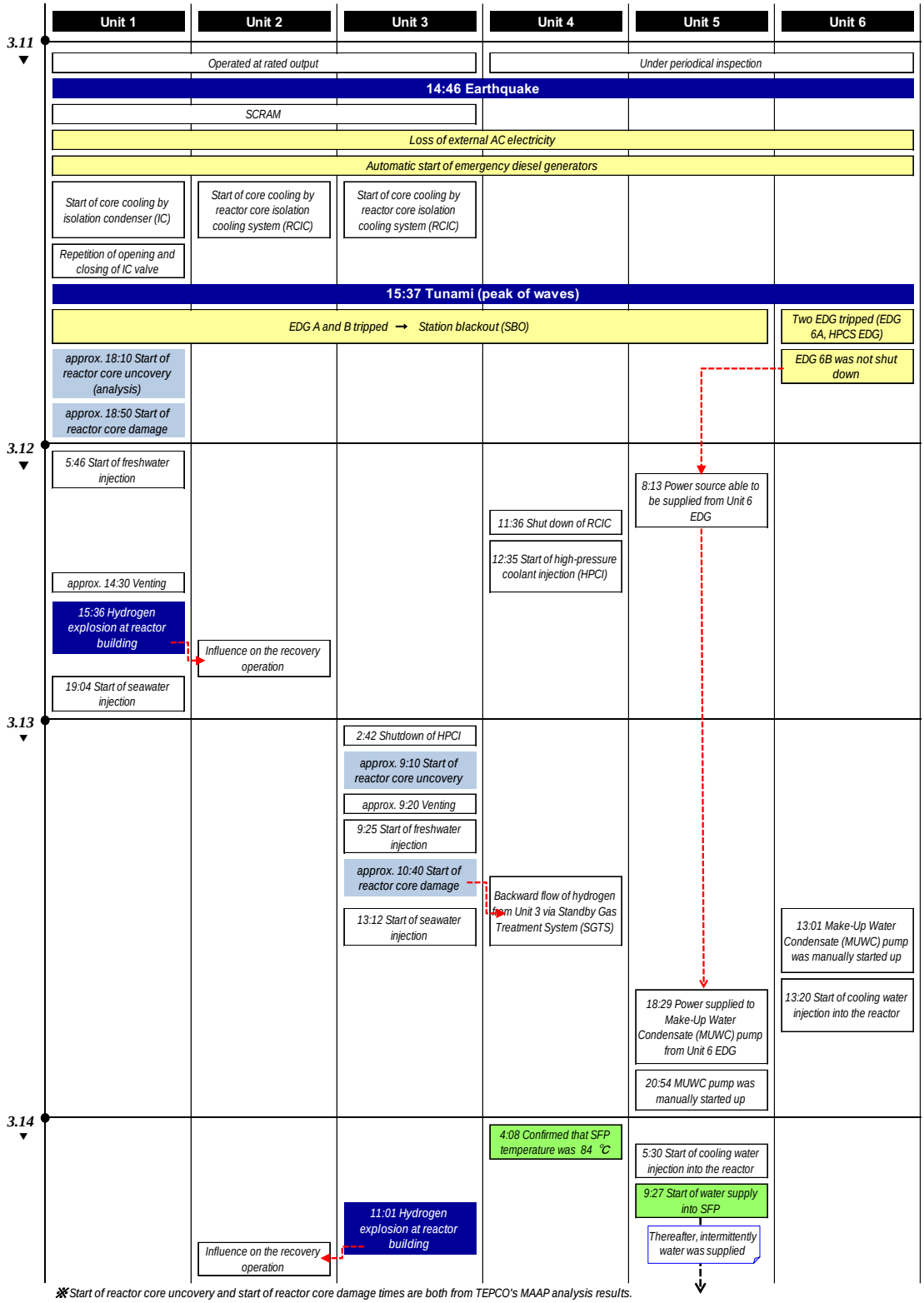

※Start of reactor core uncovery and start of reactor core damage times are both from TEPCO's MAAP analysis results.

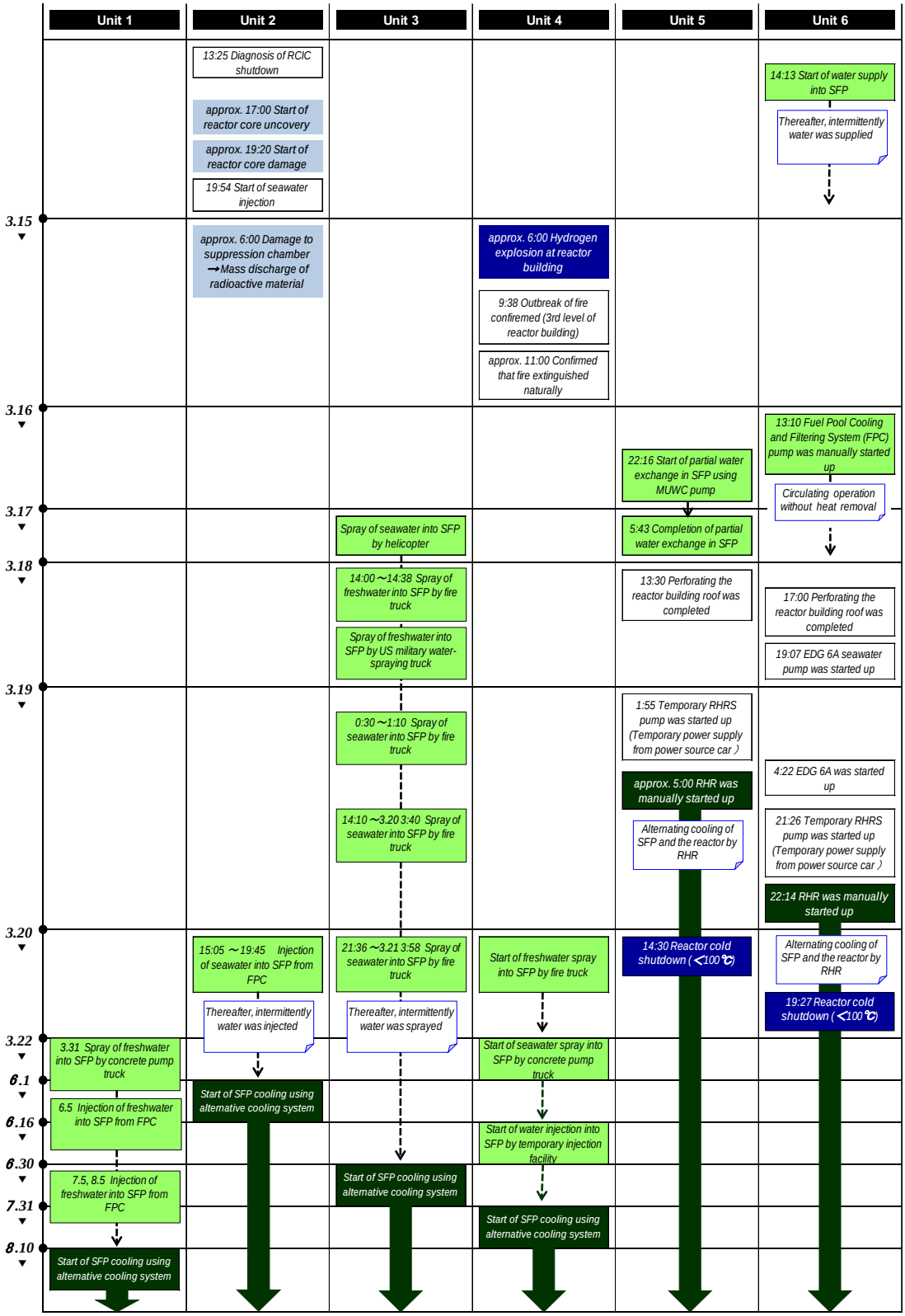
Unit 1
Unit 2
Unit 3
Unit 4
Unit 5
Unit 6
13:25 Diagnosis of RCIC shutdown
approx. 17:00 Start of reactor core uncovery
approx. 19:20 Start of reactor core damage
19:54 Start of seawater injection
14:13 Start of water supply into SFP
Thereafter, intermittently water was supplied
3.15
approx. 6:00 Damage to suppression chamber →Mass discharge of radioactive material
approx. 6:00 Hydrogen explosion at reactor building
9:38 Outbreak of fire confiremed (3rd level of reactor building)
approx. 11:00 Confirmed that fire extinguished naturally
3.16
13:10 Fuel Pool Cooling and Filtering System (FPC) pump was manually started up
22:16 Start of partial water exchange in SFP using MUWC pump
Circulating operation without heat removal
3.17
Spray of seawater into SFP by helicopter
5:43 Completion of partial water exchange in SFP
3.18
14:00～14:38 Spray of freshwater into SFP by fire truck
Spray of freshwater into SFP by US military water-spraying truck
13:30 Perforating the reactor building roof was completed
17:00 Perforating the reactor building roof was completed
19:07 EDG 6A seawater pump was started up
3.19
0:30～1:10 Spray of seawater into SFP by fire truck
14:10～3.20 3:40 Spray of seawater into SFP by fire truck
1:55 Temporary RHRS pump was started up (Temporary power supply from power source car)
approx. 5:00 RHR was manually started up
Alternating cooling of SFP and the reactor by RHR
4:22 EDG 6A was started up
21:26 Temporary RHRS pump was started up (Temporary power supply from power source car)
22:14 RHR was manually started up
3.20
15:05 ～19:45 Injection of seawater into SFP from FPC
Thereafter, intermittently water was injected
21:36～3.21 3:58 Spray of seawater into SFP by fire truck
Thereafter, intermittently water was sprayed
Start of freshwater spray into SFP by fire truck
14:30 Reactor cold shutdown (＜100℃)
Alternating cooling of SFP and the reactor by RHR
19:27 Reactor cold shutdown (＜100℃)
3.22
3.31 Spray of freshwater into SFP by concrete pump truck
Start of seawater spray into SFP by concrete pump truck
6.1
Start of SFP cooling using alternative cooling system
6.16
6.5 Injection of freshwater into SFP from FPC
Start of water injection into SFP by temporary injection facility
6.30
7.5, 8.5 Injection of freshwater into SFP from FPC
Start of SFP cooling using alternative cooling system
7.31
Start of SFP cooling using alternative cooling system
8.10
Start of SFP cooling using alternative cooling system

4.3 Chronology and situation of spent fuel pools and dry cask storage

4.3.1 Unit 1 spent fuel pool (SFP 1)

Around 15:35 on 11 March, the SFP 1 lost all AC power when emergency diesel generators stopped functioning as the seawater pumps and power panels were flooded by the tsunami. The cooling and water supply for the SFP likewise failed. At 15:36 on 12 March, the reactor building (R/B) was damaged by a hydrogen explosion, and the ceiling and debris dropped on the upper part of the pool [45].

On 31 March, fresh water was sprayed into the pool by a concrete pump truck, and sprayed again on 20 and 22 May. On 28 May, water injection from the FPC piping into the pool was tested, and full-scale injection was started on the following day. In consequence, the skimmer surge tank level increased, and it was confirmed that the pool was filled with water. Water injection was conducted about once a month to compensate for the evaporation and keep the water level of the pool until an alternative cooling system was introduced. By 5 August, approximately 578 tons of water had been injected to the pool, as shown in Table 7 [38].

On August 10, pool water cooling by the alternative cooling system was started. The water temperature was about 47 °C (at the inlet of the alternative cooling system) when the cooling was started. The water temperature reached a steady condition on 27 August, where the water temperature stabilized at about 30 °C.

Table 7: Amount of water sprayed and injected to the SFP 1 [38].

Date	Amount (t)	Measures	Injection efficiency (-)
3/31	90	Concrete pump truck	0.7
5/20	60	Concrete pump truck	0.7
5/22	90	Concrete pump truck	0.7
5/28	5	FPC	1
5/29	168	FPC	1
6/5	15	FPC	1
7/5	75	FPC	1
8/5	75	FPC	1
Total amount : approx. 578 (t)			

Table 8: Results of water analysis on the SFP 1 [38]

Detected nuclide	Half-life	Concentration (Bq/cm^3)			
		Sampled on 6/22	Sampled on 8/19	(Reference) Unit 1 SFP on 2/11	(Reference) Unit 1 T/B basement on 3/26
Cs-134	2 years	1.2×10^{4}	1.8×10^{4}	Lower than detection limit	1.2×10^{5}
Cs-137	30 years	1.4×10^{4}	2.3×10^{4}	0.078	1.3×10^{5}
I-131	8 days	68	Lower than detection limit	Lower than detection limit	1.5×10^{5}

Overflow water from the pool to the skimmer surge tank was sampled on 22 June and 19 August, and nuclide analysis of the water was conducted. Analysis results are shown in Table 8 [38]. Analysis results are as follows:

- The concentration of caesium in the pool water was about one order of magnitude lower than that of the stagnant water in the building basement. In addition, iodine-131, which is a short-half-life radionuclide (8 days), was detected. It exists very little in the spent fuel stored for a long time.
- Analysis results indicated that detected radioactive nuclides in the pool were likely to have been generated in the reactor during the accident, and that fuel damage in the pool was unlikely.

The water level and water temperature in the SFP 1, as estimated by TEPCO, are shown in Figure 19 [38]. In the evaluation, the water level is assumed to have been reduced once by 13 March, due to the influence of sloshing during the earthquake and the explosion. Then, it is estimated that the water level was maintained until the water temperature reached 70 °C, which is assumed as an evaporation starting temperature, and after that, reduced by evaporation. The water level recovered by water injections on 31 March and water injections by FPC piping in late May. It was confirmed that the SFP water level was at full capacity by an increase in the skimmer surge tank level on 28 May and 5 June.

Eventually, the alternative cooling system was started on 10 August, and the pool water has been cooled down. From the estimation, it can be determined that the water level in the SFP 1 was maintained and there was no exposure of the fuel.

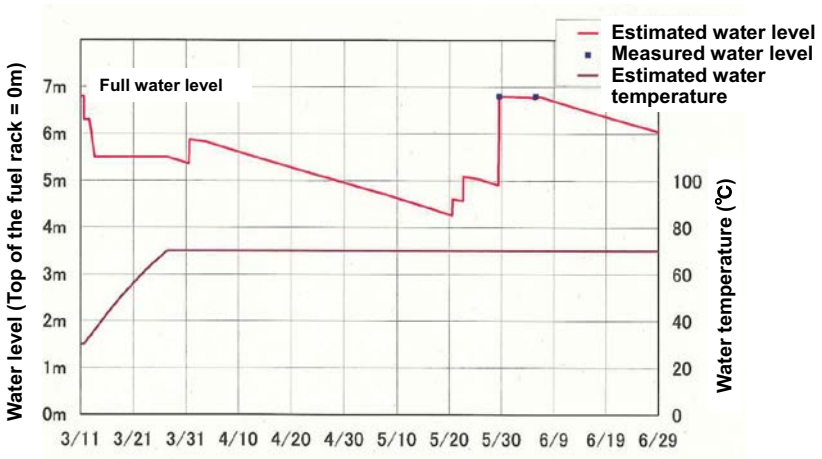

Figure 19: Water level and water temperature in the SFP 1, estimated by TEPCO [38].

4.3.2 Unit 2 spent fuel pool (SFP 2)

Around 15:35 on 11 March, the SFP 2 lost all AC power when EDGs stopped functioning as the seawater pumps and power panels were flooded by the tsunami. The cooling and water supply for the SFP likewise failed. On 20 March, seawater injection from the FPC piping into the pool was started. On 22 March, the skimmer surge tank level increased, and it was confirmed that the pool was filled with water. On 29 March, the water source was switched from seawater to fresh water. By 25 March, about 88 tons of seawater had been injected.

Since then, fresh water injection from the FPC piping was continued until an alternative cooling system was introduced. By 1 June, approximately 1,122 tons of water had been injected to the pool, as

shown in Table 9 [38]. On 31 May, pool water cooling by the alternative cooling system was started. The pool water temperature was about 70 °C when the cooling was started. The water temperature reached a steady condition on 5 June, where the water temperature stabilized at about 30 °C.

Overflow water from the pool to the skimmer surge tank was sampled on 16 April and 19 August, and nuclide analysis of the water was conducted. Analysis results are shown in Table 10 [38]. Analysis results indicated that detected radioactive nuclides in the pool were likely to have been generated in the reactor during the accident, and that fuel damage in the pool was unlikely.

Table 9: Amount of water injected to the SFP 2 [38].

Date	Amount (t)	Measures	Injection efficiency (-)
3/20	40*	FPC	1
3/22	18*	FPC	1
3/25	30*	FPC	1
3/29	15～30	FPC	1
3/30	＜20	FPC	1
4/1	70	FPC	1
4/4	70	FPC	1
4/7	36	FPC	1
4/10	60	FPC	1
4/13	60	FPC	1
4/16	45	FPC	1
4/19	47	FPC	1
4/22	50	FPC	1
4/25	38	FPC	1
4/28	43	FPC	1
5/2	55	FPC	1
5/6	58	FPC	1
5/10	56	FPC	1
5/14	56	FPC	1
5/18	53	FPC	1
5/22	56	FPC	1
5/26	53	FPC	1
5/30	53	FPC	1
6/1	25	FPC	1
Total amount : approx. 1122 (t)			

＊ : Seawater

Table 10: Results of water analysis on the SFP 2 [38].

Detected nuclide	Half-life	Concentration (Bq/cm^3)			
		Sampled on 4/16	Sampled on 8/19	(Reference) Unit 2 SFP on 2/10	(Reference) Unit 2 T/B basement on 3/27
Cs-134	2 years	1.6×10^5	1.1×10^5	Lower than detection limit	3.1×10^6
Cs-137	30 years	1.5×10^5	1.1×10^5	0.28	3.0×10^6
I-131	8 days	4.1×10^3	Lower than detection limit	Lower than detection limit	1.3×10^7

The water level and water temperature in the SFP 2, evaluated by TEPCO, are shown in Figure 20 [38]. In the estimation, the water level is assumed to have been reduced due to the influence of sloshing during the earthquake. Although the water level reduced due to the evaporation once the evaporation started, it recovered every time water was injected. The water level is considered to be maintained at near full capacity by repeated reduction and recover due to evaporation and water injection.

As the Unit 2 R/B was not significantly damaged, water was injected intermittently from the FPC system. The full capacity of the pool was confirmed when the skimmer surge tank level increased. Figure 20 shows a series of points when the skimmer surge tank level increased. Figure 20 shows that the estimated values are in good agreement with the actually measured values of the pool water levels. The estimated values are lower than the measured values (full capacity) during the middle and the end of March, because the influence of sloshing at an early phase is estimated larger than the actual value.

The water temperature gauge in the SFP 2 was available, and the water temperature was measured regularly. The measurements are shown in Figure 20, which indicates the repetition of the trend that the water temperature increased to around 70 °C immediately after water injection, and then decreased to around 50 °C within 1 to 2 days. This trend is caused by the fact that the temperature gauge indicated the atmosphere temperature when it was exposed to the atmosphere due to the drop of the pool water level below the gauge.

Since the alternate cooling system started on 31 May, the pool water has been cooled down as shown in Figure 20, and the water temperature has been kept at about 30 °C. From the results of estimations by TEPCO, it can be determined that the water level of the SFP 2 was maintained, and that there was no exposure of the fuel.

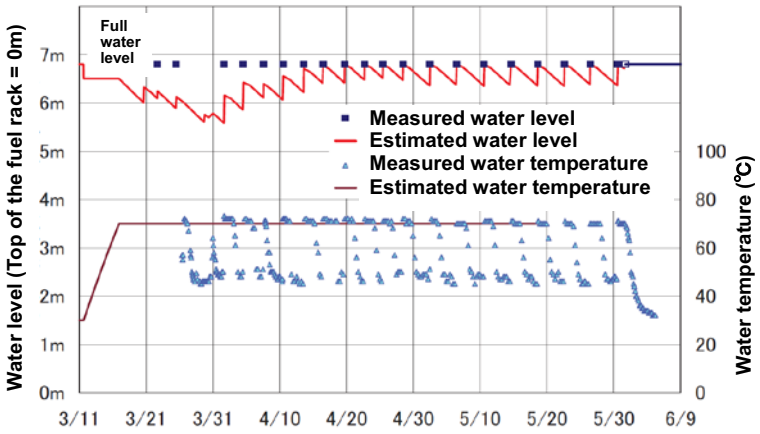

Figure 20: Water level and water temperature in the SFP 2, estimated by TEPCO [38].

4.3.3 Unit 3 spent fuel pool (SFP 3)

Around 15:35 on 11 March, the SFP 3 lost all AC power when EDGs stopped functioning as the seawater pumps and power panels were flooded by the tsunami. The cooling and water supply for the SFP likewise failed. At 11:01 on 14 March, the reactor building was damaged by a hydrogen explosion, and a large amount of debris dropped on the upper part of the pool.

Around 9:48 on 17 March, seawater was sprayed to the pool by a helicopter. Around 19:05 on 17 March, a water-spraying truck began spraying seawater into the pool, and by 25 March, mostly seawater was sprayed to the pool by a water-spraying truck and a fire truck. On 23 and 24 March, seawater injection from the FPC piping was attempted. However, the pump's discharge pressure was higher than expected, and it was judged that practically no water was injected into the pool due to blocking in the FPC line. On 27 March, a concrete pump truck began spraying seawater into the pool, and on 29 March, the water source was switched from seawater to fresh water. By 22 April, about 815 tons of water had been sprayed to the pool by a concrete pump truck.

On 12 April, the concrete pump truck equipped with a camera was introduced, and the water level of the pool was checked from camera pictures. As a result, the Unit 3 SFP was confirmed to be full for the first time. On 22 April, water injection from the FPC piping after removing a strainer was tested, and full-scale injection into the pool was started on 26 April. By 29 June, about 824.5 tons of water had been injected to the pool. The total amount of water sprayed and injected to the pool was approximately 6167.5 tons, as shown in Table 11 [38]. On 30 June, pool water cooling by the alternative cooling system was started. The pool water temperature was then about 62 °C. The water temperature reached a steady condition on 7 July, where the water temperature stabilized at about 30 °C.

Table 11: Amount of water sprayed and injected to the SFP 3 [38]

Date	Amount (t)	Measures	Injection efficiency (-)
3/17	30*	Helicopter	0.1
3/17	44*	Water-spraying truck	0.1
3/17	30	Water-spraying truck	0.1
3/18	42	Water-spraying truck	0.1
3/19	2490*	Fire truck	0.1
3/20	1137*	Fire truck	0.1
3/22	150*	Fire truck	0.1
3/23	35*	FPC	1
3/24	120*	FPC	1
3/25	450*	Fire truck	0.1
3/27	100*	Concrete pump truck	0.95
3/29	100	Concrete pump truck	0.95
3/31	105	Concrete pump truck	0.95
4/2	75	Concrete pump truck	0.95
4/4	70	Concrete pump truck	0.95
4/7	70	Concrete pump truck	0.95
4/8	75	Concrete pump truck	0.95
4/10	80	Concrete pump truck	0.95
4/12	35	Concrete pump truck	0.95
4/14	25	Concrete pump truck	0.95
4/18	30	Concrete pump truck	0.95
4/22	50	Concrete pump truck	0.95
4/26	47.5	FPC	1
5/8	60	FPC	1
5/9	80	FPC	1
5/16	106	FPC	1
5/24	100	FPC	1
5/28	50	FPC	1
6/1	40	FPC	1
6/5	60	FPC	1
6/9	55	FPC	1
6/13	42	FPC	1
6/17	49	FPC	1
6/26	45 with boron	FPC	1
6/27	60 with boron	FPC	1
6/29	30	FPC	1
Total amount : approx. 6167.5 (t)			

* : Seawater

Table 12: Results of water analysis on the SFP 3 [38].

Detected nuclide	Half-life	Concentration (Bq/cm^3)				
		Sampled on 5/8	Sampled on 7/7	Sampled on 8/19	(Reference) Unit 3 SFP on 3/2	(Reference) Unit 3 T/B basement on 4/22
Cs-134	2 years	1.4×10^5	94,000	74,000	Lower than detection limit	1.5×10^6
Cs-136	13 days	1.6×10^3	Lower than detection limit	Lower than detection limit	Lower than detection limit	4.4×10^4
Cs-137	30 years	1.5×10^5	110,000	87,000	Lower than detection limit	1.6×10^6
I-131	8 days	1.1×10^4	Lower than detection limit	Lower than detection limit	Lower than detection limit	6.6×10^5

The water level and water temperature in the SFP 3, as estimated by TEPCO, are shown in Figure 21 [38]. In the estimation, the water level is assumed to have been reduced by about 2 m by 13 March, due to the influence of sloshing during the earthquake and the explosion. However, the water level was recovered by the intensive water spraying started after 17 March, as shown in Table 11, and was maintained at near the full capacity, since the water injection was conducted on a regular basis (except for the period between the end of April and the beginning of May, when water injection was not performed due to a failure of the pump truck).

The water level has been measured based on the images recorded by the camera mounted on the pump truck since the middle of April, and the measurements have been in good agreement with the estimated values as shown in Figure 21 [38]. The water level is considered to be maintained at near full capacity by repeated reduction and recover due to evaporation and water injection. The only record of the water temperature was approximately 60 °C as shown in Figure 21, which was taken from the water sampled at the surface of the pool. Therefore, it is considered to be lower than the average pool water temperature.

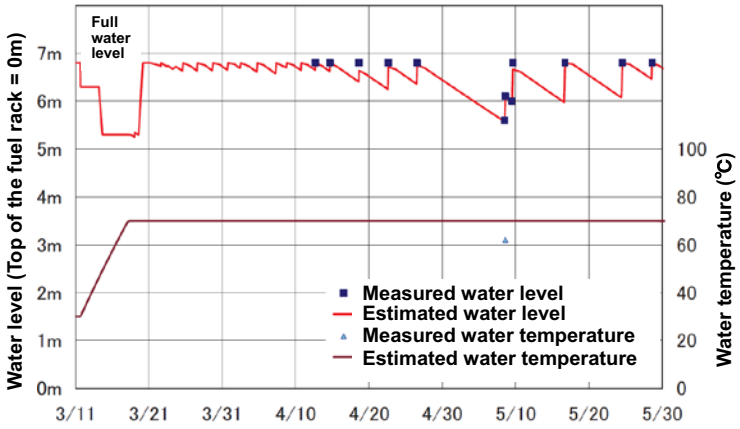

Figure 21: Water level and water temperature in the SFP 3, estimated by TEPCO [38].

Water was sampled using the concrete pump truck on 8 May. Overflow water from the pool to the skimmer surge tank was sampled on 7 July and 19 August, and nuclide analysis of the water was conducted. Analysis results are shown in Table 12 [38]. Analysis results indicated that detected radioactive nuclides in the pool were likely to have been generated in the reactor during the accident, and that fuel damage in the pool was unlikely.

On 8 May, underwater conditions in the SFP 3 were video-recorded during water sampling. Figure 22 shows some photographs taken in the pool. The conditions of the fuel could not be assessed, due to a large amount of debris dropped on the upper part of the pool, as shown in Figure 22 [46].

Figure 22: Underwater conditions in the SFP 3, video recorded on May 8, 2011 [46].

On 14 to 18 February 2013, underwater conditions in the SFP 3 were video-recorded again after removing the debris dropped on the upper part of the pool. Figure 23 shows some photographs taken in the pool [47]. From the photographs, it was confirmed that various type and size of debris had dropped into the pool and piled up on the racks. However, the fuel elements seemed to be still contained in the racks, and it was confirmed that significant fuel damage had not occurred in the pool.

Figure 23: Underwater conditions in the SFP 3, video recorded on February 14 to 18, 2013 [47].

4.3.4 Unit 4 spent fuel pool (SFP 4)

Around 15:35 on 11 March, the SFP 4 lost all AC power when EDGs stopped functioning as the seawater pumps and power panels were flooded by the tsunami. The cooling and water supply for the SFP likewise failed. Around 6:00 on 15 March, the reactor building was damaged by a hydrogen explosion, and a large amount of debris dropped into the pool. On 16 March, a helicopter flew close to the operating floor of Unit 4, at which time the water surface of the pool could be seen, but no exposed fuel was observed.

On 20 March, fresh water was sprayed into the pool by a water-spraying truck. By 21 March, about 250 tons of water had been sprayed into the pool from the ground. On 22 March, a concrete pump truck began spraying seawater into the pool, and by 14 June, approximately 5,700 tons of water had been added to the pool as a result (fresh water spraying had been continued after 30 March).

On 16 June, water injection by a temporary SFP injection facility was started, and by 31 July, about 280 tons of water had been injected by this facility. On 19 June, water injection from the in-core monitor (ICM) piping to the reactor well and dryer and separator (DS) pit was performed to reduce the level of

radiation coming from the in-core structure stored inside of the DS pit. The total amount of water sprayed and injected to the pool was approximately 6,242 tons, as shown in Table 13 [38].

On 31 July, pool water cooling by the alternative cooling system was started. The pool water temperature was around 75 °C when the cooling was started and reached a steady condition on 3 August when the water temperature stabilized at about 40 °C.

A detailed study on the SFP 4 was performed at Oak Ridge National Laboratory (ORNL). The study is reported in [48], where detailed design characteristics of SFP 4 and its decay heat load are described. In SFP 4, all of the fuel assemblies are stored vertically in 53 fuel storage racks, as shown in Figure 24 [48]. The number in each numbered box denotes the cooling time in years for the stored fuel assembly. The red boxes are those fuel assemblies recently off-loaded from the core; the gray boxes are the fresh assemblies. Table 14 summarizes the assembly design and the decay heat for each fuel type, based on its cooling time.

Table 13: Amount of water sprayed and injected to the SFP 4 [38].

Date	Amount (t)	Measures	Injection efficiency (-)
3/20	160	Water-spraying truck	0.1
3/21	92.2	Water-spraying truck	0.1
3/22	150*	Concrete pump truck	0.7
3/23	125*	Concrete pump truck	0.7
3/24	150*	Concrete pump truck	0.7
3/25	21*	FPC	0.7
3/25	150*	Concrete pump truck	0.7
3/27	125*	Concrete pump truck	0.7
3/30	140	Concrete pump truck	0.7
4/1	180	Concrete pump truck	0.7
4/3	180	Concrete pump truck	0.7
4/5	20	Concrete pump truck	0.7
4/7	38	Concrete pump truck	0.7
4/9	90	Concrete pump truck	0.7
4/13	195	Concrete pump truck	0.7
4/15	140	Concrete pump truck	0.7
4/17	140	Concrete pump truck	0.7
4/19	40	Concrete pump truck	0.7
4/20	100	Concrete pump truck	0.7
4/21	140	Concrete pump truck	0.7
4/22	200	Concrete pump truck	0.95
4/23	140	Concrete pump truck	0.95
4/24	165	Concrete pump truck	0.95
4/25	210	Concrete pump truck	0.95
4/26	130	Concrete pump truck	0.95
4/27	85	Concrete pump truck	0.95
5/5	270	Concrete pump truck	0.95
5/6	180	Concrete pump truck	0.95
5/7	120	Concrete pump truck	0.95
5/9	100	Concrete pump truck	0.95
5/11	120	Concrete pump truck	0.95
5/13	100	Concrete pump truck	0.95
5/15	140	Concrete pump truck	0.95
5/17	120	Concrete pump truck	0.95
5/19	100	Concrete pump truck	0.95
5/21	130	Concrete pump truck	0.95
5/23	100	Concrete pump truck	0.95
5/25	121	Concrete pump truck	0.95
5/27	100	Concrete pump truck	0.95
5/28	60	Concrete pump truck	0.95
6/3	210	Concrete pump truck	0.95
6/4	180	Concrete pump truck	0.95
6/6	90	Concrete pump truck	0.95
6/8	120	Concrete pump truck	0.95
6/13	150	Concrete pump truck	0.95
6/14	150	Concrete pump truck	0.95
6/16	75	Temporary water spraying system	1
6/18	99		1
6/22	56		1
6/29	7		1
6/30	13		1
7/31	25		1
Total amount : approx. 6242 (t)			

∗ : Seawater

Table 14: Fuel inventory and decay heat in SFP 4 [48]. Copyright 2012 by the American Nuclear Society, La Grange Park, IL, USA.

Fuel Type	Assembly Configuration	Number of Fuel Assemblies	Discharge Data	Cooling Duration as of March 11, 2011 (yr)	Average Assembly Decay Heat as of March 11, 2011 (W)
7 × 7RD	7 × 7	1	September 26, 1980	30.5	186.2
8 × 8	8 × 8	4	September 2, 1986	24.5	209.1
8 × 8BJ	8 × 8	2	February 26, 1995	16	250.3
		6	April 21, 1996	14.9	257.3
		10	March 19, 1999	12	278.2
		12	May 17, 2000	10.8	288.9
STEP2	8 × 8	16	March 19, 1999	12	278.2
		92	May 17, 2000	10.8	288.9
		132	October 2, 2001	9.4	304.6
		88	September 16, 2002	8.5	318.5
		78	June 25, 2005	5.7	393.6
		4	October 2, 2006	4.4	472.5
		101	February 11, 2007	4.1	506.6
		49	March 28, 2008	3	676.9
STEP3-B	9 × 9	1	October 2, 2006	4.4	472.5
		87	March 28, 2008	3	676.9
		100	September 29, 2009	1.5	1267
		548	November 30, 2010	0.3	3416
STEP3-B Fresh Fuel	9 × 9	204			0

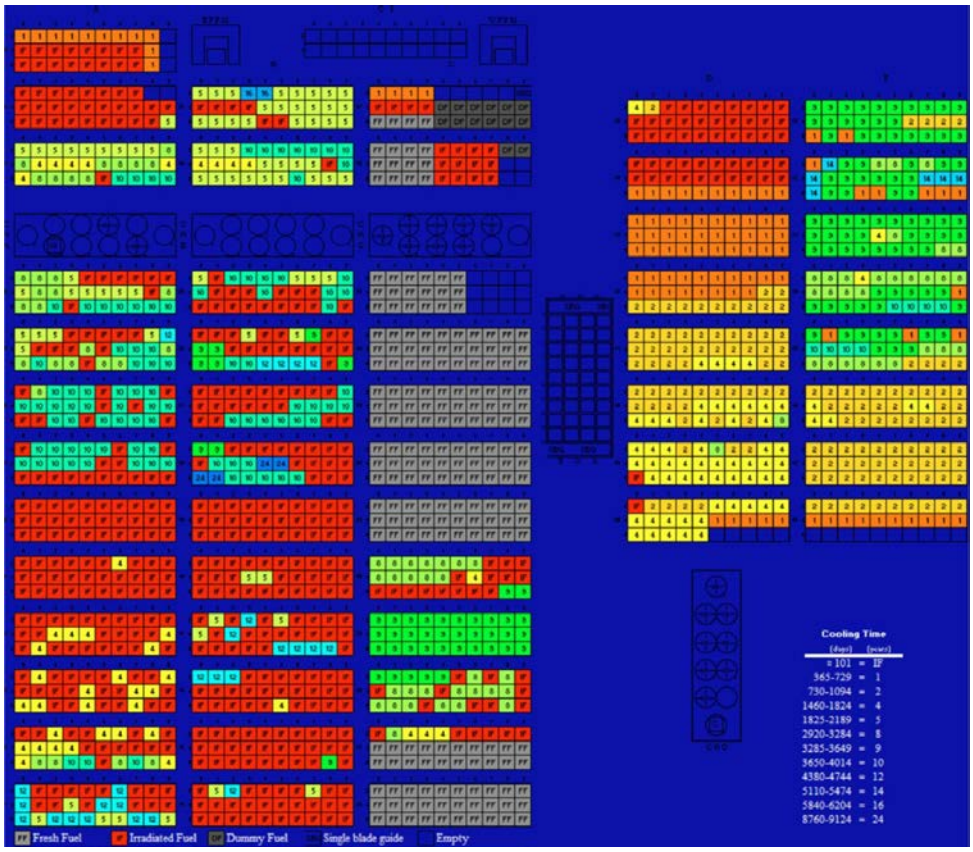

Figure 24: Fuel loading in SFP 4 [48]. See text for explanations. Copyright 2012 by the American Nuclear Society, La Grange Park, IL, USA.

When the disaster occurred on 11 March 2011, Unit 4 was defueled for maintenance. As part of the maintenance, the core shroud was due to be replaced, which necessitates a temporary drain of the reactor vessel and reactor well. According to the original schedule, the drain should have been completed by 7 March 2011, but the operations were delayed and the reactor well was still filled with water on March 11 [45]. This situation played an important role during the course of the accident and significantly slowed the decrease of the SFP 4 water level: the water-tightness of the pool gate was lost due to the pressure from the reactor well side as the SFP water level became low [34]. It induced a water inflow from the reactor well to the pool as illustrated in Figure 26.

At first, the water inflow from the reactor well was not considered and it was estimated that the fuel would be uncovered by late March. Therefore, from 20 March, water was added via helicopter, fire truck, and concrete pump truck. Eventually, the water level reduced to 1.5 m above the top of the fuel racks as the amount of evaporation was larger than the water injection, including water inflow from the reactor well, until around 20 April, as shown in Figure 25 [38].

The water level and water temperature in the SFP 4, as estimated by TEPCO, are shown in Figure 25. The assumptions made in the estimation are as follows:

- The water level is assumed to have been reduced by 1.5 m as a result of sloshing by the earthquake and the explosion.
- Inflow from the reactor well occurred before 22 April (see illustration in Figure 26). The water level was calculated by considering the water in the pool and the reactor well and dryer and separator pit collectively. After 22 April, the pool gate was closed, and no inflow from the reactor well was considered.

Later, intensive water injection conducted between 22 and 27 April (see Table 13) succeeded in recovering the water level to the full capacity. The water injection was then suspended until 5 May to study the trend of the reducing water level. Subsequently, the water level recovered again to full capacity by intensive water injection, and then the water level is considered to be maintained at near full capacity by repeated reduction and recover due to evaporation and water injection.

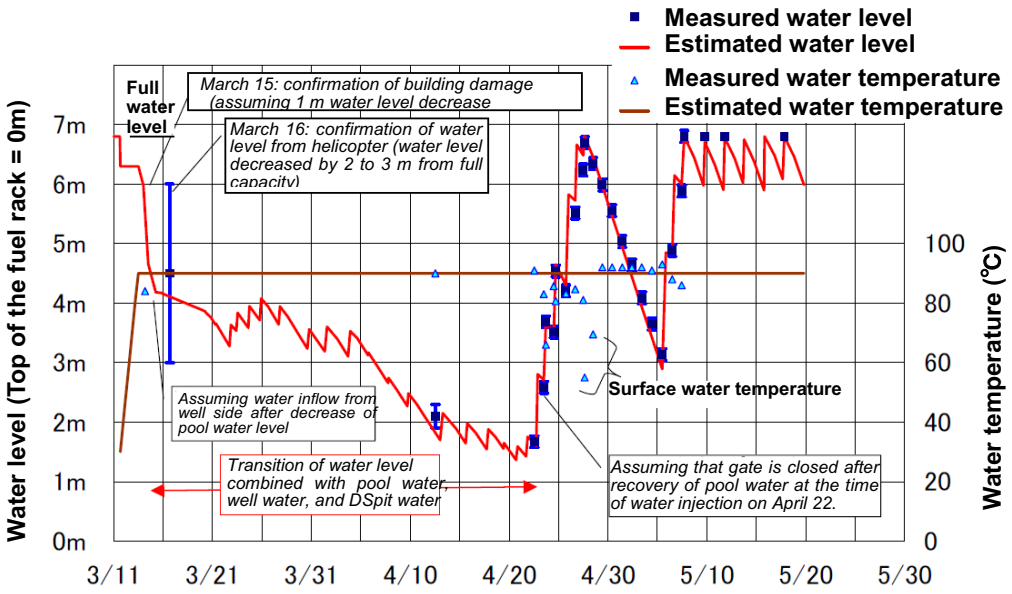

Figure 25: Water level and temperature in the SFP 4, estimated by TEPCO [38].

Since the middle of April, a thermocouple has been installed on the boom of the concrete pump truck for frequent measurements of the water level. The measured values are generally in good agreement with the estimated values, as shown in Figure 25. The water temperature was measured with the aforementioned thermocouple. Most of the measured temperatures were around 90 °C, as shown in Figure 25. This is rather high compared to the measurements at the SFP 2, which were around 70 °C. This is due to the relatively high decay heat associated with fuel in the SFP 4 (all fuel had been removed from the Unit 4 reactor pressure vessel in December 2010).

Water was sampled using the concrete pump truck on 12 April, and 7 May. Overflow water from the pool to the skimmer surge tank was sampled on 20 August, and nuclide analysis of the water was conducted. Analysis results are shown in Table 15 [38]. Analysis results indicated that the concentration of caesium in the pool was about three orders of magnitude lower than that of the water in the Unit 1 to 3 SFP, and detected iodine-131 in the pool was likely to be released from Unit 1 to 3 during the accident. The results indicated that fuel damage in the pool was unlikely.

On 7 May, underwater conditions in the pool were video-recorded during water sampling. Figure 27 shows some photographs taken in the pool [49]. From the photographs, it was confirmed that various type and size of debris dropped into the pool and piled up on the racks. However, the fuel elements seemed to be still contained in the racks, and it was confirmed that significant fuel damage had not occurred in the pool.

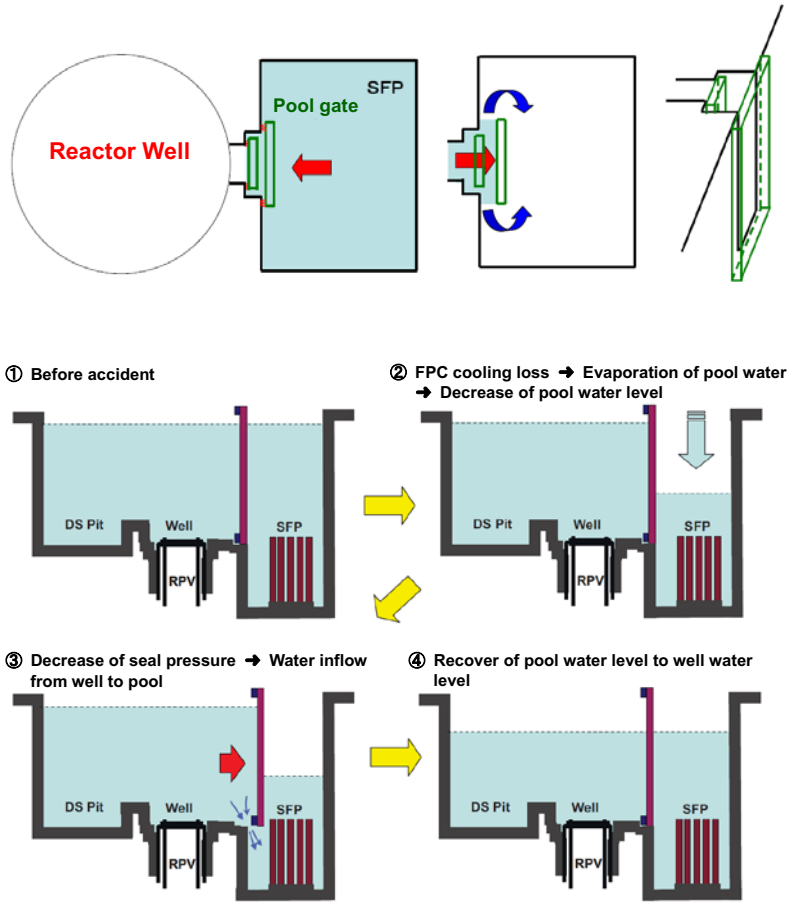

Figure 26: Water inflow mechanism from the reactor well to the SFP through a pool gate [38].

Table 15: Results of water analysis on the SFP 4 [38].

Detected nuclide	*Half-life*	*Concentration (Bq/cm^3)*					
		Sampled on 4/12	*Sampled on 4/28*	*Sampled on 5/7*	*Sampled on 8/20*	*(Reference) Unit 4 SFP on 3/4*	*(Reference) Unit41 T/B basement on 3/24*
Cs-134	*2 years*	*88*	*49*	*56*	*44*	*Lower than detection limit*	*31*
Cs-137	*30 years*	*93*	*55*	*67*	*61*	*0.13*	*32*
I-131	*8 days*	*220*	*27*	*16*	*Lower than detection limit*	*Lower than detection limit*	*360*

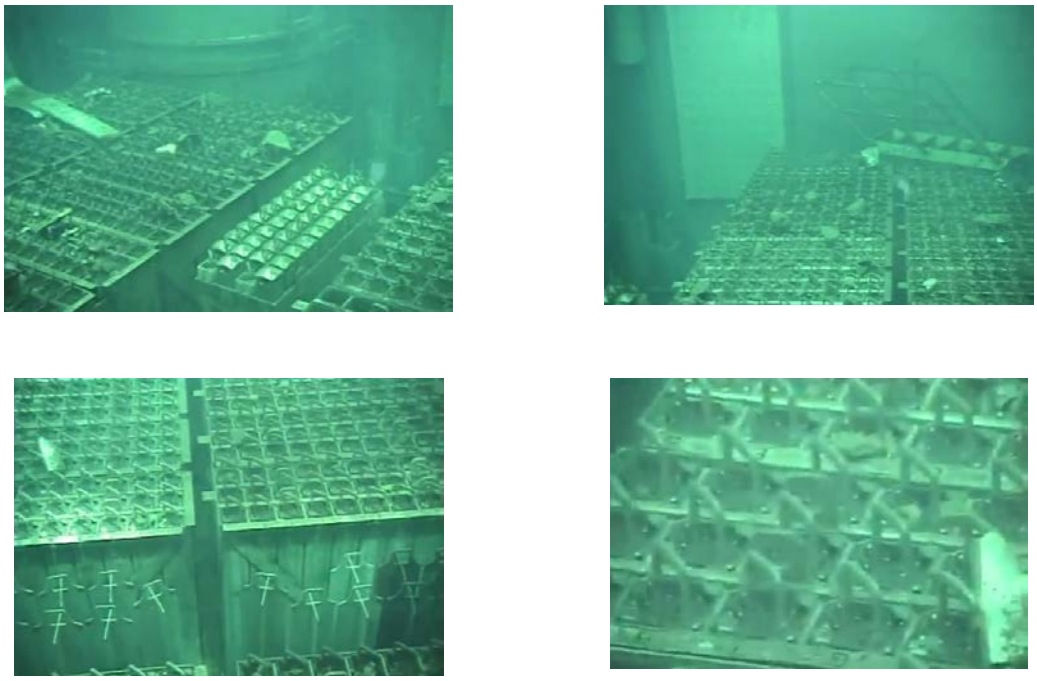

Figure 27: Underwater conditions in the SFP 4, video recorded on May 7, 2011 [49].

4.3.5 Unit 5 spent fuel pool (SFP 5)

Around 15:35 on 11 March, the SFP 5 lost all AC power when EDGs stopped functioning as the seawater pumps and power panels were flooded by the tsunami. The cooling and water supply for the SFP likewise failed. However, one air-cooled emergency diesel generator on Unit 6 continued to function and supplied electric power also to Unit 5.

On 13 March, the MUWC pump was manually started up by electric power supplied from the Unit 6 EDG. On 14 March, water supply into the pool was started using the MUWC line. Thereafter, water was intermittently supplied into the pool.

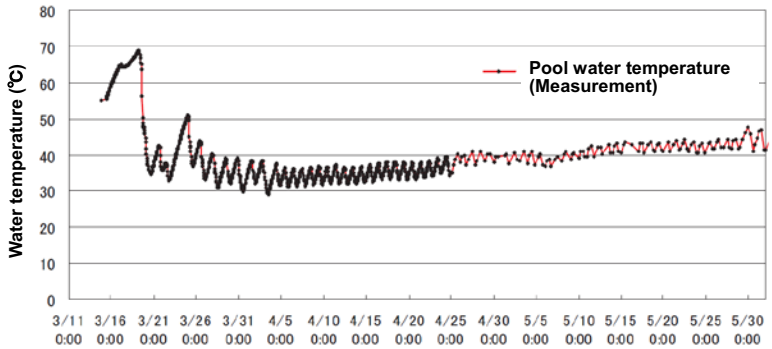

Figure 28: Measured variation of pool water temperature in the SFP 5 [38].

The water temperature started to increase gradually, as shown in Figure 28 [38]. However, on 19 March, the RHR pump was manually started up, and alternating cooling between the reactor and the pool was started by using the RHR system. As a result, the water temperature stopped increasing at 68.8 °C and

maintained a stable condition. Since the RHR was used for the reactor cooling as well, the pool water temperature increased when the cooling system was switched to the reactor, and it fluctuated between 30 and 50 °C. On 25 June, pool water cooling by the FPC system was started and a steady condition was reached, where the water temperature stabilized at about 30 °C.

4.3.6 Unit 6 spent fuel pool (SFP 6)

Around 15:35 on 11 March, two of the three EDGs on Unit 6 stopped functioning as the seawater pumps and power panels were flooded by the tsunami. Only one air-cooled emergency diesel generator on Unit 6 continued to function and supplied electric power to Unit 6, and later also to Unit 5. However, the cooling for the SFP failed due to the flooding of the seawater pumps.

On 13 March, the MUWC pump was manually started up by electric power supplied from the Unit 6 EDG. On 14 March, water supply into the pool was started using the MUWC line. Thereafter, water was intermittently supplied into the pool. On 16 March, the FPC pump was manually started up and circulation operation without heat removal was started.

The water temperature gradually increased, as shown in Figure 29 [38]. However, on 19 March, the RHR pump was manually started up, and alternating cooling between the reactor and the pool was started by using the RHR system. In consequence, the water temperature stopped increasing at 67.5 °C and maintained a stable condition. Since the RHR was used for the reactor cooling as well, the pool water temperature increased when the cooling system was switched to the reactor, and it fluctuated between 20 and 40 °C.

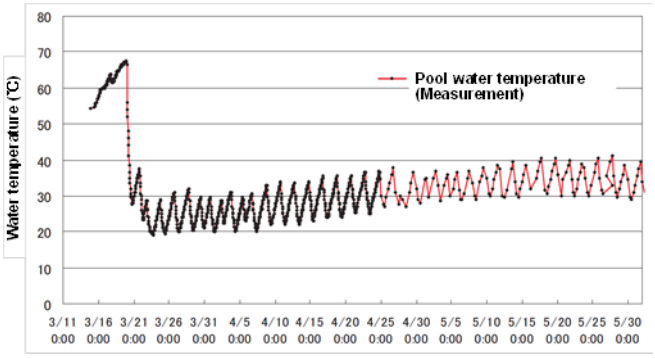

Figure 29**: Measured variation of pool water temperature in the SFP 6 [38].**

4.3.7 Common pool

Around 15:35 on 11 March, the common pool lost all AC power when EDGs stopped functioning as the seawater pumps and power panels were flooded by the tsunami. The cooling (air cooling) and water supply for the common pool likewise failed.

The water temperature gradually increased, as shown in Figure 30 [38]. On 18 March, an inspection was conducted for the common pool, and it was confirmed that a sufficient water level was maintained. On 24 March, the off-site power supply was recovered and the temporary cooling system was started. As a result, the water temperature stopped increasing at 73 °C and maintained a stable cooling condition. Since then, the water temperature stabilized between 30 and 40 °C.

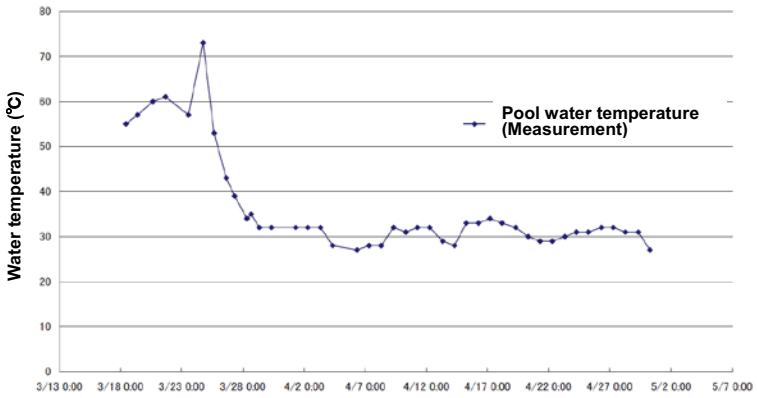

Figure 30: Measured variation of pool water temperature in the common pool [38].

4.3.8 Dry cask storage

Around 15:35 on 11 March, all AC power supply was lost at the dry cask storage building due to the tsunami caused by the earthquake. A large amount of seawater, sand and debris flowed into the dry cask storage building, and some of the casks were covered with seawater. An inspection confirmed that the casks had not moved from their respective bolted positions and the casks were not damaged by the event. Figure 31 shows the conditions inside the dry cask storage building after the tsunami [38].

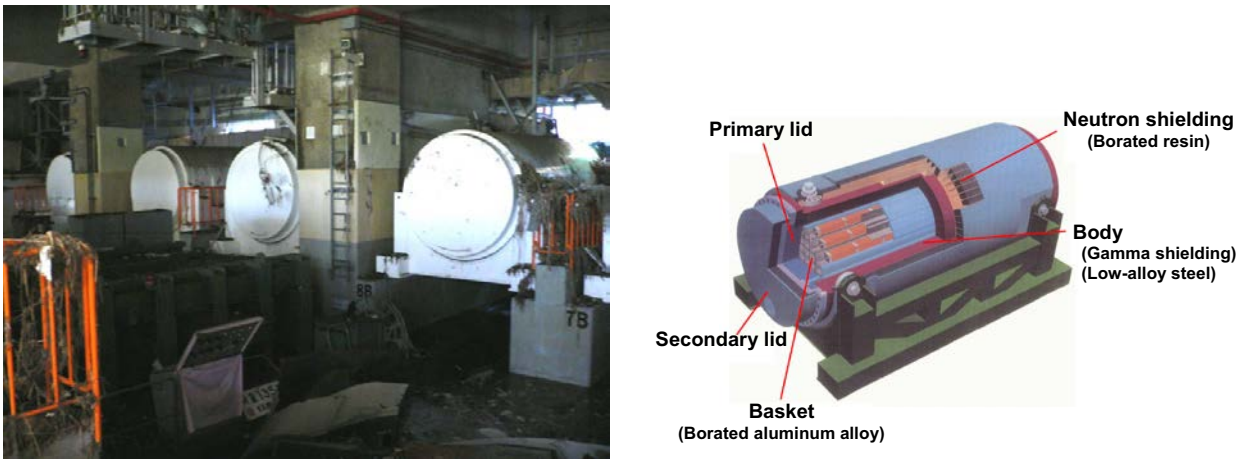

Figure 31: Conditions inside the dry cask storage building (left), and dry cask design (right) [38].

4.4 Post-accident measures taken against issues of concern

The reactor buildings of Units 1, 3 and 4 were severely damaged by hydrogen explosions, and a large amount of debris dropped into the SFPs in these units. Moreover, seawater was sprayed and injected to the SFP 2, SFP 3 and SFP 4 in the early stage of the accident. Because of this, the following issues regarding the SFPs were of particular concern after the accident:

- Influence of hydrogen explosions on the structural integrity of the reactor building and SFP;
- Impact of dropped objects on the fuel assemblies;
- Influence of seawater injection into the SFP.

After the accident, several measures have been taken to investigate these issues and to improve the situation.

4.4.1 Reinforcement of the structure supporting the Unit 4 SFP

The structural integrity of the reactor buildings and SFPs was of concern with regard to damage that might result from additional seismic events. The Unit 4 SFP was of particular concern, because of the relatively high decay heat associated with the fuel in this SFP; see Section 4.3.4. The cross-section of the Unit 4 reactor building and SFP is shown in Figure 32 [50]. The wall of the Unit 4 SFP is very thick (140 ～185 cm) and the pool is supported by a thick wall (160～185 cm), as shown in Figure 32.

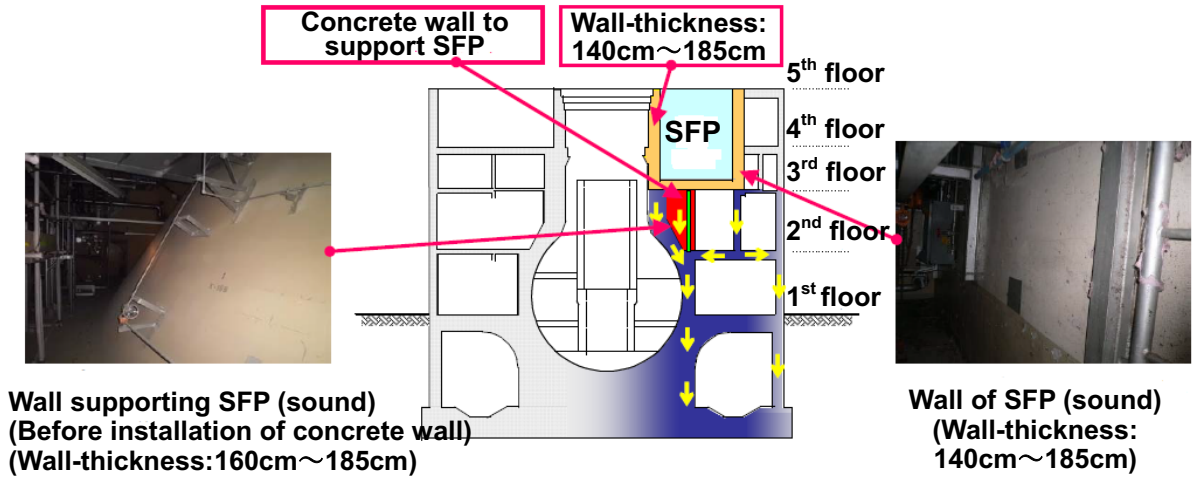

Figure 32: Cross-section of the Unit 4 reactor building and SFP [50].

As a result of seismic safety evaluations reflecting the damage of the reactor building, it was confirmed that the reactor building, including the SFP, would not be damaged in case an earthquake equivalent to the Great East Japan Earthquake (basic design earthquake ground motion: Ss) occurs again. Furthermore, reinforcing work was conducted to improve the seismic safety margin for the Unit 4 SFP. Between 31 May and 30 July 2011, steel support pillars were installed, and then concrete was poured to construct a concrete wall at the bottom part of the Unit 4 SFP, as shown in Figure 33. The seismic safety margin has been improved by more than 20 % by reinforcing the bottom part of the Unit 4 SFP.

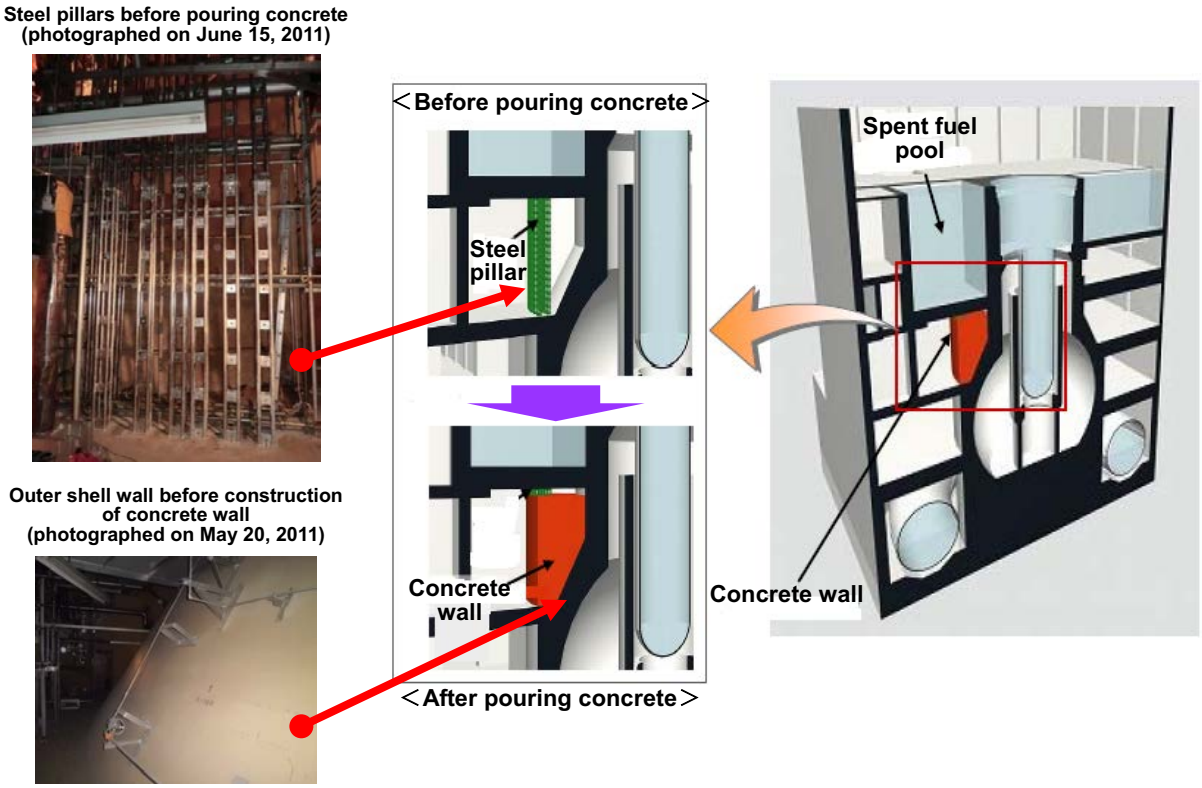

Figure 33: Seismic reinforcing work for the Unit 4 SFP [50].

4.4.2 Periodic inspection of the structural integrity of the Unit 4 reactor building and SFP

In order to confirm the structural integrity of the Unit 4 reactor building and SFP, periodic inspections are continued since 17 May 2012, for the following inspection items:

- Investigation of tilt of the SFP (measurement of water level in the SFP);
- Investigation of tilt of the reactor building (measurement of outer wall surface of the building);
- Visual inspection of the reactor building;
- Investigation of the concrete strength.

The distance from the 5th floor surface to the water levels in the SFP and the reactor well was measured, respectively. The measurement method and measurement points are shown in Figure 34 [50, 51]. Results of measurement are presented in Table 16 [50, 51]. Since the measured values at the four corners were almost the same, the results indicate that the 5th floor surface and the SFP surface are parallel. As a result, it was confirmed that the pool and building are not tilted.

The verticality of the outer wall surface was confirmed by measuring the horizontal difference between the fixed points of 1st floor and upper floors on the outer wall with optical equipment. The measurement points fixed on the outer wall surface are shown in Figure 35. For the calculation of the allowable stress specified in the Building Standards Law in Japan, it is required that the tilt of a building shall be within 1/200. The horizontal differences measured at all the fixed points were within this limiting value. The performed measurements confirmed that the building is not tilted.

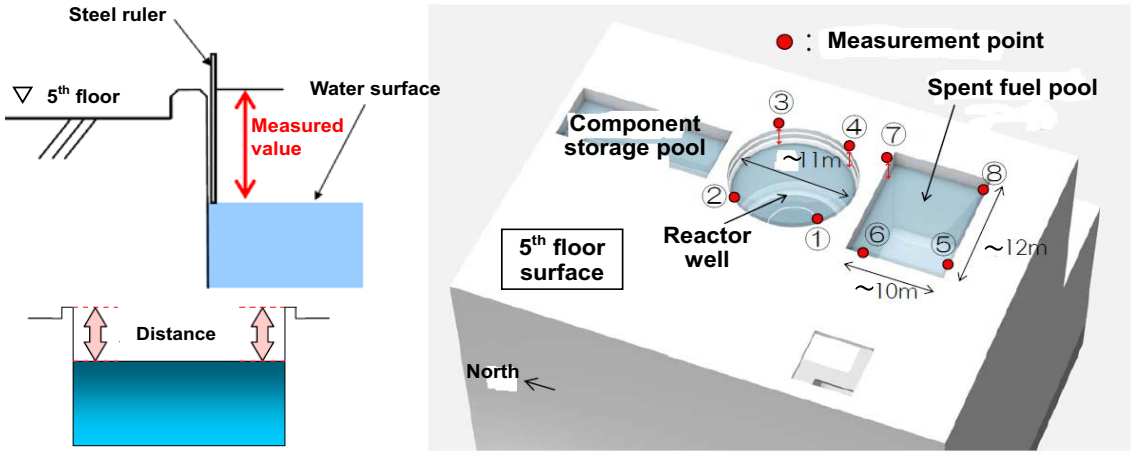

Figure 34: Measurement method and measurement points for water level in the SFP 4 [50, 51].

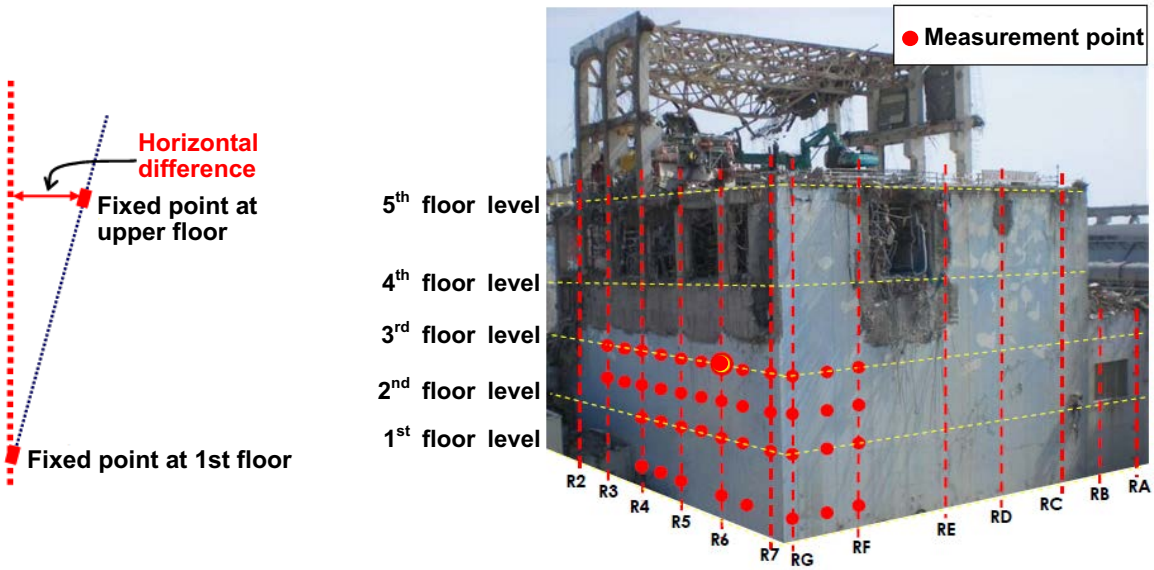

Figure 35: Measurement method and measurement points for verticality of Unit 4 building [50, 51].

Table 16: Results of water level measurements in Unit 4 SFP and reactor well [50, 51].

Unit (mm)

Reactor well	*Date*		
	2012.2.7	*2012.4.12*	*2012.5.18*
①	*462*	*476*	*492*
②	*463*	*475*	*492*
③	*462*	*475*	*492*
④	*464*	*475*	*492*

Unit (mm)

Spent fuel pool	*Date*		
	2012.2.7	*2012.4.12*	*2012.5.18*
⑤	-	*468*	*461*
⑥	-	*468*	*461*
⑦	-	*468*	*461*
⑧	-	*468*	*461*

Visual inspection was conducted to investigate the occurrence of cracks in the concrete walls and floors in the Unit 4 reactor building. The visual inspection locations are shown in Figure 36 [51], together with photographs of the inspected concrete wall surfaces of the SFP 4. As a result of the visual inspection, it was confirmed that cracks over 1 mm width are not observed in the concrete walls and floors. Moreover, cracks that may cause corrosion of reinforcing steel bars in the concrete are not observed.

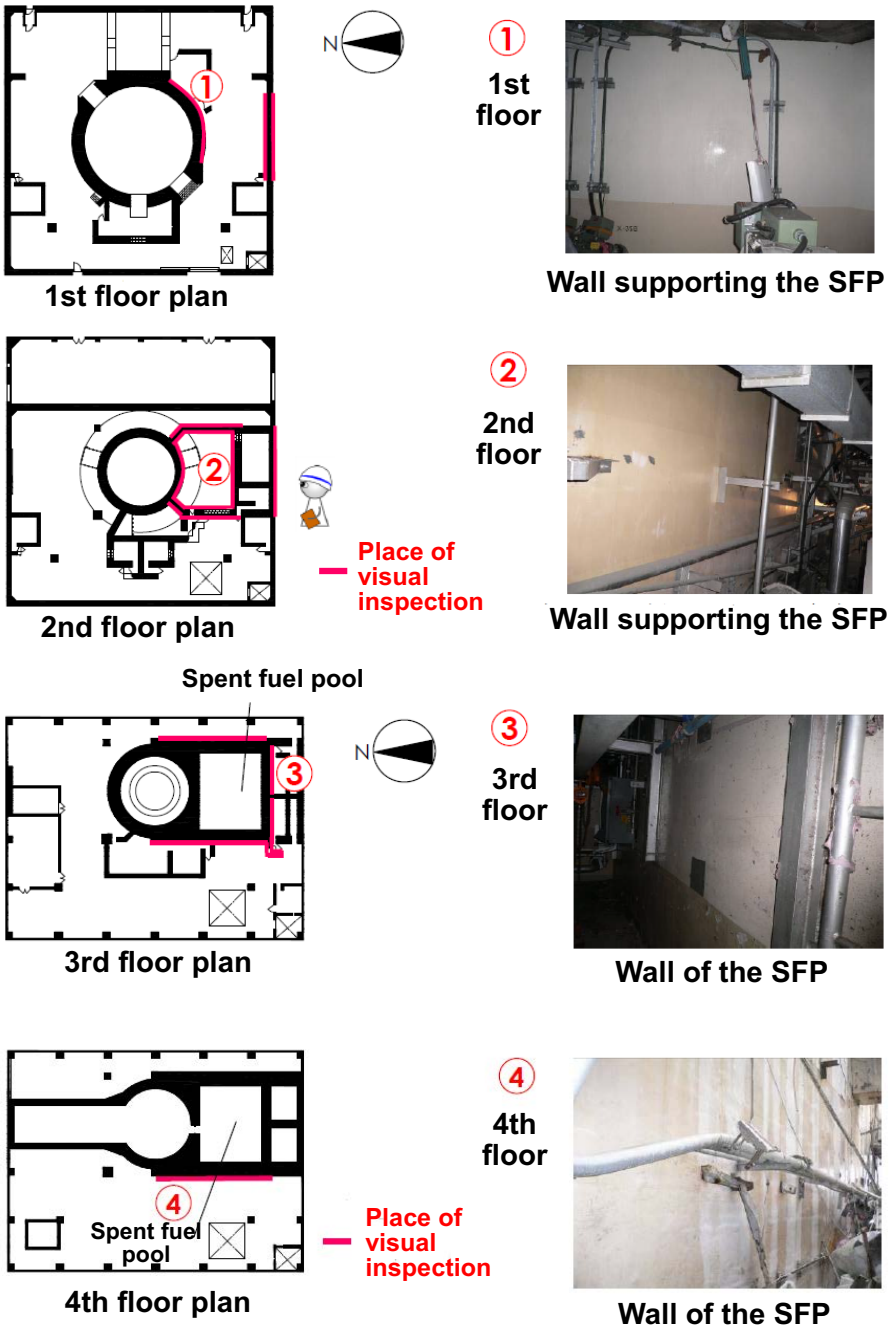

Figure 36: Visually inspected structures in the Unit 4 reactor building [51].

The concrete strength was investigated by non-destructive tests with Schmidt hammer equipment. The concrete strength measurement points at the SFP walls and floor are shown in Figure 37 [51], and

measured results are presented in Table 17 [51]. The concrete strengths measured at all points exceed the design strength (22.1 MPa). From these measurements, it was confirmed that sufficient structural strength is maintained in the Unit 4 reactor building and SFP.

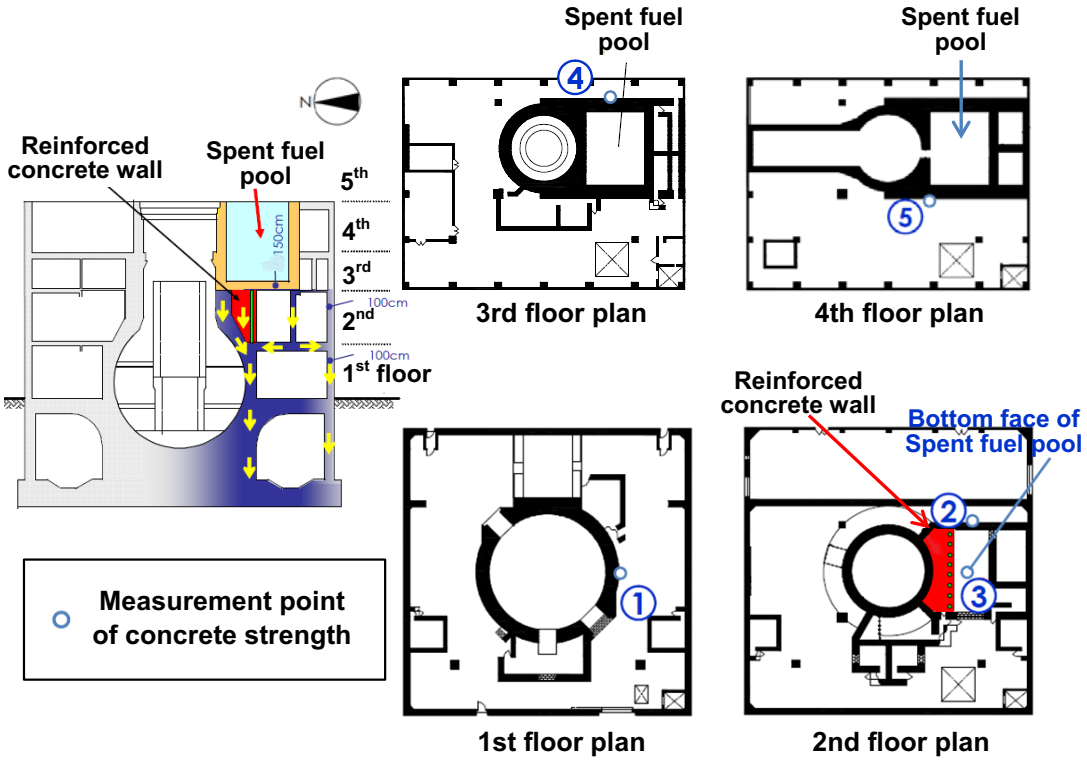

Figure 37: Measurement points for concrete strength in the Unit 4 reactor building [51].

Table 17: Results of measurements of concrete strength in the walls and floor of SFP 4 [51].

Unit (N/mm^2)

Measurement point			*Concrete strength (May, 2012)*	*Design strength*
①	*1st floor*	*Reactor shell wall supporting SFP*	*38.4*	*22.1*
②	*2nd floor*	*Wall supporting SFP*	*36.3*	
③		*Bottom face of SFP*	*33.1*	
④	*3rd floor*	*Wall of SFP*	*39.1*	
⑤	*4th floor*	*Wall of SFP*	*35.6*	

4.4.3 Evaluation of the impact of dropped objects on the fuel assemblies

In Units 1, 3 and 4, a large amount of debris dropped into the SFPs due to the hydrogen explosions. So far, investigations performed in the Unit 3 and Unit 4 SFPs have not revealed any fuel damage. In order to evaluate the impact of dropped objects on the fuel assemblies, a postulated debris drop test was performed in July 2012, using an un-irradiated 9×9 fuel assembly [52, 53]. A steel ingot of 100 kg, simulating heavy debris, was dropped onto the handle of the upper tie plate of the full length fuel assembly from a height of 5 m.

Results of the debris drop test are shown in Figure 38 [52, 53]. As revealed by the photographs of the deformed fuel assembly, the upper tie plate handle is severely deformed and fuel rods are bent in S-shape, with spacer grids as support points. However, hoisting performance of the fuel assembly and integrity (tightness) of all fuel rods were maintained after the debris drop test.

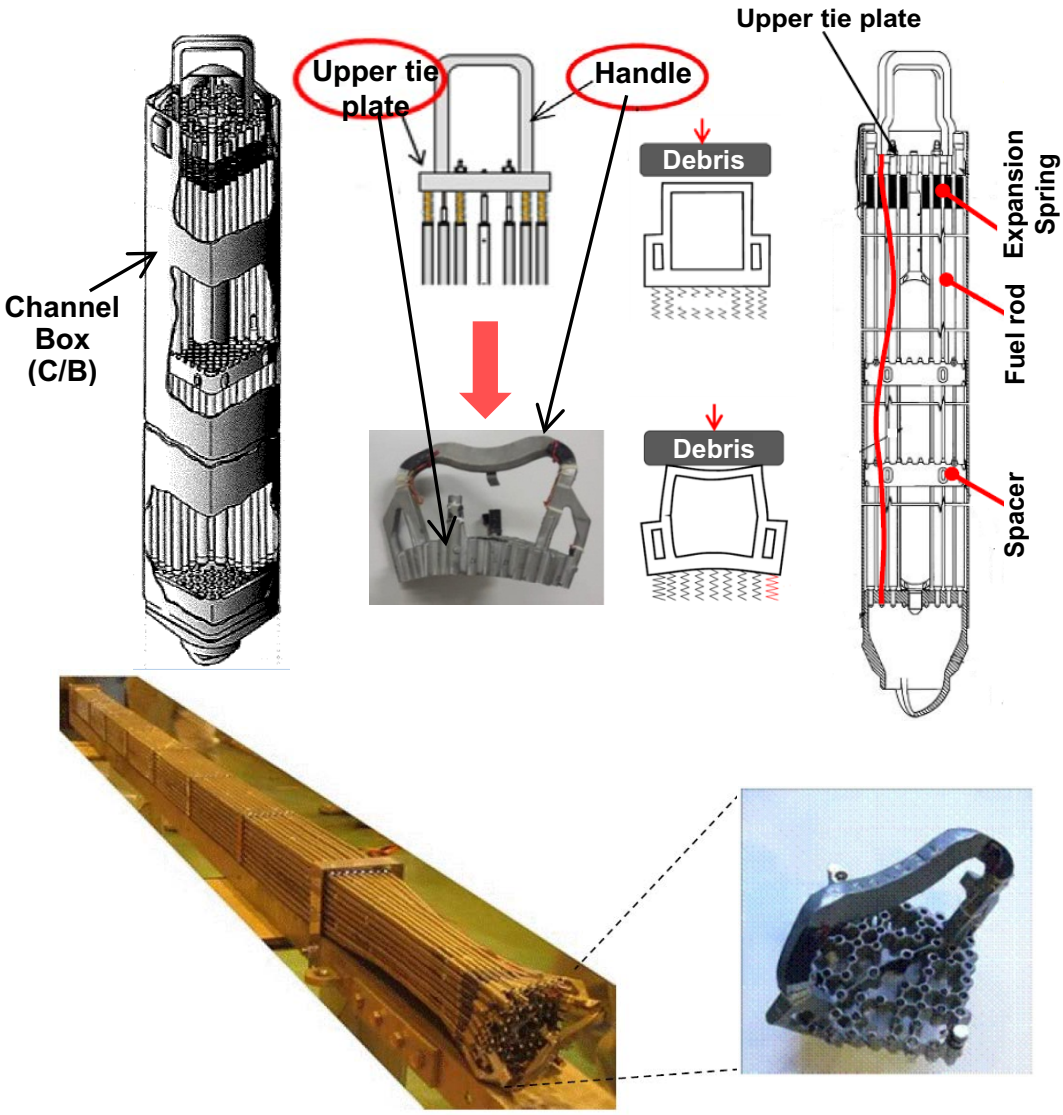

Figure 38: Results of postulated debris drop test [52, 53].

The effects of dropped objects on the fuel assemblies were examined by the postulated debris drop test, and fundamental data were obtained for evaluating the integrity of the fuel rod cladding after impact of dropped objects on the fuel assembly. From the drop test and analysis, it was confirmed that the integrity of the fuel rod cladding can be evaluated based on the extent of deformation inflicted on the upper tie plate handle by the impact.

4.4.4 Purification of the pool water at the Unit 1 to Unit 4 SFPs

Due to the loss of the pool water cooling system, emergency seawater spray and injection were conducted at the Unit 2 to Unit 4 SFPs in the early stage of the accident. Eventually, the alternative circulating cooling systems were started at the Unit 1 to Unit 4 SFPs from May to August 2011, and the water temperature in all SFPs has then been maintained below 40 °C. Since seawater was used, the concentration of chloride ion in the pool water was significantly increased, and so was the risk of accelerated corrosion. In order to reduce the risk of corrosion, the following measures have been taken to improve the quality of pool water at the Unit 1 to Unit 4 SFPs [54]:

- Removal of salts at the Unit 2 to Unit 4 SFPs;
- pH control at the Unit 3 SFP;
- Addition of hydrazine hydrate at the Unit 1 to Unit 4 SFPs.

The pool water purification conducted at the Unit 1 to Unit 4 SFPs is presented below.

Results of pool water quality measurements before purification are shown in Table 18 [54]. Except for the Unit 1 SFP, in which seawater was not injected, the concentrations of chloride ion in the pool water were above 1500 parts per million (ppm), as shown in Table 18. This concentration is approximately one-tenth of that in seawater. Removal of salts in the pool water was started in August 2011, using the reverse osmosis membrane apparatus and the ion exchange equipment connected to the alternative cooling system. Moreover, radioactive nuclides in the pool water at the Unit 2 and Unit 3 SFPs were removed using the adsorption removing system with zeolite to reduce the degradation of the reverse osmosis membrane by radiation. The removal of salts was completed by March 2013. Results of pool water quality measurements after purification are presented in Table 19 [54]. The concentrations of chloride ion as of July and August, 2013, were less than the safety regulation value of 100 ppm at the Unit 2 to Unit 4 SFPs, as shown in Table 19.

Table 18: Results of pool water quality measurements before purification [54].

	Time of sampling	pH	Chloride ion (ppm)	Cs-134 (Bq/cm^3)	Cs-137 (Bq/cm^3)
SFP 1 (Unit 1)	August, 2011	8.2	3.9	1.8×10^4	2.3×10^4
SFP 2 (Unit 2)	August, 2011	7.5	1,508	1.1×10^5	1.1×10^5
SFP 3 (Unit 3)	May, 2011	11.2	-	-	-
	August, 2011	9.2	1,769	7.4×10^4	8.7×10^4
SFP 4 (Unit 4)	August, 2011	7.7	1,944	4.4×10^1	6.1×10^1

In addition, the pool water pH at the Unit 3 SFP was 11.2 as of May 2011, as shown in Table 18. It was likely caused by the effluent (mainly calcium hydroxide) from the concrete dropped into the pool. In

the strong alkaline environment, acceleration of corrosion was a concern for the aluminium storage racks. Therefore, boric acid solution was injected into the Unit 3 SFP to control the pH of the pool water. As a result, the pH was decreased to 9.2 in August 2011, as shown in Table 18 [54].

Table 19: Results of pool water quality measurements after purification [54].

	Date of sampling	pH	Chloride ion (ppm)	Cs-134 (Bq/cm^3)	Cs-137 (Bq/cm^3)
SFP 1 (Unit 1)	June 19, 2013	8.1	7	5.6×10^3	1.3×10^4
SFP 2 (Unit 2)	June 16, 2013	8.7	13	4.7×10^1	1.4×10^2
SFP 3 (Unit 3)	June 17, 2013	8.2	13	3.7×10^2	7.7×10^2
SFP 4 (Unit 4)	August 9, 2013	7.9	30	1.3×10^0	5.6×10^0

Also, hydrazine hydrate has been added to reduce dissolved oxygen in the pool water at the Unit 1 to Unit 4 SFPs from May 2011 [54]. The intermittent injection of hydrazine hydrate is continued to deoxygenate the pool water at the Unit 1 to Unit 4 SFPs. After completion of pool water purification, the pool water is periodically inspected to maintain and control its quality.

4.5 Lessons learned

With regard to the SFPs, the lessons learned from the Fukushima Daiichi accident are the following:

- The SFP has a long grace time for cooling recovery compared with the reactor core. However, it contains a large amount of radioactive material in the spent fuel. Therefore, it would lead to a significant influence on the environment if the cooling function is lost and the stored fuel is damaged. Alternative means should be provided to allow the continued provision of water to the SFPs from the outside, without resorting to improvised approaches, such as a helicopter water drop or a concrete/fire pump [41, 55].
- The pool water temperature is measured near the pool water surface. If the water level decreases, the thermometer is exposed to the atmosphere. The water level is not directly measured at the pool. Instead, the water level of the skimmer surge tank, into which the water overflows when the pool is filled with water, is measured to understand the water level of the pool indirectly. Therefore, if the pool water level is lower than the skimmer surge tank level, it cannot be measured correctly. A wide range of water-level measurements and temperature measurements for SFPs should be made available to the operators in the control room [41, 55].
- The explosions at the Units 1, 3 and 4 reactor buildings caused structural damage to the SFPs in these units, but it is concluded that the integrity of the pool liner was maintained. Furthermore, investigation results indicate that any fuel damage was not likely caused by debris from the reactor building explosions. However, it should be recognized that the core accidents influenced the SFPs as well [40, 41].

5 ACCIDENT PHENOMENOLOGY

SFP accidents that result in radioactive release are highly unlikely. The SFP accident progression from initiation, to alarm, to dose consequences is slower in comparison to that of most reactor core accidents, progressing for days before any significant consequences occur. Due to the slow progression, operator intervention is highly likely to arrest the accident in its early stages, before onset of fuel degradation and radioactive release.

The SFP accident phenomenology presented in the following chapter is weighted on its complexity and its ease of explanation, not on its relative importance or its relative duration during the accident. Figure 39 illustrates that the accident progresses from a single dominant phenomenon, in the early stages, to a progressively more complex multiple interdependent phenomena situation. The figure presents the accident stages, using two different metrics, the status of the water and the status of the fuel, and then links these stages to timings and active phenomenology. Rough timings are given for two hypothetical scenarios; loss of cooling and loss of coolant accidents. These timings will vary greatly, not least depending on the residual power of the fuel. At the bottom of Figure 39 are the phenomena and how their respective applicability aligns with the accident stages.

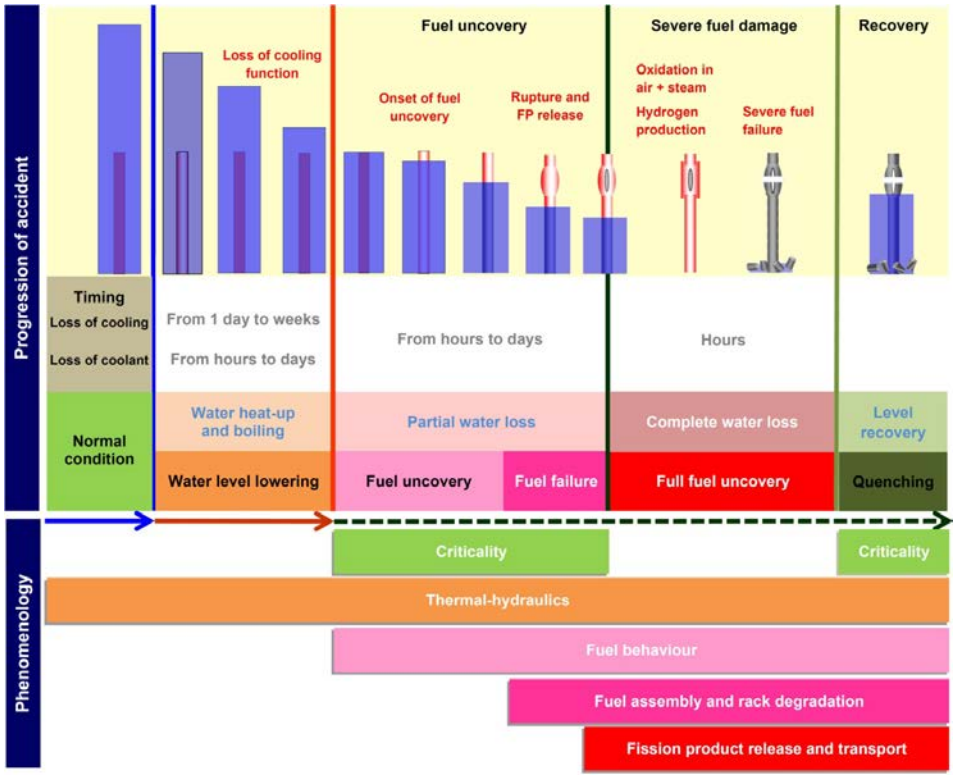

Figure 39: Stages and phenomenology of SFP loss of cooling/coolant accidents.

In the following, readers may notice a bias towards descriptions of phenomenology in the later, more severe accident progression stages. This bias should not be interpreted as a statement on the probability of reaching these later accident stages. It should also be noted that some of the phenomena described in the following sections do not apply to CANDU SFPs. For example, natural (non-enriched) uranium is used in CANDU fuel, which means that there are no criticality concerns and thus, no criticality control design features are necessary. Moreover, contrary to LWR fuel, CANDU spent fuel is stored horizontally and in storage racks that are open to both horizontal and vertical flow; see Section 2.2.2. This means that the thermal-hydraulic behaviour differs between CANDU and LWR SFPs, especially when the fuel racks are partially uncovered.

5.1 Criticality

5.1.1 Criticality aspects of SFP and storage rack design

From the neutronics point of view, SFPs are designed to be subcritical systems. The amount of fissile material contained in an SFP, as well as its geometrical configuration, varies from unit to unit; special care in the arrangement design is therefore always taken in order to maintain a given subcriticality margin which guarantees criticality safety under both operational and accident conditions for the entire lifetime of the SFP itself [56]. For example, US 10 CFR §50.68 b.4 specifies that, if no credit is taken for soluble boron and in the case of an SFP flooded with unborated water, k-eff[3] of the spent fuel racks loaded with fuel of the maximum reactivity must not exceed 0.95 at a 95 % probability and 95 % confidence level.

Spent fuel assemblies must be cooled for a sufficiently long time in order to cope with the decay heat generated by fission products; light water is generally used to accomplish this. It should be remembered that water is both a neutron absorber and a neutron moderator. The role of neutron absorption of water for an FA inside a core is minimized by design, so that a loss of moderator accident typically results in a negative reactivity insertion, simply because moderation effects were designed to be higher than absorption ones. On the contrary, the water gap between two assemblies stored in an SFP may be rather large, just because there should be enough cooling flow and neutronic decoupling; the role of absorption of this water element is therefore of great impact on k-eff, so that a loss of coolant accident in an SFP may result in a positive reactivity insertion for “low density” SFP rack designs. It should also be remembered that water density in an SFP is far higher than in hot core conditions, implying for sure slightly better moderation, but also much more effective neutron absorption. Hence, a decrease in water density, for instance at the onset of water boiling due to loss of cooling functions, may result in a positive reactivity insertion too. All this, together with the need to cope with the calculation uncertainties, as well as with a possible absence of monitoring and/or means for stopping criticality, forms one important rationale for the rather high (5 %) subcriticality margin typically imposed by regulatory authorities on the design and layout of SFP racks. It should also be remarked that spent fuel is a rather intense source of neutrons, therefore, should criticality conditions be met, the onset of power excursion may be rather fast.

5.1.2 Consequences of SFP criticality

A criticality accident in the SFP may, in principle, occur by movement or displacement of FAs and/or neutron absorbing material in the rack structure, and/or by loss of neutron absorption by an increase in coolant void fraction. For the latter scenario, consequences may be very different depending on the precise dewatering dynamics and on the rack design. The amount of excess reactivity inserted in the system may vary in time rather quickly, even with pulsing behaviour. Strongly coupled interactions between neutronics and thermal-hydraulics at the short-range scale can be foreseen. After some time, various neutronics and/or thermal-hydraulic counter-reactions may decrease the inserted reactivity, perhaps even stopping criticality.

[3]. k-eff (or k-effective) is the effective neutron multiplication factor (ratio between neutron production and neutron loss in a system containing fissile material). This factor represents the possibility for a system to undergo a sustainable fission chain reaction, in which case k-eff $\geq$ 1.

However, in this time lapse, the fuel cladding might get severely damaged by overheating, resulting in release and dispersion of fission products, including short-lived isotopes generated while the system was critical. Fuel damage mechanisms occurring during reactivity initiated accidents (RIAs) in reactor cores have been described in a recent CSNI report [57]. The material in that report is focused mainly on consequences of control rod drop (BWR) and control rod ejection (PWR) accidents, which lead to large and fast reactivity insertion, prompt criticality, and large energy depositions during a short (10-70 ms) power pulse. Criticality accidents in SFPs would probably be much slower and result in less energy deposition compared to the aforementioned accident scenarios; experimental studies on the fuel rod behaviour under such conditions would improve the understanding of the fine details of the phenomena.

As will be shown in the following, extensive fuel damage may decrease reactivity and allow subsequent SFP reflooding, which can be considered a good post-accident measure to avoid any further fuel damage. Also the amount of fuel damaged by a criticality excursion is difficult to predict; the excursion may affect a localized portion of an SFP or its entirety, depending on how the SFP has been loaded. Experimental activities related to the understanding of the complex behaviour of SFPs in case of reactivity insertions could be useful in this regard.

5.1.3 Computational analyses of SFP criticality accidents

After the Fukushima Daiichi accident (see Chapter 4), some studies have been performed to assess the criticality margin of SFPs under different types of conditions. At the Japan Nuclear Energy Safety Organization (JNES)[4], the activities have been mainly concentrated on BWR fuel. A peculiar problem of this type of fuel is given by the presence of enclosing boxes; after the onset of fuel uncovering due to loss of coolant or loss of cooling capability, a difference in the water level between the inner part of the fuel assembly and the outside of the storage rack may occur, mainly due to the water density difference between them. Water convective motion is in fact stopped in the upper part of the fuel assembly. Moreover, the gap between FA box and rack in the uppermost, uncovered part of the assembly acts as a kind of radial thermal insulation shield. Therefore, the water outside the rack is at a much lower temperature than the water inside the FA; see Figure 40.

Water inside the FA may start to boil. At the onset of boiling, there may be so high a difference in water density between these two zones that a significant water level difference may appear; calculations of this water level difference have been performed with RELAP5. This difference, in turn, creates a large axial difference in the neutronic properties of water: in the lower part, neutron absorption prevails, while in the upper part, the water density is so low that absorption in the assembly gap is reduced and the inner part of the FA is in conditions typical of BWR cores. As a result, the neutronic coupling between two neighbouring FAs is enhanced. In Figure 41, the k-eff calculations for three different types of racks are given as a function of the water level difference. In two cases, when the water level difference is greater than about 50 cm (corresponding to a fuel assembly decay power of about 2.5 kW; compare Table 14), k-eff may be > 1. It can also be seen that racks made with borated structural materials do not present this risk. An experimental campaign was conducted at the Toshiba Nuclear Critical Assembly (NCA) to have better evaluations of the phenomena described here. The campaign was concluded in 2013.

[4]. From 1 March 2014, the organization is part of the Nuclear Regulation Authority (NRA) in Japan.

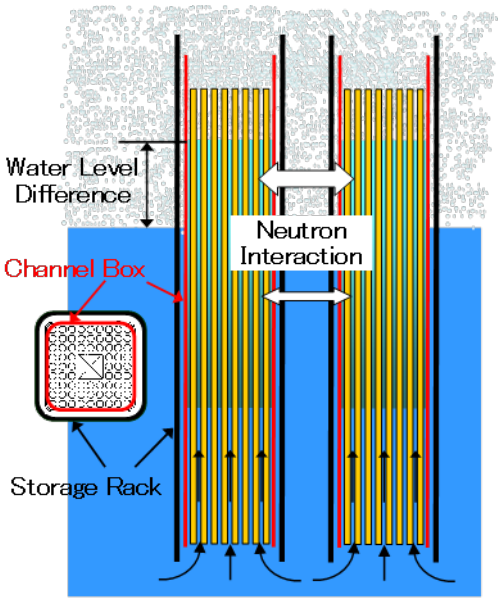

Figure 40: **Fuel uncovering and onset of water level difference for BWR fuel.**

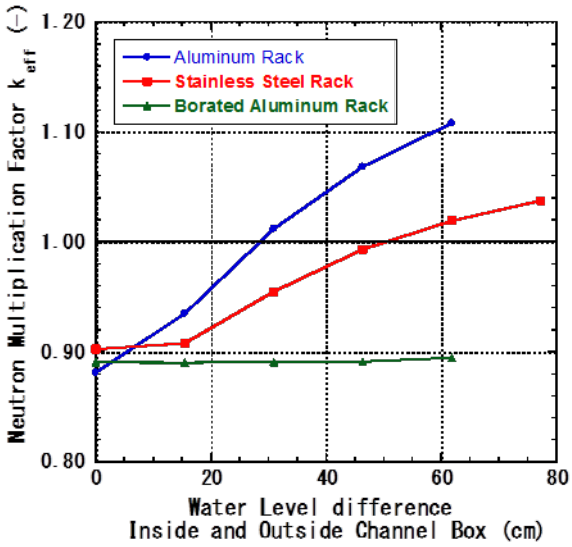

Figure 41: k-eff as a function of water level difference for two neighbouring assemblies.

In 2012, the Electric Power Research Institute (EPRI) published a report [58], which included an assessment, made with contributions by ORNL, of (re-)criticality concerns for the refilling of a drained SFP at the Fukushima Daiichi Unit 4 (henceforth called SFP 4). It should be remembered that the SFP 4 used only non-borated stainless steel racks without any neutron absorber panel, of the high-density type, relying nonetheless to a certain degree on some assembly separation for neutronic decoupling (so called "flux trap"). The report included therefore also a parametric analysis of the effect of assembly separation [58]. The SFP 4 contained 53 fuel storage modules, consisting of 3×10 rack units. The rack units were

rectangular, with pitches of 19.4 cm in one direction and 16.85 cm in the other; the inner cells containing the fuel assemblies were square with an outer side of 15.2 cm. As far as (re-)criticality was concerned, the report proposed to evaluate the reactivity inserted by water refilling in the case of a geometry that was distorted from the safe original one because of severe cladding degradation after drainage; this new geometry consisted in fuel pellets collapsed by gravity on the pool floor and grouped into heaps. For this configuration, and assuming pure water, the reactivity inserted in the system was extrapolated from previous studies on spent fuel casks and estimated to about -0.12, therefore greatly reducing or nullifying the risk of (re-)criticality. The conclusion was that there was no risk in refilling a drained SFP containing severely damaged fuel. A further criticality margin could also be foreseen, if one assumed instead seawater, which contains substantial amounts of chlorine; the neutron absorption cross-section of chlorine at 0.025 eV is about 40 b, which is not huge, but still relevant to somewhat increase the safety margin. As for assembly separation, ORNL prepared a model of the rack modules with square rack units with separation ranging from 0 cm (compacted SFP filling) to 20 cm.

The calculated variation of k-eff with FA separation (lower axis) or FA pitch (upper axis) is reported in Figure 42. The FA separation is naturally defined as the difference between the assumed FA pitch and the inner cell outer side. Three points are shown, which represent the SFP 4 average assembly pitch (18.12 cm), the highest pitch (19.62 cm, being roughly the highest real separation for SFP 4) and the lowest pitch (being roughly representative of the lowest real separation for SFP 4), respectively. It can be seen that keeping at least 1.1 cm of separation between assemblies is fundamental for the case of SFP 4.

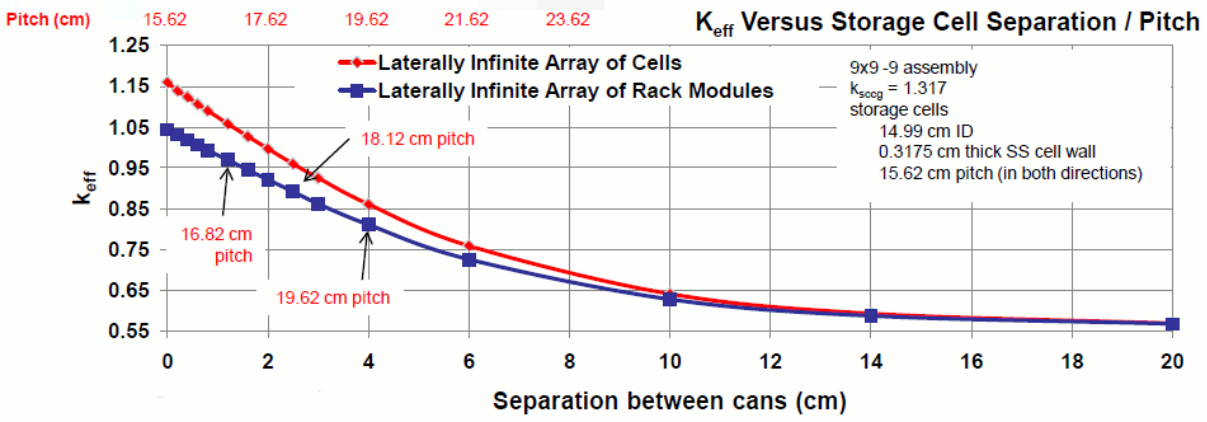

Figure 42: Rack module k-eff as a function of fuel assembly separation [58].

M. Kromar and B. Kurinčič [59] provided results pertaining to the SFP of the PWR NPP in Krško, Slovenia. In the dry or partially drained SFP, the fuel discharged from the last or two last refuellings can still have enough decay heat to breach the cladding and produce fuel pellet relocation. The analysis was focused on modelling the simplest collapse of the fuel rods, assuming they lost their integrity and that they collapsed to the bottom of the assembly. The process of collapse was assumed to start at the assembly centre. The authors examined cases of different percentage of fuel degradation: 0, 6, 25, 52, 74 and 100 %. The modelled FAs were housed in stainless steel racks of the older design, without any additional neutron absorbers. The design analyses of the NPP Krško racks show that the maximum pool reactivity takes place at the low water density – optimum moderation region. Low water density might occur when the pool water content is low and water boiling is so strong that significant void formation can arise.

The conclusions of the study were as follows: If the boron concentration in the pool water remains at least 2000 ppm, fuel degradation leads to lower pool multiplication, regardless of the pool water temperature and density. An almost insignificant reactivity rise of approximately 100 per cent mille (pcm)

is observed with the low water density in the optimum moderation region below 0.4 g/cm^3 and slightly degraded fuel. With no boron in the pool water, slightly degraded fuel exhibits higher reactivity than intact FAs. An increase in k-eff of up to 2 % is observed near the optimum moderation peak. Finally, it should be noted that fuel degradations higher than 50 % lead to lower pool reactivity in all cases. It may be concluded that too much fuel compaction leads to a so severe under-moderation of the degraded fuel that a net decrease of reactivity is achieved.

During the Fukushima Daiichi accident, also Institut de Radioprotection et de Sûreté Nucléaire (IRSN) performed some fast calculations to assess whether a criticality excursion was likely to occur in case of a SFP loss of cooling accident (dry-out). These calculations were performed with the CRISTAL package standard route [60]. The results show that the k-eff of the SFP can increase when a water-air mixture is modelled within the storage, compared to full water density within the pool. This k-eff increase can be higher than 5 % at the most challenging composition of the water-air mixture. The initial study dealing with the Fukushima Daiichi SFPs was supplemented by a PWR 17×17 textbook case, in order to identify the main parameters and conditions leading to such a k-eff increase [61]. The textbook model used for the study of the effects of decrease of the water density in an SFP consisted of (see Figure 43) a nominal 17×17 PWR UO_2 fuel design with 5 % enrichment (fresh fuel assumption). The pitch between the FAs was varied between 23 and 50 cm, and the storage rack was modelled by a 1.8 mm stainless steel basket around each FA. Finally, the water density (within the FAs and between them) was varied to simulate the water-air mixture in case of pool heat-up or refill. This mixture was modelled only on the uppermost 1.5 metres from the top of the FAs, which is called the “dry” part of the pool, opposite to the so-called “immersed” part of the pool, which corresponds to the remaining 2.5 metres lowermost part still containing water at 1 g/cm^3.

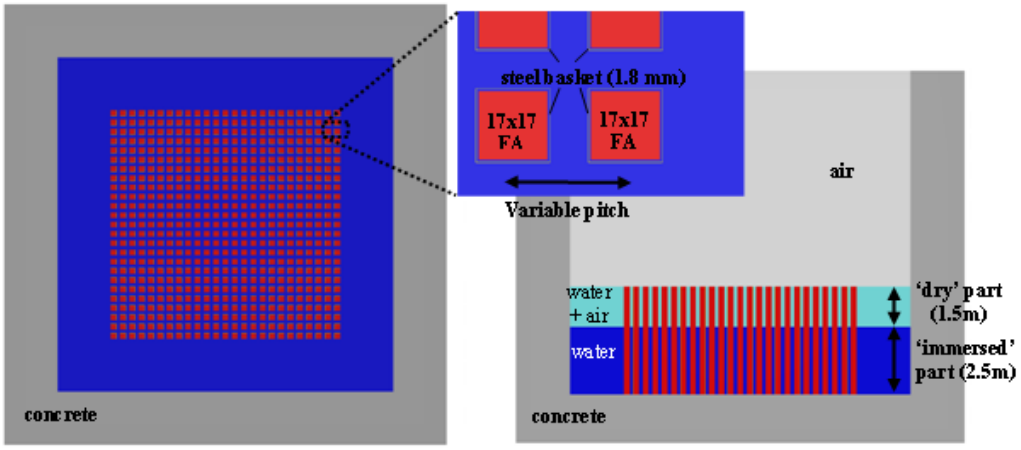

Figure 43: SFP configuration for IRSN studies.

From this reference case, several sensitivity studies were performed, such as on the impact of boron (either present in the stainless steel of the storage rack, or dissolved in the immersed part of the pool, or in the “dry” part of the pool in order to simulate a refilling by poisoned water), the impact of fuel initial enrichment and burnup, and also the impact of the height of the “dry” part and the number of FAs in the pool, etc. [61].

The results obtained for the textbook case described above are reported in Figure 44. The calculated value of Δk-eff, which is the difference between k-eff of the dry-out configuration and the safe one, was categorized into four zones:

- Δk-eff ≤ 0; which corresponds to a "dry-out" configuration less reactive than the safe design case (thus called the "Safe Zone");
- 0 < Δk-eff ≤ 2.5 %; which corresponds to an increase in k-eff lower than the required safety margins accounted for under abnormal conditions (so-called "Zone of reduced margins");
- 2.5 % < Δk-eff ≤ 5 %; which corresponds to an increase in k-eff comparable to the usual safety margins accounted for under abnormal conditions, but still lower than the usual overall safety margins (so-called "Risk Zone");
- Δk-eff > 5 %; which corresponds to an increase in k-eff higher than the usual overall safety margins (so-called "High Risk Zone").

Figure 44 below mainly shows that a large increase in k-eff (higher than 5 %) is indeed possible in case of loss of water within a fuel assembly storage. It shows also that:

- there is no k-eff increase when the FA pitch is less than 25 cm;
- there is no k-eff increase for a water density equal (or close) to 0 g/cm^3;
- the increase in k-eff occurs for the broadest range of water density for an FA pitch of about 30 cm; for large pitches, the risky water density range is very narrow;
- the worst water density range (leading to a significant k-eff increase whatever the assembly pitch) is between 0.15 and 0.2 g/cm^3 (i.e. for a water-air mixture with a void fraction of about 80-85 %).

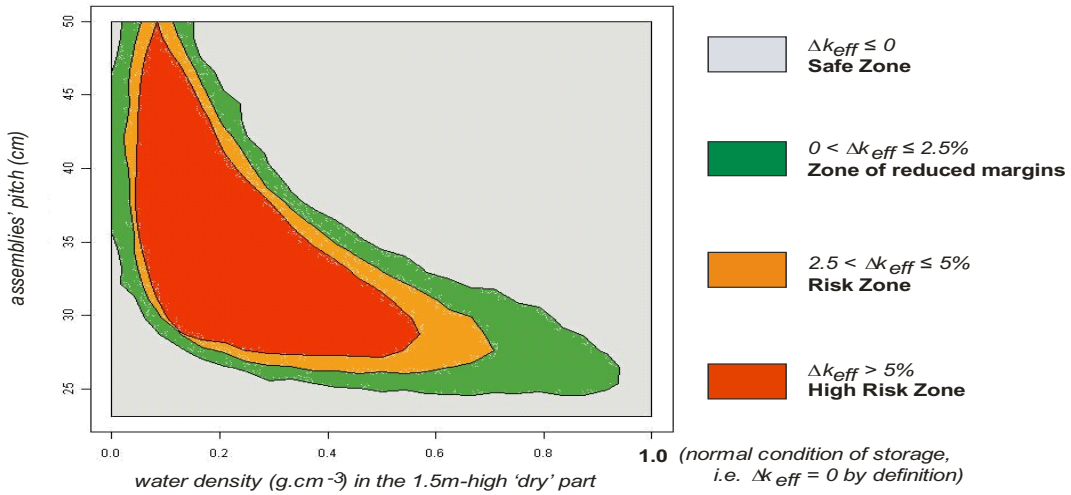

Figure 44: Pool multiplication factor at 0 ppm boron for the different degradation cases [61].

These results were obtained with configurations for the "dry-out" cases close to the pessimistic assumptions typically used for safety analyses (except, of course, the water density). Sensitivity analyses performed afterwards addressed if and how the risky zones were reduced with more realistic assumptions. The main conclusions drawn from the various sensitivity analyses performed are [62]:

- the presence of boron in the immersed part of the pool has almost no effect on the Δk-eff results, but boron in the "dry" part of the pool reduces significantly the risk zone [61];
- if the storage racks are borated, there is a boron content above which there is no more k-eff increase, whatever the assembly pitch. This means that for "high density storage racks", (with a small pitch and

thus with borated structures), there are no major criticality issues, but for "low density storage racks", (non-borated structures and thus with intermediate pitches), there can be a criticality risk in case of low water density (both boiling and spraying phases). Low density storages present higher criticality risks than high density storages in case of a dry-out;

- accounting for fuel depletion obviously reduces the risky zones, but still, a high risk zone remains even with a burnup of 10 GWd/MTU in the top end of the assemblies [61];
- the number of stored FAs has no important effect on the k-eff increase, except of course for very small storages, for which a loss of water leads to significant neutron leakage;
- the increase in k-eff is lower for a “dry” height of fuel less than 1.5 m, still being significant starting from a “dry” height of about 50 cm.

Dedicated criticality safety analyses were also performed in Germany [63] to answer the question whether a criticality accident in an SFP has still to be considered for emergency planning of NPPs in permanent shut-down, awaiting decommissioning. For that purpose, a number of hypothetical beyond design basis configurations have been considered, intentionally exceeding the requirements of the German safety rule KTA 3602 [64] and especially the double contingency principle. Among them, compaction, distortion or destruction of the storage racks, loss of fuel assembly integrity, loss of soluble boron and combinations of these scenarios have been investigated. Fresh and irradiated FAs have been considered, both of PWR and BWR types. Some configurations with k-eff > 1 were identified, but most of these were shown to be physically unrealistic, some by plausibility, others by reduction of model conservatism. Most of these configurations implied unirradiated fuel and, in case of PWRs, total loss of soluble boron. In this generic study, typically little burnup or little remaining soluble boron were sufficient to keep the arrangement subcritical.

Though being obviously of hypothetic kind, for a few remaining configurations, probabilistic analyses would be required for a quantitative assessment. This was beyond the scope of the work, which was to evaluate physical boundary conditions yielding a reactivity increase in SFPs. No potential triggering events have been identified in these analyses, nor have probabilities of occurrence of those configurations been determined. One main underlying aspect of all considerations was that ordered FA structures feature higher reactivity compared to distorted or fragmented ones. No consequence analysis was performed.

Inadvertent Criticality Events (ICEs) have been also dealt with very qualitatively in [2] for the case of reflooding of a BWR Mark I SFP drained after a beyond-design-basis earthquake; the general conclusion was that ICEs may be possible for specific combinations of conditions (e.g. for a region of the pool storing higher reactivity FAs, where the boron poison in the rack panels has been significantly displaced as a result of the earthquake). However, potential consequences of an ICE have been considered as being bound by activity release scenarios, and thus, have not been evaluated further.

5.2 Thermal-hydraulics

Under normal operation, decay heat from the spent fuel is removed by a combination of natural convection flow of the pool water through the storage racks and forced convection of the pool water through an external cooling system [65]. There is also some heat removal from the SFP by conduction through the side walls and the floor of the pool, and by radiation, convection and evaporation from the pool surface. These phenomena contribute to only a few percent of the total heat removal during normal operation, since the bulk water temperature in the pool is kept low (typically less than 310-320 K) by the cooling system. However, under off-normal situations, when the pool water temperature increases, the aforementioned phenomena become important.

The axial flow through an LWR spent fuel assembly is induced by the temperature-difference driven buoyancy. At normal conditions in the pool, the axial flow velocity is typically 0.1-0.2 m/s [65, 66], which is sufficient to efficiently cool the fuel. The temperature difference between the fuel rod cladding and the

water is less than 5 K, and the difference in water temperature between the top and bottom of the FAs is usually less than 10 K. These are typical temperature differences and flow velocities for normal operating conditions in the SFP; they depend on the decay power and design of the considered FA.

In the following, we will consider thermo-hydraulic conditions in four different scenarios, or stages, which may arise during loss of cooling accidents in LWR SFPs. As illustrated in Figure 45, the scenarios are: a) Fuel assemblies completely covered with water, b) FAs partly uncovered but intact, c) FAs partly uncovered and damaged, d) FAs completely uncovered. These scenarios can be viewed as different stages of an accident, but it must be recognized that all stages illustrated in Figure 45 may not be reached during an accident. For instance, a fast drain-down accident in an SFP with comparatively old and cold fuel assemblies is unlikely to result in fuel damage with large geometrical distortion, as illustrated in Figure 45c). Also, the duration of each stage will depend strongly on the scenario of the particular accident. Thermo-hydraulic phenomena are expected to be significantly different in CANDU SFPs, due to the open rack structure with horizontally aligned fuel elements; see Section 2.2.2.

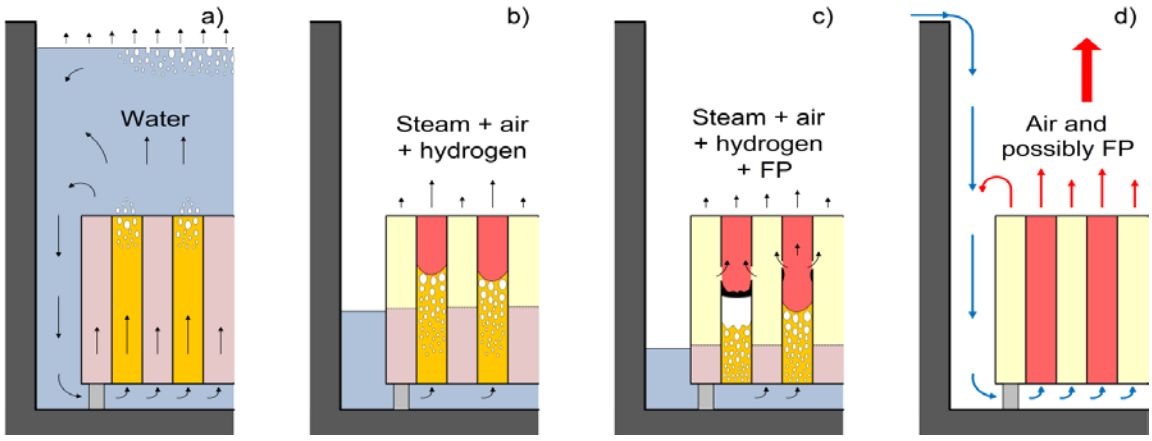

Figure 45: Thermo-hydraulic conditions in four different scenarios (or stages) of an SFP loss-of-cooling/coolant accident. Fuel assemblies with high decay power are indicated with dark shades of yellow (water filled part) and red (gas filled part).

5.2.1 Fuel assemblies completely covered with water

As already mentioned in Section 3.1, many accident scenarios involve partial or complete loss of SFP cooling capacity. This results in a heat-up of the pool inventory, and if no corrective actions are taken, the pool water will gradually evaporate and eventually uncover the fuel assemblies. Fuel damage is very unlikely as long as the FAs are completely covered with water, since natural convection of the pool water will provide sufficient cooling of the fuel. As shown in Section 2.1.2, most modern rack designs for spent LWR fuel storage have a closed cell design, with inlet holes for convective flow only at the bottom of each cell. Since this design allows lateral cross flow only in the regions below and above the racks, the overall shape of the natural convection flow pattern in the pool depends largely on the distribution of hot and cold FAs [66]. With natural convection in a large number of parallel heated channels that are fed by the same downcomer, flow reversal is possible in low-power FAs [67]. This may lead to premature nucleate boiling in some channels and unstable natural circulation flow may occur [68]. Consequently, the cooling of the FAs is perturbed, and in some channels, the flow could be reduced, leading to further voiding [69].

As the pool water heats up, boiling will usually first occur in the upper part of high-power FAs and/or at the pool surface [66]; see Figure 45a). If the pool water level is high above the fuel racks, there may be an intermediate region with non-boiling water between the fuel racks and the pool surface. This is because the saturated water, exiting from high-power FAs, is mixed with cooler water as the fluid rises. However, boiling may occur again closer to the pool surface, where the hydrostatic pressure is lower; see Figure 45a). Whether boiling first occurs at the pool surface or at the exit of hot FAs depends on the lateral distribution of hot/cold FAs and the pool water level. When the pool water level approaches the top of the racks, the non-boiling region of the pool will shrink and the void fraction in the upper part of the FAs will increase as a result of lower hydrostatic pressure. As explained in Section 5.1, the increasing void fraction may pose a criticality problem.

Fairly simple methods can be used to estimate the time needed for evaporating the pool water level down to the top of the fuel assemblies, given the total heat load of the spent fuel, the pre-accident water volume and water temperature in the pool, and any corrective actions in terms of make-up water injection or forced cooling [25, 48, 70, 71]. The applied models differ mainly with respect to how heat and mass transfer by evaporation of water from the pool surface is modelled.
In the models, evaporation from the surface is considered the dominating mechanism for heat removal from an SFP with inoperable cooling system. It becomes significant when the water temperature exceeds about 340 K [48, 66]. This is illustrated by Figure 46, which shows the relationship between pool water temperature, evaporation rate and decay power of the fuel during steady-state conditions, as calculated by Wang et al. [48]. In Figure 46, the latter two quantities are normalized with respect to pool surface area, which means that the results can be used for estimating the steady-state pool water temperature and evaporation rate for fuel pools with arbitrary surface area, given the total heat load from the stored fuel. It should be remarked that the calculated results in Figure 46 apply to a case with air at 293 K and 50 % relative humidity above the pool surface, representing Fukushima Daiichi unit 4 post-accident conditions. Heat and mass transfer by evaporation from a free surface is less effective at higher air temperature and humidity [48, 72]. Measured fuel pool temperatures for Fukushima Daiichi units 2 and 4 (pool surface area 120.8 m^2) from late April to early May 2011 are included in Figure 46 for illustration.

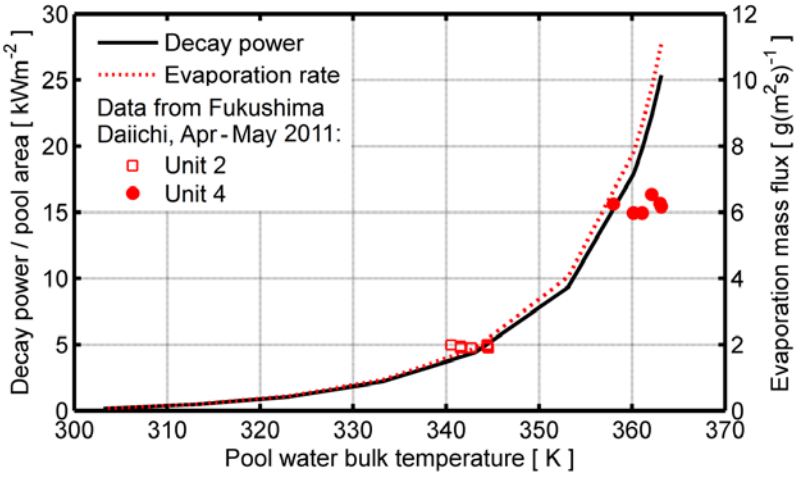

Figure 46: Calculated relationship between pool water temperature, evaporation rate and spent fuel decay power during steady-state conditions [48]**. Air at 293 K and 50 % relative humidity is assumed above the pool surface. Data are measured pool temperatures, plotted versus decay power** [48]**.**

Figure 46 suggests that bulk boiling does not necessarily occur in an SFP with inoperable cooling system, since heat removal by evaporation becomes significant at pool temperatures well below the boiling point. However, the large amount of evaporated water during a loss-of-cooling accident is a challenge for the ventilation system of the SFP building, which is not designed for handling the steam produced from an SFP in boiling or near-boiling condition. Accident management procedures therefore usually involve opening of doors and hatches, if such exist, to release steam to the environment.

Yet, water vapour may still condense inside the building and accumulate in locations that could cause safety related systems to fail. Other consequences of the evaporation is that suction to the SFP cooling system will be lost as soon as the pool water level drops below the strainers at the top of the pool, or alternatively, when boiling occurs at the strainers. Consequently, it will be impossible to restart the pool cooling system under these conditions. If the pool water level drops to less than about 0.6 m above the spent FAs, analyses show that the increased β- and γ-radiation field would prevent access to the spent fuel building [2]. This might hamper mitigation measures, surveillance and control.

Finally, radiation from the water covered spent fuel assemblies leads to production of hydrogen by radiolysis of the water. Although it is not clear whether hydrogen may be produced in sufficient quantities to exceed the hydrogen-air flammability threshold in the SFP building, the phenomenon may play a role for SFP accidents involving loss of ventilation in the pool building. Hydrogen produced by radiolysis is expected to be a minor problem in comparison with hydrogen that may be produced by high temperature oxidation of zirconium alloys in steam; see Section 5.4.1. Studies are ongoing in Belgium, France and some other countries to determine if particular measures (material and/or organisational) may be needed, such as the installation of passive autocatalytic recombiners (PARs) in the fuel building [73].

5.2.2 Fuel assemblies partly uncovered but intact

As the pool water drops below the top of the spent fuel assemblies, it does not necessarily result in immediate heat-up of the uncovered part of the fuel: As long as the water level is not too far below the top of the FAs, the uncovered part may be cooled by steam flow and water level swell from boiling in the lower part, as illustrated in Figure 45b). Calculations with MELCOR [74] suggest that cladding peak temperatures in the uncovered part of the fuel assemblies may be kept < 800 K even when the collapsed water surface is 1.5 - 2.0 m below the top of the spent FAs [2, 75, 76]. Yet, it must be recognized that the thermo-hydraulic phenomena occurring in the partly uncovered fuel assemblies are complex. The swell level inside spent FAs at different heat load has received comparatively little attention in past research programs, and only a limited amount of test data is available. The swell level is dependent on the bubble rise velocity inside the closed rack area, on the flow resistance of the spacer grids and on the pitch and the diameter of the fuel rods. For each fuel assembly design, different swell levels will be expected for identical heat loads. Thermo-hydraulic tests on partly uncovered fuel assemblies are underway in France within the IRSN DENOPI program. The planned tests will address the issue of single- and two-phase flow natural convection in an SFP after loss of cooling, as well as air ingress and spray efficiency on a partly uncovered full-scale fuel assembly with electrical heater rods; see Section 6.3.1.

The steam generation and the water swell in a particular fuel assembly, and hence, the effectiveness of cooling in the uncovered upper part, depend on the extent of boiling below the water surface. This, in turn, depends on the immersed length of the FA and its decay power. Computational analyses suggest that the peak cladding temperature can in fact be *lower* in high-power fuel assemblies than in neighbouring medium-power assemblies, since the former have higher steam production and better cooling in the uncovered part [76, 77]. However, temperatures in the uncovered part are difficult to predict by computational models, mainly because of the complex two-phase flow pattern. At high temperature, heat transfer by radiation in the lateral direction between adjacent FAs and between FAs and the rack structure, as well as heat generation by oxidation of the fuel cladding, add further complexity to the calculations. It should also be recalled from Section 5.1 that differences in swell level between adjacent FAs, as illustrated in Figure 40 and Figure 45b), may reduce the margin to nuclear criticality.

5.2.3 Fuel assemblies partly uncovered and damaged

As the water level drops, the cladding peak temperature in the uncovered part of an FA increases for two reasons; less steam is produced by boiling in the bottom part, and the steam overheating increases in proportion to the uncovered length. Eventually, the peak temperature may escalate as a result of rapid cladding oxidation with available steam and/or air. Since the oxidation processes are strongly exothermal, they result in a self-sustained zirconium fire, leading to structural degradation of the fuel assembly and release of fission products; see Sections 5.4 and 5.5. The onset of these processes depends on the thermal runaway kinetics of the zirconium-steam-air reactions. As shown in Section 6.2.1.1, the reaction kinetics for various cladding alloys have been thoroughly studied in steam and air environments separately, but there is a paucity of tests done in steam-air mixtures. The chemical environment in a partly uncovered fuel assembly at high temperature is expected to be complex: As indicated in Figure 45b-c), steam will dominate close to the water, but as the rising steam reacts with the zirconium metal, the steam gradually becomes starved of oxygen. The uppermost part of the FA may therefore contain a mixture of steam, hydrogen and air. The environment is thus more complex than for a completely uncovered fuel assembly, and the risks involved with hydrogen production must be considered; see Section 5.4.

During gradual uncovering of the spent fuel, e.g. by boil-off or slow draining of the pool water, computational analyses [76, 77] indicate that low- to medium-power fuel assemblies are those that will start to heat up first; they have less steam production and water swell than high-power FAs, and therefore poorer cooling of the uncovered part. However, the heat-up rate is fairly low, since the decay power is moderate and the surrounding rack structure and fuel assemblies act as heat sinks. As the water level decreases, successively higher powered assemblies will start to heat up. Since the heat-up rate increases in proportion to the decay power, the peak temperatures in high-power FAs will ultimately catch up with those in medium-power assemblies. It is as yet unclear at what fuel assembly power the critical conditions for igniting a zirconium fire in partially uncovered fuel assemblies will first occur.

As damage progresses in the upper part of the FA, debris will relocate downward and obstruct the axial flow through the fuel assembly; see Section 5.4.6. At the same time, melting and candeling of the rack material in the damaged region may open pathways for cross flow between adjacent rack cells, as illustrated in Figure 45c). The flowpaths and thermo-hydraulic conditions in the damaged fuel rack thus become complex and difficult to model in computer simulations.

With prevalent closed-cell rack designs for storage of spent LWR fuel, the worst possible scenario with regard to fuel coolability is deemed to arise with nearly completely uncovered fuel assemblies, having only their bottom ends immersed in non-boiling water [78]. This scenario is considered worse than a situation with completely uncovered FAs, in which natural convection of air provide cooling; see below. The water will plug the bottom inlets to the storage racks and preclude air circulation, and if non-boiling, the water will emit negligible steam for cooling the uncovered part of the FAs. This worst case scenario would occur transitionally when refilling a drained SFP by injecting cold water into the bottom of the pool through the normal cooling system. As soon as the water level reaches the bottom of the FAs, natural circulation of air through the FAs will stop and fuel temperatures start to increase. Refilling the drained pool by spraying (top-down cooling) could be a better alternative [2, 77], especially if fast refilling cannot be achieved.

5.2.4 Fuel assemblies completely uncovered

As illustrated in Figure 45d), natural convection by air is the dominating cooling mechanism when the spent fuel assemblies are completely uncovered. Experiments on the thermo-hydraulic behaviour of completely uncovered BWR and PWR fuel assemblies in air have recently been carried out at Sandia National Laboratories in the USA [12]; see Section 6.1.1. Except for these experiments, our understanding of the behaviour is based largely on computational analyses. Software developed specifically for the problem [25, 78, 79], as well as general-purpose programs for computational fluid dynamics (CFD), have been used to analyse the natural circulation airflow in completely drained SFPs and the surrounding

buildings. For example, Boyd [80] studied the air coolability of completely uncovered spent fuel in decommissioned BWRs by use of the FLUENT[5] program, and the same code was later used for simulating natural convection airflow in completely drained PWR fuel pools [77]. These analyses suggest that a large scale flow pattern develops inside the pool building: Hot air exiting the top of the fuel assemblies forms a plume that rises to the ceiling. It then spreads laterally within a hot layer. If the layer of hot air beneath the ceiling is evacuated by the ventilation system or by opening roof hatches, the air in the building may remain thermally stratified as cool air enters at lower elevation to replace the hot air that exits through the ceiling. The cool air is then drawn into the SFP, where it spreads laterally under the racks and enters the FAs from below. However, if the building ventilation is inadequate, the analyses suggest that the room will gradually heat up and the hot gas layer will ultimately drop into the SFP, hampering the natural convection and resulting in significant fuel heat-up.

The aforementioned computational studies thus identify ventilation of the pool building as important for the coolability of completely uncovered fuel assemblies, in particular since a strong non-linear relationship is reported to exist between the calculated cladding peak temperature and the air temperature at the bottom of the SFP [77, 80]. Another conclusion from the computational analyses is that the availability of downward flow paths for the cool air to the bottom of the SFP is crucial for the natural circulation airflow. These flow paths include the downcomer space between the storage racks and the pool wall, the transport cask region and possibly some empty rack cells. Lateral heat transfer from spent FAs with high decay power to low-power assemblies or empty rack cells is also important under air cooling, which means that the spent fuel storage pattern affects coolability; see Section 2.1.3.

The CFD analyses reported in [77, 80] indicate that, under favourable conditions, the spent fuel may be coolable by natural circulation of air only. Key factors reported to affect the coolability are the spent fuel decay power and storage configuration, the building ventilation, and the availability and configuration of downward flow paths into the SFP. Calculations with different severe accident codes show the possibility of sufficiently cooling the spent fuel with air flow for several days, already within a few months after the fuel has been removed from the reactor into the SFP [2, 81]. Under less favourable conditions, however, the cladding temperature will transgress the threshold for runaway oxidation and a zirconium fire ensues. Calculations suggest that the point of ignition would be about one fifth from the top of the fuel assembly [79], unless the FA contains part-length fuel rods, as is the case in modern BWR fuel designs. In these designs, ignition is likely to occur near the top of the fully populated section of the FA [2].

5.3 Fuel behaviour

As-fabricated light water reactor fuel consists of solid or annular ceramic pellets of uranium dioxide, UO_2, or mixed oxide (MOX) $(U,Pu)O_2$, enclosed in zirconium alloy cladding tubes with an outer diameter from about 9.5 to 11 mm in current fuel designs [82]. The fuel assemblies comprise 64 to 100 (BWR) or 190 to 300 (PWR) of these fuel rods. The rods are slightly less than 4 m long, and held in place laterally by spacer grids [82]. CANDU fuel assemblies (normally called “bundles”) are roughly half a metre long and consist of 28-43 fuel rods. CANDU fuel contains natural uranium, while the uranium in LWR fuel is enriched to about 3 to 5 wt% ^{235}U, i.e. by a factor of 4 to 7 from its natural abundance of 0.7 wt%. The fabrication, basic properties and in-reactor behaviour of oxide fuels and zirconium alloys are thoroughly reviewed in [83, 84] and [85], respectively.

The UO_2 fuel in a typical LWR is exposed to a neutron flux that induces two principal types of nuclear reactions, namely fission, and neutron capture plus beta decay. The former occurs predominantly by collision of a thermal (≈ 0.03 eV) neutron with the ^{235}U nucleus, which produces fission fragments plus 2-3 neutrons (≈ 5 MeV) and other energy contributions (≈ 198 MeV), mainly comprising kinetic energy of the fission fragments. The latter form a bimodal distribution of elements with respect to atomic mass. Even though many hundreds of fission-product isotopes are generated in the reactor, most have very short half-

[5]. Currently known as ANSYS-Fluent ; see Section 7.1.1.

lives and decay within days to weeks after their formation. The neutron-capture reactions, normally followed by beta decay, involve epithermal neutrons and lead to the formation of transuranium elements (Z > 92), of which Pu is the most ample. Fissile isotopes generated in this manner, such as ^{239}Pu, can then be fissioned, contributing up to one-third of the energy produced in a LWR with UO_2 fuel. Figure 47 shows depletion and growth of several important nuclides in UO_2 LWR fuel versus time spent in the reactor, with details described in [86].

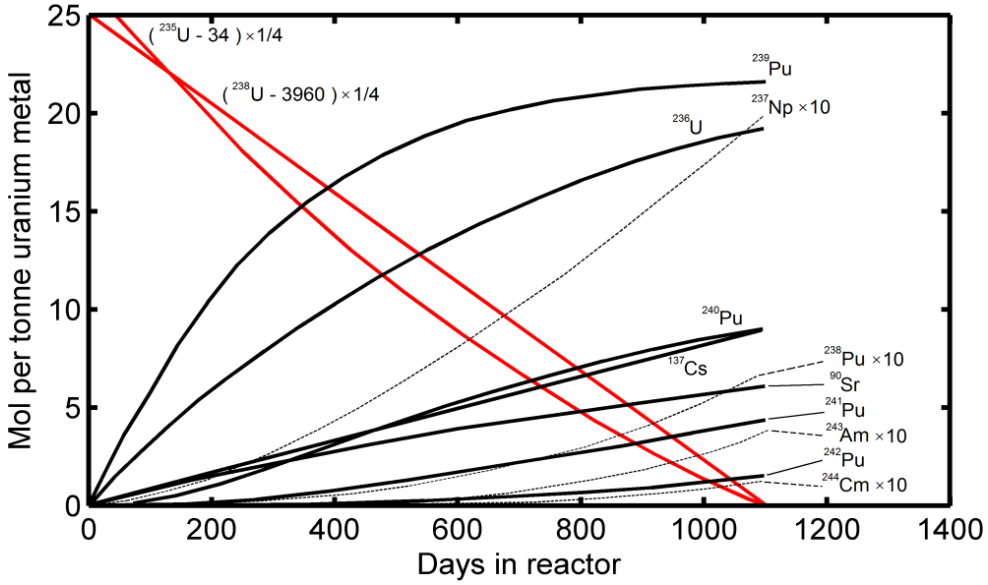

Figure 47: Depletion and growth of various isotopes in UO2 LWR fuel versus time spent in the reactor. Dashed curves are multiplied by 10. Reproduced from [86].

5.3.1 State of spent fuel

The constituents and characteristics of spent nuclear fuel have been a subject of many studies over the years and have been appraised in a number of past and recent review articles and reports [86-95]. The composition of the fuel at discharge from the reactor depends, inter alia, on the initial fuel type, the level of fissile element enrichment, and fuel burnup. The latter is commonly expressed as megawatt days per kilogram heavy metal (MWd/kgU in case of UO_2 fuel) or in percent fissions per initial metal atom (%FIMA). Current discharge burnups are typically in the range of 40 to 65 MWd/kgU for LWR fuel rods, and about 8 MWd/kgU for CANDU fuel. Fuel burnup is the most important parameter for characterizing the state of spent fuel, but it should be remarked that some important aspects of spent fuel correlate poorly with fuel burnup alone. For example, the amount of gaseous fission products residing in the fuel rod free volume and the extent of cladding corrosion also depend strongly on the local temperature history experienced by the fuel pellet and the cladding tube.

At the end of life of LWR UO_2 fuel in the reactor, about 95 % of the used fuel still consists of UO_2. The rest includes fission products and transuranium elements, many of them being radioactive. These components appear in many different forms, and they are usually categorized based on their volatility; see Section 5.5 and the works in [96-99]. An example of the concentration of fission and neutron capture products in UO_2 LWR fuel, irradiated to 30 MWd/kgU, is shown in Table 20 [90].

The distribution of fission and neutron capture products is not uniform within the fuel pellet, due to the fact that the fission density is lower in the interior than at the surface of the pellet (neutron self-shielding), and that fission products migrate by thermal- and radiation-induced diffusion. The steep radial temperature gradient, with temperatures as high as 1700 K at the centreline and decreasing to about 700 K at the pellet rim during normal reactor operation, is very important for this diffusion. Accordingly, the distribution of fission products in the spent fuel is strongly affected by the power history experienced by the fuel during operation. Thermal excursions or overpower transients enhance diffusion and may also cause coarsening of the fuel grains and extensive micro-cracking [100-102].

Table 20: Concentration of fission and neutron capture products in weight part per million (wppm) in UO2 LWR fuel irradiated to 30 MWd/kgU; after [90].

Element	Content (wppm)	Element	Content (wppm)	Element	Content (wppm)	Element	Content (wppm)
Xe	5657	Zr	3639	Ag	92	Eu	155
I	259	Mo	3498	La	1269	Gd	142
Cs	2605	Tc	799	Ce	2469	Np-237	468
Sr	794	Ru	2405	Pr	1161	Pu (tot)	9459
Ba	1741	Rh	484	Nd	4190	Am (tot)	484
Te	529	Pd	1684	Sm	815	Cm (tot)	39

Fission product gases, such as Xe and Kr, and volatile elements, such as Cs and I, migrate to fuel grain boundaries, and eventually can get released to the fuel rod free volume, which is pre-pressurized with helium gas. In spent fuel rods that have experienced normal operating conditions during their lifetime, the gaseous fission products residing in the rod free volume amount merely to a few percent of the gas produced. Fuel rods that have been temporarily operated at high power may on the other hand have significantly larger gap gas inventories. The gap gas inventory is similar in PWR, VVER and BWR fuel rods, but one should note that, because of the higher reactor operating pressure, PWR and VVER rods are fabricated with filled helium gas to a much higher pressure than BWR rods; typically to 2.5 (PWR/VVER) and 0.4 (BWR) MPa, respectively, at room temperature.

In addition to generation and release of gaseous fission products, there is also production of helium during irradiation of UO_2 and MOX fuel. The helium is generated mainly by α-decay of transuranium elements, primarily ^{242}Cm in the short term ($\approx$ 2 years) and later ^{244}Cm, ^{238}Pu and ^{241}Am, as well as α-particles formed by ternary fission [103, 104]. The amount of helium release is correlated to the fission gas release, and measurements show that most of the helium is released at high (>20 %) fission gas release fractions [103]. Since MOX fuel contains significant amounts of Pu isotopes that have shorter path to Cm production (and thereby helium generation), the production of helium is much greater in MOX fuel than in UO_2 fuel [104]. The production and release of helium continues after irradiation. However, the release process is relatively slow and the contribution to the rod internal pressure is small for storage times less than 10 years [105].

LWR spent fuel rods have significantly lower burnup at their ends than in their central part, due to the neutron flux distribution in the core. CANDU fuel rods, by contrast, have higher burnup at their ends, due to flux peaking at the bundle ends. The fuel burnup for both rod designs is heterogeneous across the fuel pellet, namely, it increases markedly at the edge of the pellet, resulting in the so-called “rim effect” or high-burnup structure (HBS) [106]. This partial re-structuring of high burnup fuel is believed to ease fuel pellet fragmentation, fuel axial relocation and dispersal of fuel fines upon cladding rupture; see Sections 5.3.4 and 5.5.5.

The LWR fuel cladding behaviour and degradation at high fuel burnup are briefly discussed in [107, 108]. The main issues are cladding corrosion, cladding hydrogen pickup and embrittlement, rod axial growth, and grid-to-rod fretting wear. A general observation regarding cladding corrosion is that uniform corrosion is more prevalent for PWR than for BWR cladding, mainly because the PWR cladding outer surface temperatures are higher [109, 110]. The existing oxide layer of the spent fuel influences the oxidation kinetics of the cladding at high temperature, should an SFP cooling accident occur. Furthermore, a mixture of Fe and Cr spinel, termed CRUD, collects on the cladding from deposition of Fe, Ni and Cr ions that have entered the coolant by corrosion of stainless steel piping in the primary coolant loop. Since it is loosely bound to the subjacent zirconium oxide and contains various amounts of radionuclides, such as ^{51}Cr, ^{59}Fe, ^{54}Mn, ^{58}Co and ^{60}Co, release of CRUD from spent fuel may aggravate the radiological problem during SFP accidents.

Another consequence of water-side corrosion, particularly in PWRs, is absorption of up to about 20 % of the oxidation product hydrogen in the cladding metal. The terminal solid solubility of hydrogen in zirconium alloys is sufficiently low that brittle precipitates of zirconium hydride accumulate with increasing burnup. This may result in a significant loss of ductility for the cladding tube at normal operating temperatures [111], but the effects of hydrogen at higher temperature are less pronounced [112]. Effects of hydrogen at high temperature are seen mainly for the rupture behaviour, as will be discussed in Section 5.3.5.

5.3.2 Decay heat

The energy produced by the fuel after cessation of the fission process by reactor shutdown is referred to as decay heat. This energy comes from the emission of gamma rays, beta and alpha particles caused by the radioactive decay of fission products and actinides in irradiated fuel. It is an important factor in the analysis of postulated loss-of-coolant accidents and evaluation of emergency core-cooling system performance [113]. This delayed energy represents about 7 % of the total recoverable energy from fission. Around 25 % of this energy is released in the first 10 s after fission cessation, and about 50 % is released within 100 s after fission cessation [113]. There are several processes responsible for heat generation after reactor shutdown. Most of them loose their significance within hours after reactor shutdown, but two are long-term processes and thus relevant for spent fuel [114]:

- *Fission products*. Unstable nuclides will undergo radioactive decay while others, along with many stable fission products, will also be depleted via neutron capture. After reactor shutdown, numerous radioactive fission products remain, which in their subsequent decay produce the major part of the decay heat up to storage times of about 60-80 years for UO_2 fuel. ^{134}Cs is the main contributor for storage times less than about four years. For older fuel, the major contributing isotopes are ^{90}Sr/^{90}Y and ^{137}Cs/^{137}Ba [115].
- *Heavy elements/actinides* dominate the decay heat generation in UO_2 fuel that has been stored more than 60-80 years. The isotopes, such as ^{239}U, ^{239}Np, and ^{239}Pu are produced by neutron capture of ^{238}U via (n,γ) reaction. Also other heavy elements and actinides are generated through (n,α), (n,γ) and (n,2n) reactions and subsequent α and β decays. Examples are the α-emitting ^{238}Pu, americium and curium isotopes, and the curium and californium isotopes that decay via spontaneous fission [111]. For storage times less than ten years, actinide decay contributes a maximum of about 30 % of the total decay heat in UO_2 fuel. For storage times beyond three years, the main contributors are ^{238}Pu, ^{241}Am and ^{244}Cm [115].

The decay heat generated in a specific fuel assembly depends mainly on its power density at end of life (for short living nuclides of half-life $t_{1/2} < 2$ years, such as ^{134}Cs), on its burnup (for long living nuclides with $t_{1/2} > 20$ years, such as the actinides), on both (for intermediate half-lives 2 years $< t_{1/2} < 20$ years, such as ^{90}Sr and ^{137}Cs) and on its storage time in the SFP (because of radioactive decay). Therefore, calculations have to be executed for groups of FAs with similar in-reactor life and storage time to get realistic values for their nuclear decay heat. The calculation can be done for instance with the ORIGEN

computer program [112,113], which has been extensively validated with experimental data [109,114]. Figure 48 shows the time evolution of decay heat produced in a typical BWR UO_2 fuel assembly [115].

According to Figure 48, the assembly decay power drops from about 75 kW to about 0.2 kW between one hour and 40 years of cooling time, i.e., the time from end of the irradiation period. For PWR assemblies and CANDU bundles, the decay power follows the same trend as in a BWR for the same fuel type, but is scaled by the mass of the fuel, i.e. about a factor of 3 for PWR [115] and about 0.1 for CANDU [116].

Systematic decay heat computations for PWR and BWR assemblies fuelled with UO_2 and MOX have been reported in [115]. Computations were made on FAs with discharge burnup levels of 35, 40, 45, and 50 MWd/kgU. The results are presented in terms of the fuel assembly decay heat for MOX and UO_2 fuels and the decay heat ratio of MOX to UO_2 as a function of time up to 15000 days after discharge. The decay heat ratio offers an easy way to compare the MOX decay heat relative to that of UO_2 fuel, and the results show that, for periods beyond the first day, MOX fuel has a higher specific decay power than UO_2. In general, the decay heat ratio (MOX/UO_2) increases with increasing time after discharge and decreases with increasing discharge burnup [115]. In addition, the calculated (MOX/UO_2) decay heat ratios at decay times greater than 10 days are very similar for PWR and BWR fuel assemblies.

The computer models used for calculating decay heat are verified against measurements on spent fuel assemblies, usually carried out with calorimetric [116, 117] or gamma-scan techniques [118, 119]. These measurements also provide the basis for guidelines and standards for decay heat calculations of spent nuclear fuel [120-125]. Measurement campaigns on spent FAs with burnups up to 50 MWd/kgU and cooling times of 11 to 27 years have recently been made [126-128]. The earlier experimental data, i.e. prior to 1994 [123], which was used to support the development of the current U.S. NRC Regulatory Guide 3.54 [120], included measurements on PWR and BWR assemblies with burnup up to 39 and 28 MWd/kgU, respectively, and were limited to cooling times less than 12 years.

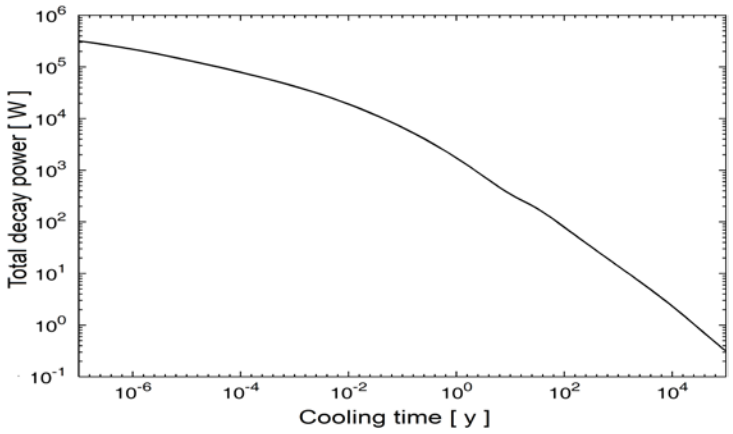

Figure 48: The total decay power versus time (year) produced in a nuclear fuel assembly calculated with ORIGEN-S for a BWR 8×8 fuel assembly with 3 % 235U enrichment and a burnup of 40 MWd/kgU distributed equally over four reactor cycles [118].

5.3.3 Ballooning of fuel rod cladding tubes

In the event of an SFP loss of cooling accident, the fuel rod internal overpressure in combination with elevated fuel cladding temperature will cause the cladding tube to expand in its radial direction, which eventually may lead to tube rupture. As mentioned in Section 5.3.1, at fabrication, fuel rods are commonly pre-pressurized with helium gas at room temperature to 0.4-0.6 MPa and 2.0-3.0 MPa in BWR and PWR

rods, respectively. With accumulation of gaseous fission products and helium released from the fuel to the rod free volume during reactor operation and subsequent storage, the internal gas pressure at room temperature may reach as high as 3.5 MPa and 7.5 MPa in BWR and PWR/VVER fuel rods, respectively [129-131].

The basic parameters controlling the cladding tube deformation are stress, temperature and creep strength; the latter being affected mainly by oxidation, grain size, chemical composition, the anisotropy and the structural phase composition of the material. When the cladding temperature rises above 800 K, the creep becomes fast enough to cause significant inelastic deformation in times of the order of minutes. Most of the data and models on Zircaloy cladding creep in LOCA conditions were produced and assayed during the 1970s and 1980s in various programs and have been reviewed in [112, 132-135]. A short pedagogical review of cladding deformation and failure during reactor accidents including LOCA is given in [136]. An experimental database of the E110 alloy cladding tubes used in VVER type reactors pertaining to LOCA conditions is outlined in [137], and a more detailed account of ballooning experiments on VVER cladding in LOCA conditions can be found in [138].

If the temperature is uniform in the internally overpressurized cladding tube, the high-temperature creep deformation can become unstable: If the diameter of the tube increases at any axial position, the local stress is increased due to the larger diameter and reduced wall thickness, provided that the rod internal pressure does not reduce significantly. This positive feedback enhances the creep rate, which may lead to a runaway deformation ("ballooning") before cladding rupture. However, the cladding temperature in overheated fuel rods is rarely uniform [139]. Erbacher and Leistikow [135, 140], found a systematic relationship between the hoop burst strain and the azimuthal temperature difference on the cladding tube: Small azimuthal temperature variations (ATVs) on the cladding cause a relatively uniform decrease of the cladding wall thickness around the circumference, which leads to relatively large ballooning. Conversely, large ATVs lead to a localized reduction in wall thickness on the hot part of the tube circumference before rupture, and hence, give rise to relatively moderate deformations on a larger scale. A similar effect of the axial temperature variation can be expected.

The cladding high-temperature creep deformation is strongly affected by the phase transformation from the low temperature hexagonal closed-packed (hcp) α-phase to body-centred cubic (bcc) β-phase that zirconium alloy cladding materials undergo in the temperature range from about 1040 to 1250 K [85]. In as-fabricated cladding material, the starting temperature of the $\alpha \rightarrow (\alpha+\beta)$ phase transition is about 1090 K for Zircaloy-4 and around 1040 K for the Zr-1wt%Nb alloy. Similarly, the start of the $(\alpha+\beta) \rightarrow \beta$ phase transition is about 1250 K for Zircaloy-4 and 1210 K for Zr-1wt%Nb [141]. The phase transition temperatures of Zircaloy-2 are considered to be the same as those for Zircaloy-4.

It should be remarked that the phase transition temperatures depend strongly on the oxygen content of the metal [142], which implies that the high temperature creep deformation is affected by cladding oxidation. Oxidation effects were examined by Burton et al. [143, 144], who performed creep tests in the temperature range of 1000 to 1925 K on as-received and pre-oxidized Zircaloy-2 specimens in vacuum. The tests indicated that oxygen has no effect on the creep of β-phase alloy, until the solubility limit of oxygen is reached. However, the creep rate of the α-phase alloy is considerably lowered by the existence of dissolved oxygen. When the alloy was heat treated to produce a two-phase structure of α-phase dispersed in a β-phase matrix, the creep rate observed was dominated by the β-phase [143, 144].

Zircaloy cladding creep measurements in the high-α, (α+β) and β-phase temperature domains from various programs up to 1978 have been assessed by Rosinger and co-workers [145, 146]. Additional data were generated by Donaldson et al. [147-149] during the 1980s, and more recently by Kaddour et al. [141, 150], including also Zr-1wt%Nb cladding samples. They have been assessed in [151, 152] and summarized in Table 21; see also [136].

Table 21: Cladding creep data, i.e. creep strain rate, in α, (α+β) and β domains of Zr-alloys assessed in [151]. Here, Zry stands for Zircaloy and Zr1Nb for Zr-1wt%Nb alloy.

No of meas.	Temp. (K)	Stress (MPa)	Material	Reference
80+115	940-1075	9-59	α-Zry	[141, 145, 149]
60+106	1090-1190	1.5-60	(α+β)-Zry	[145-147]
37+102+102	1255-1710	1-10	β-Zry	[145, 146, 148]
16	1233-1373	1-4	β-Zr1Nb	[141, 150]

Most of these measurements were conducted in inert atmosphere (argon gas and vacuum), which means that they do not address the effects of cladding oxidation on the creep behaviour. An exception is the work by Moulin et al. [153], in which cladding high temperature creep tests were carried out in both vacuum and oxygen environment.

5.3.4 Fragmentation and axial relocation of the fuel pellet column

During normal reactor operation, the fuel pellets crack and form fragments, typically 0.1-1.0 mm in size, due to thermal stresses induced by the steep temperature gradient within the fuel pellets [154, 155]. Also, as mentioned in Section 5.3.1, fuel irradiated to high burnup (e.g. ≥ 50 MWd/kgU) forms a high-burnup structure in the outer portion (rim) of the fuel pellet. The restructured fuel is a highly porous material that can be turned into fine (< 0.1 mm) fragments under LOCA conditions [156-158], due to the thermal-mechanical response of the fuel to the unusual temperature distribution, with high temperature in the peripheral part of the pellet.

Fuel fragmentation affects the propensity for fuel axial relocation and also the degree of fuel dispersion, should the cladding tube fail. Here, fuel axial relocation refers to vertical displacement of fuel fragments *inside* the ballooned cladding tube; axial relocation as a result of fuel rod melting (candelling) is described in Section 5.4.6. The relocation of fuel fragments inside the cladding may produce axial gaps within the fuel pellet column or move additional fuel material to the enlarged volume of the ballooned region, or both. The relocation may thus concentrate the heat load to the ballooned region of the rod, and if the ballooned region fails, the amount of fuel dispersed through the breach may be increased; see Section 5.5.1. Experimental results generated from various programs, conducted over the past 35 years, on fuel fragmentation, relocation and dispersion under LOCA conditions have recently been appraised and summarized by the U.S. NRC in a topical review report [156]. One of the findings from this work is that recent tests [159-161] suggest an aggravating effect of high fuel burnup on fuel fragmentation and dispersal.

5.3.5 High-temperature rupture of fuel cladding

Cladding failure by creep rupture upon ballooning under high temperature conditions is a complicated phenomenon involving many variables. For example, the macroscopic rupture behaviour depends, inter alia, on the temperature, the prevailing phase composition of the alloy, the heating rate, the creep rate, and the oxygen and hydrogen concentration of the metal [162, 163]. Creep rupture of Zircaloy cladding tubes under conventional (in-core) LOCA is supposed to be due to the progressive loss of cross-sectional area by material flow, rather than caused by nucleation, growth and coalescence of cavities on grain boundaries. However, Burton [143] has pointed out that for lower temperatures or for higher oxygen contents, creep rupture by cavitation may become important. More specifically, Burton's criterion is that roughly a 1 wt% oxygen level could induce cavitation at temperatures below 800 °C for cladding stress levels around 20 MPa.

There is a large published database on high temperature rupture of Zircaloy cladding materials, obtained from experiments with temperature ramps and differential pressures until failure occurred. The data generated prior to 1979 have been tabulated and systematized in [164], where also empirical correlations for cladding burst strain versus burst temperature were proposed for safety analysis. Additional data, up to 1983, have been reviewed by Rosinger and co-workers [165-167], Erbacher et al. [135, 168] and Parsons et al. [132]. Rosinger [169] has assessed the Zircaloy cladding burst data, and has provided a simple rough model for predicting cladding failure during a LOCA. The evaluated data consist of about 700 points and comprise a wide range of test conditions: constant pressure or closed-tube tests in inert gas or vacuum and constant pressure or closed-tube tests in steam or oxygen atmosphere. Some of the burst data are on irradiated cladding materials. Further data on cladding rupture under LOCA conditions obtained from various tests programs conducted during the 1970s and 1980s are systematized in [134]. The data include both ex- and in-reactor, single- and multi-rod tests.

The high-temperature creep rupture behaviour of Zr-Nb type cladding materials has been addressed in more recent studies: The M5 (Zr-1wt%Nb) alloy was studied on as-fabricated cladding samples within the French EDGAR programme [170] under both isothermal and transient temperature conditions. A few data on the ZIRLO (Zr-1.0Nb-0.7Sn-0.1Fe by wt%) cladding material are also available in open literature [160, 171, 172], and the E110 cladding used in VVERs has been investigated and compared with that of Zircaloy-4 [138]. The latter experiments comprised single-rod and multi-rod ballooning tests on unirradiated cladding tube samples. The single-rod samples were as-received, pre-oxidized to various oxide layer thicknesses or pre-iodized. The water-side oxidation was reported to have an appreciable effect on the rupture strength of the E110 alloy [138].

Effects of oxide layer thickness and high hydrogen concentration on the ballooning and rupture properties of unirradiated Zircaloy-4 cladding have been studied by Kim et al. [173]. Some as-fabricated cladding samples were oxidized to oxide layer thicknesses of 20 and 50 μm or hydrogenated to contents of 300 and 1000 wppm hydrogen. All the pre-oxidized samples ruptured below 1273 K and their deformation at time of rupture was appreciably less than that of the as-fabricated samples. The hydrogen-charged samples had lower burst ductility than the as-fabricated ones for temperatures below 1073 K and higher values beyond this temperature [173]. Effects of oxidation have also been reported in [167], while effects of hydrogen were studied in [174].

Since the creep rupture mechanism is intrinsically time dependent, the heating rate has a fairly strong effect on the failure behaviour: increasing the heating rate leads to higher burst temperatures [162]. As mentioned in Section 5.3.3, also the temperature distribution affects the cladding burst behaviour: Large azimuthal temperature variations during the course of cladding deformation lead to a localized reduction in wall thickness on the hot part of the tube circumference, and so, give rise to relatively low overall burst strains. There are a number of investigations that provide a reasonable explanation for this effect, e.g. [132, 133, 139, 175-177].

Finally, experimental studies indicate that the pressurization (loading) rate of the cladding during the ballooning period has an important effect on burst pressure [138]. In case of fast pressurization, the cladding rupture will take place at significantly higher pressure, compared to slow pressurization rates. During an SFP LOCA, the fuel rod internal pressure will increase slowly, concurrently with the temperature increase, while the external pressure is almost constant. For this reason, the cladding burst will take place at lower pressure compared to reactor LOCA conditions, when the fast drop of primary system pressure leads to fast increase of the pressure difference between the inside and outside of the fuel rod.

5.4 Fuel assembly and rack degradation

The physical and chemical phenomenology during a postulated severe accident in a SFP is different from the phenomenology of a severe accident in a reactor core, due to different configurations and boundary conditions. The most important differences for the modelling of an SFP accident are the low heat load of the fuel assemblies in the SFP (< 20 kW/FA) compared with the heat load in the reactor core

(> 100 kW/FA) and the much lower ambient pressure compared with a reactor transient. These factors reduce strongly the rate of accident progression and heat-up; in particular the oxidation phenomena observed in the low temperature region below 1200 K become much more important. This is in contrast with a severe accident in a reactor core, where the heat-up to temperatures above 1200 K happens rather fast. Therefore, severe reactor accident codes may need adjustments for use in simulations of SFP loss of coolant or loss of cooling accidents; see Section 7.4. Model validations for SFP boundary conditions by integral and separate effect tests are important for the prediction of SFP accident scenarios.

5.4.1 Oxidation in steam, oxygen and nitrogen mixtures

Different chemical reactions with the oxidant (overheated steam, oxygen and nitrogen) take place in a gaseous atmosphere at temperatures significantly above water boiling temperatures. According to the oxidation rate models, the oxidation reaction is very slow at lower temperatures and increases exponentially with increasing temperature. The following reactions between the oxidants and the zirconium alloy cladding material will take place:

$$Zr + O_2 \rightarrow ZrO_2 + 1101\ kJ/mol \quad (1)$$

$$Zr + 2H_2O \rightarrow ZrO_2 + 2H_2 + 528\ kJ/mol \quad (2)$$

$$Zr + ½N_2 \rightarrow ZrN + 365\ kJ/mol \quad (3)$$

The reactions (2) and (3) are strongly suppressed in presence of oxygen. Under conditions of oxygen starvation, followed by oxygen recovery, additional so called back reactions will take place:

$$2H_2 + O_2 \rightarrow 2H_2O + 573\ kJ/mol \quad (4)$$

$$ZrN + O_2 \rightarrow ZrO_2 + ½N_2 + 736\ kJ/mol \quad (5)$$

In the presence of steam and under oxygen starved conditions, the zirconium nitride will be oxidized by:

$$ZrN + 2H_2O \rightarrow ZrO_2 + ½N_2 + 2H_2 + 163\ kJ/mol \quad (6)$$

In principle, all six reactions (they are all exothermic) will take place in parallel, according to the availability (partial pressure) of the oxidants and according to their temperature dependent reaction rates. It should be mentioned that the energy release of the reactions given above strictly applies to standard temperature and pressure, and in particular, is temperature dependent. Most of the severe accident (SA) codes only take into account the reactions (1), (2) and (4). The latter one is implemented in the containment models of hydrogen combustion. Reaction (3) is only taken into account in the SA codes ATHLET-CD, ICARE/CATHARE and ASTEC; see Appendix D. In MELCOR and some versions of SCDAP-based codes, there is a differentiation between the oxidation kinetics in oxygen and air, based on air oxidation separate effect tests by Argonne National Laboratory (ANL) [178, 179], but only using the nitrogen as catalyst and not as reactive specie. The remaining reactions (5) and (6) are not modelled in any severe accident code. To include these reactions, separate effect tests have to be executed with different mixtures of the oxidants at different temperatures to obtain a data base for the estimation of the reaction rate laws; see Section 6.2.1.1. Experiments at Karlsruhe Institute of Technology (KIT) in Germany [180] showed that reaction (3) is extremely slow with pure zirconium, but comparatively rapid with sub-stoichiometric zirconium oxide and with oxygen-stabilized α-zirconium. The formation of ZrN increases the porosity of the oxidised layer, due to the higher density of ZrN compared with ZrO_2. Consequently, the oxidation rates after oxygen recovery strongly increase, because of the loss of oxide protectiveness. The reactions described above of course can occur not only between zirconium and the different oxidants, but also between other metals (e.g. steel from the spent fuel racks oxidized in steam or air).

As mentioned in Section 5.2.1, the production of hydrogen in a SFP building may pose a particular danger of a possible combustion, because the presence of enough air in the SFP building cannot be excluded and the absence (typically) of hydrogen management equipment [181].

5.4.2 Chemical heat and nuclear heat

In the SFP, the FAs have lost most of the heat load due to the decay of the short living fission products. The heat load for a typical 17×17 PWR spent fuel assembly is therefore between 1 and 15 kW, depending on the reactor power density, the fuel storage time and burnup. While the chemical heat of the oxidation below 1500 K makes only a minor contribution to the total heat load during a reactor accident, as the nuclear heat is much higher, it is a major driving force in the spent fuel accident after reaching about 1200 K. Temperature feedback effects on the oxidation process may then initiate a temperature escalation, resulting in cladding and fuel degradation. After complete oxidation of the metallic part of the spent fuel (zirconium and steel), the chemical heat is missing and the nuclear heat alone will drive the further accident progression.

5.4.3 Oxidation layer breakup and porosity

During a long lasting oxidation process in a SFP under steam environment, the oxide layer of the cladding material may break at temperatures below 1300 K by reaching a certain thickness [182]. This is accompanied by accelerated oxidation at the affected locations. The so-called breakaway thickness increases strongly with temperature, from about 10 µm at 900 K to 70-100 µm at 1300 K [183]. In case of a reactor accident, the heat load of the fuel assembly is much higher than 100 kW, so that the temperature increases rather fast and 1300 K will be reached before the oxide layer would exceed the breakaway thickness. In a SFP, where the heat load of the FAs is significantly below 20 kW, the heat up is much slower, so that the oxide breakaway thickness can be reached at low temperatures and then lead to an additional heat-up by increasing reaction rates.

The mechanism appears to be a consequence of two factors: In the temperature range below 1300 K, the oxide has a monoclinic microstructure. This causes the oxide scale to take on a layered morphology, which is susceptible to flaking off under the compressive stresses that arise due to the volume change from metallic to oxide. At higher temperatures, the microstructure is tetragonal, causing a columnar morphology that is much more robust to compressive stress. In addition, cladding materials are very hard at temperatures up to about 1000 K and cannot easily deform to relieve the stress produced in the oxide layer. This stress leads to the breakup of the oxide crust if a given temperature dependent thickness is exceeded. At temperatures above about 1000 K (the range in which ballooning occurs during LOCA transients), the cladding material becomes more plastic and apt to relax stresses from the oxide layer. This reduces the tendency for oxide breakaway at higher temperatures. However, it is somewhat more complicated than that, since strong breakaway behaviour has been observed at temperatures in the 1250 to 1300 K range, which coincides with the monoclinic-tetragonal transition temperature. The controlling mechanism may be related to a destabilizing effect of transition between microstructures.

Separate effect tests, summarized in Section 6.2.1.1, have shown that the parabolic kinetics (the oxidation rate decreases at a given temperature as the oxide thickness increases) changes to nearly-linear kinetics if breakaway occurs; in fact, the transition from pre- to post-breakaway is not instantaneous, but occurs progressively, possibly after a delay. Accelerated oxidation may occur as the post-breakaway state develops. The broken oxide layer presents a much weaker barrier to the diffusion of oxygen atoms (from steam or oxygen molecules). Reaching the breakaway conditions will increase the oxidation rates by more than one order of magnitude by reducing the protectiveness of the oxide layer. Figure 49 shows the post breakaway linear growth velocity for the oxide layer versus temperature, as measured in isothermal separate effect tests [180, 182, 184]. It can be clearly seen, that with increasing temperature, also the post breakaway linear oxide layer growth velocity increases. At temperatures above 1000 °C, no breakaway occurs in steam or oxygen oxidation. At a temperature of 600 °C, it takes about 5 weeks to completely

oxidize the cladding, but at a temperature of 700 °C, complete oxidation of the cladding is reached after half a week. So, even if no temperature escalation will be reached, loss of cladding integrity by oxidation may lead to fission product release.

Exposure of oxidizing cladding to nitrogen can trigger breakaway-like behaviour at all temperatures, which shows a similar effect although the controlling processes are different. In this case, any loss of integrity of the oxide scale enables nitrogen to penetrate and form porous nitrides beneath the oxide and break up the overlying oxide, if the oxide is not completely stoichiometric. This is frequently the case, especially if the steam or oxygen mole fraction is rather low. The zirconium nitride thus formed breaks up the microstructure and increases the porosity, allowing the gases reactant to penetrate more readily, thus the process is self-perpetuating or even self-enhancing.

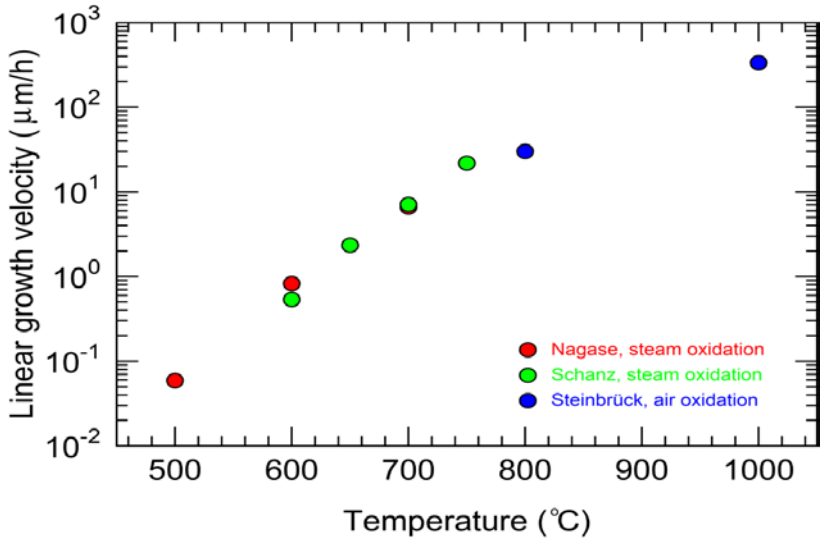

Figure 49: Temperature dependency of post breakaway oxide layer linear growth velocity. Data from [180, 182, 184]**.**

Post-breakaway oxidation has been found in experiments to accelerate the consumption and starvation of oxidant. Synergies between the damaged oxide layer, the re-oxidation of nitride according to equation (5), and the effect of starvation on the stoichiometry may promote very rapid oxidation and severe excursion during later reflood, if coolant injection is recovered. Such effects have been observed in integral tests on electrically heated fuel assemblies; see Section 6.2.2.3.

5.4.4 Radial and axial heat transfer

Heat removal from the FAs in a SFP accident is due to heat convection, heat conduction and heat radiation. In a closed rack design, heat convection and heat conduction is only possible in the axial direction, but radiation will transfer the heat both axially along the FA and radially between adjacent FAs. The spent fuel racks in the pool act as radiation barriers, which reduce the radial heat transfer between assemblies. In case of a total loss of coolant accident, the heat up starts at the same time for all FAs. In case of a boil-down accident, however, it is expected that stored FAs will start to heat up at different points in time, due to differences in their decay power. While the total heat load of the SFP is responsible for the boil down velocity, a distributed load pattern will influence the accident progression in the very late phase of cladding degradation: in earlier phases, the temperature differences are too small for significant heat radiation between FAs with different heat loads. A distributed storage pattern of fuel elements with similar heat loads will delay the accident progression; see Section 2.1.3.

5.4.5 Eutectic metal reactions and melting

Eutectic reactions occur between the zirconium-alloy cladding materials and uranium oxide as well as between B_4C and steel. The latter reaction is possible in an SFP cooling accident only if the control rods are stored among spent fuel assemblies. This is the case, e.g. for VVER-1000, where used B_4C control rods are generally stored by inserting them in spent FAs. In some SFPs, especially with high density storage, the racks are loaded with boron-aluminium absorbers. The eutectic reactions mostly lead to an earlier liquefaction of the materials, which means, the relocation into the lower pool area will start earlier; see Section 6.2.2.1. Because of the low heat load and the low heating rate, most of the metals will be oxidized before reaching melting temperatures. In large scale experiments under SFP boundary conditions [12], no melt pool inside the FAs could be observed, but part of the aluminium metal melted and was candelling downwards in the FA. This behaviour is not prototypical, because zirconium will form eutectic melt with UO_2, but not with MgO.

5.4.6 Candelling and relocation

After reaching temperatures above 1700 K, the steel of the racks and even earlier (slightly above 900 K) part of the built-in absorption material (borated aluminium sheets at the rack walls), which has only slightly lower temperatures than the fuel cladding because of the slow heat-up process, will start to melt. These materials will flow downwards (candelling) and solidify in cooler regions of the FA. The accompanying loss of support may also lead to relocation of partially degraded cladding and fuel materials and it will open a cross flow pathway due to failure of the rack. The materials will relocate into the water filled gap between the pool bottom and the lower end of the active fuel, causing a stronger steam production and possibly energetic interaction because of their high temperature. If there had been oxidant starvation in the upper fuel region, this would cause a strong temperature increase due to renewed oxidation.

CANDU spent fuel bundles are stored in multiple layers of racking in the SFP. The fuel bundles that are not submerged in water during a loss of cooling/coolant accident will heat up and deform. The heatup will lower the strength of each of the racks, likely leading to a situation that the total weight of all the uncovered/overheated fuel bundles/racks rests on the rack that is just beneath the water level. When the accumulated total weight exceeds the load bearing capability of the rack, the rack gives in and transfers the entire load to the next underneath. The process continues, resulting in a cascading effect and a sudden relocation of the bundles/racking materials onto the bottom of the pool. The collapse of the racks in the SFP could re-submerge fuel temporarily and stop hydrogen generation until the remaining water in the pool boils off.

5.4.7 Corium-concrete interaction

After the complete boil down of the water in the SFP, the oxidation rate of the cladding materials will be strongly reduced, and therefore, the dominant heat source of the accident scenario will be absent. It is uncertain if the nuclear heat alone will be sufficient to heat up the fuel, zirconium oxide, steel oxide and remaining metal to the melting temperature of the corium and start the concrete degradation by corium-concrete interaction. This is dependent on the total nuclear heating of the spent fuel. A distributed load pattern will decrease the possibility of a corium-concrete interaction further, because of a wide spreading of the high heat load fuel debris on the bottom of the SFP; see

Figure 6. The corium-concrete interaction is further discussed in Section 5.5.4.

5.5 Fission product release and transport

The main factor that governs volatile fission product (FP) release from the fuel is the fuel temperature. Release from the SFP during an accident is therefore proportional to the extent of fuel degradation in the

pool, i.e. the fraction of fuel exposed to high temperature and the duration of this exposure. For description of release from the fuel, the various fission products may be classified into the following groups [98]:

- *Volatiles*: release of volatiles is not significantly, i.e., beyond the effect of the structural changes of the fuel matrix, influenced by redox conditions on release (Xe, Kr, Cs, I). Release of volatiles from the fuel is usually complete before the fuel starts to melt.
- *Semi-volatile and low-volatile FPs*: the release rate of semi-volatile FPs (Mo, Rh, Ba, Pa, Tc) and low-volatile FPs (Ru, Ni, Sr, Y, La, Ce, Eu) is very sensitive to the oxidizing or reducing conditions.
- *Non-volatile FPs*: negligible release before the fuel melts (Zr, Nd, Pr).

The possibility of air ingress into the pool during a severe accident increases the risk of large Ru release and also significant release of fuel fines. In the following, the main phenomena of FP release are described for four subsequent stages of fuel degradation.

5.5.1 Cladding rupture

Cladding rupture may occur at lower temperature for SFP cooling accidents than for reactor accident scenarios, since there are end-of-life fuel rods with maximum internal pressure in the pool and the outer pressure is atmospheric. The complete fuel rod plenum and gap inventory of noble gas is considered to be released at the cladding rupture event. As mentioned in Section 5.3.1, this inventory normally amounts merely to a few percent of the gas produced [185], but in rods that have experienced overpower transients during its in-reactor lifetime, it could reach around 20 % of the total noble gas inventory (see e.g. Figure 18 in [92]). Certain amounts of volatile iodine and caesium might be released at cladding rupture as well. However, it seems that very limited data about iodine and caesium release from a spent fuel rod on cladding rupture are available. Some valuable results were produced in the experimental series FLASH; results of the FLASH-5 test with irradiated fuel indicated that the release fraction of noble gases, iodine and radioactive caesium was between 1 and 2 % of the inventory during the simulated LOCA scenario [186]. Also, the evaluation of measured activity data from the Paks cleaning tank incident (see Section 3.3) provided important information on the release of different radioactive isotopes from damaged fuel. The analyses of the Paks incident showed that 1-3 % of the inventory of iodine, caesium and noble gases was released from the fuel [34].

Due to possible fuel fragmentation, small fragments of fuel might be expelled from the failed cladding at the fuel rod depressurization. As mentioned in Section 5.3.4, recent tests suggest an effect of fuel burnup on the propensity for fuel fragment dispersal upon cladding rupture. Fragmented fuel pellets can also relocate from the upper part of the rod above the cladding breach. Usually, cladding failure occurs near the top of PWR fuel rods, so the amount of relocated fuel will not be significant. For BWR fuel rods, cladding failure is likely to occur at the top of the fully populated section of the FA; therefore, relocation of fuel fragments from the full length rod sections above the cladding breach might be significant.

5.5.2 Fuel heat-up

Due to the air in the SFP building, fuel heat-up during an SFP cooling accident may occur in an oxygen-rich atmosphere. Below 175 °C, exposure of fuel to air is not an issue [187]. However, at a temperature of only 500 °C, UO_2 oxidation is particularly rapid. Oxygen penetrates rapidly the grain boundaries, converting them to U_3O_8, which occupies about 30 % more volume than the parent UO_2. The boundaries split and the grains separate from the matrix. They can then be attacked from all sides, continue to oxidize and fragment further. The final particle size, typically with 50 % of the mass in particles less than 10 μm in diameter, can be small enough that the particles (also called fuel fines) become airborne [188].

U_3O_8 is the equilibrium phase in air at 1100 °C. At higher temperatures, fuel fragmentation is less severe, partly because oxidation proceeds more as a front moving through the fuel pellet and partly because U_3O_8 becomes less brittle. Above 1200 °C in air, UO_3 is formed, which is a gas under these conditions

[188]. The described fuel volatilization at high oxygen potential can be compared with UO_2 volatilization in vacuum, which starts to be significant only at 2000 K [189]. Particles released during fuel volatilization at relatively low temperature may still contain large fractions of its initial FP inventory, even volatiles.

The only reference where an estimation of release of fuel fines from the pool can be found is NUREG-1738 [25]. There, the release of fuel fines was simply taken the same as for the Chernobyl accident; the fraction of fuel released as fuel fines is estimated to about 4 % [190]. This source term was considered to be bounding, because the Chernobyl accident involved more extreme conditions than can be expected for accidents in SFPs [25]. The size of fuel particles released from Chernobyl is estimated to be 10 µm (Activity Median Aerodynamic Diameter, AMAD) [190]. Released fuel particles contained about 80-90 % of the activity of non-volatile radionuclides, such as ^{95}Zr, ^{95}Nb, ^{140}La, ^{144}Ce and transuranium elements embedded in the uranium matrix of the fuel. Activity of such a particle was 0.1-1 kBq.

If the fuel is oxidized to compositions close to U_3O_8, the high oxygen potential permits to oxidize elements that are normally in the metallic state, e.g. Mo, Tc or Ru, and eventually makes the formation of complex phases more likely, e.g. $(Ba,Sr)MoO_3$, Cs_2MoO_4, RuO_3, RuO_4 or MoO_2 [191, 192]. These compounds are much more volatile than the elements, so that high releases would be expected under strongly oxidizing conditions. Fission product release experiments conducted in air-rich environments are summarized in Section 6.2.1.2.

In Appendix 4B of NUREG-1738 [25], the Ru release fraction from the SFP was proposed to be 0.75, the same as for volatile fission products[6]. Ruthenium is assumed to be released in the oxidic form. This source term of ruthenium is considered in NUREG-1738 to be bounding for several reasons. Firstly, the rubble bed formed by the spent fuel after heat-up to about 2500 K is expected to limit the potential for ruthenium release to a value less than that for volatile fission products. Secondly, following the Chernobyl accident, ruthenium in the environment was found to be in the metallic form [190, 193]. Metallic ruthenium (^{106}Ru, $t_{1/2}$ = 371.5 d) has about a factor of 50 lower dose conversion factor for inhalation than the oxidic ruthenium. Size of particles containing Ru released from Chernobyl is estimated to be 10 µm (AMAD) [190]. Particles were formed of metallic condensate with activities 0.5-10 kBq (per-particle).

The release of volatile fission products from hyperstoichiometric uranium oxide will be enhanced by favourable changes of the diffusion coefficient, and by the structural transformation of the fuel. Additionally, the very high volatility of the matrix itself and fuel fragmentation, as described above, will boost the release of volatile fission products. Otherwise, the influence of redox conditions on volatile FP release is minor.

Complete release of volatiles can be assumed from degraded-molten fuel. The total release of volatiles would then be proportional to the fraction of degraded fuel in the pool. It should be noted that ^{137}Cs ($t_{1/2}$ = 30.05 y) was considered as the radionuclide with most important radiological consequences from the inventory of 10 years old spent fuel [194]. Size of particles containing volatile fission products (Cs and I) released from Chernobyl is estimated to be 0.4-0.7 µm (AMAD) [190]. Particles containing Cs were fairly insoluble [190].

5.5.3 Fuel melting

Release of volatile fission product from the molten fuel will be (almost) complete. For other fission products, release from the molten fuel is governed by vaporization of species from the melt. The equilibrium vapour pressure above the melt obeys Henry's law [195], and the vaporization rate is thought to be surface limited [196].

[6]. For comparison, the Chernobyl source term reported in 190. *Chernobyl: Assessment of radiological and health impacts (2002 update of "Chernobyl: Ten Years On")*, 2002, OECD Nuclear Energy Agency, Paris, France. is: Ru > 3.5 %, Xe 100 %, Cs 30-40 %.

5.5.4 Molten fuel concrete interaction

Molten fuel interaction with concrete of the pool basemat would be very similar to what is known for scenarios of molten corium concrete interaction (MCCI) in the reactor cavity for reactor accidents, as described elsewhere, see e.g. [197]. The difference would be in specific decay heat (lower for the SFP scenario), amount of corium (larger for SFP scenario) and area of the basemat (larger for SFP scenario). The specific mass of corium per area of basemat would be similar. The concrete ablation rate would be lower, due to lower specific decay heat, but production rate of hydrogen and other non-condensable gases might be even higher. It is very likely that the hydrogen concentration would reach the limit for global hydrogen burn, even in very large free volume of the building in a few days [198]. Global hydrogen burn means destruction of the non-hermetic reactor building. Passive autocatalytic hydrogen recombiners are usually not installed in SFP buildings. For SFPs located in an isolated containment, MCCI in the pool would cause similar challenge to containment integrity as for MCCI in the reactor cavity (assuming reactor without core catcher or in-vessel retention capability).

5.5.5 Transport of released fission products

Transport of released fission products to the environment would be qualitatively different for an SFP located inside the isolated reactor containment than for an SFP in a non-hermetic building or non-isolated (open or failed) containment. Phenomena relevant for FP transport in the case of an SFP severe accident in the isolated containment are the same as for in-reactor severe accident described elsewhere, e.g. [197]. In the following text, it is assumed that the SFP is located in a non-hermetic building. Transport of fission products released from the fuel to the environment is driven by the bulk flow of steam and gas from the pool. For the loss of cooling or partial loss of coolant accidents, the bulk flow is driven at first by steam from the coolant boil-off and later by thermal expansion of gas in the pool and its buoyancy due to sensible heat. For the complete loss of coolant accident, it is gas thermal expansion from the beginning of scenario.

In case of air ingress to the overheated stored fuel assemblies and zirconium fire, the flow driven by thermal expansion of gas and its buoyancy is considered to be able to transport large aerosols and fuel fines to the environment. The possibility of retention of released material above the release point in the assembly would be very limited. Fuel fines and larger aerosols might be trapped by turbulent impaction on obstacles, such as spacer grids or upper nozzles. Significant deposition of Ru compounds can also be expected, even on relatively hot surfaces [98]. However, these deposits would be resuspended on assembly collapse. SFPs are usually not covered. For the VVER plant design, the SFP is covered by panels. Still, there are enough openings to avoid pressure rise above the pool, and retention due to the coverage would be limited.

Retention of material transported by the escaping gas from the SFP building depends on the construction of the building. The key parameter is the free building volume, which means that large buildings have larger retention capability. Concentration of transported materials would be diluted by mixing in a large volume, gas would be cooled and steam condensed on constructions inside of the building. In a large building, the effective velocity of gas towards opening(s) would be low to provide time for aerosols to deposit on surfaces, mainly by gravitational settling. Large buildings also provide volume to dilute hydrogen released from oxidation and decrease risk of destructive global hydrogen burn. Another important factor is the size of the building leak opening(s): Too large opening size would decrease retention capability, too small opening would increase risk of building failure due to overpressure by escaping gas or local hydrogen burns. Finally, it is the ultimate strength of the building, measured by maximum static internal overpressure and maximum dynamic load, which should allow the building to withstand the accident. After several days of MCCI, it is very likely that the amount of produced burnable gas would be sufficient to destroy non-hermetic buildings by a large burn. It would cause some resuspension of deposited material. Beneficial effect of large building volume was analysed for VVER-440/213 type of plants with a large reactor building common to twin units [198]. However, the effect of zirconium fires was not considered in this study.

6 EXPERIMENTS WITH RELEVANCE TO SFP COOLING ACCIDENTS

In the following, we review separate effect tests (SETs) and integral tests with relevance to SFP cooling accidents, carried out worldwide since the 1980s. The considered tests were done to shed light on the fuel behaviour and degradation mechanisms under high temperature accident conditions, and to generate data needed for verification and calibration of computer codes. It should be made clear that most of the reviewed tests were not primarily intended to study SFP accidents, but were targeted to study reactor LOCA: This means that they reproduce fairly high temperatures, high heating rates and steam environment. The only integral tests that have been specifically targeted to SFP cooling accidents are those conducted by Sandia National Laboratories, USA, within the SFP Heatup and Propagation Project (BWR fuel) and the OECD/NEA Sandia Fuel Project (PWR fuel). Integral and separate effect tests have also been done to reproduce conditions and phenomena in the Paks cleaning tank incident; see Section 3.3.

The considered integral tests are experiments done on fuel (sub)assemblies with electrically heated fuel rods; no integral tests have been done on spent (irradiated) fuel. The tests vary considerably with respect to scope and objective, but they are all deemed to provide knowledge necessary for understanding and modelling important phenomena related to SFP accidents.

6.1 Experiments focused on SFP cooling accidents

6.1.1 Tests conducted at Sandia National Laboratories

In 2001, the U.S. Nuclear Regulatory Commission staff performed an evaluation of the potential accident risk in a SFP at decommissioning plants in the United States. The resulting report, NUREG-1738 [25], describes a modelling approach for a typical decommissioning plant with design assumptions and industry commitments, the thermal-hydraulic analyses performed to evaluate spent fuel stored in the SFP at decommissioning plants, the risk assessment of SFP accidents, the consequence calculations, and the implications for decommissioning regulatory requirements. Some of the assumptions in the accident progression in NUREG-1738 were known to be conservative, especially the estimation of fuel damage and source term.

The U.S. NRC continued SFP accident research by applying best-estimate computer codes to predict the severe accident progression following various postulated accident initiators. The computer code studies identified various modelling and phenomenological uncertainties that prompted a need for experimental confirmation for both PWR and BWR SFPs. The experiments were conducted at Sandia National Laboratories, where the BWR programme was run from April 2004 until November 2006. The PWR experimental programme (2009-2013) was part of an international effort established with the Organization for Economic Co-operation and Development and includes the 13 countries: Czech Republic, France, Germany, Hungary, Italy, Japan, Norway, Republic of Korea, Spain, Sweden, Switzerland, United Kingdom, and the United States (with the U.S. Nuclear Regulatory Commission as the operating agency).

The main objective of the experimental work was to provide basic thermal-hydraulic data associated with a loss-of-coolant accident. The accident conditions of interest for the SFP were simulated in a full-scale prototypic fashion (electrically heated, prototypic fuel assemblies in a prototypic SFP rack) so that

the experimental results closely represent actual fuel assembly responses. A major impetus was to facilitate severe accident code validation and reduce modelling uncertainties within the computer codes.

6.1.1.1 Sandia BWR experimental program

Three scales of fuel assemblies were used in the experiments. Initial tests were conducted at a small scale in order to assess the performance and suitability of zirconium clad electrically-heated spent fuel rod simulators. The fuel rods were filled with high density MgO ceramic pellets, sized to precisely match the thermal mass of spent fuel. Two tests were conducted in order to demonstrate that the heater design was capable of initiating a zirconium fire. The second scale examined a single, full-length highly prototypic fuel assembly (stainless steel, Zircaloy, and Incoloy versions) inside a prototypical pool rack cell. The stainless steel rod assembly was unheated and only used for the hydraulic characterization. The Incoloy fuel assemblies were used to conduct high temperature tests while minimizing complications of oxidizing Zircaloy surfaces. The Zircaloy version of the full-length FA was used for tests that were taken to conditions of high temperature oxidation and ignition. The final scale was five Zircaloy short (1/3 length) assemblies in a 3×3 pool rack. The short array of assemblies was designed to simulate a slice from the middle to upper portion of an array of full-length FAs. This was accomplished in the final ignition test by accurately controlling both the flow rate and temperature of air introduced into the bottom of each partial assembly.

Two types of testing were conducted: (i) separate effect tests and (ii) integral tests. In the separate effects tests, the experiments were designed to investigate a specific heat transfer or flow phenomenon, such as thermal radiative coupling or induced natural convective flow. These tests were non-destructive and involved some non-prototypic materials (e.g. stainless steel and Incoloy). In the integral tests, all hydraulic flow and heat transfer phenomena were investigated simultaneously. These tests were specified with boundary conditions that led to the destruction of the experimental apparatus and thus involved a limited number of more complex experiments. Post-mortem examination of the integral test assemblies revealed gross distortion of the pool rack and channel box, rubblization of the tubing bundle, and accumulation of debris on the bottom tie plate that resulted in flow blockage. Flow blockage was also evident from molten aluminium (originating from Boral plates built into the pool rack) that collected on and below the bottom tie plates. A unique aspect of this project was the deliberate close coupling of the experiments with numerical analysis, where the principal code used was the severe accident code MELCOR [12]; see Appendix D.

6.1.1.2 Sandia PWR experimental programme

The study was conducted in two phases. Phase 1 focused on axial heating and burn propagation. A single full-length 17×17 PWR test assembly was constructed with a prototypic fuel skeleton (Figure 50) and zirconium-alloy clad heater rods. The assembly was characterized in two different-sized storage cells.

Phase 1 started with separate effect tests, where the assembly hydraulic and thermal-hydraulic responses were investigated. It concluded with an ignition test to determine where in the assembly ignition first occurs and the nature of the burn in the axial direction of the assembly. The pool cell was completely insulated to model boundary conditions representing a “hot assembly”, which is a typical bounding scenario.

Phase 2 addressed axial and radial heating and burn propagation, including effects of fuel rod ballooning. Five full-length assemblies were constructed. The centre assembly was of the same heated design as used in Phase 1. The four peripheral assemblies were unheated, but highly prototypic, incorporating prototypic cladding tubes and end plugs. These boundary conditions experimentally represent a “cold assembly” situation, which complements the bounding scenario covered by Phase 1. Similarly, this phase started with separate effect tests, including hydraulic and thermal-hydraulic

measurements. Studies using this test assembly concluded with a fire test, in which the centre assembly was heated until ignition occurred. The fire eventually propagated axially and radially to the peripheral assemblies, as predicted. Fuel rods in two of the four peripheral assemblies were pressurized with argon, and the fuel rods ballooned when the zirconium-alloy cladding reached a high enough temperature. The two peripheral assemblies without pressurized rods were compared to evaluate the effect of ballooning.

Figure 50: Single fuel assembly for Phase 1 PWR testing in construction stage.

Figure 51 gives the normalized measured peak cladding temperatures and flow rates as a function of normalized time for the centre and peripheral assemblies. Both temperature data series have been truncated because of the failure of the thermocouples at elevated temperatures. The first major disturbance in the flow occurs at approximately 1.06 of the normalized hour and corresponds to the loss of electrical power in the centre assembly. A sharp decrease in the peripheral assembly flow rates was recorded after 1.37 of the normalized hours, which coincides with the time when the ignition front had progressed across the entire cross section of the peripheral assemblies. Debris was observed exiting the bottom of the inlet pipes and may be the cause of the erratic signals at times greater than 1.58 of the normalized hours.

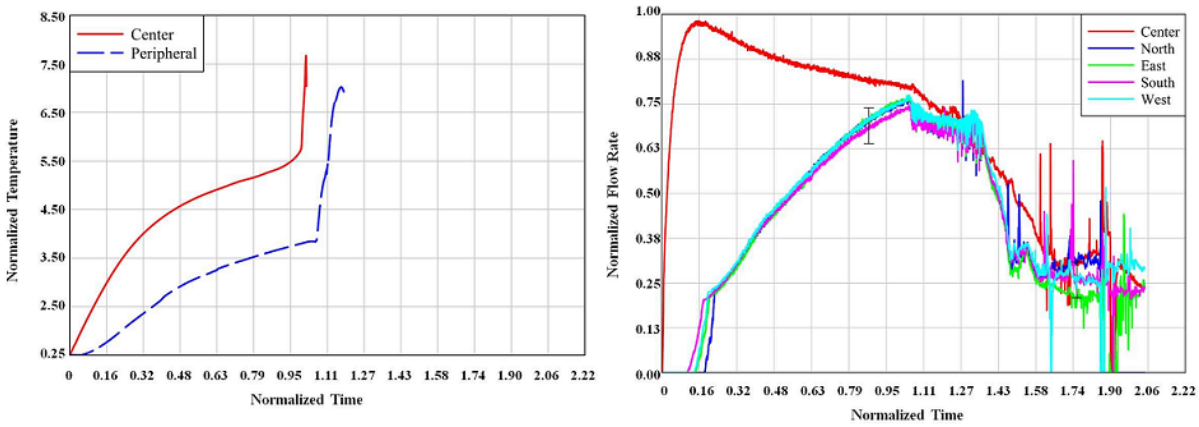

Figure 51: Normalized temperatures and flow rates as a function of time for Phase 2 test data.

6.1.2 Experimental simulation of the Paks cleaning tank incident

The conditions of the Paks cleaning tank incident (see Section 3.3) were simulated in integral experiments in the CODEX test facility [199]. Small scale separate effect tests were performed in Hungary to support the understanding of several special phenomena [200].

6.1.2.1 Integral simulation of the cleaning tank incident in the CODEX facility

The CODEX facility included electrically heated fuel rod bundles, and the whole scenario of the Paks incident was simulated in tests CODEX-CT-1 and CODEX-CT-2. The most important difference between these two tests was the operation of an off-gas valve on the top of the cleaning tank model. In the CODEX-CT-1 test, the hydrogen produced by metal-water reactions was released from the test section so that the internal pressure in the cleaning tank model was kept constant. During the CODEX-CT-1 test, 270 l of H_2 was released, the atmosphere contained 60-80 vol% hydrogen, and the average degree of oxidation was above 20 %. In the CODEX-CT-2 test, the produced hydrogen was not released from the tank model during the dry phase.

The CODEX-CT experiments illustrated that part of the coolant could bypass the fuel assemblies in the cleaning tank and did not take part in removing decay heat. In case of low coolant flow rate, a steam volume could be formed in the tank, and after that, the upper part of the bundles was not cooled. The maximum temperature in the upper volume of the cleaning tank was probably in the range of 1200-1300 °C, while the bottom part of the fuel assemblies was cooled by water.

The long time (seven hours) oxidation in the cleaning tank could have produced a several hundred μm thick oxide scale on the zirconium surfaces. A significant part of the hydrogen produced in the steam-Zr reaction was absorbed by the Zr components. The maximum hydrogen concentration in the metal could reach 20000 wppm, comparable to that in pure ε-phase zirconium hydride. The high temperature period of the incident took place in hydrogen-rich steam atmosphere, where the maximum hydrogen concentration could be above 80 vol%. If the hydrogen could not be released from the cleaning tank, the oxidation of zirconium could be suppressed and the less oxidized surfaces could produce a temperature excursion during the final quenching.

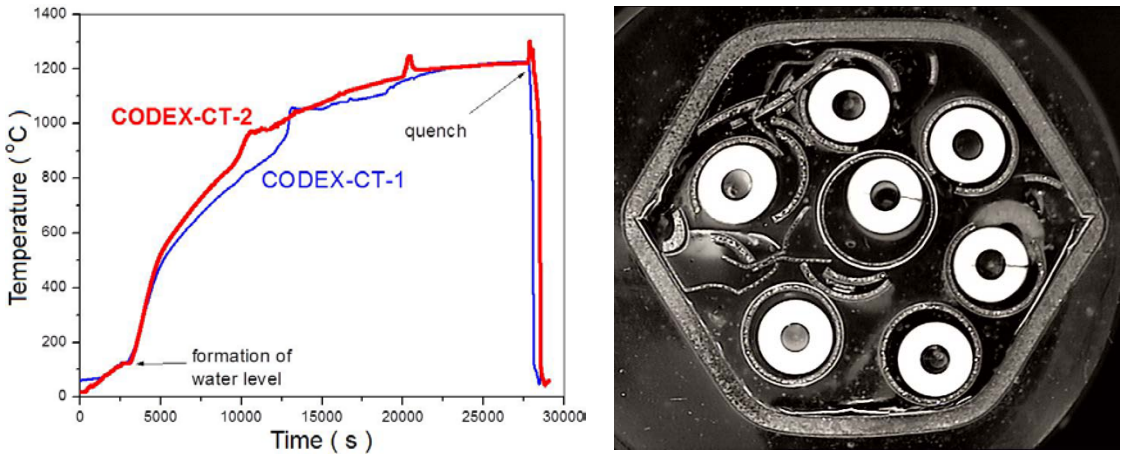

Figure 52: Rod temperature histories (left) in the CODEX-CT experiments and cross section of a test fuel bundle (right), showing ballooning and fragmentation of the cladding [199].

The post-test state of the test fuel rods showed many similarities with the conditions observed after the incident at the Paks NPP. For this reason, it is likely that the thermal conditions and the chemical reactions

in the tests represented those in the incident. Post-test examinations of the CODEX bundles indicated that the high degree of embrittlement was a combined result of oxidation and hydrogen uptake by the zirconium components [199].

6.1.2.2 Separate effect tests to investigate specific phenomena of the incident

In order to improve the understanding of the phenomena that took place during the Paks cleaning tank incident, several series of separate effect tests have been carried out in Hungary:

- The COHYRA experiments provided detailed information and new numerical correlations on the oxidation, hydrogen uptake and embrittlement of the E110 type cladding in high temperature hydrogen-rich steam. The collected experimental data are available in the OECD NEA IFPE Database [137, 201].
- Investigation of high temperature interactions between the cladding and the spacer grid during ballooning of fuel rods indicated that the local stresses did not create cracks in the vicinity of the contact and the cladding did not become weaker in this region. The mechanical testing of ballooned and oxidised bundles showed that the radial load could be easily transferred by the spacer grid and this fact explained the reason for breaking of many fuel rods at the position of the spacer grid during the Paks incident [200].
- According to high temperature tests with short fuel rod samples, interactions between the steel spring and the zirconium cladding did not lead to failure of the cladding in the investigated range of parameters (up to 1200 ºC). The external spiral shape observed on some fuel rods in the Paks incident was explained by a combined effect of mechanical and chemical interactions between the cladding and the spring in steam atmosphere [200].
- High temperature tests with small fuel bundles confirmed the possibility of upward shifts of fuel assemblies due to a rocket force type effect during reflood. The intense production of steam inside of the bundle could lift up the assembly if it was covered by shroud and was not fixed. Such situations potentially can take place in SFPs with VVER or BWR fuel assemblies [200].

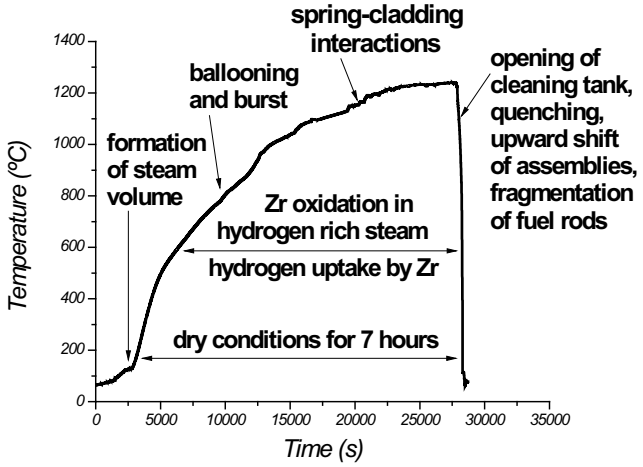

Figure 53: Some specific phenomena observed in the Paks cleaning tank incident [200].

6.2 Experiments related to SFP cooling accidents

In addition to the tests described above, which were targeted directly to SFP accidents, there are also tests that address phenomena of relevance to SFP accidents, although most of the experiments were aimed primarily to study fuel degradation during severe reactor accidents in which air enters the overheated core. Table 22 provides a bridge between the phenomena described in Chapter 5 and the different experiments of this kind that are detailed in the sequel.

Table 22: Link between the accident phenomenology described in Chapter 5 and the different experiments detailed in the following subsections.

Phenomena	Related experiments	
	Separate effect tests	Integral tests
Thermal-hydraulics	Siphon breakers: (KAERI)	Boildown: QUENCH (KIT) Reflooding: QUENCH (KIT), PARAMETER (LUTCH)
Fuel behaviour, fuel assembly and rack degradation	Cladding high temperature oxidation in air: (ANL, IRSN, JAEA, KFKI AEKI, KIT) B_4C interaction: BECARRE (IRSN)	PHEBUS FP (IRSN) QUENCH (KIT) CODEX AIT (KFKI AEKI) PARAMETER (LUTCH)
Fission product (FP) release and transport	FP release in air-rich environment: (CEA, CRL, JAEA, ORNL, UKAEA)	PHEBUS FP (IRSN)

6.2.1 Separate effect tests

6.2.1.1 Cladding air oxidation tests

Although early tests [202-208] showed that the high temperature oxidation kinetics of zirconium is different in air than in steam, air oxidation of Zr-based cladding materials was not thoroughly investigated until recently. Most of the data have been produced over the last decade, with the aim to investigate and formulate computational models for cladding degradation either under SFP loss-of-coolant accidents or in the late phase of severe reactor accidents, where an overheated and previously steam-cooled core is exposed to air or nitrogen through a breach in the reactor pressure vessel (RPV). Since these two accident scenarios are different, SETs on air oxidation have been carried out over a fairly wide range of conditions. Most tests have been done on Zircaloy-4 cladding, but data are available also for Zr-Nb type materials like M5, ZIRLO and, to a lesser extent, E110. Differences in air oxidation behaviour among these materials are observed mainly for temperatures below 1300 K.
For Zircaloy-4, high temperature oxidation test have also been conducted in nitrogen, nitrogen-steam and air-steam mixtures. Table 23 is a summary of tests done on cladding in as-fabricated (bare) condition. There are also SETs on the impact of cladding preoxidation in steam/oxygen on subsequent exposure to high temperature air or nitrogen; these are summarized in Table 24.

All tests summarized in Table 23 and Table 24 were done on unirradiated materials. Spent fuel characteristics were simulated by pre-test oxidation, in one case combined with hydrogen charging [179]. All tests were done at atmospheric pressure with flowing argon used as a carrier gas to the reactive species.

The use of argon may have some influence on gas diffusion, but this seems not to have been evaluated. Another similarity among the tests is that weight gain measurements were used to quantify the oxidation/nitriding kinetics. The weight gain versus time provides information on the *average* kinetics for a sample, and is a good measure as long as the oxidation or nitriding is uniform. However, this is not always the case at high temperature. It should also be remarked that nearly all tests were carried out on mechanically unloaded samples, which means that they do not capture the accelerating effect of cladding deformation (ballooning) on the oxidation. This effect is attributed to continuous breaking of the protective oxide layer as the cladding balloons; a few available tests [178] suggest that the oxidation may be up to 20 % faster during deformation. Another restriction is that nearly all tests have been done at constant temperature. Data from only a few non-isothermal air oxidation tests with constant heating rates up to 4 K/min [209] and 50 K/min [210] are available in the open literature.

Table 23: Summary of separate effect tests on high temperature air oxidation/nitriding of bare (non-preoxidized) cladding tubes. Test types: Thermogravimetry (TG), periodic retrieval (PR) and end retrieval (ER). Specimen types: Open-end (OE) and closed-end (CE) tube segments; see text.

Tested materials	Test type	Sample type, length (mm)	Testing temp (K)	Testing gas	Refe-rence	Comments, remarks
Zr-4	ER	OE, 30	1173-1423	Air, O_2, N_2, H_2O	[207]	Also tests on pre-hydrided samples
Zr-4, Zr-2	ER, PR	OE, 27	623-773	Air	[206]	Also tests on samples dipped in saltwater
Zr-4, M5, ZIRLO	PR	CE, 75	573-1173	Air	[178]	
ZIRLO	PR	CE, 75	573-873	Air	[179]	Tests on pre-hydrided samples
Zr-4, E110	TG	OE, 8	1073-1473	Air, O_2	[211]	
Zr-4	ER	OE, 20	1073-1673	Air + H_2O	[211]	50 % air + 50 % steam
Zr-4, E110	ER	OE, 8	1073-1473	Air, O_2, N_2	[212]	Tests with limited oxidation/nitriding
Zr-4	TG	OE, 10	1073-1673	Air, O_2, N_2	[180]	
Zr-4	ER	OE, 20	1073-1773	Air + H_2O	[180]	9 air/steam mixtures
Zr-4	ER	OE, 20	1273-1473	N_2 + H_2O	[180]	5 nitrogen/steam mixtures
Zr-4, M5, ZIRLO	TG	OE, 20	973-1853	Air	[210]	Also tests with 5-50 K/min heating
Zr-4	TG	OE, 7/20	873-1473	Air	[213]	
M5	TG	OE, 20	873-1273	Air	[213]	
Zr-4	TG	OE, 20	1073-1473	N_2	[214]	

The tests listed in Table 23 and Table 24 differ with regard to applied test specimen designs, gas flow rates and weight gain measuring techniques. Diverse preoxidation conditions were also used among the tests in Table 24. The specimen design used in most tests was an open end tube section, allowing oxidation of both the inner and the outer surface. Lengths from 7 to 30 mm were used. Long samples are advantageous to minimize the relative effect of the end surfaces, but disadvantageous with regard to gas ingress to the inner surface. For this reason, closed end tube sections have been used in some studies [178-180]. The specimen dimensions may affect the measured reaction kinetics, if the gas flow rate is insufficient to make up for the gas reacted with the metal. This problem is most probable for large samples, low gas flow rates and high reaction rates, i.e. for high temperatures and the fast initial oxidation phase of bare samples.

From Table 24, it is clear that preoxidation was done in either steam or oxygen at diverse temperatures. Preoxidation temperatures around 800 K were used in several studies to generate cladding oxide layers, believed to be typical for spent fuel, within a reasonable time. However, recent tests [214] show that these oxide layers are much less protective than oxide scales that are formed slowly under simulated PWR conditions. Another problem is that, for some cladding materials, preoxidation in steam at 800 K leads to much higher hydrogen concentrations than typically found in cladding that has corroded during normal in-reactor operation [213]. This can be avoided by preoxidizing the samples in oxygen instead of steam.

Table 24: Summary of separate effect tests on high temperature air oxidation/nitriding of preoxidized cladding tubes. Test types: Thermogravimetry (TG), periodic retrieval (PR) and end retrieval (ER). Specimen types: Open-end (OE) and closed-end (CE) tube segments; see text for details.

Tested materials	Test type	Sample type, length (mm)	Testing temp (K)	Testing gas	Preox temp (K)	Preox gas	Refe-rence	Comment, remark
Zr-4	ER	CE, 150	873-1173	Air	823	H_2O	[178]	Internal pressure 0.35-2.76 MPa
Zr-4, M5, ZIRLO	PR	CE, 75	573-1173	Air	823	H_2O	[178]	Some tests with 2.5% O_2 + 97.5% N_2
ZIRLO	PR	CE, 75	573-873	Air	823	H_2O	[179]	Tests on pre-hydrided samples
Zr-4, E110	TG	OE, 8	1073-1473	Air, N_2	1073-1473	O_2	[211]	
Zr-4	TG	OE, 10	1073-1673	Air, N_2	1073-1673	O_2	[180]	
M5, ZIRLO	TG	OE, 20	1273-1473	Air, N_2	1273-1473	O_2	[210]	
Zr-4	TG	OE, 10/20	873-1473	Air	773	H_2O	[213]	
M5	TG	OE, 20	973-1273	Air	773	H_2O	[213]	
Zr-4	TG	OE, 20	1073-1473	Air, N_2	773	O_2	[214]	
Zr-4, M5	TG	OE, 10	1123-1273	Air	PWR-like	H_2O	[214]	Slow preoxidation in autoclave

As indicated in Table 23 and Table 24, different techniques were used to measure the weight gain versus time. Thermogravimetry (TG), with on-line recording of the sample's weight during the test, allows

a precise determination of transitions (breakaways) in the oxidation kinetics. Periodic retrieval (PR) of the samples for weighing outside the test chamber gives cruder resolution of the kinetics. It also necessitates cooling/heating cycles that may affect the oxide layer [206], and there is also a risk of losing oxide flakes during handling. The weight gain was measured only once for the tests marked ER (end-of-test retrieval) in Table 23 and Table 24. To evaluate the oxidation kinetics with this technique, a large number of tests are needed on identical samples that have different exposure times.

In addition to the SETs in Table 23 and Table 24, the open literature contains a few more detailed studies of the oxidation/nitriding processes and the oxide layers formed in air. A study by Steinbrück et al. involved annealing of Zircaloy-4 samples, having oxygen concentrations in the range from 0 to 35 wt% (from pure β-Zr to stoichiometric ZrO_2), in nitrogen gas at 1473 K for one hour to determine the kinetics and mechanisms of nitrogen reactions with different parts of an oxidized cladding tube [180]. Micro-Raman spectroscopy was used by Idarraga and co-workers [215, 216] to study oxide layers formed on initially bare samples of Zircaloy-4 and M5 cladding exposed to air at 1073-1273 K. The oxides were characterized in order to determine the oxide structures associated with protective and non-protective behaviour. Micro-Raman line scans from the oxide-metal interface to the scale surface were performed to study the variations in oxide crystal structure and chemical composition as a function of position in the oxide. A comparative analysis of electron transport properties of oxide layers formed in steam and air at temperatures around 750 K on Zircaloy-4 and Zr-1wt%Nb cladding tubes is also available in the literature [217].

6.2.1.2 Tests on release of fission products and actinides in air-rich environment

Experimental programs with SETs on the release of fission products and actinides from spent fuel under accident conditions have been conducted at several facilities. A fairly recent, however inexhaustive, overview of experiments can be found elsewhere [218]. Here, we briefly summarize studies done at various facilities, with emphasis placed on tests done in air: As explained in Section 5.5, when the fuel cladding has been completely oxidized, the air environment may significantly increase the oxygen-to-metal ratio of the fuel. This accelerates the release of certain fission products, e.g. low-volatile species like ruthenium [195]. We consider only SETs done on spent fuel; experiments on trace-irradiated fuel or un-irradiated fuel with simulated fission products (simfuel) are not reviewed here. Experiments of the latter kind, addressing ruthenium behaviour in air-rich environments, are reviewed in [219].

Tests performed to date have been done out-of-reactor by annealing small samples of spent fuel under controlled temperature and environment conditions, notably in hydrogen, steam, air or mixtures thereof. The gas composition and temperature controls the oxygen potential globally. All tests have been conducted at atmospheric pressure, except for four tests done at 1 MPa [220]. Most tests have been isothermal, with temperature and hold time as key parameters, but results from non-isothermal tests with stepwise or constant rate heating are also available. Samples comprising either bare fuel pellet fragments or short segments of spent fuel rods (pellets housed in their original cladding) have been tested. Most available data are from tests on CANDU UO_2 fuel, which has low or no enrichment of ^{235}U and lower discharge burnup than LWR fuel. Only four tests have so far been done on MOX fuel [98, 220]. The out-of-reactor storage time for the tested fuel ranges from months to decades, which means that the fuel samples had significant differences in radionuclide inventory. In the most recent studies, fuel samples have been re-irradiated shortly before testing in order to rebuild the inventory of short-lived isotopes.

Several series of SETs on fission product release from spent UO_2 fuel have been conducted at Oak Ridge National Laboratory, USA [221]. Three of the tests were done in air: Two tests in the HBU series, conducted on 305 mm long Zircaloy-4 clad PWR fuel rod segments irradiated to about 30 MWd/kgU, were done in dry air [222]. Both test rods were hermetically sealed, except for a simulated pin-hole type failure in the form of a Ø 1.6 mm hole drilled through the cladding at the centre of the fuelled section. The testing temperature and hold time were 773 K and 20 h for rod HBU-5 and 973 K and 5 h for rod HBU-6 [222].

Notwithstanding the low temperatures, both rods released considerable amounts of ruthenium during the tests, probably as a result of air oxidation of the fuel pellets. A later test at ORNL, VI-7, was done in moist air at a peak temperature of 2300 K [223]. The test rod was a 152 mm long BWR fuel rod segment, irradiated to 40 MWd/kgU. End caps were pressed onto both ends of the sample to keep the fragmented fuel pellets in place, but they did not provide gas seals. The sample was held at the peak temperature for 20 min, which was obviously too short for fuel oxidation and the associated acceleration of fission product release to occur [221, 223].

Since 1983, more than 300 annealing tests have been done on irradiated UO_2 fuel in various experimental programs on fission product release at the Chalk River Laboratories (CRL), Canada. The tests have been done at temperatures from 800 to 2350 K on bare fuel fragments, fuel fragments enclosed in Zircaloy foil bags, and on short Zircaloy-clad fuel rod segments with unsealed caps fitted onto the ends [218, 224]. Tests with clad fuel generally show delayed release of fission products compared to tests on bare UO_2 under otherwise identical conditions. The delay is primarily associated with the time required to oxidize the cladding, after which the UO_2 begins to oxidize and cause enhanced release rates [225]. Tests at CRL have been conducted in flowing steam, hydrogen, air and mixtures thereof. Some of the CRL tests done in air are summarized here.

The Metallurgical Cell Experiment 1 (MCE1) test series was conducted on bare UO_2 CANDU fuel fragments with a burnup of 10.7 MWd/kgU. Five of the eight samples were tested in air, and held at constant temperatures of 1970 to 2350 K for about 15 minutes. The remaining samples were tested in $Ar+H_2$ mixtures at comparable temperatures and hold times [226]. The observed release fractions were significantly higher for the air-exposed samples.

The Hot Cell Experiment (HCE) series HCE1, HCE2 [227], HCE3 [228], and HCE4 [229] were conducted at the CRL during the 1990s. Most tests were done in steam, but each series also comprised one or a few tests done in air environment. Most specimens were 20-25 mm long fuel rod segments with unsealed end caps, but also bare UO_2 samples were used in the HCE1 and HCE2 series. The HCE2 series was special in the sense that samples of both CANDU and PWR UO_2 fuel were examined. The objective was to compare the release kinetics of these two fuels in steam and air environments at temperatures between 1620 and 1920 K [227]. It should be remarked that the tested PWR fuel had a burnup of 57 MWd/kgU, which is about seven times the typical discharge burnup of CANDU fuel.

The UCE12 experiment series at CRL [225] was targeted to assess the effects of oxidizing environments on fission product release during an accident, and to compare the release from bare UO_2 with that from fuel rod segments in order to understand the role of the cladding. A total of 20 tests were done on CANDU fuel samples with a burnup of 15-18 MWd/kgU. Peak temperatures ranged from 1370 to 1900 K, and tests were done in argon, steam, air and steam followed by air [225]. Of particular interest are test 14, which was done on bare UO_2 fragments, test 16, carried out on a fuel rod segment with end caps at both ends, and test 20, which was done with a fuel rod segment having only one end cap. These tests were all done in air under identical conditions, except for the aforementioned differences in sample configuration. The results show that the cladding has a retarding effect on fission product release, also when it is severely oxidized [225].

During the 1980s and 1990s, out-of-reactor annealing tests on bare as well as clad samples of irradiated UO_2 were carried out at the Harwell laboratory of the UK Atomic Energy Authority (UKAEA), using different sweep gas mixtures. Very little information on these tests can be found through electronic databases, and it is unclear to what extent the test results are available in open literature. Some data on the release kinetics of both ^{106}Ru and volatile fission products from bare samples of UO_2 fuel exposed to air have been presented for temperatures in the range of 570-870 K [230]. Another reported study covers fuel oxidation and release of gaseous fission products at even lower temperatures [231].

Two programmes with SETs on high-temperature fission product and actinide release from PWR fuel specimens have been conducted at the Grenoble centre of the French Commissariat à l'Energie Atomique

et aux Energies Alternatives (CEA) [218]. The HEVA programme, which was run between 1983 and 1989, comprised eight tests conducted in various mixtures of steam and hydrogen at peak temperatures between 1900 and 2370 K [232]. The VERCORS programme, which was run from 1989 to 2002, was an extension of HEVA with modified apparatus, higher temperatures and augmented instrumentation [98]. It comprised in total 17 tests in three different series of experiments. Most tests were run in steam, hydrogen or mixtures thereof; one test was run in a mixture of 90 % He and 10 % air. With the exception of two tests on bare UO_2 fragments, the tested samples consisted of short PWR fuel rod segments, comprising three spent fuel pellets in their original cladding. Two half-pellets of fresh depleted uranium served as plugs at either end of the segment. Two of the VERCORS tests were done with MOX fuel samples; the other tests used UO_2 fuel with burnups ranging from 38 to 72 MWd/kgU. The fuel samples were in most cases re-irradiated shortly before testing, in order to re-establish the inventory of short-lived isotopes. A recent summary of the VERCORS programme is given in [98]. A new CEA test programme, named VERDON, is underway within the International Source Term Programme (ISTP). The test matrix comprises four tests, similar to those conducted at the end of the VERCORS programme. At present, three of the tests have been carried out: one test on high-burnup UO_2 fuel in mixed H_2/H_2O environment and two tests on MOX fuel, respectively in air/H_2O and H_2O environment. The fourth test is to be done on MOX fuel with reducing environment.

The Japan Atomic Energy Agency (JAEA) has conducted a series of ten annealing tests on high burnup fuel within the VEGA program, which was run from 1999 to 2004 [220]. The tests were done in either steam or helium, using UO_2 or MOX fuel with burnups ranging from 43 to 56 MWd/kgHM. The UO_2 fuel was sampled from both BWR and PWR spent fuel rods, and the MOX fuel originated from the Fugen Advanced Thermal Reactor (ATR). The peak temperature was between 2770 and 3120 K in the tests, which is higher than in other tests reported to date. The VEGA facility is also unique in the sense that it can be pressurized up to 1 MPa, and four of the tests were run at this pressure. Except for three tests carried out on short fuel rod segments, including the cladding, the tests were done on bare fuel samples. Two of the clad samples were re-irradiated before testing to re-establish the inventory of short-lived isotopes [220].

6.2.1.3 Tests on siphon breaker effectiveness

Separate effect tests on the effectiveness of siphon breakers have recently been conducted at the Korea Atomic Energy Research Institute (KAERI) [14]. The experimental setup consisted of a large water tank with a line connected at the bottom of the tank, and a penetration level at the upper part. This line could be connected to the atmosphere at two different levels located below the bottom of the tank. Different siphon breaking devices were installed on the line: siphon breaking holes with diameters between 30 and 55 mm, and siphon breaking lines with diameters between 25.4 and 63.5 mm. Several pressure transducers were installed as well as an ultrasonic flow metre. Three parts of the line were equipped with flow visualization in order to interpret the siphon breaking phenomenon.

The test matrix spanned a range of parameters, such as break vertical location, break size, type of siphon breaker (line or hole), and dimension of the siphon breaker. The tests conducted showed that "*siphon breaking is triggered by filling a horizontal pipe with air at its highest position*". However, the experiments were not able to determine if triggering of the siphon breaking is linked to the integrated quantity of entrained air or to the air flow rate.

6.2.2 Integral tests

6.2.2.1 International Phébus fission product programme

The international Phébus Fission Product programme (Phébus FP) [233], conducted by IRSN, investigated key phenomena involved in LWR severe accident sequences through five in-reactor integral experiments in the Phébus reactor at Cadarache, France. The facility provided prototypic reactor conditions, which allowed the study of basic phenomena governing core degradation all the way to the late phase, hydrogen production, fission product release and transport, circuit and containment phenomena, and iodine chemistry. Although these tests were not targeted to study the severe accident progression in a SFP, most of the findings of the Phébus FP tests are applicable to SFPs.

Five tests were performed between 1993 and 2004. FPT-0 to FPT-3 used a 1 m high bundle of 21 fuel rods. The fuel degradation was studied parametrically with respect to the coolant flow rate, the control rod type (Ag-In-Cd, "AIC" or B_4C absorber material), fuel irradiation and the value of the bundle power at end of the test. FPT-4 addressed release of low volatile FPs and actinides from a pre-fabricated debris bed. The main conclusions are given in [218, 233-235]. In summary, they are:

- Cladding oxidation (runaway) was more violent than expected in FPT-0 on the basis of earlier experiments and led to improved understanding of oxidation laws and degradation. The criteria were revised and good simulations are now obtained for a large spectrum of different situations;
- Liquefaction of fuel and the transition from a rod-like geometry to that of a melt pool takes place at temperatures of 2500 ±200 K, well below the melting temperature of pure UO_2 (3100 K).
  The severe degradation appears to be linked to important chemical interactions between the fuel and structural materials, principally the Zircaloy cladding;
- The presence of control rod materials accelerates and enhances core degradation, with the effect of B_4C being somewhat greater than that of AIC. Oxidation of the B_4C in FPT-3 led to no significant CH_4 production; it led mainly to CO and CO_2 formation, depending on temperature and steam availability;
- Re-frozen melt pools in the PWR cases consisted mainly of U/Zr/O oxidic mixtures with small amounts of stainless steel oxides.

These integral experiments were supplemented by separate-effects tests to understand better the phenomena observed, and to serve as a basis for model development and improvement. Specifically, the European Commission (EC) funded International Source Term Programme [236] included small-scale tests on air oxidation of Zr-based cladding (MOZART series [214]) and on B_4C oxidation and interactions with structural materials (BECARRE series at IRSN Cadarache). Also relevant is the VERDON series of tests mentioned in Section 6.2.1.2, which are part of the ISTP. These tests are done at CEA, Cadarache, France, to study fission product release and its links with core degradation, including effects of air ingress and burnup.

6.2.2.2 Karlsruhe QUENCH tests

The QUENCH experimental programme is conducted in Karlsruhe[7], Germany, in order to investigate the effect of reflood on bundle degradation. The program, which started in 1996, is on-going and about 20 tests have been done up to now [237, 238]. A number of integral bundle experiments with 21-31 electrically heated fuel rod simulators of 2.5 m length, using zirconia (ZrO_2) as fuel substitute, have been conducted. The influence of different parameters on bundle degradation and reflood were investigated:

[7]. Until October 2009: Forschungzentrum Karlsruhe, thereafter Karlsruhe Institute of Technology.

degree of pre-oxidation, temperature at reflood initiation, flooding rate, effect of neutron absorber materials (B_4C, AIC), air ingress, type of cladding alloy, and steam starvation conditions.

Among the different QUENCH experiments, the air ingress tests QUENCH-10 and QUENCH-16 are of particular interest for SFP accidents. These tests confirmed the strong accelerating effect of air on fuel assembly degradation, especially when pre-oxidation in steam is limited and when oxygen starvation occurs during the air ingress phase. These tests are further described in Section 6.2.2.3, along with other integral fuel degradation test done in mixed steam/air environments.

Another experiment with relevance for SFP cooling accidents is the boil-down test QUENCH-11, which was performed with the main purpose of investigating fuel bundle behaviour during boil-off and subsequent quenching at a low water injection rate [239, 240]. A steady boil-off and a corresponding top-down uncovery of the test bundle was achieved by applying power from an electric auxiliary heater at the bundle bottom in addition to the electric bundle power. When the water level had fallen, water was injected into the lower plenum at a rate of 1 g/s, enabling a nearly stable water level and an extension of the boil-off phase. Quenching of the bundle was performed at a maximum measured bundle temperature of 2040 K with a rather low water flow rate, i.e. 18 (17+1) g/s, compared to the standard water injection rate of approximately 50 g/s. The conditions led to enhanced cladding and shroud oxidation, quite similar to standard conditions of forced-convection steam flow. In the upper part, the test bundle was significantly degraded by oxidation and melt formation.

6.2.2.3 Integral fuel degradation tests with mixed steam/air environment

There are some recent integral tests that address phenomena of relevance to SFP loss of cooling accidents, although the experiments were aimed primarily to study fuel degradation during severe reactor accidents in which air enters the overheated core. More precisely, these tests simulated loss of reactor coolant accidents involving a first phase with high temperature steam (or oxygen) oxidation of the fuel assemblies, followed by a phase with air oxidation, resulting from air ingress through an assumed breach in the reactor pressure vessel.

Integral tests of this kind have to date been carried out at three different facilities. All the tests were done out-of-reactor on part-length sub-size fuel assemblies of PWR or VVER design with electrically heated rods. The rods had no or negligible internal overpressure during the tests, which means that possible accelerating effects of creep deformation on cladding oxidation and degradation were not addressed. As shown in Table 25, the tests differed with respect to fuel rod and test assembly design, and also regarding the chemical environment, temperature and duration of the steam and air oxidation phases. In two of the tests, the fuel was brought back to room temperature by cooling in argon, while quenching with room temperature water was used in the remaining tests.

The CODEX-AIT (Core Degradation Experiment – Air Ingress Test) experiments were conducted at KFKI AEKI, Hungary, with the aim of examining the effects of air on cladding and fuel pellet oxidation [241]. Two tests were done during 1998-1999 on the same 9×9 square assembly design, but the tests differed with regard to the oxidizing conditions; see Table 25. The AIT-1 test assembly was preoxidized in argon-oxygen rather than steam, in order to avoid hydrogen production in the test rig. During the preoxidation, a fast and uncontrollable temperature escalation up to almost 2300 K occurred before the assembly was cooled with flowing argon. The AIT-2 test assembly was supposed to be preoxidized in argon-steam, but due to a valve leak, the environment was argon-steam-air. Both tests were terminated by cooldown in cold argon, following the air oxidation phase. Due to the imprecision in the cladding preoxidation conditions, the CODEX-AIT tests are less suitable for model calibration and validation. However, these seminal tests clearly indicated accelerated cladding oxidation and degradation processes in

air compared with steam [241]. Oxidation of the UO_2 fuel pellets to higher oxides (U_3O_8) was expected in the high-temperature air environment, but was not observed in the tests.

Table 25: Summary of integral tests on fuel degradation in high temperature air, following a period with high temperature preoxidation in steam or oxygen.

	CODEX AIT-1	CODEX AIT-2	QUENCH 10	QUENCH 16	PARAME-TER-SF4
Test assembly design:					
Size and arrangement	9 rods, square		21 rods, square		19 rods, hex
Cladding material	Zircaloy-4		Zircaloy-4		E110
Cladding OD (mm)	10.75		10.75		9.13
Fuel pellet material	UO_2		ZrO_2		UO_2
Heated length (mm)	600		1024		1275
Steam oxidation phase:					
Environment	Ar+O_2	Ar+H_2O+air	Ar+H_2O	Ar+H_2O	Ar+H_2O
Temperature (K),	1220-2250,	1020, 1800	1620-1690,	1300-1430,	1420-1470,
hold time (s)	~100	1170,1800	6780	4000	5890
Air oxidation phase:					
Air flow rate (g/s)	3.5	2.5	1.0	0.2	0.5
Argon flow rate (g/s)	0.0	0.7	3.0	1.0	2.0
Start temperature (K)	1170	1020	1190	1000	1170
Peak temperature (K)	2270	2150	2200	1870	2030
Hold time (s)	500	1000	1800	4040	1450
Reflooding phase:					
Coolant	Cold Ar	Cold Ar	RT water	RT water	RT water
Temperature excursion?	No	No	No	Yes	Yes
Peak temperature (K)	-	-	-	2420	2300
Resulting damage:					
Posttest state of test assembly and the enclosing shroud	Mainly intact structure. Top spacer broken and relocated.	Relocation of fragmented and molten material.	Severe damage to assembly and shroud.	Relocated melt from upper half of the assembly.	Relocation of fragmented and molten material. Shroud failed.

The QUENCH-10 and QUENCH-16 experiments were done at Forschungszentrum Karlsruhe[8], Germany, using test assemblies with 21 PWR type fuel rods. The assemblies were thus larger than in the CODEX-AIT tests, and another difference was that the electrically heated rods contained annular pellets of ZrO_2 rather than UO_2; see Table 25. The QUENCH-10 test was done in 2004 with the aim to study the effect of air on extensively preoxidized fuel assemblies; the preoxidation phase in argon+steam resulted in an oxide scale that was up to 500 µm thick [242]. The QUENCH-16 test, carried out in 2011, examined the behaviour in air following mild preoxidation in steam; the oxide thickness after preoxidation was less than 130 µm in this case [238, 243]. Another objective with QUENCH-16 was to investigate nitride formation during prolonged (>800 s) oxygen starvation conditions in the air oxidation phase. The air flow rate was therefore exceptionally low in this test; see Table 25. Post-test examinations showed that zirconium nitrides formed inside the cladding oxide layer as a result of oxygen starvation in the upper part of the test assembly. The structure of the nitride containing oxide was very porous and non-protective. The QUENCH tests were terminated by reflooding the assemblies bottom-up with room temperature water. A strong and

[8]. From October 2009: Karlsruhe Institute of Technology.

unexpected oxidation excursion took place during the reflood phase in QUENCH-16, but not in QUENCH-10. The oxidation excursion resulted in extensive hydrogen production and temperatures well above the Zircaloy-4 melting point of 2120 K. It was accompanied by axial relocation and oxidation of metallic melt from the upper half of the test assembly. The oxidation excursion during reflooding was attributed to massive steam penetration through the porous oxide/nitride layer and reactions with the underlying cladding metal as well as with zirconium nitride [243].

The PARAMETER-SF4 experiment was conducted in 2009 at the LUTCH Laboratory, Podolsk, Russia [244]. It was an approximate counterpart to the QUENCH-10 test, carried out on VVER-1000 type fuel configuration (hexagonal assembly) and material (E110 Zr-1wt%Nb cladding). Also, the steam preoxidation phase was milder than in the QUENCH-10 test; see Table 25. During the air oxidation phase, oxygen starvation occurred in the upper part of the assembly during the final 350 s as the air flow rate was kept low. The test assembly was reflooded bottom-up with room temperature water, and similar to the QUENCH-16 test, a rapid temperature excursion up to about 2300 K was observed during reflooding. The temperature excursion, accompanied by a sharp overpressure transient in the test rig, resulted in damage of the shroud that enclosed the test assembly. This, together with extensive melting and relocation of molten material in part of the test assembly, made it difficult to quantitatively determine the extent and axial variation of cladding oxidation and other parameters [245].

6.3 Current and planned experimental campaigns

6.3.1 The IRSN DENOPI project

The IRSN DENOPI project, 2014 - 2019, supported by the French government in the framework of post-Fukushima activities, is devoted to the experimental study of SFPs under loss of cooling and loss of coolant accident conditions. The project is divided into 3 parts:

1. Two-phase convection phenomena in SFPs under loss of cooling conditions

Current knowledge of the natural convection in a SFP under loss of cooling condition, i.e. prior to uncovery of the fuel assemblies, is mainly based on expert judgment. The approach proposed in the DENOPI project is to conduct experiments on models of an SFP at reduced scale to contribute to the development and validation of two-phase flow convection models across the entire SFP. The experiments will be conducted at conditions of normal operation, loss of cooling, and recovery of the cooling system before any FA uncovery. The reduced scale pool will be equipped with a specific metrology to measure flow characteristics locally. The effect of high power fuel assemblies during refuelling operations will be studied. Temperature and velocity measurements will be conducted in the area above the racks in order to understand flows and to validate the computer codes used.

2. Physical phenomena at the scale of a fuel assembly under loss of coolant conditions

There are very few experimental data from tests with partially uncovered fuel assemblies. A better knowledge of these configurations would allow answering important questions, such as:

- the conditions for air penetration into the fuel assemblies, depending on the water level and the power of the assemblies;
- the void fraction in the FAs during boil-off, which is an important parameter in the evaluation of criticality issues;
- the efficiency of a water spray to cool the FAs in case of a loss of coolant accident.

The thermo-hydraulic experiments planned under this phase of the project will be conducted first at a reduced scale, then at full assembly scale. The cladding will not be made of zirconium alloys, in order to avoid the oxidation reactions. The tests will be performed with a geometric configuration representative of a whole cell assembly. The instrumentation will characterize the thermal-hydraulic behaviour of an assembly under conditions representative of different phases of the accident. Air penetration into the fuel assembly will be monitored by measuring oxygen concentrations at different levels of the assembly.

3. Oxidation of zirconium by an air/steam mixture

Experiments on oxidation and nitriding of zirconium alloy fuel cladding will be performed. The objective is to better estimate the margin to runaway of these exothermal reactions, leading to the destruction of the cladding. Separate effect tests will be conducted to investigate exothermic oxidation of the fuel cladding material exposed to steam and air mixtures. Experimental results will be used to validate certain hypotheses (stationarity, limiting step, etc.) and to develop a kinetic model. This will be used to improve the modelling and validation of the ASTEC severe accident code; see Appendix D. Mechanical tests will be conducted to estimate the ability of fuel rods weakened by oxidation and/or nitriding to maintain their integrity during a spray of water or handling in the post-accident phase.

6.3.2 Experiments at the Karlsruhe Institute of Technology

The separate effect test programs at Karlsruhe Institute of Technology are continuously going on according to the requirements. Current and future experiments are focussed on better understanding the detailed mechanisms and effects of nitrogen on the oxidation kinetics of zirconium alloy cladding. Extensive high-temperature oxidation test series have recently been run in mixed oxygen-nitrogen and steam-nitrogen atmospheres. The results show a significant effect of nitrogen on the oxidation kinetics over a wide range of compositions, down to 0.1 vol.% nitrogen in the mixture [246, 247].

KIT is also planning to perform another semi-integral bundle test in the QUENCH facility, with special focus on SFP conditions, including steam-air mixtures. Such a test could be e.g. conducted in the framework of the EC-sponsored Severe Accident Facilities for European Safety Targets (SAFEST) programme.

7 SIMULATION TOOLS

Modelling loss of cooling accidents in SFPs implies describing complex and coupled phenomena: the thermal-hydraulic behaviour of the pool, the nuclear criticality, and in case of a severe accident; the fuel behaviour, all the way to fuel assembly and rack degradation, as well as the fission product release and transport. At present, there are no specifically designed computer codes in use for the simulation of SFP loss of cooling or loss of coolant accidents. The safety analyses rely on simulation tools that were developed mainly for analysis of reactor core accidents, such as thermal-hydraulic system codes, nuclear criticality codes, fuel behaviour and severe accident codes. It should be pointed out, however, that an intensive work is currently being performed to improve the validation of computer codes with respect to SFP accidents, particularly in the field of severe accidents. Table 26 makes a connection between the phenomenology discussed in Chapter 5 and the computer codes described in the current chapter.

Table 26: Link between the accident phenomenology described in Chapter 5 and the different computer codes detailed in this chapter.

Phenomenology	Computer code (Code responsible body)
Thermal-hydraulics	Computational fluid dynamics codes: ANSYS-CFX and ANSYS-FLUENT (ANSYS), NEPTUNE-CFD (EDF) System codes: ATHLET (GRS), TRACE (U.S. NRC), CATHARE (CEA), COBRA-SFS (PNL)
Nuclear criticality	Composition of the fuel assemblies (depletion codes): VESTA (IRSN), DARWIN (CEA), TRITON (ORNL), OREST/KENOREST (GRS) Nuclear criticality codes: APOLLO (CEA), DRAGON (EPM, Canada), CRISTAL (IRSN), SCALE (U.S. NRC)
Fuel behaviour	Early phase of the accident - fuel rod transient codes: TRANSURANUS (ITU), FRAPTRAN (U.S. NRC), RAPTA-5 (VNIINM), TESPA-ROD (GRS), DRACCAR (IRSN) Late phase of the accident - severe accident codes: ATHLET-CD (GRS), ASTEC (IRSN-GRS), MAAP (EPRI), MELCOR (U.S. NRC)
Fuel assembly and rack degradation	Severe accident codes: ATHLET-CD (GRS), ASTEC (IRSN-GRS) MAAP (EPRI), MELCOR (U.S. NRC)
Fission product release and transport	Severe accident codes: ATHLET-CD (GRS), ASTEC (IRSN-GRS) MAAP (EPRI), MELCOR (U.S. NRC)

7.1 Thermal-hydraulic codes

7.1.1 Computational fluid dynamics codes

With regard to thermal-hydraulics of SFPs, computational fluid dynamics codes are used to address issues where three-dimensional (3D) phenomena are of prime importance. Examples of CFD codes are ANSYS-CFX, ANSYS-Fluent and NEPTUNE-CFD. Simulations performed with these types of codes are not, for the moment, officially used in the plant safety reports, but are performed in support of specific safety cases [248]. For example, CFD simulations can be used to:

- investigate and/or gain understanding of several problems, which have been identified during nuclear power plant operations, e.g. inadequate water temperature or water level measurements, or damage on SFP structures;
- demonstrate the coolability of the SFP [66], in normal, incident and accident conditions, e.g. after a modification of the location of the cool water injection or after a modification of the racks, in particular in case the total storage capacity of the SFP is increased;
- address specific problems linked with SFP boiling after a loss of cooling accident, such as the possibility of bubble entrainment in the SFP cooling system when restarting it under boiling conditions. This could induce a definitive and total loss of cooling, in case of pump cavitation. Another application is to determine the water/steam density distribution in the boiling SFP, to be used in analyses with nuclear criticality safety codes to assess criticality risks.

CFD codes can also be used to investigate the thermo-aeraulics of the SFP building, for example to assess the design of the mitigation means, in case of incident or accident conditions [77, 80].

Although CFD codes have the capacity to address problems at a local scale in 3D, the analyses of interest here are typically done on a large part of the SFP: for example, the totality of one of the compartments of the pool. The specificity of these analyses is thus the wide water volume to be taken into account, compared with RPV simulations, in which zoom on a specific zone is classically made: from pump to core inlet, or from core outlet to middle of the hot legs, for example. For the moment, this large scale modelling necessitates the use of:

- simplified modelling of the storage racks, fuel assemblies and SFP structures;
- relatively large and coarse meshes;
- porous medium approximations in some locations (e.g. to represent FAs inserted in racks).

The simulations of the SFP are single phase calculations, in natural or mixed convection conditions. In some cases, according to the accident scenarios, boiling may occur. Some single phase simulations are made even in these conditions, with simplified assumptions.

The CFD codes are classically validated on a few tests, representing natural, mixed or forced convection, but in general on a smaller scale compared to the SFP scale and with air. Moreover, natural convection is a relatively complex problem to address and models suffer from lack of validation. There are for the moment almost no data available to assess CFD codes for multiphase flow situations in this type of conditions (natural convection at nearly atmospheric pressure). Another limitation with today's CFD analyses is the simplified representation of the geometry: this is linked with computing and modelling capabilities. To illustrate this point, at present, it is not possible to represent the FAs (with fuel rods, grids, etc.) in the racks: the number of equations to be solved would be prohibitive and the model to represent boiling at the fuel rod surface, for example, is not yet mature. Another problem that has to be addressed is the representation of the heat exchange at the pool free surface.

7.1.2 System codes

The thermal-hydraulic system codes can be used to assess the SFP thermal-hydraulics in incident and accident conditions at a large scale. As with CFD codes, these simulations are not reported in the safety reports, but are performed in support of specific safety cases. For example, system code simulations can be performed to evaluate, during a loss of cooling accident, the evolution of the water inventory of the SFP and the void fraction in the FAs, and to verify if the fuel elements are adequately cooled via natural circulation flow.

Examples of system codes are ATHLET (Analysis of Thermal-Hydraulics of Leaks and Transients, GRS, Germany), CATHARE (Code for Analysis of Thermal-Hydraulics during an Accident of Reactor and safety Evaluation, CEA, France), and TRACE (TRAC/RELAP Advanced Computational Engine, U.S. NRC, USA).

The system codes generally simulate one-dimensional (1D) natural circulation in an open-loop consisting of a down-flow path (downcomer) connected to a number of heated up-flow paths, and a large uniform volume representing the upper part of the pool; see Figure 54. The density difference between the fluid in the downcomer and in the FA supplies a pressure differential, which drives the flow around the open-loop. The downcomer is used to represent the space between a storage rack and the nearby wall of the pool. The mass flow rate is then calculated as a balance between the buoyancy force and the flow path frictions. Flow pressure loss coefficients along each path are supplied by the user as input, and so is the inlet temperature at the top of the downcomer. This temperature is customarily taken as the maximum pool temperature allowed by the plant technical specifications.

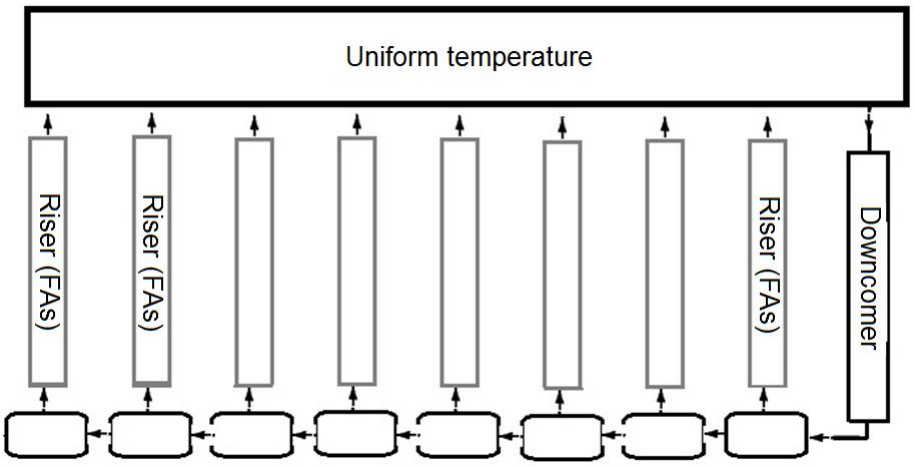

Figure 54: Typical SFP model used with thermal-hydraulic system codes.

From a geometrical point of view, the system thermal-hydraulic codes cannot represent all the SFP structures. A symmetric behaviour is generally assumed within the pool, and therefore only a limited number of fuel assemblies are modelled. This number is usually chosen equal to the number of FAs required to span the distance from the edge of the downcomer to the centre of the spent fuel storage. A detailed representation requires 3D modelling, but in comparison with CFD codes, the modelling is done at a larger scale and with e.g. simplified porous media assumptions.

System codes suffer from lack of validation for the operating conditions of storage pools (nearly atmospheric pressure, complex natural or mixed convection flow paths), because the majority of validation test cases are related, so far, to the simulation of the primary and secondary side piping networks of LWRs at higher pressure under forced convection conditions. Limitations, which are due, e.g. to the simplified

model equations with respect to viscosity and turbulence effects or the simulation of the walls, have to be assessed. However, 3D system code models are under active development, so that significant improvements related to both the 3D modelling basis, as well as the representation of the 3D geometry in question are possible in the future.

7.2 Nuclear criticality safety codes

The calculation codes which could be used to assess whether an SFP is likely to undergo a sustainable fission chain reaction under loss of cooling accident conditions are the same as those used to demonstrate the nuclear criticality safety (NCS) of the SFP in the safety cases. NCS calculations are static calculations and require material compositions and geometry data to calculate the k-effective (henceforth called k-eff; see Section 5.1) of a given configuration. Thus, only some input data should be changed from the usual models, according to the knowledge (or to the assumptions) of how the SFP conditions are changed under the loss of cooling accident.

For SFPs, the parameters having the most important impact on k-eff are:

- The composition of the fuel assemblies;
- The geometrical configuration, in particular the pitch between fuel assemblies;
- The density of the coolant/moderator;
- The material of the storage racks (steel or aluminium, borated or not).

In case of loss of cooling accident conditions, the water density (full density, water-air mixture or even air) within the pool, which could be different from one part of the pool to another, becomes particularly important for k-eff calculations. Water acts indeed as both a moderating material, favouring the neutron chain reaction, and an absorbing material, limiting the risk of a critical excursion. Depending on the moderation ratio, the first or the latter effect is more pronounced. Finally, the geometry of the fuel assembly (cladding degradation, debris formation, etc.) due to the accident situation is also an important parameter to assess.

There are various NCS computer codes with different modelling capabilities and different calculation methods, based on different nuclear data libraries. All these codes could be of interest for analysing the SFP under accident conditions, depending on the kind of scenario studied and on the more or less detailed description of this scenario. One should note that the composition of the fuel assemblies is an input data for NCS computer codes. Thus, preparatory calculations are required to obtain the composition of spent fuels (not always the case for the demonstration of SFP safety, where conservative assumptions are generally used for ensuring safety margins, while for accident conditions, the knowledge of the actual k-eff before the accident is required). These calculations are performed by so-called depletion codes, examples of which are VESTA (IRSN, France), DARWIN (CEA, France), TRITON (ORNL, USA), MONTEBURNS (LANL, USA), SERPENT (VTT, Finland) and OREST/ KENOREST (GRS, Germany). These depletion codes are not more detailed in the present report.

In terms of geometry modelling capabilities, NCS computer codes cover from 1D geometry problems (e.g. simplified debris bed issue), to 3D geometry problems (e.g. complete SFP description). The different calculation methods used by the NCS computer codes to estimate the k-eff value of a given configuration are:

- Pure Monte Carlo point wise calculations. Examples of these codes are MORET5 (IRSN, France), TRIPOLI (CEA, France), MCNP (LANL,USA), MVP (JAEA, Japan) and MONK (Serco Assurance, UK);
- Pure deterministic calculations. Examples are APOLLO2 (CEA, France), and DRAGON (EPM, Canada), using different ways of solving the neutron transport equation (P_{ij}, S_N, MOC). These methods are based on multi-group cross-sections and are generally limited to 1D and 2D configurations;

- "Hybrid" routes, as used in, e.g. the CRISTAL (IRSN and CEA, France) and SCALE (ORNL, USA) packages. Such a route consists in a first deterministic calculation of the fissile material (array of fuel rods) to get problem-specific, explicit or homogenized multi-group cross-sections, followed by a 3D Monte Carlo k-eff calculation of the SFP, including an infinite array of FAs or an explicitly modelled storage rack being fully or partially loaded with several FAs of identical or varying isotopic composition (i.e., burnup). This route is at present the most common used for NCS studies (best compromise between calculation time and physics approximations, with regards to the multi-parametric studies usually performed to demonstrate NCS).

In almost each case (codes/methods), different nuclear data libraries, based on the main nuclear data evaluation (JEFF, ENDF/B, JENDL, etc.), can be used. In general, the validation of the NCS computer codes is performed by:

- comparisons between calculations and experiments (several thousands of criticality benchmark experiments are internationally available to perform such comparisons), and/or
- inter-code comparisons.

For SFP, the configuration of an array of fuel rods submerged in liquid water is very well covered and documented for the validation of the NCS computer codes. Furthermore, there are barely any major discrepancies between calculations and experiments in this kind of configuration (whatever the code/method is).

In the peculiar case of SFP under loss-of-cooling accidents, the validation of the NCS computer codes depends on the accident condition studied. In particular, the harder the neutron spectrum is (for very low water densities for example), the less there are experiments to cover the case. Also the prediction of potentially irregular geometric configurations of fuel structural materials and coolant, or without coolant, due to severe accident scenarios, poses difficulties on modelling and validation.

7.3 Fuel rod behaviour codes

The early phase of an SFP accident, up to loss of rod-like geometry, can be simulated by fuel behaviour codes intended for transient analyses, such as TRANSURANUS (KIT, Germany), FRAPTRAN (PNNL,USA), RAPTA-5 (VNIINM, Russia) and TESPA-ROD (GRS, Germany). The numerical models in these codes simulate relevant thermo-mechanical phenomena in the fuel rods and describe in detail the changes in the fuel pellet and in the cladding tube, and determine the integral parameters of the fuel rod. The codes include special models to handle high-temperature phenomena. Fuel failure is also indicated by the calculations. Some special codes, e.g. DRACCAR (IRSN, France) and FRETA-B (JAEA, Japan), are capable of describing the mechanical interaction between the ballooned fuel rods and simulate flow blockage within a fuel assembly [112].

The transient fuel behaviour codes need input data from steady-state fuel rod simulation codes, in order to take into account effects of fuel burnup and irradiation history. Additional input from system codes is also often needed to define thermal-hydraulic boundary conditions for the fuel rod analyses. The fuel behaviour codes normally have more detailed models for several early phase phenomena than the severe accident codes, but they are not applicable to accident conditions beyond the loss of rod like geometry. Moreover, they usually lack models for cladding high temperature oxidation in air-containing environments.

7.4 Severe accident codes

Severe accident codes have been developed and improved for a long time for reactor pressure vessel purposes, and the capabilities of the codes have been verified and validated to simulate scenarios in the RPV in an accurate way. Most codes are based on a "classical" thermal-hydraulics system code for design-basis accidents, see Section 7.1.2, with different kinds of models for the core region, considering e.g. 1D,

3D or porous media approaches. More detailed descriptions of some of the most widely used severe accident codes (MELCOR, ATHLET-CD, MAAP-SFP and ASTEC) are given in Appendix D.

In general, all severe accident codes have models to simulate the main phenomena (e.g. pool boiling, zirconium alloy oxidation in steam and air) during postulated scenarios in SFPs, like loss of coolant or loss of cooling, leading to a heat-up of the pool with subsequent full dry-out. The validation and application of the current model basis against SFP scenarios and phenomena are ongoing. Currently in Europe, a lot of work is performed on integral tests like QUENCH and PARAMETER to evaluate, for example, air ingress modelling; see Section 6.2.2.3.

In addition, postulated SFP scenarios with full or partial dewatering due to loss of coolant or loss of cooling are investigated and simulated with severe accident codes [81, 249]. Analyses of these simulations [81, 249] show that a lack of knowledge can be identified for cladding oxidation phenomena in air or steam/air mixtures. Besides the oxidation, which is modelled quite sufficiently, the role of nitride formation and its impact on a subsequent accelerated oxidation of oxidised/nitrided cladding due to embrittlement is mostly not separately modelled and validated. Some air oxidation models/correlations might indirectly consider the presence of nitrogen and its role in the cladding oxidations process, if nitrogen was present during the experiments. Probably, one of the main open issues is the boundary conditions governing the SFP LOCA scenarios during the transient. The geometrical boundary conditions of a SFP with its 3D characteristics and the heterogeneous distribution of fuel assemblies with different thermal loads are also challenging for severe accident codes, which were developed for a more uniform (cylindrical) geometry in the RPV.

Furthermore, the results show that the coolability is quite sensitive to the current dominant atmosphere. The studies show that the heat generated by the fuel assemblies could be removed by air even in cases of a postulated transient with complete loss of coolant, while in other simulations, the coolability of the fuel assemblies depended on the current air flow through the fuel assemblies at different positions in the pool. Additionally, the water level in the fuel assembly, the state of boiling and the power of the fuel assembly strongly influence the coolability. Another item, which is not yet completely investigated and quantified, is the flooding of dewatered fuel assemblies by water injection, when pre-oxidation and maybe nitride formation may influence the coolability and the integrity of the cladding [81, 249]. Finally, the results of some scenarios show that even fuel melting and slumping into the SFP bottom is predicted.

The latest results for the application of severe accident codes on a spent fuel assembly in pure air atmospheres were achieved within the OECD/NEA Sandia Fuel Project; see Section 6.1.1.2. Two benchmark exercises were performed on the two phases of the project (one for each ignition test). Phase 1 dealt with the axial burn propagation of one full-length PWR fuel assembly under so called “hot neighbour conditions”. In Phase 2, the radial and axial burn propagations of five full-length PWR fuel assemblies in a 1×4 configuration with a heated central assembly surrounded by unheated assemblies, representing “cold neighbour conditions”, were investigated [250, 251].

The results of the Phase 1 benchmark show that severe accident codes (ATHLET-CD and MELCOR) and users were able to capture the time of ignition with reasonable accuracy and with a relative small range for the peak cladding temperature. After ignition, the calculated results deviate from the experimental data, due to the very oscillating oxidation processes leading to a long-term zirconium fire in the experiment. Furthermore, the availability of accurate hydraulic data was recognized as important for obtaining a correct modelling of the experiment. Provided that adequate models were used for radiation heat transfer and oxidation breakaway, all the codes showed a reasonable capability to capture the ignition time and location for these approximately “concentric” test conditions [250].

In Phase 2, the objectives of the experiment were only partially met. Until ignition, the simulations with ASTEC, ATHLET-CD and MELCOR reproduced reasonably the experimental results, but even for that different modelling and model options were used to achieve the scenario with the same code. Due to a rough nodalization of the five assemblies, the radial burn propagation was underestimated, leading to

discrepancies in comparison to the experiment as well as in a code-to-code comparison. The codes have restrictions on the number of elements or rings, but a more detailed radial nodalization could improve the results, considering that the nodalization has to be fine enough to have several nodes in the "non-heated" fuel assemblies, but also to have a good matching of the heat transfer governing the radial transport, essentially radiation. From the results of Phase 2, some general conclusions can be drawn:

- It is difficult to accurately reproduce the thermal kinetics in the peripheral FAs with axisymmetrical modelling, in which only average temperatures can be compared;
- Modelling the radial heat transfer by radiative mechanisms is not easy via view factors, because they are quite uncertain;
- The extrapolation to a real pool would require models that are able to capture the main phenomena already observed in this test configuration;
- For adapting models developed for reactor applications (e.g. radiation) to SFPs, enhanced user guidelines have to be developed and further modelling efforts could be necessary.

With regard to the first two conclusions, it should be noted that a better representation of the geometry and heat transfer could be achieved with the LOCA code DRACCAR [252]; see Appendix D. In this code [253, 254], each structure has its own thermal-mechanical behaviour that can also interact with neighbours by thermal radiation or mechanical contact. With this modelling, the temperature gradients in the cells are correctly reproduced and the exchange surfaces and the geometry also. In this case, no adjustments of the heat transfer coefficients are made necessary, and the code results can be trusted, particularly the ignition time and location as well as the kinetics of the accident.

The results of the simulation of the OECD/NEA Sandia Fuel Project show – in agreement with the experimental findings – that the phenomena under air atmospheres/air ingress are not fully understood and modelled. All codes considered air oxidation, but nitride formation was modelled only in one code explicitly and re-oxidation of ZrN was not modelled at all. All reactions in air atmosphere influence the temperature excursion, because they are exothermal; see Section 5.4.1. Additionally, ZrN forms a porous layer, leading to fast subsequent oxidation in oxygen or steam. For these phenomena, further model development is necessary on the basis of more separate effect and integral tests, although they are partially direct or indirect considered in current models [251, 255].

It is usually adequate to apply correlations, when evaluating fission-product release from over-heating and degrading fuel rods. Relative to SFP loss-of-cooling accident conditions, such correlations have been validated for reactor accidents that are characterized by fast thermal transients and steam-hydrogen atmospheres. SFP accidents can be considered potentially exceptional for these correlations, since these accidents can involve a wider range of conditions: slower temperature rise, longer times for fuel and FP interaction with cladding, and extremes of the ambient gas mixture (steam-hydrogen-air-nitrogen). In general, evaluating FP release from overheated fuel requires good knowledge of fuel-FP-cladding chemistry. While this knowledge is implicitly present in the reactor accident correlations, the wider-ranging conditions of SFP accidents could generate different, or a different balance of, chemical species. In such a context, chemical thermodynamics is a powerful approach commonly used to gain insights into fuel chemistry and help predict FP migration and release. Comprehensive computational tools exist, which are based on critically-assessed thermodynamic databases, e.g. [256, 257]. Hence, initially at least, it would be prudent not to rely solely on reactor-accident correlations without some complementary investigation using thermodynamic tools.

A special comment should be made on SA codes for CANDUS: While the analytical tools needed to analyse the CANDU SFP design basis accidents are relatively simple, the analysis of a severe SFP accident requires more advanced tools. Unlike LWR technology, where the fuel pool and the reactor core share similarities in structure and configuration, hence granting the ability to leverage existing severe accident codes, the CANDU SFP (open racks) is significantly different than the reactor core configuration (horizontal pressure tubes). The result is that no complete and comprehensive CANDU severe SFP accident analysis tool is currently available.

8 CONCLUSIONS AND RECOMMENDATIONS

This report is the third in a series of status reports [73, 181] produced by the CSNI as a follow-up of the Fukushima Daiichi accident. The purpose of the report was to briefly review existing SFP designs, safety systems and accident mitigation measures in OECD member countries, to summarize past experience from events and incidents in these pools, to assess current experimental and analytical knowledge on phenomena relevant to SFP cooling accidents, and to briefly review available computational tools, with focus on their applicability and validation status for SFP accidents.

8.1 Conclusions

Chapter 2 of the report provided a description of at-reactor SFPs for light water and CANDU reactors. The design of spent fuel racks, the pool cooling system, the instrumentation and measures for safety, accident prevention and mitigation were presented. Appendix A summarized the current spent fuel storage situation in OECD member countries with the aim of providing brief overviews of spent fuel management strategies, national requirements/criteria for SFPs and representative design data for at-reactor SFPs and storage racks, currently used for LWR and CANDU nuclear power plants. The improvements made after the Fukushima Daiichi accident were also summarized. Appendix B detailed, country by country, the different measures taken after the accident. The main findings from Chapter 2 are as follows:

- At-reactor SFPs are designed to store several times the number of fuel assemblies present in the reactor core, providing adequate cooling, and criticality safety and radiation protection. The design of the SFPs differs not only between reactor technologies (PWR, PHWR, BWR, VVER, etc.), but also between technologies generations and often from site to site. Though there are a wide variety of designs, the fundamental design parameters and safety provisions are consistent.
- All SFPs are large robust monolithic structures. The pool walls are generally made of more than one metre thick steel lined concrete. Fuel assemblies are stored in racks that provide spacing for coolant flow and in some cases also for criticality control. The pools are filled with several additional metres of water above the spent fuel to provide biological shielding. An active cooling and purification system maintains optimal conditions for the stored fuel.
- The possibilities of loss of cooling and loss of coolant accidents are accounted for in the basic design of all SFPs. The cooling systems have built in redundancies and are connected to emergency backup power to maintain their function. Pool penetrations are kept to a minimum. The cooling systems either have siphon breakers or the depth of the inlet and outlet pipes are limited to prevent draining of the pool. The large volume of water provides a significant thermal mass, which slows the accident progression and gives respite for operator intervention.
- Following the Fukushima Daiichi accident, additional measures have been undertaken to improve SFP safety even further. These measures differ greatly due to the large variation on designs, but can be generally stated as improvements in accident response procedures, additional backup electricity or water supplies, and instrumentation improvements.

Chapter 3 dealt with possible accident scenarios. An overview of operational experience feedback from at-reactor SFPs was presented, together with a representative selection of events that have occurred in LWRs. Appendix C presented some significant precursor events and accidents that have happened with SFPs, and it also summarized the results of two past assessment of events with loss of SFP cooling or water inventory. The main conclusions from Chapter 3 are:

- Although numerous events that involve loss of SFP cooling or partial loss of SFP water inventory have occurred in the past, operational experience shows that none of these events have led to severe accidents with pool fuel uncovery and/or fuel damage. With regard to activity release consequences, the 1983 Bruce-A Unit 4 fuel transfer incident in Canada and the 2003 Paks cleaning tank incident in Hungary may be referenced. However, these incidents by their specific natures were not representative of SFP accidents.
- Experience shows that loss of SFP cooling is in most cases caused by inoperable cooling pumps, and that inadvertent diversion of coolant flow or loss of ultimate heat sink are other occurring causes. Thanks to the slow nature of these events, operators have always successfully restored cooling long before the SFP water reached the maximum allowed temperature. Nevertheless, the possibility for operators to perform the appropriate measures must be guaranteed even in adverse conditions (e.g. reactor accident, see Chapter 4).
- Accidents with loss of SFP water inventory may be faster, especially if they occur by failure of temporal gates or seals during refuelling, other activities or human errors. However, the design of the SFP and its connected systems generally preclude drain-down below the top of stored fuel assemblies. Events with loss of water inventory by up to 4 m have been reported. None of them has led to fuel uncovery or to any dramatic temperature increase of the remaining pool water.
- The evaluated events provide valuable feedback that can help to avoid similar incidents in the future. Although general conclusions are difficult to draw, due to the variation in design of SFPs and related systems, operational experience shows that reliable SFP instrumentation is crucial for detecting abnormal events in a timely manner and that accident management procedures and training are vital for responding to the events efficiently. Besides preparation of SFP accident management procedures and training of the staff, important preventive actions also involve testing, maintenance and configuration control of gates, seals, anti-siphon devices and emergency equipment.

Chapter 4 was entirely dedicated to the behaviour of the SFPs and the dry cask storage at the Fukushima Daiichi nuclear power station during and after the 2011 accident. The power station had six at-reactor SFPs, one at each unit, a common pool, and a dry cask storage facility. As a consequence of the tsunami, cooling flow was lost in the Unit 1 to Unit 4 SFPs, following the loss of all AC power at Units 1 to 5. The Unit 6 air-cooled emergency diesel generator survived the tsunami and was used to maintain cooling and water supply for the Unit 5 and Unit 6 SFPs. With no pool cooling to remove decay heat at the Unit 1 to Unit 4 SFPs, emergency water injection was conducted by using a helicopter, concrete pump trucks, fire trucks, and by making use of various connected piping systems. Eventually, pool water cooling by the alternative cooling system was started at all SFPs, and the water has been cooled down and maintained at temperatures below 40 °C. Regarding the SFPs, the conclusions from the Fukushima Daiichi accident are the following:

- When SFP cooling was lost, a concern arose that the SFPs may boil dry and result in fuel failure. In response to this concern, station personnel took numerous extraordinary actions to ensure sufficient cooling of the spent fuel until the alternative cooling system could be installed. These actions were most likely decisive for averting what could have become severe accidents.
- Analyses and inspections reveal that the structural integrity of all SFPs was maintained, and that the water level never dropped below the top of fuel assemblies in any of the pools. Results of video inspections and water analyses indicate that, in all pools, almost no fuel is damaged.

- Investigations show that the fuel racks appear to be intact and that debris from the reactor building explosions is unlikely to have caused any fuel damage when falling into the SFPs.
- It is concluded that all SFPs at the Fukushima-Daiichi nuclear power station survived the accident, that the spent fuel was not uncovered or damaged, and that the loss of SFP cooling never evolved into severe accidents. However, numerous extraordinary actions for emergency water injection were needed to avert such accidents.

Chapter 5 described the phenomenology of SFP loss of cooling and loss of coolant accidents. It covered the criticality issue and the thermal-hydraulic behaviour of a SFP under different stages with an emphasis on severe accident. The fuel behaviour and fuel assembly and rack degradation, as well as the fission product release and transport during loss of cooling or loss of coolant accidents were addressed. The findings from Chapter 5 can be summarized as follows:

- Phenomena related to high temperature fuel degradation and fission product release are well known from separate effect tests and integral experiments, carried out in the past three decades to study loss of reactor cooling accidents. Although the conditions expected in SFP accidents differ from those in reactor accidents by a more heterogeneous distribution of fuel assemblies, lower decay power, air-containing environment and lower pressure, the degradation and release phenomena are fundamentally the same. Differences, induced e.g. by the expected mixed air/steam environment in SFP accidents, have been identified and investigated in recent experiments. Nevertheless, quantitative realistic estimation of the source term for postulated severe accident in SFP is still a challenge. The problem is that certain involved phenomena have very strong influence on the release rate. It is difficult to evaluate the extent to which a particular phenomenon takes place for a given severe accident scenario.
- As for the large-scale thermal-hydraulic behaviour of the SFP and the thermo-aeraulics of the pool building during accident scenarios, our current understanding is based largely on computational analyses with CFD and thermal-hydraulic system codes. Experimental campaigns have recently been conducted in the USA to support these analyses for completely uncovered fuel assemblies, and experiments on water covered and partly uncovered assemblies are underway in France. The computational analyses at hand indicate that partial uncovering of spent fuel assemblies does not necessarily result in immediate heat-up of the uncovered part: as long as the water level is not too far below the top of the assemblies, the uncovered part can be cooled by steam flow and water swell from boiling in the lower part.
- Nuclear criticality is a phenomenon of concern for SFP accidents, except for CANDUs, in which natural uranium fuel is used. After the Fukushima Daiichi accident, computational analyses have been performed to assess the criticality margin of LWR SFPs under different postulated accident conditions. The analyses, which cannot be considered complete or exhaustive, indicate that criticality is not an issue as long as the spent fuel assemblies remain covered with water. Moreover, if the fuel gets severely damaged and compacted, the calculated margin to criticality is generally increased, which suggests that reflooding an SFP that contain severely damaged fuel, even with unborated or sea water, may not pose a criticality problem. Substantial reductions in calculated criticality margin are seen for accident scenarios with extensive loss of pool water inventory and/or neutron absorbing material from the storage racks.

Chapter 6 was a brief review of integral tests and separate effect tests with relevance to SFP accidents. Among the integral tests, the experiments recently conducted in the OECD/NEA Sandia Fuel Project, were given particular attention. The separate effect tests covered by the review were mainly on severe accident: cladding air oxidation and fission product release in air-rich environments. The main conclusions from Chapter 6 are:

- The current database with relevance to SFP cooling accidents consists largely of experiments that were conducted primarily to study the late phase of LWR loss of coolant accidents, with air ingress

to the core. Separate effect tests of this kind, applicable to SFP cooling accidents, include numerous tests on cladding high temperature oxidation in air and mixed air/steam environments, and fuel fission product release under air-rich conditions. These well controlled separate effect tests are instrumental in the development and calibration of computer models.

- Integral tests, while fewer in number due to higher costs, are essential to investigate the feedback effects caused by interacting phenomena. Valuable integral tests with relevance to SFP cooling accidents, although intended primarily to study reactor accidents, are the integral fuel degradation tests with mixed steam/air environment in the QUENCH, CODEX and PARAMETER series, and the international PHEBUS FP programme on melt progression and fission product release.
- The only integral tests that have been specifically targeted to SFP cooling accidents are those conducted by Sandia National Laboratories, USA, within the SFP Heatup and Propagation Project (BWR fuel) and the OECD/NEA Sandia Fuel Project (PWR fuel). The main objective of these tests was to produce basic thermal-hydraulic data for completely uncovered fuel assemblies in SFP loss-of-coolant accidents. They have resulted in severe accident code benchmarking and evolution of the computer code models for SFP applications.
- More integral tests dedicated specifically to SFP accidents are planned, e.g. through the French IRSN DENOPI programme, 2014-2019. This programme is intended to investigate the two-phase convection phenomenon in SFPs under loss of cooling conditions, the conditions for air penetration into partly uncovered fuel assemblies, the efficiency of a water spray in case of a loss of coolant accident and the oxidation of zirconium by an air/steam mixture. A new integral test in the Karlsruhe QUENCH series is also planned with special focus on SFP accident conditions.

Chapter 7 dealt with simulation tools used for analysis of SFP accidents. These tools include computer codes for analysis of nuclear criticality safety, thermal-hydraulics, fuel rod behaviour and severe accidents. Details on widely used severe accident codes were given in Appendix D. The main findings from Chapter 7 are:

- Several criticality safety codes are available to assess the neutron multiplication properties of SFPs. These codes, which are generally used for analysis not only of accidents but also of normal operating conditions, represent the state-of-the art in neutron transport physics and have been widely validated both by inter-code comparison and by comparison with criticality benchmark experiments. Although these codes are extensively assessed against experiments, the uncertainties in some input parameters, as well as the simplifications in the modelling of some geometries, irregular or distorted due to a severe accident, or of systems characterized by a hardened neutron spectrum, may pose some difficulties to the simulations of SFP accidents and to their validation.
- Thermal-hydraulic system codes and severe accident codes have been developed mainly for reactor applications, but they are being adapted to SFP accident analysis. These codes are usually restricted to 1D or 2D representations of the considered geometry, and 3D CFD simulation tools are therefore being used as a complement for thermo-hydraulic analyses.
- While CFD tools have the capacity to address problems at the local scale in 3D, SFP analyses are usually done at a larger scale. The large simulation domain imposes simplified modelling of the storage racks (porous medium approximation) and relatively coarse meshes. Moreover, natural convection is a complex problem to address and there are for the moment almost no data to assess CFD simulation tools for multiphase flow situations in natural convection at nearly atmospheric pressure.
- The models for fuel degradation processes in LWR severe accident codes were developed for reactor applications. Typical SFP accident scenarios involve fuel arrangements (heterogeneous) and boundary conditions (low fuel power, low pressure, mixed air/steam environment) that are different from those in reactor accidents. This poses a challenge for the extrapolation of the

degradation models to SFP applications, even though the model basis covers most of the phenomena expected in SFP accidents.

- The early phase of an SFP accident, up to loss of rod-like geometry, can also be simulated by fuel rod behaviour codes intended for transient analyses. These tools have more detailed models for thermo-mechanical phenomena than thermal-hydraulic system and severe accident codes. However, they usually lack models for cladding high temperature oxidation in air-containing environments.
- Existing user guidelines for thermal-hydraulic and severe accident codes were developed for applications to reactor configurations. For the application of these codes to SFP accident analysis, the user guidelines are currently limited and need to be improved. Finally, at present, there is no severe accident code for CANDU SFP applications.

8.2 Recommendations

Current knowledge of SFP loss of cooling and loss of coolant accidents and their consequences is based on experiments and computer analyses. The current experimental database contains some recent tests that were intended specifically to study SFP accidents with LWR fuel, but the bulk of data derive from tests done to study the behaviour of reactor cores (both LWR and CANDU) in loss of coolant accidents. Likewise, currently available computational tools are intended primarily for analyses of reactor accidents and more specific modelling for SFP is desirable in these tools. Nevertheless, the main phenomena involved in SFP cooling accidents are largely understood. Uncertainties exist, for example as to the thermo-hydraulic and neutronic behaviour of partially uncovered fuel assemblies in typical rack structures and the hydrogen production. Also the high-temperature oxidation kinetics and burst behaviour of internally pressurized zirconium alloy cladding tubes in mixed air-steam environments need more attention, both experimentally and with regard to modelling.

Additional experiments, specifically targeted to SFP accidents in LWRs, are underway to study the aforementioned phenomena. These experiments are important and will reduce uncertainties and improve computational models, but further dedicated experiments are needed. This is especially true for the CANDU technology, which has particular fuel assembly and storage rack designs. It is recommended that the Phenomena Identification and Ranking Technique (PIRT) is used to systematically identify phenomena that are both of high importance and high uncertainty, and thus, of primary interest for further studies. The present status report is an adequate starting point for such an activity.

The simulation tools currently used for analyses of SFP cooling accidents in LWRs include computer codes for nuclear criticality safety, thermal-hydraulics, fuel rod behaviour and severe accidents. For the latter codes, it should be recognized that applied models for fuel degradation phenomena were developed for reactor applications, and that there are limitations and uncertainties involved in their application to SFPs. The severe accident code benchmark carried out as part of the OECD/NEA Sandia Fuel Project helped to identify these limitations for an accident scenario involving completely uncovered fuel. It is recommended that the NEA organizes similar benchmark activities for other SFP accident scenarios, as pertinent experimental data become available. These activities may also include computer programs for thermo-hydraulics and nuclear criticality safety.

Another recommendation is that formal user guidelines are produced for the application of LWR severe accident and thermo-hydraulic system codes to SFP cooling accidents. This would ensure best practice in analyses and reduce user effects.

For the CANDU technology, there is currently no complete and comprehensive severe-accident code that can be used for SFP accident analysis. The reason is that the conditions and the fuel configuration in the SFP are much different from those in the CANDU reactor core, which makes existing tools for analysis of severe CANDU reactor accidents unfit for SFPs. It is recommended that a severe-accident analysis tool for CANDU SFPs be developed.

The present report summarizes results of experiments and computational analyses carried out to date to gain understanding of phenomena with significance to SFP cooling accidents. Considering that some knowledge gaps currently exist and that ongoing and planned research projects are expected to produce results that will hopefully narrow these gaps within the foreseeable future, it is recommended that:

- a CSNI state of the art report on SFP loss-of-cooling and loss-of-coolant accidents is written as the results of these research projects become available;
- a follow-on activity is launched on SFP combining probability of SFP accidents, which was beyond the scope of this document, and mitigation a strategy.

9 REFERENCES

1. *Survey of wet and dry spent fuel storage*, 1999, Report IAEA-TECDOC-1100, International Atomic Energy Agency, Vienna, Austria.
2. Barto, A., et al., *Consequence study of a beyond-design-basis earthquake affecting the spent fuel pool for a U.S. Mark I boiling water reactor*, 2013, Report SECY-13-0112-Enclosure-1 (ADAMS accession no. ML13256A342), U.S. Nuclear Regulatory Commission, Washington, DC, USA.
3. *Storage of spent nuclear fuel*, 2012, Specific Safety Guide SSG-15, International Atomic Energy Agency, Vienna, Austria.
4. Ibarra, J.G., et al., *Operating experience feedback report: Assessment of spent fuel cooling*, 1997, Report NUREG-1275, U.S. Nuclear Regulatory Commission, Washington, DC, USA.
5. Benjamin, A.S., et al., *Spent fuel heatup following loss of water during storage*, 1979, Report NUREG/CR-0649, U.S. Nuclear Regulatory Commission, Washington, DC, USA.
6. *The annual maintenance and construction plan of Tsuruga Power Station for fiscal year 2010*, 2010, The Japan Atomic Power Company, Tokyo, Japan.
7. 2003, Report HLR-046, Rev. 2, Hitachi, Ltd., Tokyo, Japan.
8. 1999, Report HLR-064, Rev. 2, Hitachi, Ltd., Tokyo, Japan.
9. Budaev, M.A., et al. *Hydrogen generation under cooling pond drainage during full blackout accident on nuclear power plant*, 2013. In: The 8th International Scientific and Technical Conference: Safety Assurance of NPP with VVER, May 28-31, 2013, Podolsk, Russian Federation.
10. Hozer, Z., et al., *Safety analysis of a VVER-440 spent fuel storage pool*. International Journal of Nuclear Energy Science and Technology, 2007. 3(3): pp. 302-313.
11. Anisimov, O.P., et al. *Current state of WWER SNF storage in Russia and the perspectives*, 2006. In: Sixth International Conference on WWER Reactor Fuel Performance, Modelling and Experimental Support, September 19-23, 2005, Albena, Bulgaria: International Atomic Energy Agency.
12. Lindgren, E.R. and S.G. Durbin, *Characterization of thermal-hydraulic and ignition phenomena in prototypic, full-length boiling water reactor spent fuel pool assemblies after a postulated complete loss-of-coolant accident*, 2013, Report NUREG/CR-7143, U.S. Nuclear Regulatory Commission, Washington, DC, USA.
13. *Potential draining of the spent fuel storage due to the absence of a siphon breaker on its cooling circuit line*, 2012, Report IRS-8243, IAEA International Reporting System for Operating Experience, Vienna, Austria.
14. Kang, S.H., et al., *Experimental study of siphon breaking phenomenon in the real-scaled research reactor pool*. Nuclear Engineeering and Design, 2013. 255: pp. 28-37.

15. *Regulatory Guide 1.13 Rev 2: Spent fuel storage facility design basis.* 2007, U.S. Nuclear Regulatory Commission: Washington, DC, USA.

16. Frost, C.R. and S.J. Naqvi. *Design considerations for water pool storage of irradiated CANDU fuel by Ontario Hydro,* 1986. In: International Conference on CANDU Fuel, October 6-8, 1986, Chalk River, ON, Canada: Canadian Nuclear Society.

17. Frost, C.R. *Operating experience with Ontario Hydro's irradiated fuel bays,* 1984. In: Irradiated Fuel Storage: Operating Experience and Development Program, October 17-18, 1984, Toronto, ON, Canada: Ontario Hydro.

18. Chuanqing, L. and D.C. Hancock, *Fuel handling system for Qinshan Phase III Nuclear Power Plant.* China Journal of Nuclear Power Engineering, 1999. 20(6).

19. *EU stress tests and follow-up*, European Nuclear Safety Regulators Group: Available via internet at http://www.ensreg.eu/EU-Stress-Tests.

20. *The International Reporting System for Operating Experience (IRS)*, Internationl Atomic Energy Agency: Available via internet at http://nucleus.iaea.org/CIR/CIR/IRS.html.

21. *Generic Communications*, U.S. Nuclear Regulatory Commission: Available via internet at http://www.nrc.gov/reading-rm/doc-collections/gen-comm/.

22. *U.S. Nuclear Regulatory Commission: Licensee Event Report Search (LERSearch)*, U.S. Nuclear Regulatory Commission: Available via internet at https://lersearch.inl.gov/Entry.aspx.

23. *European Clearinghouse on NPP Operational Experience Feedback*, European Union Joint Research Centre: Available via internet at https://clearinghouse-oef.jrc.ec.europa.eu.

24. Martin Ramos, M., *Analysis of fuel related events,* 2009, Report SPNR/CLEAR/09 11 006, European Clearinghouse on NPP Operational Experience Feedback, Petten, The Netherlands.

25. Collins, T.E. and G. Hubbard, *Technical study of spent fuel pool accident risk at decommissioning nuclear power plants,* 2001, Report NUREG-1738, U.S. Nuclear Regulatory Commission, Washington, DC, USA.

26. Throm, E.D., *Regulatory analysis for the resolution of generic issue 82: Beyond design basis accidents in spent fuel pools,* 1989, Report NUREG-1353, U.S. Nuclear Regulatory Commission, Washington, DC, USA.

27. *Assessment of the risk of fuel assemblies being uncovered in the spent fuel pool,* 2006, Report IRS-7764, IAEA International Reporting System for Operating Experience, Vienna, Austria.

28. Novak, J.a.M., G. . *Dry Fuel Handling: Station Experience and Ontario Hydro (CNS) Programs,* 1986. In: Proceedings of the (First) International Conference on CANDU Fuel, October 6-8, Chalk River, Ontario.

29. Hastings, I.J., et al. *Behaviour in Air at 175-400°C of Irradiated UO2 Fuel*, 1984. In: Irradiated Fuel Storage – Operating Experience and Development Programs, October 17-18, Ontario, Canada

30. Hastings, I.J., et al., *Post irradiation Dimensional Stability and Fission Product Behaviour of Deliberately Defected UO2 Fuel at 200 and 400°C.* Nucl. Technol., 1985. 70: pp. 268 – 273.

31. Hastings, I.J., et al. *Post irradiation Stability and Fission Product Behaviour of Defected UO2 fuel at 400°, 600° and 900°C in Air*, 1985. In: American Ceramic Society Annual Meeting, May 5-9, Cincinnati, Ohio, USA, pp. 121-138.

32. *OECD-IAEA Paks fuel project: Final report,* 2009, Report TDL-002, International Atomic Energy Agency, Vienna, Austria.

33. *Report to the chairman of the Hungarian Atomic Energy Commission on the Authority's investigation of the incident at Paks nuclear power plant on 10 April 2003,* 2003, Hungarian Atomic Energy Authority, Budapest, Hungary.

34. Hozer, Z., et al., *Activity release from damaged fuel during the Paks-2 cleaning tank incident in the spent fuel storage pool.* Journal of Nuclear Materials, 2009. 392(1): pp. 90-94.

35. Hozer, Z., et al., *Numerical analyses of an ex-core fuel incident: Results of the OECD-IAEA Paks Fuel Project.* Nuclear Engineering and Design, 2010. 240(3): pp. 538-549.

36. *Nuclear safety review for the year 2003,* 2004, Report IAEA/NSR/2003, International Atomic Energy Agency, Vienna, Austria.

37. *Report of the expert mission to assess the results of the Hungarian Atomic Energy Authorities investigation of the 10 April 2003 fuel cleaning incident at Paks NPP,* 2005, Report IAEA-TCR-02581/IAEA-NSNI-112F, International Atomic Energy Agency, Vienna, Austria.

38. *Impact at the Fukushima Daiichi nuclear power station due to the Great East Japan Earthquake,* 2012, Report (in Japanese) http://www.tepco.co.jp/cc/press/betu12_j/images/120509j0101.pdf, Tokyo Electric Power Company, Tokyo, Japan.

39. *The official report of the the Fukushima Nuclear Accident Independent Investigation Commission: Executive summary,* 2012, Report from The National Diet of Japan, The Fukushima Nuclear Accident Independent Investigation Commission (NAIIC), Tokyo, Japan.

40. *Special report on the nuclear accident at the Fukushima Daiichi nuclear power station,* 2011, Report INPO 11-005, Institute of Nuclear Power Operations, Atlanta, GA, USA.

41. *Investigation on the spent fuel pools,* 2012, Presentation (in Japanese) http://www.nsr.go.jp/archive/nisa/shingikai/800/28/006/6-2.pdf, Nuclear and Industrial Safety Agency (NISA), Japan.

42. Nishihara, K., et al., *Estimation of fuel composition in Fukushima-Daiichi nuclear power plant,* 2012, Report JAEA-Data/Code 2012-018, Japan Atomic Energy Agency, Tokai-mura, Japan.

43. *Additional report of the Japanese Government to the IAEA: The accident at TEPCO's Fukushima Nuclear Power Stations - Second report,* 2011, Government of Japan, Nuclear Emergency Response Headquarters, Tokyo, Japan.

44. *Fukushima nuclear accident analysis report (Interim report),* 2011, Report, http://www.tepco.co.jp/en/press/corp-com/release/betu11_e/images/111202e14.pdf, Tokyo Electric Power Company, Tokyo, Japan.

45. Gauntt, R.O., et al., *Fukushima Daiichi accident study (status as of April 2012),* 2012, SAND2012-6173, Sandia National Laboratories, Albuquerque, NM, USA.

46. *Videoclip from Fukushima Daiichi SFP 3, May 8, 2011,* 2011, Available at http://www.tepco.co.jp/tepconews/library/movie-01j.html?bcpid=45149870002&bclid=49031294002&bctid=52072676002, Tokyo Electric Power Company, Tokyo, Japan.

47. *Videoclip from Fukushima Daiichi SFP 3, February 14-18, 2013,* 2013, Available at http://www.tepco.co.jp/tepconews/library/movie-01j.html?bcpid=45149870002&bclid=347241149002&bctid=412805945002, Tokyo Electric Power Company, Tokyo, Japan.

48. Wang, D., et al., *Study of Fukushima Daiichi nuclear power station unit 4 spent-fuel pool.* Nuclear Technology, 2012. 180: pp. 205-215.

49. *Videoclip from Fukushima Daiichi SFP 4, May 7, 2011,* 2011, Available at http://www.tepco.co.jp/tepconews/library/movie-01j.html?bcpid=45149870002&bclid=49031294002&bctid=52072681002, Tokyo Electric Power Company, Tokyo, Japan.

50. *The integrity evaluation of the reactor building at Unit 4 in the Fukushima Daiichi nuclear power station,* 2012, Presentation, http://www.meti.go.jp/english/earthquake/nuclear/decommissioning/pdf/20120605_01b.pdf, Ministry of Economy, Trade and Industry, Tokyo, Japan.

51. *Inspection results of the integrity of the Unit 4 reactor building at the Fukushima Daiichi nuclear power station,* 2012, Presentation (in Japanese), http://www.tepco.co.jp/nu/fukushima-np/images/handouts_120525_07-j.pdf, Tokyo Electric Power Company, Tokyo, Japan.

52. *Removal of fuel assemblies from the Unit 4 SFP at the Fukushima Daiichi nuclear power station,* 2013, Presentation (in Japanese), http://www.tepco.co.jp/nu/fukushima-np/series/images/131030_01.pdf, Tokyo Electric Power Company, Tokyo, Japan.

53. *Fukushima Daiichi Nuclear Power Station: Fuel removal from reactor 4 spent fuel pool,* 2013, Presentation, http://www.mofa.go.jp/files/000019236.pdf, Tokyo Electric Power Company, Tokyo, Japan.

54. *Post-accident activities and future plans at the Fukushima Daiichi nuclear power station,* 2013, Report (in Japanese), http://www.aesj.or.jp/~wchem/3gennkou%20.pdf, Tokyo Electric Power Company, Tokyo, Japan.

55. *Fukushima Daiichi: ANS Committee report,* 2012, American Nuclear Society, Special Committee on Fukushima, La Grange Park, IL, USA.

56. Grimm, P., et al. *Parametric studies on the reactivity of spent fuel storage pools*, 1984. In: Fifth International Meeting on Thermal Nuclear Reactor Safety, September 9-13, 1984, Karlsruhe, Germany: Nuclear Research Center Karlsruhe, KfK 3880/1, Vol. 1, pp. 626-633.

57. *Nuclear fuel behaviour under reactivity-initiated accident (RIA) conditions: State-of-the-art report 2010,* 2010, Report NEA/CSNI/R(2010)1, OECD Nuclear Energy Agency, Paris, France.

58. *Summary of the EPRI early event analysis of the Fukushima Daiichi spent fuel pools following the March 11, 2011 earthquake and tsunami in Japan,* 2012, Report 1025058, Section 8 and appendices A, G and H, Electric Power Research Institute, Palo Alto, CA, USA.

59. Kromar, M. and B. Kurincic. *Criticality safety investigation of the NPP Krsko wet spent fuel storage in the hypothetical degraded configuration*, 2011. In: Twentieth International Conference on Nuclear Energy for New Europe, September 12-15, 2011, Bovec, Slovenia, pp. 314.1-314.8.

60. Gomit, J.-M., et al. *CRISTAL V1: Criticality package for burn up credit calculations*, 2003. In: Seventh International Conference on Nuclear Criticality Safety (ICNC2003), October 20-24, 2003, Tokai-mura, Japan: Japan Atomic Energy Research Institute, JAERI-CONF-2003-019, Part 2, pp. 80-84.

61. Caplin, G., et al. *Criticality accident in case of a spent fuel pool dry-out*, 2011. In: EUROSAFE Forum 2011, November 7-8, 2011, Paris, France.

62. Caplin, G. and A. Sargeni. *Why a criticality excursion was possible in the Fukushima Spent Fuel Pools*, 2014. In: ANS Reactor Physics Topical Meeting 2014 (PHYSOR 2014), September 28 - October 3, Kyoto, Japan.

63. Kilger, R., et al. *Generic criticality considerations for spent fuel pool storage racks under beyond design basis accident conditions*, 2013. In: ANS NCSD 2013: Criticality Safety in the Modern Era - Raising the Bar, September 29 - October 3, 2013, Wilmington, NC, USA.

64. *Storage and handling of fuel assemblies and associated items in nuclear power plants with light water reactors*, 2003, Standard KTA 3602, Kerntechnischer Ausschuss, Salzgitter, Germany.

65. Weech, M.E. and Y.J. Lee, *Heat transfer in spent fuel storage.* Nuclear Engineering and Design, 1981. 67: pp. 379-389.

66. Hung, T.-C., et al., *The development of a three-dimensional transient CFD model for predicting cooling ability of spent fuel pools.* Applied Thermal Engineering, 2013. 50: pp. 496-504.

67. Gartia, M.R., et al., *Analysis of metastable regimes in a parallel channel single phase natural circulation system with RELAP5/MOD3.2.* International Journal of Thermal Sciences, 2007. 46(10): pp. 1064-1074.

68. Bousbia Salah, A. and J. Vlassenbroeck. *Survey of some safety issues related to some specific phenomena under natural circulation flow conditions*, 2012. In: EUROSAFE 2012, November 5-6, 2012, Brussels, Belgium.

69. Duffey, R.B., et al. *Two-phase flow stability and dryout in parallel channels in natural circulation*, 1993, (BNL-48897). In: National Conference and Exposition on Heat Transfer, August 8-11, 1993, Atlanta, GA, USA.

70. Kaliatka, A., et al., *Analysis of the processes in spent fuel pools in case of loss of heat removal due to water leakage.* Science and Technology of Nuclear Installations, 2013. 2013.

71. Nimander, F., *Investigation of spent nuclear fuel pool coolability*, 2011, Master Thesis, Royal Institute of Technology, Stockholm, Sweden.

72. Shah, M.M. *Analytical formulas for calculating water evaporation from pools*, 2008. In: ASHRAE Transactions (2008 ASHRAE Annual Meeting), 114.

73. *OECD/NEA/CSNI status report on filtered containment venting,* 2014, Report NEA/CSNI/R(2014)7, OECD Nuclear Energy Agency, Paris, France.

74. Gauntt, R.O., et al., *MELCOR computer code manuals,* 2000, Report NUREG/CR-6119, U.S. Nuclear Regulatory Commission, Washington, DC, USA.

75. Ogino, M. *Analysis of fuel heat-up in a spent fuel pool during a LOCA*, 2012. In: Technical Workshop on the Accident of TEPCO's Fukushima Dai-ichi NPS, July 23-24, 2012, Tokyo, Japan.

76. Jäckel, B. *Spent fuel pool boil down calculations with MELCOR 1.8.6*, 2013. In: Fifth European MELCOR User Group Meeting, May 2-3, 2013, Stockholm, Sweden.

77. Wagner, K.C. and R.O. Gauntt, *Mitigation of spent fuel pool loss-of-coolant inventory accidents and extension of reference plant analyses to other spent fuel pools,* 2006, Sandia Letter Report, Sandia National Laboratories, Albuquerque, NM, USA.

78. Benjamin, A.S. and D.J. McCloskey, *Spent fuel heatup following loss of water during storage.* Nuclear Technology, 1980. 49: pp. 274-294.

79. Nourbakhsh, H.P., et al., *Analysis of spent fuel heatup following loss of water in a spent fuel pool: A user's manual for the computer code SHARP*, 2002, NUREG/CR-6441, U.S. Nuclear Regulatory Commission, Washington, DC, USA.

80. Boyd, C.F., *Predictions of spent fuel heatup after a complete loss of spent fuel pool coolant,* 2000, Report NUREG-1726, U.S. Nuclear Regulatory Commission, Washington, DC, USA.

81. Fleurot, J., et al. *SARNET synthesis of spent fuel pool accident assessments using accident codes*, 2013. In: Sixth European Review Meeting on Severe Accident Research (ERMSAR 2013), October 2-4, 2013, Avignon, France.

82. *Fuel design data.* Nuclear Engineering International, 2007. 52: pp. 32-41.

83. Lambert, J.D.B. and R. Strain, *Oxide fuels*, 1993. In: Materials Science and Technology, A Comprehensive Treatment, Nuclear Materials Part I, B.R.T. Frost, Editor. VCH: Weinheim, Germany. pp. 111-190.

84. Konings, R.J.M., et al., *Nuclear fuels*, 2010. In: The Chemistry of the Actinide and Transactinide Elements, Fourth edition, L.R. Morss, N.M. Edelstein, and J. Fuger, Editors. Springer: Dordrecht, The Netherlands. pp. 3665-3811.

85. Lemaignan, C. and A.T. Motta, *Zirconium alloys in nuclear applications*, 1994. In: Materials Science and Technology, A Comprehensive Treatment, Nuclear Materials Part II, B.R.T. Frost, Editor. VCH: Weinheim, Germany. pp. 1-51.

86. Cohen, B.L., *High-level radioactive waste from light-water reactors.* Reviews of Modern Physics, 1977. 49: pp. 1-20.

87. Oversby, V.M., *Nuclear waste materials*, 1994. In: Materials Science and Technology, A Comprehensive Treatment, Nuclear Materials, Part II, B.R.T. Frost, Editor. VCH: Weinheim, Germany. pp. 391-442.

88. Forsyth, R., *Spent nuclear fuel: A review of properties of possible relevance to corrosion processes*, 1995, Report TR 95-23, SKB, Stockholm, Sweden.

89. Hedin, A., *Spent nuclear fuel – how dangerous is it?*, 1997, Report TR-97-13, SKB, Stockholm, Sweden.

90. Buck, E.C., et al., *The geochemical behaviour of Tc, Np and Pu in spent nuclear fuel in an oxidizing environment*, 2004. In: Energy, Waste and the Environment: A Geochemical Perspective, R. Giere and P. Stille, Editors. The Geological Society of London Special Publication: London. pp. 65-88.

91. Bruno, J. and R.C. Ewing, *Spent nuclear fuel.* Elements, 2006. 2: pp. 343-349.

92. *Impact of high burnup uranium oxide and mixed uranium–plutonium oxide water reactor fuel on spent fuel management*, 2011, IAEA Nuclear Energy Series Report NF-T-3.8, International Atomic Energy Agency, Vienna, Austria.

93. Burns, P.C., et al., *Nuclear fuel in a reactor accident.* Science, 2012. 335: pp. 1184-1188.

94. Guenther, R.J., et al. *Detailed characterization of LWR fuel rods for the U.S. civilian radioactive waste management program*, 1989. In: Scientific Basis for Nuclear Waste Management XII, Berlin, Germany: R.C. Ewing and W. Lutze, Editors, MRS Proceedings, 127, pp. 325-336.

95. Guenther, R.J., et al., *Characterization of spent fuel approved testing material - ATM 104*, 1991, Report PNL-5109-104, Pacific Northwest Laboratory, Richland, WA, USA.

96. Kleykamp, H., *The chemical state of the fission products in oxide fuels.* Journal of Nuclear Materials, 1985. 131: pp. 221-246.

97. Kleykamp, H., *The chemical state of fission products in oxide fuels at different stages of the nuclear fuel cycles.* Nuclear Technology, 1988. 80: pp. 412-422.

98. Ducros, G., et al., *Synthesis of the VERCORS experimental programme: Separate-effect experiments on fission product release in support of the PHEBUS-FP programme.* Annals of Nuclear Energy, 2013. 61: pp. 75-87.

99. Shcherbina, N., et al., *Partitioning of selected fission products from irradiated oxide fuel induced by thermal treatment.* Journal of Nuclear Materials, 2013. 437: pp. 87-94.

100. Schrire, D. and G. Lysell. *Fuel microstructure and fission product distribution in BWR fuel at different power levels,* 1991. In: International Topical Meeting on LWR Fuel Performance, Avignon, France: European Nuclear Society, 2, pp. 518-527.

101. Forsyth, R.S., et al., *Fission product concentration profiles (Sr, Xe, Cs and Nd) at the individual grain level in power-ramped LWR fuel,* 1988, Report TR-88-24, SKB, Stockholm, Sweden.

102. Lysell, G. and S. Bengtsson, *Investigation of fuel behaviour at different power levels, SKI-bump II,* 1994, Report N(H)-94/13, Studsvik Nuclear, Nyköping, Sweden.

103. Yang, R.L. and T.C. Rowland. *The helium enigma: In-reactor pressurization of BWR fuel rods,* 1982. In: ANS Winter Meeting, November 14-19, 1982, Washington, DC, USA: Transactions of the American Nuclear Society, 43, p. 336.

104. Kamimura, K., et al. *Helium generation and release in MOX fuels*, 1999. In: MOX Fuel Cycle Technologies for Medium and Long Term Deployment, May 17–21,1999, Vienna, Austria: IAEA, Report IAEA-CSP-3, pp. 263-270.

105. Piron, J.P., et al. *Helium behaviour in spent UO_2 and MOX fuels*, 2002. In: Fission Gas Behaviour in Water Reactor Fuels, September 26-29, 2000, Cadarache, France: OECD Nuclear Energy Agency, pp. 311-320.

106. Rondinella, V.V. and T. Wiss, *The high-burnup structure in nuclear fuel.* Materials Today, 2010. 13(12): pp. 24-32.

107. Rudling, P., et al., *High burnup fuel issues.* Nuclear Engineering & Technology, 2008. 40: pp. 1-8.

108. Olander, D., *Nuclear fuels – Present and future.* Engineering Journal, 2009. 13: pp. 1–28.

109. *Waterside corrosion of zirconium alloys in nuclear power plants,* 1998, Report IAEA-TECDOC-996, International Atomic Energy Agency, Vienna, Austria.

110. Allen, T.R., et al., *Material performance and corrosion/waste materials*, 2012. In: Comprehensive Nuclear Materials (Vol. 5), R.J.M. Konings, Editor. Elsevier: Amsterdam, The Netherlands. pp. 49-68.

111. Motta, A.T. and L.-Q. Chen, *Hydride formation in zirconium alloys.* JOM, 2012. 64: pp. 1403-1408.

112. *Nuclear fuel behaviour in loss-of-coolant cccident (LOCA) conditions: State-of-the-art report,* 2009, Report NEA No. 6846, OECD Nuclear Energy Agency, Paris, France.

113. Gauld, I.C. *Validation of ORIGEN-S decay heat predictions for LOCA analysis,* 2006. In: PHYSOR-2006, ANS Topical Meeting on Reactor Physics, September 10-14, 2006, Vancouver, BC, Canada.

114. Tobias, A., *Decay heat.* Progress in Nuclear Energy, 1980. 5: pp. 1-93.

115. Ade, B.J. and I.C. Gauld, *Decay heat calculations for PWR and BWR assemblies fueled with uranium and plutonium mixed oxide fuel using SCALE,* 2011, Report ORNL/TM-2011/290, Oak Ridge National Laboratory, Oak Ridge, TN, USA.

116. Gunn, S.R., *Radiometric calorimetry: A review* Nuclear Instruments and Methods, 1964. 29: pp. 1–24.

117. Ramthun, H., *Recent developments in calorimetric measurements of radioactivity.* Nuclear Instruments and Methods, 1973. 112: pp. 265–272.

118. Jansson, P., *Studies of nuclear fuel by means of nuclear spectroscopic methods*, 2002, Doctoral Thesis, Uppsala University, Uppsala, Sweden.

119. Jansson, P., et al., *Gamma-ray spectroscopy measurements of decay heat in spent nuclear Fuel.* Nuclear Science and Engineering, 2002. Volume 141: pp. 129-139.

120. *Regulatory Guide 3.54 Rev. 1: Spent fuel heat generation in an independent spent fuel storage installation*. 1999, U.S. Nuclear Regulatory Commission: Washington, DC, USA.

121. *American national standard for deay heat power in light water reactors*. 2005, American Nuclear Society: La Grange Park, IL, USA.

122. *Calculation of the deacy power in nuclear fuels of light water reactors - Part 1: Uranium oxide nuclear fuel for pressurized water reactors,* 2014, Standard DIN 25463-1, Deutsches Institut Für Normung e.V., Beuth Verlag, Berlin, Germany.

123. Hermann, O.W., et al., *Technical support for a proposed decay heat guide using SAS2H/ORIGEN-S data*, 1994, Report NUREG/CR-5625 (ORNL-6698), U.S. Nuclear Regulatory Commission (Oak Ridge National Laboratory), Washington, DC, USA.

124. *ISO 10645:1992, Nuclear energy - Light water reactors -- Calculation of the decay heat power in nuclear fuels*, International Organization for Standardization: Geneva, Switzerland.

125. *Calculation of the deacy power in nuclear fuels of light water reactors - Part 2: Mixed uranium-plutonium oxide (MOX) nuclear fuel for pressurized water reactors*, 2014, Standard DIN 25463-2, Deutsches Institut Für Normung e.V., Beuth Verlag, Berlin, Germany.

126. Sturek, F., et al., *Measurements of decay heat in spent nuclear fuel at the Swedish interim storage facility CLAB,* 2006, Report R-05-62, Swedish Nuclear Fuel and Waste Management Company (SKB), Stockholm, Sweden.

127. Murphy, B.D. and I.C. Gauld, *Spent fuel decay heat measurements performed at the Swedish central interim storage facility,* 2010, Report NUREG/CR-6971, U.S. Nuclear Regulatory Commission, Washington DC, USA.

128. Ilas, G. and I.C. Gauld, *SCALE analysis of CLAB decay heat measurements for LWR spent fuel assemblies.* Annals of Nuclear Energy, 2008. 35: pp. 37–48.

129. Massih, A.R. and H.C. Schutte. *A probabilistic method for evaluation of fuel rod behavior in a reactor core*, 1998. In: Technical Meeting of the Groups of the German Nuclear Society (KTG), February 2-3, 1998, Karlsruhe, Germany.

130. Heins, L. and H. Landskron. *Fuel rod design by statistical methods for MOX fuel*, 1999. In: MOX Fuel Cycle Technologies for Medium and Long Term Deployment May 17-21, 1999, Vienna, Austria: Report IAEA-SM-358.

131. Kim, K.T., et al., *Development of a simplified statistical methodology for nuclear fuel rod internal pressure.* Journal of the Korean Nuclear Society, 1999. 31: pp. 257-266.

132. Parsons, P.D., et al., *The deformation, oxidation and embrittlement of PWR fuel cladding in a loss-of-coolant accident: A state of the art report,* 1986, CSNI Report 129, OECD NEA, Paris, France.

133. Shewfelt, R.S., *The ballooning of fuel cladding tubes: Theory and experiment.* Res Mechanica, 1988. 25: pp. 261-294.

134. Grandjean, C., *A state-of-the-art review of past programs devoted to fuel behavior under LOCA conditions. Part one: Clad swelling and rupture, assembly flow blockage,* 2005, Report SEMCA-2005-313, IRSN, Saint Paul-lez-Durance, France.

135. Erbacher, F.J. and S. Leistikow, *A review of Zircaloy fuel cadding behavior in a loss-of-coolant accident,* 1985, Report KfK 3973, Kernforschungszentrum Karlsruhe GmbH, Karlsruhe, Germany.

136. Alam, T., et al., *A review on the clad failure studies.* Nuclear Engineering and Design, 2011. 241: pp. 3658– 3677.

137. Perez-Feró, E., et al., *Experimental database of E110 claddings exposed to accident conditions.* Journal of Nuclear Materials, 2010. 397: pp. 48–54.

138. Hozer, Z., et al., *Ballooning experiments with VVER cladding.* Nuclear Technology, 2005. 152(3): pp. 273-285.

139. Jones, P.M., et al., *Modelling of azimuthal effects arising from interaction between clad deformation and heat transfer under LB LOCA conditions.* Nuclear Engineeering and Design, 1984. 79,: pp. 267–276.

140. Erbacher, F.J., et al., *Cladding deformation and emergency core cooling of a pressurized water reactor in a LOCA,* 1990, Report KfK 4781, Kernforschungszentrum Karlsruhe GmbH, Karlsruhe, Germany.

141. Kaddour, D., et al., *Experimental determination of creep properties of zirconium alloys together with phase transformation.* Scripta Materialia, 2004. 51: pp. 515–519.

142. Chung, H.M. and T.F. Kassner, *Pseudobinary Zircaloy-oxygen phase diagram.* Journal of Nuclear Materials, 1979. 84: pp. 327–339.

143. Burton, B., *Creep fracture processes in Zircaloy.* Journal of Nuclear Materials, 1983. 113: pp. 172-178.

144. Burton, B., et al. *Interaction of oxidation and creep in Zircaloy-2,* 1979. In: Zirconium in the Nuclear Industry (Fourth Conference): American Society for Testing and Materials, pp. 561-585.

145. Rosinger, H.E., et al., *The steady-state creep of Zircaloy-4 fuel cladding from 940 to 1873 K,* 1978, Report AECL-6193, Atomic Energy of Canada Limited, Pinawa, MB, Canada.

146. Rosinger, H.E., et al., *Steady-state creep of Zircaloy-4 fuel cladding from 940 to 1873 K.* Journal of Nuclear Materials, 1979. 82: pp. 286-297.

147. Donaldson, A.T. and T. Healey, *Creep deformation of Westinghouse Zircaloy-4 fuel cladding in alpha plus beta phase temperature range,* 1984, Report TRPD/B/0564/N85, Central Electricity Generating Board, Berkeley, UK.

148. Donaldson, A.T., et al. *Biaxial creep deformation of Zircaloy-4 PWR fuel cladding in the alpha, (alpha+beta), and beta phase temperature ranges,* 1985. In: Nuclear Fuel Performance Conference, March 25-29, 1985, Stratford-upon-Avon, UK: British Nuclear Energy Society (BNES), 2, pp. 83-89.

149. Donaldson, A.T., et al., *Creep behaviour of Westinghouse Zr-4 fuel tubes between 973 and 1073 K,* 1985, Report TRPD/B/0008/N82, Central Electricity Generating Board, Berkeley, UK.

150. Kaddour, D., *Fluage isotherme et anisotherme dans les domaines monophasés (α et β) et biphasés (α + β) d'un alliage Zr-1 %NbO,* 2004, Doctoral Thesis, Ecole Nationale Supérieure des Mines de Paris, Paris, France.

151. Massih, A.R., *An evaluation of high-temperature creep of zirconium alloys: data versus models,* 2014, Research report SSM-2014:20, Swedish Radiation Safety Authority, Stockholm, Sweden.

152. Massih, A.R., *High-temperature creep and superplasticity in zirconium alloys.* Journal of Nuclear Science and Technology, 2013. 50: pp. 21–34.

153. Moulin, G., et al., *High temperature creep properties of zirconium and Zircaloy-4 in vacuum and oxygen environments.* Journal of Nuclear Materials, 2007. 362: pp. 309–315.

154. Oguma, M., *Cracking and relocation behaviour of nuclear fuel pellet during rise to power.* Nuclear Engineering and Design, 1983. 76: pp. 35–45.

155. Coindreau, O., et al., *Nuclear fuel rod fragmentation under accidental conditions.* Nuclear Engineering and Design, 2013. 255: pp. 68-76.

156. Raynaud, P.A.C., *Fuel fragmentation, relocation, and dispersal during the loss-of-coolant accident,* 2012, Report NUREG-2121, U.S. Nuclear Regulatory Commission, Washington, DC, USA.

157. Oberländer, B. and W. Wiesenack, *Overview of Halden reactor LOCA experiments (with emphasis on fuel fragmentation) and plans,* 2014, Report IFE/KR/E-2014/001, Institute for Energy Technology, Kjeller, Norway.

158. Hiernaut, J.P., et al., *Fission product release and microstructure changes during laboratory annealing of a very high burn-up fuel specimen.* Journal of Nuclear Materials, 2008. 377: pp. 313-324.

159. Kolstad, E., et al. *High burnup fuel behaviour under LOCA conditions as observed in Halden reactor experiments*, 2011. In: Fuel Beaviour and Modelling Under Severe Transient and Loss of Coolant Accident (LOCA) Conditions, October 18-21, 2011, Mito, Japan.

160. Flanagan, M. and P. Askeljung. *Observations of fuel fragmentation mobility and release in integral high-burnup fueled LOCA tests*, 2012. In: Halden Workshop on LOCA, May 29-30, 2012, Lyon, France.

161. Askeljung, P., et al. *NRC LOCA testing program at Studsvik: Recent results on high burnup fuel*, 2012. In: TopFuel - Reactor Fuel Performance 2012, September 2-6, 2012, Manchester, UK: European Nuclear Society.

162. Erbacher, F.J., et al. *Burst criterion of Zircaloy fuel claddings in a loss-of-coolant accident*, 1982. In: Zirconium in the Nuclear Industry: Fifth Conference, ASTM STP-754, August 4-7, 1980, Boston, MA, USA: D.G. Franklin, Editor American Society for Testing and Materials, pp. 271-283.

163. Manngård, T. and A.R. Massih, *Modelling and simulation of reactor fuel cladding under loss-of-coolant accident conditions.* Journal of Nuclear Science and Technology, 2011. 48: pp. 39-49.

164. Powers, D.A. and R.O. Meyer, *Cladding swelling and rupture models for LOCA analysis,* 1980, Report NUREG-0630, U.S. Nuclear Regulatory Commission, Washington, DC, USA.

165. Neitzel, H.J. and H.E. Rosinger, *The development of burst criterion for Zircaloy fuel cladding under LOCA conditions,* 1980, Report KfK 2893, Kernforschungszentrum Karlsruhe, Karlsruhe, Germany.

166. Varty, R.L. and H.E. Rosinger, *Comparison of fuel sheath model with published experimental data,* 1982, Report AECL-6806, Atomic Energy of Canada Limited, Pinawa, MB, Canada.

167. Ferner, J. and H.E. Rosinger, *The effect of oxygen on the failure of reactor fuel sheaths during a postulated loss-of-coolant accident,* 1983, Report AECL-7791, Atomic Energy of Canada Limited, Pinawa, MB, Canada.

168. Erbacher, F.J., *Cladding tube deformation and core emergency cooling in a loss of coolant accident of a pressurized water reactor.* Nuclear Engineering and Design, 1987. 103: pp. 55-64.

169. Rosinger, H.E., *A model to predict the failure of Zircaloy-4 fuel sheathing during postulated LOCA conditions*. Journal of Nuclear Materials, 1984. 120: pp. 41-54.

170. Forgeron, T., et al. *Experiment and modeling of advanced fuel rod cladding behavior under LOCA conditions: alpha-beta phase transformation kinetics and EDGAR methodology*, 2000. In: Zirconium in the Nuclear Industry, 12th International Symposium, STP-1354: G.P. Sabol and G.D. Moan, Editors, American Society for Testing and Materials.

171. Chapin, D.L., et al. *Optimized ZIRLO qualification program for EDF reactors*, 2009. In: TopFuel 2009, September 6-9, 2009, Paris, France: European Nuclear Society.

172. Flanagan, M., *Mechanical behavior of ballooned and ruptured cladding*, 2012, Report NUREG-2119, U.S. Nuclear Regulatory Commission, Washington, DC, USA.

173. Kim, J.H., et al., *Effects of oxide and hydrogen on the behavior of Zircaloy-4 cladding during the loss-of-coolant accident (LOCA)*. Nuclear Engineering and Design, 2006. 236: pp. 2386-2393.

174. Brachet, J.-C., et al. *Influence of hydrogen content on the α/β phase transformation temperatures and on the thermal-mechanical behaviour of Zy-4, M4 (ZrSnFeV) and M5^{TM} (ZrNbO) alloys during the first phase of LOCA transient*, 2002. In: Zirconium in the Nuclear Industry, 13th International Symposium, STP-1423: G.D. Moan and P. Rudling, Editors, American Society for Testing and Materials, pp. 673-701.

175. Ferner, J. and H.E. Rosinger, *The effect of circumferential temperature variation on fuel-cladding failure*. Journal of Nuclear Materials, 1985. 132: pp. 167-172.

176. Rosinger, H.E. and J. Ferner, *A study of the effect of circumferential temperature variation on fuel-sheath failure*. Res Mechanica, 1986. 19: pp. 143-146.

177. Shewfelt, R.S. and D.P. Godin, *Ballooning of thin-walled tubes with circumferential temperature variations*. Res Mechanica, 1986. 18: pp. 21-33.

178. Natesan, K. and W.K. Soppet, *Air oxidation kinetics for Zr-based alloys*, 2004, Report NUREG/CR-6846, U.S. Nuclear Regulatory Commission, Washington, DC, USA.

179. Natesan, K. and W.K. Soppet, *Hydrogen effects on air oxidation of ZIRLO alloy*, 2004, Report NUREG/CR-6851, U.S. Nuclear Regulatory Commission, Washington, DC, USA.

180. Steinbrück, M., et al., *Prototypical experiments on air oxidation of Zircaloy-4 at high temperatures*, 2007, Report FZKA-7257, Forschungszentrum Karlsruhe, Karlsruhe, Germany.

181. *Status report on hydrogen management and related computer codes*, 2014, Report NEA/CSNI/R(2014)8, OECD Nuclear Energy Agency, Paris, France.

182. Nagase, F., et al., *Oxidation kinetics of low-Sn Zircaloy-4 at the temperature range from 773 K to 1573 K*. Journal of Nuclear Science and Technology, 2003. 40(4): pp. 213-219.

183. Steinbrück, M. and M. Grosse. *Deviations from the parabolic kinetics during oxidation of zirconium alloys*, 2013. In: Seventeenth International Symposium on Zirconium in the Nuclear Industry, February 3-7, 2013, Hyderabad, India.

184. Schanz, G., *Semi-mechanistic approach for the kinetic evaluation of experiments on the oxidation of zirconium alloys*, 2007, Report FZKA-7329, Forschungszentrum Karlsruhe, Karlsruhe, Germany.

185. Bailly, H., et al., *The nuclear fuel of pressurized water reactors and fast neutron reactors*. 1999, Cachan, France: Lavoisier Publishing.

186. Stephenson, W., et al., *Realistic methods for calculating the releases and consequences of a large LOCA*, 1992, Report EUR-14179-EN, Commission of the European Communities, Luxembourg.

187. Hanson, B.D., *The burnup dependence of light water reactor spent fuel oxidation,* 1998, Report PNNL-11929, Pacific Northwest National Laboratory, Richland, WA, USA.

188. Hunt, C.E.L., et al., *Fission-product release during accidents: An accident management perspective.* Nuclear Engineeering and Design, 1994. 148: pp. 205-213.

189. Hiernaut, J.P., et al., *Thermodynamic study of actinides and lanthanides during total vaporisation of a very high burn-up UO_2 fuel.* Journal of Nuclear Materials, 2008. 378(3): pp. 349-357.

190. *Chernobyl: Assessment of radiological and health impacts (2002 update of "Chernobyl: Ten Years On"),* 2002, OECD Nuclear Energy Agency, Paris, France.

191. Hiernaut, J.P., et al., *Volatile fission product behaviour during thermal annealing of irradiated UO_2 fuel oxidised up to U_3O_8.* Journal of Nuclear Materials, 2008. 372(2-3): pp. 215-225.

192. Lewis, B.J., et al., *Low volatile fission-product release and fuel volatilization during severe reactor accident conditions.* Journal of Nuclear Materials, 1998. 252(3): pp. 235-256.

193. Devell, L., et al., *The Chernobyl reactor accident source term: Development of a consensus view,* 1995, Report NEA/CSNI/R(95)24, OECD Nuclear Energy Agency, Paris, France.

194. Alvarez, R., et al., *Reducing the hazards from stored spent power-reactor fuel in the United States.* Science and Global Security, 2003. 11: pp. 1-51.

195. Iglesias, F.C., et al., *Fission product release mechanisms during reactor accident conditions.* Journal of Nuclear Materials, 1999. 270: pp. 21-38.

196. Benson, C.G., et al., *Fission product release from molten pools: Final report,* 1999, Report AEAT-5893, AEA Technology, Harwell, UK.

197. Wilson, R., et al., *Report to the American Physical Society of the study group on radionuclide release from severe accidents at nuclear power plants.* Reviews of Modern Physics, 1985. 57(3): pp. S1-S144.

198. Vokac, P. *Simulations of VVER-440/213 severe accident scenarios at shutdown using the MELCOR code,* 2013. In: The 8th International Scientific and Technical Conference: Safety Assurance of NPP with VVER, May 28-31, 2013, Podolsk, Russian Federation.

199. Hozer, Z., et al., *Quenching of high temperature VVER fuel after long term oxidation in hydrogen rich steam.* Annals of Nuclear Energy, 2010. 37: pp. 71-82.

200. Hozer, Z., et al., *Experimental simulation of the Paks-2 cleaning tank incident through separate effect and integral tests.* Nuclear Engineeering and Design, 2011. 241(3): pp. 573-581.

201. Perez-Feró, E., et al., *Experimental database of E110 claddings under accident conditions, NEA-1799 IFPE/AEKI-EDB-E110*, International Fuel Performance Experiments (IFPE) Database, OECD Nuclear Energy Agency: Available via internet at https://www.oecd-nea.org/science/wprs/fuel/ifpelst.html.

202. Rosa, C.J. and W.W. Smeltzer, *The oxidation of zirconium in oxygen-nitrogen atmospheres.* Zeitschrift für Metallkunde, 1980. 71(7): pp. 470-475.

203. Hayes, E.T. and A.H. Roberson, *Some effects of heating zirconium in air, oxygen and nitrogen.* Journal of the Electrochemical Society, 1949. 96(3): pp. 142-151.

204. Probst, H.B., et al., *Scaling of zirconium at elevated temperatures,* 1959, USAEC Report AECU-4113, United States Atomic Energy Commission, Cleveland, OH, USA.

205. Evans, E.B., et al. *Critical role of nitrogen during high temperature scaling of zirconium,* 1972. In: Symposium on High-temperature Gas-metal Reactions in Mixed Environments, May 9-10, 1972, Boston, MA, USA: Metallurgical Society of AIME, pp. 248-281.

206. Suzuki, M. and S. Kawasaki, *Oxidation of Zircaloy cladding in air*. Journal of Nuclear Materials, 1986. 140(1): pp. 32-43.

207. Leistikow, S., et al., *Study on high temperature steam oxidation of Ziracloy-4 cladding tubes,* 1976, Report KFK-2262, Kernforschungszentrum Karlsruhe, Karlsruhe, Germany.

208. Leistikow, S. and H.V. Berg. *Investigation under nuclear safety aspects of Zircaloy-4: Oxidation kinetics at high temperature in air,* 1987. In: Second Workshop of German and Polish Research on High Temperature Corrosion of Metals, December 2-4, 1987, Julich, Germany: W.J. Quadakkers, H. Schuster, and P.J. Ennis, Editors, pp. 114-132.

209. Coindreau, O., et al., *Air oxidation of Zircaloy-4 in the 600-1000 C temperature range: Modeling for ASTEC code application.* Journal of Nuclear Materials, 2010. 405: pp. 207-215.

210. Steinbrück, M. and M. Böttcher, *Air oxidation of Zircaloy-4, M5 and ZIRLO cladding alloys at high temperatures.* Journal of Nuclear Materials, 2011. 414: pp. 276-285.

211. Ver, N., *Determination of kinetic parameters of the oxidation of zirconium alloys in steam/air mixtures,* 2007, Report AEKI-FRL-2007-401-01/01, AEKI KFKI, Budapest, Hungary.

212. Matus, L., et al., *Summary of separate effect tests with E110 and Zircaloy-4 in high temperature air, oxygen and nitrogen,* 2008, Report AEKI-FL-2008-401-04/01, AEKI KFKI, Budapest, Hungary.

213. Duriez, C., et al., *Zircaloy-4 and M5 high temperature oxidation and nitriding in air*. Journal of Nuclear Materials, 2008. 380: pp. 30-45.

214. Duriez, C., et al., *Reaction in air and in nitrogen of pre-oxidised Zircaloy-4 and M5 claddings.* Journal of Nuclear Materials, 2013. 441(1-3): pp. 84-95.

215. Idarraga, I., et al., *Potentialities of raman imaging for the analysis of oxide scales formed on Zircaloy-4 and M5 in air at high temperature*. Oxidation of Metals, 2013. 79(3-4): pp. 289-302.

216. Idarraga, I., et al., *Raman investigation of pre- and post-breakaway oxide scales formed on Zircaloy-4 and M5 in air at high temperature*. Journal of Nuclear Materials, 2012. 421: pp. 160-171.

217. Frank, H., *Influence of oxidation media on the transport properties of thin oxide layers of zirconium alloys.* Acta Polytechnica, 2007. 47(6): pp. 36-42.

218. Lewis, B.J., et al., *Overview of experimental programs on core melt progression and fission product release behaviour*. Journal of Nuclear Materials, 2008. 380: pp. 126-143.

219. Giordano, P., et al., *Recent advances in understanding ruthenium behaviour under air-ingress conditions during a PWR severe accident.* Progress in Nuclear Energy, 2010. 52: pp. 109-119.

220. Hidaka, A., *Outcome of VEGA program on radionuclide release from irradiated fuel under severe accident conditions.* Journal of Nuclear Science and Technology, 2011. 48(1): pp. 85-102.

221. Lorenz, R.A. and M.F. Osborne, *A summary of ORNL fission product release tests with recommended release rates and diffusion coefficients,* 1995, Report NUREG/CR-6261, U.S. Nuclear Regulatory Commission, Washington, DC, USA.

222. Lorenz, R.A., et al., *Fission product release from highly irradiated LWR fuel,* 1980, Report NUREG/CR-0722, U.S. Nuclear Regulatory Commission, Washington, DC, USA.

223. Osborne, M.F., et al., *Data summary report for fission product release test VI-7,* 1995, NUREG/CR-6318, U.S. Nuclear Regulatory Commission, Washington, DC, USA.

224. Liu, Z., et al., *A summary of CRL fission-product release measurements from UO_2 samples during post-irradiation annealing (1983-1992)*, 1994, Report COG-92-377, CANDU Owners Group, Toronto, ON, Canada.

225. Dickson, R.S., et al. *Cesium release from CANDU fuel in argon, steam and air: The UCE12 experiment*, 1994. In: Fifteenth Annual Conference of the Canadian Nuclear Society, June 5-8, 1994, Montreal, QC, Canada.

226. Cox, D.S., et al. *Fission product releases from UO_2 in air and inert conditions at 1700-2350 K: Analysis of the MCE-1 experiment*, 1991. In: American Nuclear Society International Topical Meeting on the Safety of Thermal Reactors, July 21-25, 1991, Portland, OR, USA.

227. Cox, D.S., et al., *Fission product release kinetics from CANDU and LWR fuel during high-temperature steam oxidation experiments*, 1999. In: Fission Gas Release and Fuel Rod Chemistry Related to Extended Burnup, IAEA-TECDOC-697. IAEA: Vienna, Austria. pp. 153-164.

228. Barrand, R.D., et al. *Release of fission products from CANDU fuel in air, steam and argon atmospheres at 1500-1900 C: The HCE3 experiment*, 1999. In: Sixth International Conference on CANDU Fuel, September 26-29, 1999, Niagara Falls, ON, Canada.

229. Dickson, L.W. and R.S. Dickson. *Fission product releases from CANDU fuel at 1650 C. The HCE4 experiment*, 2001. In: Seventh International CNS CANDU Fuel Conference, September 23-27, 2001, Kingston, ON, Canada: Canadian Nuclear Society, pp. 3B21-3B30.

230. Williamson, R. and S.A. Beetham, *Fission product release during air oxidation of irradiated uranium dioxide*, 1990. In: Fission Product Transport Processes in Reactor Accidents, J.T. Rogers, Editor. Hemisphere Publishing: New York, USA. pp. 175-186.

231. Bennett, M.J., et al., *Influence of manufacturing route and burn-up on the oxidation and fission gas release behaviour of irradiated uranium dioxide in air at 175-400 C.* Nuclear Energy, 1988. 27(1): pp. 49-54.

232. Leveque, J.P., et al., *The HEVA experimental programme.* Nuclear Technology, 1994. 108: pp. 33-44.

233. Clément, B. and R. Zeyen, *The objectives of the Phébus FP experimental programme and main findings.* Annals of Nuclear Energy, 2013. 61: pp. 4-10.

234. de Luze, O., et al., *Early phase fuel degradation in Phébus FP: Initiating phenomena of degradation in fuel bundle tests.* Annals of Nuclear Energy, 2013. 61: pp. 23-35.

235. Barrachin, M., et al., *Late phase fuel degradation in the Phébus FP tests.* Annals of Nuclear Energy, 2013. 61: pp. 36-53.

236. Clément, B. and R. Zeyen. *The Phebus fission product and source term international programmes*, 2005. In: International Conference on Nuclear Energy for New Europe, September 5-8, 2005, Bled, Slovenia.

237. Steinbrück, M., et al., *Synopsis and outcome of the QUENCH experimental program.* Nuclear Engineeering and Design, 2010. 240(7): pp. 1714-1727.

238. Stuckert, J. and M. Steinbrück, *Experimental results of the QUENCH-16 bundle test on air ingress.* Progress in Nuclear Energy, 2014. 71: pp. 134-141.

239. Hering, W., et al., *Results of boil-off experiment QUENCH-11*, 2007, Report FZKA 7247, Forschungszentrum Karlsruhe, Karlsruhe, Germany.

240. Hering, W., et al., *Analytical pre-test support of boil-down test QUENCH-11,* 2008, Report FZKA 7305, Forschungszentrum Karlsruhe, Karlsruhe, Germany.

241. Hozer, Z., et al., *Interaction of failed fuel rods under air ingress conditions.* Nuclear Technology, 2003. 141: pp. 244-256.

242. Schanz, G., et al., *Results of the QUENCH-10 experiment on air ingress,* 2006, Report FZKA 7087, Forschungszentrum Karlsruhe, Karlsruhe, Germany.

243. Stuckert, J., et al., *Results of the QUENCH-16 bundle experiment on air ingress,* 2013, Report KIT-SR-7634, Karlsruhe Institute of Technology, Karlsruhe, Germany.

244. Kisselev, A.E., et al. *Application of thermal hydraulic and severe accident code SOCRAT/V2 to bottom water reflood experiment PARAMETER-SF4,* 2010. In: Nuclear Energy for New Europe 2010, September 6-9, 2010, Portoroz, Slovenia.

245. Fernandez-Moguel, L. and J. Birchley, *Simulation of air oxidation during a reactor accident sequence: Part 2 - Analysis of PARAMETER-SF4 air ingress experiment using RELAP5/SCDAPSIM.* Annals of Nuclear Energy, 2012. 40: pp. 141-152.

246. Steinbrück, M. and S. Schaffer. *High-temperature oxidation of Zircaloy-4 in oxygen-nitrogen mixtures,* 2014. In: International Symposium on High-Temperature Corrosion and Oxidation, June 23-27, 2014, Hakodate, Hokkaido, Japan.

247. Steinbrück, M., et al. *High-temperature oxidation of Zircaloy-4 in steam-nitrogen mixtures,* 2014. In: The Nuclear Materials Conference (NuMat2014), October 27-30, 2014, Clearwater Beach, FL, USA.

248. *Best practice guidelines for the use of CFD in nuclear reactor safety applications,* 2007, Report NEA/CSNI/R(2007)5, OECD Nuclear Energy Agency, Committee on the Safety of Nuclear Installations, Paris, France.

249. Fleurot, J., et al., *Synthesis of spent fuel pool accident assessments using severe accident codes.* Annals of Nuclear Energy, 2014. 74: pp. 58-71.

250. Adorni, M., *Benchmark Sandia Fuel Project Phase I: Ignition testing,* 2012, Final Report OECD Nuclear Energy Agency, Paris, France.

251. Hollands, T., *Benchmark Sandia Fuel Project Phase II: Ignition testing,* 2013, Final Report OECD Nuclear Energy Agency, Paris, France.

252. Jacq, F., et al. *Multi-physics modeling in the frame of the DRACCAR code development and its application to spent-fuel pool draining accidents,* 2013. In: EUROSAFE Forum, November 4-5, 2013, Cologne, Germany.

253. Bascou, S., et al. *Computational analysis of multi-pin ballooning during LOCA and post-LOCA transient using the multi-physics code DRACCAR,* 2012. In: TopFuel 2012, September 2-6, 2012, Manchester, UK.

254. Ricaud, J.-M., et al., *Multi-pin ballooning during LOCA transient: A three-dimensional analysis.* Nuclear Engineeering and Design, 2013. 256: pp. 45– 55.

255. Herranz, L.E., et al., *Modeling of the SFP-PWR ignition test with MELCOR,* 2013, Report DFN/SN-4/OP-13, CIEMAT, Division de Fision Nuclear, Madrid, Spain.

256. Thompson, W.T., et al., *Thermodynamic treatment of uranium dioxide based nuclear fuel.* International Journal of Materials Research, 2007. 98(10): pp. 1004-1011.

257. Barrachin, M., et al., *Progress in understanding fission-product behaviour in coated uranium-dioxide fuel particles.* Journal of Nuclear Materials, 2009. 385(2): pp. 372-386.

258. *Belgian stress tests: National report for nuclear power plants,* 2011, Federal Agency for Nuclear Control, Brussels, Belgium.

259. *Belgian stress tests: National action plan for nuclear power plants,* 2012, Federal Agency for Nuclear Control, Brussels, Belgium.

260. *CNSC integrated action plan on the lessons learned from the Fukushima Daiichi nuclear accident,* 2013, Report CC172-100/2013E-PDF, Canadian Nuclear Safety Commission, Ottawa, ON, Canada.

261. Adorjan, F., ed. *National report of Hungary on the targeted safety re-assessment of Paks nuclear power plant, compiled for the European Commission by the Hungarian Atomic Energy Authority* 2011: Budapest, Hungary.

262. *Outline of new regulatory requirements for light water nuclear power plants (severe accident measures),* 2013, Provisional translation, available at http://www.nsr.go.jp/english/data/new_regulatory_requirements3.pdf, Nuclear Regulation Authority, Tokyo, Japan.

263. *Stress tests carried out by Spanish nuclear power plants: Final report,* 2011, Spanish Nuclear Safety Council (CSN), Madrid, Spain.

264. *B.5.b Phase 2 & 3 Submittal Guideline,* 2006, Report NEI 06-12 (Rev. 2), Nuclear Energy Institute, Washington, DC, USA.

265. *European stress tests for nuclear power plants: The Swedish national report,* 2011, Swedish Radiation Safety Authority, Stockholm, Sweden.

266. *Swedish action plan for nuclear power plants: Response to ENSREG's request,* 2012, Swedish Radiation Safety Authority, Stockholm, Sweden.

267. Miller, C., et al., *Recommendations for enhancing reactor safety in the 21st century: The Near-Term Task Force review of insights from the Fukushima Dai-ichi accident,* 2011, (ADAMS accession no. ML111861807), U.S. Nuclear Regulatory Commission, Washington, DC, USA.

268. *Order modifying licenses with regard to requirements for mitigation strategies for beyond-design-basis external events,* 2012, Order EA-12-049, U.S. Nuclear Regulatory Commission, Washington, DC, USA.

269. *Order modifying licenses with regard to reliable spent fuel pool instrumentation,* 2012, Order EA-12-051, U.S. Nuclear Regulatory Commission, Washington, DC, USA.

270. *Assessment of spent fuel pool cooling,* 1997, NRC Information Notice IN 97-14, U.S. Nuclear Regulatory Commission, Washington, DC, USA.

271. *Loss of shutdown cooling due to station blackout during refueling outage,* 2012, Report IRS-8229, IAEA International Reporting System for Operating Experience, Vienna, Austria.

272. *Dual unit loss of offsite power resulting from inadequate relay modification,* 2012, Report IRS-8292, IAEA International Reporting System for Operating Experience, Vienna, Austria.

273. *EDG failed to start after undetected loss of two phases on 400 kV incoming offsite supply,* 2013, Report IRS-8315, IAEA International Reporting System for Operating Experience, Vienna, Austria.

274. *Irradiated fuel, both in the vessel and the spent fuel pool, without forced cooling during refueling outage,* 2007, Report IRS-7912, IAEA International Reporting System for Operating Experience, Vienna, Austria.

275. *Inoperable SFP cooling pumps results in loss of safety function,* 2007, Licensee Event Report LER 2007-007, San Onofre Nuclear Generating Station, San Clemente, CA, USA.

276. *Both trains of spent fuel pool cooling inoperable results in a loss of safety function*, 2009, Licensee Event Report LER 2009-004, San Onofre Nuclear Generating Station, San Clemente, CA, USA.

277. *Drop in the level of the wet refueling pool and flooding of reactor building areas*, 2002, Report IRS-7568, IAEA International Reporting System for Operating Experience, Vienna, Austria.

278. *Insufficient testing of functionality of siphon breaker valve at spent fuel basin due to lack in inspection program*, 2012, Report IRS-8299, IAEA International Reporting System for Operating Experience, Vienna, Austria.

279. *Deterministic safety analysis for nuclear power plants*, 2009, Specific Safety Guide SSG-2, International Atomic Energy Agency, Vienna, Austria.

280. *Approaches and tools for severe accident analysis for nuclear power plants*, 2008, Safety Report Series No. 56, International Atomic Energy Agency, Vienna, Austria.

281. Lindgren, E.R. and S.G. Durbin, *Laminar hydraulic analysis of a commercial pressurized water reactor fuel assembly*, 2013, Report NUREG/CR-7144, U.S. Nuclear Regulatory Commission, Washington, DC, USA.

282. Birchley, J., et al., *PSI oxidation model for Zircaloy-4: Background, description, input specification and assessment summary*, 2013, Report TM-42-13-11, Paul Scherrer Institut, Villigen, Switzerland.

283. Armijo, J.S., *Letter from the Advisory Committee on Reactor Safeguards to the U.S. Nuclear Regulatory Commission*. 2013, U.S. Nuclear Regulatory Commission (ADAMS accession no. ML13198A433): Washington, DC, USA.

284. Austregesilo, H., et al., *ATHLET-CD Mod 2.2 Cycle C - User's Manual*, 2012, Report GRS-P-4/Vol.1, Gesellschaft für Anlagen- und Reaktorsicherheit (GRS), Garching, Germany.

285. Birchley, J., et al. *WP5.1: Conduct and analytical support to air ingress experiment QUENCH-16*, 2012. In: Fifth European Review Meeting on Severe Accident Research (ERMSAR-2012), March 21-23, 2012, Cologne, Germany.

286. *MAAP4: Modular Accident Analysis Program for LWR Power Plants*, 1994-2005, User's Manual, Fauske and Associates, LCC, Burr Ridge, IL, USA.

287. Paik, C.Y. *Spent fuel pool model in MAAP5*, 2011. In: EPRI MAAP Users Group Training Meeting, August 10-12, 2011, Daejon, Republic of Korea.

288. Powers, D.A., et al., *A review of the technical issues of air ingression during severe reactor accidents*, 1994, Report NUREG/CR-6218, U.S. Nuclear Regulatory Commission, Washington, DC, USA.

289. van Dorsselaere, J.P., et al., *The ASTEC integral code for severe accident simulation.* Nuclear Technology, 2009. 165: pp. 293-307.

290. Albiol, T., et al., *SARNET: Severe accident research network of excellence*. Progress in Nuclear Energy, 2010. 52(1): pp. 2-10.

APPENDIX A:
SPENT FUEL STORAGE SITUATION IN OECD MEMBER COUNTRIES

This appendix summarizes the current spent fuel storage situation in some OECD member countries with the main purpose to provide brief overviews of spent fuel management strategies, national requirements/criteria for SFPs, and representative design data for at-reactor SFPs and storage racks currently used in LWR and CANDU power plants.

Table A.1: Summary of spent fuel management strategies.

COUNTRY	ORIGINAL CONFIGURATION OF SFP MAINTAINED	DRY CASK (ONSITE STORAGE)	CENTRALIZED INTERIM STORAGE	REPROCESSING	DIRECT DISPOSAL
BELGIUM	No, for some plants	Yes	Yes, Wet and Dry[9]	Not any longer[10]	Long term policy still to be developed
CANADA	Yes	Yes[11]	No[12]	No	Future plans[13]
CZECH REPUBLIC	Yes[14]	Yes	No	No	No
FRANCE	Yes	No	Yes[15]	Yes	No
GERMANY	-	Yes	Yes, for some plants	Not any longer	Currently not, but foreseen
HUNGARY[16]	No[17]	Yes[18]	Yes, Dry	No	Planned, site investigation in progress
ITALY	Yes[19]	-	-	Yes[20]	-
JAPAN	Yes	Yes	Yes	Yes	No
KOREA (REPUBLIC OF)	No[21]	No	Yes, Dry[22]	Under plan	Under review
SPAIN[23]	No[24]	Yes, for some plants	Planned, Dry [25]	-	-
SWEDEN	No[26]	No	Yes, Wet	No	Planned
USA	No	Yes	No	No	No

[9]. Dry storage at Doel site (SCG building); wet storage at Tihange site (DE building).
[10]. The last Belgian fuel elements sent to La Hague have been reprocessed in late 2001.
[11]. Dry cask storage after 7 to 10 years.
[12]. All plants have moved to dry cask storage.
[13]. Site for deep geological repository for high level waste not yet selected.
[14]. The original configuration of the SFP is maintained – high density storage.
[15]. For all the NPPs of Electricité de France, the management strategy is to use a centralized storage, before reprocessing.
[16]. The spent fuel is stored in high density racks of the SFP for 3-5 years. After that, the spent fuel is transported to the Modular Vault Dry Storage (MVDS) facility that is located close to the NPP. There is one common interim storage facility for all four units. According to the plans, the spent fuel will be sent to final disposal in a domestic deep geological repository after several decades of dry storage.
[17]. There are no plans to return to low density configuration.
[18]. Modular Vault Dry Storage facility.
[19]. Spent fuel shipped abroad for reprocessing. The fuel elements will be reprocessed to recover valuable materials and condition the final waste for return to Italy for disposal.
[20]. Since the beginning of its nuclear program, Italy has pursued the option of reprocessing abroad the spent fuel produced in its NPPs.
[21]. There are no plans to return to low density configuration.
[22]. Feasibility of interim storage facility to store the spent fuel is currently being explored.
[23]. Spanish NPPs have accomplished re-racking modifications; some of the SFPs are almost full, so those plants have built interim onsite dry cask storage.
[24]. All NPPs in Spain have moved to high density spent fuel configurations in order to provide additional storage. No plan to return to low density configurations.
[25]. A centralized interim dry storage will become operational in 2018.
[26]. With the exception of one BWR unit.

Table A.2: Summary of status of national requirements/criteria for SFPs (part 1/2).

COUNTRY	STATUS OF NATIONAL REQUIREMENTS/CRITERIA FOR SPENT FUEL POOLS
BELGIUM	U.S. NRC Standard Review Plan 9.1.3 (General Design Criterion 61) U.S. NRC Standard Review Plan 9.1.2 U.S. NRC Regulatory Guide 1.13 (Spent Fuel Storage Facility Design Basis) WENRA reference levels for existing NPP Additional requirement from BElgian Stress Test (BEST) action plan Arrêté royal du 30 novembre 2011 "Prescriptions de sûreté des installations nucléaires"
CANADA	Pool must have space for an emergency core dump at all times. Sufficient time for operator intervention to terminate or mitigate accident: Normally demonstrated as > 24 h until bulk pool boiling is reached in a loss of cooling accident. Structural integrity maintained.
CZECH REPUBLIC	Safety requirements are imposed by national legislation. European "stress tests" were performed after the Fukushima accident. Conclusions of this activity are summarized in the National Action Plan on Strengthening Nuclear Safety of Nuclear Facilities in the Czech Republic. Currently an update of national legislation is ongoing to accommodate recent changes in WENRA reference levels. See references for details. *References* 1. Decree of the SÚJB No. 195/1999 Coll., on Basic Design Criteria for Nuclear Installations with Respect to Nuclear Safety Radiation Protection and Emergency Preparedness. 2. Decree of the SÚJB No. 106/1998 Coll., on Nuclear Safety and Radiation Protection Assurance during Commissioning and Operation of Nuclear Facilities. 3. "Post Fukushima National Action Plan on Strengthening Nuclear Safety of Nuclear Facilities in the Czech Republic" ("National Action Plan"). 4. National Report of Dukovany NPP and Temelín NPP prepared under the initiative of the European Commission in response to the Fukushima Daiichi nuclear power plant accident ("stress tests"). 5. WENRA: Updated Reference Levels for Existing NPP - November 2013
HUNGARY[27]	According to the requirements of the Hungarian Atomic Energy Authority, the SFP must be able to provide the following functions: • Criticality must be prevented with an acceptable threshold, • Decay heat removal must be guaranteed in any operational condition, • The free capacity of the SFP must be enough for emergency offload of a full reactor core, • Biological shielding must be guaranteed for the operating staff, technical solutions must be available for the storage of leaking or damaged fuel.
ITALY	Not anymore relevant, given the decommissioning status of the Italian NPPs
JAPAN	For fuel handling system 1. The storage and handling systems for fresh and spent fuels shall be designed so as to meet the following requirements: • The storage systems shall have appropriate containment and air purification systems. • The storage systems shall have appropriate storage capacity. • The handling systems shall have capability to prevent the dropping of fuel assemblies during their operation. 2. The storage and handling systems (except for dry storage casks) for spent fuels shall be designed so as to meet the following requirements, in addition to the aforementioned. • Proper shielding for radiation protection shall be implemented. • The storage systems shall have systems capable of fully removing decay heat and transporting it to an ultimate heat sink, and with associated purification systems. • Prevention of excessive decrease of cooling water inventory in the storage systems and proper leakage detection shall be possible. • The storage systems shall not lose their safety functions even in case of postulated dropping of fuel assemblies during handling. 3. The fuel storage and handling systems shall be so designed that criticality can be prevented. 4. The storage and handling systems for fresh and spent fuels shall be designed so that the water level and water temperature of the spent fuel storage facility (except using dry storage casks), the radiation level in the fuel handling area and other abnormalities can be detected, so that such a situation can be properly communicated to the site personnel or corrective measures can be automatically taken. Also, they shall be designed so that the situation of any events can be monitored through more than one parameter even in case of loss of off-site power.

[27]. The spent fuel is stored in high density racks of the SFP for 3-5 years. After that, the spent fuel is transported to the MVDS facility that is located close to the NPP. There is one common interim storage facility for all four units. According to the plans, the spent fuel will be sent to final disposal in a domestic deep geological repository after several decades of dry storage.

Table A.2: Summary of status of national requirements/criteria for SFPs (part 2/2).

COUNTRY	STATUS OF NATIONAL REQUIREMENTS/CRITERIA FOR SPENT FUEL POOLS
KOREA (REPUBLIC OF)	For PWR: 1. Water level corresponding to the minimum level allowed by technical specification: 7 m above the top of the fuel assemblies. For both PWR and PHWR: 1. A cooling train maintains the SFP water temperature at or below 60 °C when heat exchanger is supplied with component cooling water at the design flow and temperature. 2. Implementation of the improvement action items issued in Korea NPP safety review report performed as part of countermeasures after the Fukushima Daiichi accident: (a) Supply of makeup water by using fire engine, etc., and (b) Installation of a connector for the makeup water supply in order to obtain means for alternative heat removal under the loss of function of pumps and heat exchangers in the SFP cooling system. *References* 1. Ulchin Units 3 and 4, Final Safety Analysis Report (FSAR) 2. Shin-kori Units 3 and 4, Final Safety Analysis Report (FSAR) 3. Wolsong Units 1,2,3 and 4, Final Safety Analysis Report (FSAR)
SPAIN	U.S. NRC Regulatory Guide 1.13 rev. 2, Spent Fuel Storage Facility Design Basis CSN Instruction IS-26, of 16th June 2010, on Basic Nuclear Safety Requirements Applicable to Nuclear Installations CSN Instruction IS-27, of 16th June 2010, on General Nuclear Power Plant Design Criteria
U.S.A	General Design Criteria (GDC) 2, 4, 61, 62,and 63, which provide criteria for protection from natural phenomena, protection from dynamic effects, fuel storage and handling safety, criticality prevention, and monitoring of fuel storage, respectively. Implementing guidance for GDC 2, 4, 61, and 63 is contained in U.S. NRC Regulatory Guide 1.13, Rev. 2, "Spent Fuel Storage Facility Design Basis."

Table A.3: Representative data of PWR and VVER SFPs and storage racks (part 1/2)

GENERAL INFORMATION	BELGIUM	CZECH REPUBLIC		FRANCE		GERMANY	HUNGARY	ITALY
REACTOR TYPE	PWR (440 to 1050 MWe)	VVER-1000 (1000 MWe)	VVER-440/213 (470 MWe)	PWR (900 to 1450 MWe)	EPR[1] (1650 MWe)	PWR (1170 to 1410 MWe)	VVER-440 (470 MWe)	PWR[2] (260 MWe)
NUMBER OF FA IN THE CORE	121 to 157	-	-	-	-	193	-	-
CONTAINMENT TYPE	Large dry	Large dry	Bubble condenser	-	-	Large dry	Bubble condenser	Large dry
POOL LOCATION RELATIVE TO CONTAINMENT	Outside primary containment, adjacent	Inside primary containment	Outside primary containment, adjacent	Outside primary containment, adjacent	Inside primary containment	Inside primary containment	Outside primary containment, adjacent	Outside primary containment, adjacent
FUEL STORAGE POOL CAPACITY (FAs)	373 to 820	705	950	310 to 630	~ 1100	~ 800	706 + 350[3]	162+other in-core comp.
POOL BOTTOM LOCATION RELATIVE TO PLANT GRADE	-	Above grade	Above grade	Above grade	Above grade	Above grade	Above grade	Below grade
NUMBER OF FUEL RODS PER ASSEMBLY	179 to 264	312	126	264	264	300	126	208
INITIAL HEAVY METAL MASS PER ASSEMBLY (kg)	-	465	126	450 to 535	-	620	126	308
GEOMETRIC DIMENSIONS OF THE FUEL POOL								
LENGTH (m)	-	13.05	6	~ 12	12	~ 9.0	6	15.3
WIDTH (m)	-	6.21	3.76	~ 5.5	9	~ 11.5	3.7[4]	10.4
DEPTH (m)	-	8.1	15.07	12.5 to 14.2	14.4	~ 13.5	15	11
GEOMETRIC DIMENSIONS OF THE STORAGE RACKS								
MATERIAL	-	Borated stainless steel	Borated stainless steel	Stainless steel	Borated stainless steel	Borated stainless steel	Stainless steel	Borated stainless steel	Stainless steel
FRAME	Square	Hexagonal	Hexagonal	Square	Square	Square	Square	Hexagonal	Open
CROSS FLOW BETWEEN RACK CELLS	-	No	No	No	No	No	No	No	Yes
CRITICALITY CONTROL	-	Solid neutron absorbers and borated water	Solid neutron absorbers and borated water	Fuel element spacing and borated water	Solid neutron absorbers and borated water	Solid neutron absorbers and borated water	Solid neutron absorbers and burn-up credit	Solid neutron absorbers and borated water	Fuel element spacing
CENTRE-TO-CENTRE FUEL ELEMENT SPACING (mm)	-	288	162	410	280	286	280	160	508

[1]. One unit under construction.
[2]. Data refers to Trino Vercelelse unit, presently under decommissioning. Trino Vercellese is the only remaining NPP in Italy still having some fuel elements (47 assemblies as of October 2011: 39 with UOX fuel and 8 with MOX fuel; shipment abroad for reprocessing was foreseen for the following years) in its SFP.
[3]. 350 refers to temporary storage on upper racks.
[4]. The cross section of the pool is not a rectangle, but a pentagon.

Table A.3: Representative data of PWR and VVER SFPs and storage racks (part 2/2).

GENERAL INFORMATION	JAPAN	KOREA (REPUBLIC OF)		SPAIN				SWITZERLAND	USA
REACTOR TYPE	PWR	OPR1000 (1000 MWe)	APR1400[32] (1340 MWe)	KWU (1046 MWe)	WEST. (1098 MWe)	WEST. (1038 MWe)	WEST. (1055 MWe)	PWR	PWR (480 to 1310 MWe)
NUMBER OF FA IN THE CORE	121 to 193	-	-	177	157	157	159	-	-
CONTAINMENT TYPE	Large dry	Large dry	Large dry	Large dry	Large dry	Large dry	Large dry	Large dry	Large Dry / Sub-Atmospheric
POOL LOCATION RELATIVE TO CONTAINMENT	Outside primary containment, adjacent	Outside primary containment, adjacent	Outside primary containment, adjacent	Inside primary containment	Outside primary containment, adjacent	Outside primary containment, adjacent	Outside primary containment, adjacent	Outside primary containment, adjacent / Inside primary contain.	Outside primary containment, adjacent
FUEL STORAGE POOL CAPACITY (FAs)	Confidential	266 + 1232	351 + 1345	805	1594	1421	1804	-	544 to 2363
POOL BOTTOM LOCATION RELATIVE TO PLANT GRADE	-	Above grade	Above grade	Above grade	Above grade	Below grade	Above grade	-	At or below grade
NUMBER OF FUEL RODS PER ASSEMBLY	179 to 264	236	236	236	264	264	264	-	208 to 264
INITIAL HEAVY METAL MASS PER ASSEMBLY (kg)	Confidential	429	431	Confidential	Confidential	Confidential	Confidential	-	462
GEOMETRIC DIMENSIONS OF THE FUEL POOL									
LENGTH (m)	Confidential	8.6	12.8	9	14.83	9.43	11.78	-	6.7
WIDTH (m)	Confidential	10.4	10.8	8.4	7.28	9.43	9.21	-	12.2
DEPTH (m)	Confidential	12.6	12.8	12.65	12.33	12.04	10.57	-	13.1
GEOMETRIC DIMENSIONS OF THE STORAGE RACKS									
MATERIAL	Borated stainless steel, Stainless steel	Stainless Steel	Stainless Steel	Borated stainless steel	Borated stainless steel	Borated stainless steel	Borated stainless steel	Borated aluminium	Stainless steel
FRAME	Square	Square	Square	Square	Square	Square	Square	-	Square
CROSS FLOW BETWEEN RACK CELLS	No	No	No	No	No	No	No	-	No
CRITICALITY CONTROL	Solid neutron absorbers and borated water	Solid neutron absorbers and borated water	Solid neutron absorbers and borated water	Fuel element spacing and borated water	Fuel element spacing and borated water	Fuel element spacing and borated water	Fuel element spacing and borated water	Solid neutron absorbers and borated water	Solid neutron absorbers and borated water
CENTRE-TO-CENTRE FUEL ELEMENT SPACING (mm)	Confidential	229 to 280	226 to 266	Confidential	Confidential	Confidential	Confidential	-	260[33]

[32]. Four units under construction.
[33]. High density.

Table A.4: Representative data of BWR SFPs and storage racks

GENERAL INFORMATION	GERMANY	JAPAN	SPAIN		SWITZERLAND	USA	
REACTOR TYPE	BWR (1280 MWe)	BWR (460 to 1100 MWe)	BWR-6 (G.E.) (1096 MWe)	BWR (G.E.) (466 MWe)	BWR (370 to 1220 MWe)	BWR (600 to 900 MWe)	BWR (1000 to 1400 MWe)
NUMBER OF FA IN THE CORE	784	400 to 764	624	400	-	-	-
CONTAINMENT TYPE	Reinforced Concrete with Inner Steel Liner	Mark I/II	Mark III	Mark I	Mark I/II	Mark I/II	Mark III
POOL LOCATION RELATIVE TO CONTAINMENT	Outside primary containment, inside reactor building (secondary containment)	Outside primary containment, inside reactor building	Outside primary and secondary containment, in separate building	Outside primary containment, inside reactor building	Outside primary containment, inside reactor building / In separate building	Outside primary containment, inside reactor building	Outside primary containment, in separate building
FUEL STORAGE POOL CAPACITY (FAs)	~ 3230	900 to 1770	5404 (in 2 SFPs)	2609	-	2301 to 4117	3104 to 4348
POOL BOTTOM LOCATION RELATIVE TO PLANT GRADE	Above grade	Above grade	Below grade	Above grade	Above grade	Above grade	At or below grade
NUMBER OF FUEL RODS PER ASSEMBLY[34]	Up to 91	60 to 74	60 to 92	60 to 92	-	49 to 92	49 to 92
INITIAL HEAVY METAL MASS PER ASSEMBLY (kg)	200	Confidential	Confidential	Confidential	-	184	190
GEOMETRIC DIMENSIONS OF THE FUEL POOL							
LENGTH (m)	~ 13.0	7.16 to 10.37	~ 12	12.04	-	10.8	7.9
WIDTH (m)	~ 11.5	12.04 to 12.20	~ 11	7.16	-	12.2	12.2
DEPTH (m)	~ 11.5	11.8 to 11.91	13.1	11.8	-	11.8	12.2
GEOMETRIC DIMENSIONS OF THE STORAGE RACKS							
MATERIAL	Stainless steel	Aluminium Borated aluminium Stainless steel	Stainless steel	Borated stainless steel	Borated stainless steel	Stainless steel	Stainless steel
FRAME	Square	Square	Square	Square	-	Square	Square
CROSS FLOW BETWEEN RACK CELLS	No	No	No	No	-	No	No
CRITICALITY CONTROL	Solid neutron absorber and burnup-credit	Fuel element spacing and solid neutron absorber	Fuel element spacing and solid neutron absorber	Fuel element spacing and solid neutron absorber	Solid neutron absorber	Solid neutron absorber	Solid neutron absorber
CENTRE-TO-CENTRE FUEL ELEMENT SPACING (mm)	170	Confidential	Confidential	Confidential	-	160[35]	-

[34]. Range depending on FA type (SFPs can be mixed).

[35]. High density.

Table A.5: Representative data of CANDU SFPs and storage racks.

GENERAL INFORMATION	CANADA	KOREA (REPUBLIC OF)
REACTOR TYPE	PHWR (CANDU) (515 to 880 MWe)	PHWR (CANDU6) (660 MWe)
NUMBER OF FA IN THE CORE	-	-
CONTAINMENT TYPE	Single and multi-unit/Vacuum building	Single and multi-unit/Vacuum building
POOL LOCATION RELATIVE TO CONTAINMENT	Inside confinement / Spent fuel building, adjacent to containment	Spent fuel building, adjacent to containment
FUEL STORAGE POOL CAPACITY (FAs)	50 000 - 200 000	44 688
POOL BOTTOM LOCATION RELATIVE TO PLANT GRADE	At or below grade	Below grade
NUMBER OF FUEL RODS PER ASSEMBLY	28 or 37	37
INITIAL HEAVY METAL MASS PER ASSEMBLY (kg)	~ 22	23.6
GEOMETRIC DIMENSIONS OF THE FUEL POOL		
LENGTH (m)	~ 40	19.84
WIDTH (m)	~ 10	11.89
DEPTH (m)	~ 8	9.77
GEOMETRIC DIMENSIONS OF THE STORAGE RACKS		
MATERIAL	Stainless steel	Stainless steel
FRAME	Open	Open
CROSS FLOW BETWEEN RACK CELLS	Yes	Yes
CRITICALITY CONTROL	Fuel element spacing only	Fuel element spacing only
CENTRE-TO-CENTRE FUEL ELEMENT SPACING (mm)	~ 119.6	102

APPENDIX B: POST-FUKUSHIMA ACTIONS TAKEN IN OECD MEMBER COUNTRIES TO ASSESS AND IMPROVE SFP SAFETY

In the following, a brief summary is given on assessments and improvements made regarding safety of SFPs in OECD member countries after the 2011 Fukushima Daiichi accident.

Belgium

The nuclear power plants in Belgium have been assessed within the EU stress test program. The scope of the Belgian stress tests covers all the seven PWRs currently in operation, including the AR SFPs of each reactor unit, and the dedicated spent fuel storage facilities at both reactor sites. Information about the Belgian stress tests and the resulting national action plan is available in [258, 259]. An extract of Belgian actions related to SFPs are listed in Table B.1.

Canada

Following the Fukushima Daiichi accident, an action plan has been established by the Canadian Nuclear Safety Commission (CNSC) [260]. With regard to SFPs, industry in Canada has enhanced the number of possible sources of cooling water and the delivery methods. An additional emergency source of water, obtained from the lake or intake channel and injected into the SFP via a series of installed flexible hosing, has been added at some sites. All sites are required to have mobile pumper(s) and/or fire truck(s), either on site or readily available. The mobile pumps have sufficient capacity to provide SFP makeup water. These pumps also have the ability to draft water directly from local environmental sources.

Canadian utilities have also established additional provisions (Protected Equipment Zones) to protect in-service SFP cooling equipment when redundant systems are out of service and are introducing severe accident mitigation guideline provisions for SFPs under a CANDU Owners Group Joint Project. Generic SAMG provisions for CANDU SFPs will be issued in 2014, and station specific guidelines will follow from individual utilities. Additionally, utilities have conducted analyses to confirm structural behaviour of SFP under heat-up conditions and the structural integrity of SFP and structures under beyond design basis seismic conditions. Provisions have been established to monitor bay level and temperature following loss of cooling capability / loss of power / common mode events, and siphon break predefined maintenance checks have been introduced, where required, to confirm the integrity of anti-siphon provisions.

France

Following the events at Fukushima Daiichi, Electricité de France (EDF) carried out analyses of its installations through additional safety assessments, by examining the consequences of occurrence of extreme situations, leading to total loss of power supplies and/or the heat sink for all the units on a site. For SFPs, steps have been taken or are being studied to ensure that fuel assemblies, whether stored in storage racks or during handling, remain immersed at all times:

- Improved reliability of the prevention of the risk of draining through verification and strengthening, if necessary, of the possible draining routes (e.g. connected piping, compartment doors, wrap of the fuel transfer tube, etc.);
- Checking behaviour of the systems, structures and components in case of powerful earthquakes, together with their ability to maintain their functions (e.g. ability of the storage racks to ensure sub-criticality after a powerful earthquake, resistance of the pool 's civil engineering structure, etc.);
- Implementation of an ultimate extra replenishing supply, independent of the supplies used in normal operation, to compensate for water evaporation in the pool in a situation involving loss of the heat sink;
- Improvement of the instrumentation to manage water make-up in the situations considered, and determine the status of the storage pool;
- Reinforcing the electrical power production resources, by installing shielded, autonomous generators to restore power to the functions necessary to handle the emergency;
- Study of the production of hydrogen by radiolysis in situations involving loss of ventilation, which confirmed that opening of an outlet prevents reaching the hydrogen flammability threshold in the SFP building;
- Placing resources at the operator's disposal to enable a fuel assembly that is being handled to be placed in a storage rack, as from the first moments of any such event and independently from any power source.

Most of these provisions belong to the “hard core” defined by EDF, which is aimed at preventing fuel meltdown and avoid large-scale, durable radioactive discharges under extreme situations, potentially consecutive to an earthquake or a flood exceeding the design basis cases.

Moreover, implementation of a crisis centre, withstanding all the occurrences envisaged, is planned on each site: in particular, it will enable all concerned to determine the storage pool parameters under the situations considered. EDF has also implemented a Nuclear Emergency Response Team (FARN), ready to intervene in the control, maintenance and logistics fields on a site in an accident situation to restore water and electricity supplies in less than 24 hours.

Germany

In Germany, nine units are still in operation, while eight units are in permanent shutdown. The SFP is located within the containment in German PWRs, while it is located in the reactor building, outside the containment, in BWRs. In normal operation and during design basis accidents, the spent fuel cooling systems as well as emergency cooling systems have the aim to cool the SFP.

Experimental research and simulations of SFP related topics are performed in different projects at different institutions. Currently, there are no specific Severe Accident Management Measures described in the Accident Management Manual for the conditions after uncovering of the top of FAs in the SFP. The systematic implementation of a SAMG for the operating NPPs is foreseen. Additional preventive and mitigative procedures and guidelines for full power and low power shut down states as well as the cooling of the SFP are to be developed.

The German Reactor Safety Commission (RSK) gave the following provisional insights from the 2011 accident in Japan concerning further measures and reassessments of the severe accident management program, amongst others:

- Assuring the effectiveness of accident management measures even under aggravated boundary conditions caused by external hazards;

- Assuring the effectiveness of accident management measures at station blackout;
- Review of the accident management concept with regard to injection possibilities for the cooling of FAs and for ensuring subcriticality;
- Increased consideration of the wet storage of FAs in the accident management concept;
- Identification of safety margins still available in the beyond-design-basis range and the application of corresponding procedures based on the implementation of SAMG;

In the decommissioned NPP Obrigheim (KWO), the procedure of the external flooding of the spent SFP "after uncovering top of the fuel" will be treated further in the oversight process.

Hungary

Four VVER-440 units are in operation in Hungary. The SFPs are located in the reactor hall, outside of the containment. In case of total loss of cooling, boiling in the SFP starts after four hours, according to the most conservative case, and fuel damage starts 19 hours after the occurrence of the accident. These time intervals can be significantly extended by use of alternative water sources. Alternative electrical power sources are currently not available on the site of the nuclear power plant, but corrective measures are planned to be executed in this regard. Criticality accidents may occur in special geometry configurations only; their risk is not that high to obtain first priority from the reduction of the radioactive release among the interventions. Consequently, flooding of the SFP with coolant containing boron acid in at least 13.5 g/l concentration has to be started as soon as possible [261]. Among the Hungarian post-Fukushima measures, the following SFP related actions are planned:

- Water make-up to the SFP from an external source has to be made possible by the construction of a supply pipeline having adequate design against external hazards, with potential connection from the yard. Water inventory with adequate boron concentration has to be supplied through this line to the SFP. Operating instructions on the practical application have to be developed;
- Diverse diesel generators have to be installed to support the power supply of safety equipment that have a role in preventing severe accidents and/or managing an accident in the long term.

Japan

New regulatory requirements were developed in Japan, taking into account the lessons learned from the Fukushima Daiichi accident. More stringent regulations have been developed with an underlying assumption that severe accidents could occur at any moment. The following two measures against severe accidents are required for SFPs in the new regulations; see [262] and the summary of requirements for these measures in Table B.2:

A) Preventive measures against fuel damage in SFPs;

B) Measures for cooling, shielding, maintaining the sub-criticality and monitoring of SFPs.

Republic of Korea

With regard to SFPs, two post-Fukushima follow-up actions have been taken:

- An external cooling line has been installed to further enhance the SFP cooling capability, and an additional cooling source (water) for it is provided through fire trucks at the plant site;
- A severe accident mitigation guideline for SFPs is currently being developed. It is scheduled to be completed by the end of 2015.

Spain

The EU stress tests were carried out during 2011 for all operating reactors in Spain. The Spanish nuclear fleet in operation currently comprises 6 sites and a total of 8 units; there are also two sites that have temporary spent fuel storage facilities. The results were reported to the European Nuclear Safety Regulatory Group (ENSREG) [263].

- Establish a diverse means of SFP makeup with at least a concurrent makeup capability of 114 m^3/h beyond the normal SFP makeup capability;
- Establish a flexible means of SFP makeup of at least 114 m^3/h, using portable, power-independent pumping capability;
- Establish a flexible means of providing at least 45.4 m^3/h of spray to the SFP, using a portable, power-independent pumping capability.

The solutions listed in the preceding paragraphs can be accomplished one by one or in combination [264].

- Identify the types and location of materials maintained on-site that could be used to reduce leakage rates. Confirm that procedures/guidance will list the capabilities that may be available for use by Emergency Response Organization;
- Development of Extensive Damage Mitigation Guidelines to include the above mentioned strategies and the equipment necessary to accomplish them;
- Installation of new instrumentation for temperature, water level and radiation in the fuel building pool area, for other measuring instruments with seismic category, wider range and with the environmental qualification in accordance to the importance of their role;
- Providing additional on-site diesel generators for power supply;
- Providing extra diesel generators and mobile pumps that will be placed in central Spain to be transported to any of the sites in 24 hours;
- Development of studies on H_2 explosion risks in buildings adjacent to the containment (e.g. fuel building).

Sweden

In 2011, the EU stress tests were carried out for the ten operating reactors in Sweden, and the results were reported to ENSREG [265]. With regard to SFPs, some weaknesses were identified in the instrumentation and control systems. Needs for diversified cooling, e.g. by mobile equipment or by installation of pipelines to feed firewater into the pools, were also recognized. A similar stress test was also done for the central interim storage facility CLAB, which is an underground wet storage facility that houses most of the spent fuel produced at Swedish NPPs and research reactors awaiting deep geological disposal. Based on the stress test results, an action plan was established by the Swedish regulator [266]. For the at-reactor SFPs, the following actions are required from the licensees as a starting point (completion expected in 2014):

- Reassess the integrity of the SFP: Integrity and robustness of the SFP during prolonged extreme situations at the site shall be further evaluated and reassessed;
- Consider improvements of the capability to cool the SFP: For cooling of the SFP, the following improvement shall be considered: Permanent filling pipes from a protected location to the SFPs in units that do not yet have this kind of pipe lines;

- Investigate the instrumentation of the SFP: Instrumentation for measurement of necessary parameters in the spent fuel storage (water level, temperature) in the event of severe accidents as well as the resistance of the equipment to harmful environment conditions shall be investigated.

Switzerland

- All SFPs must have a second independent cooling circuit installed by the end of 2017;
- A powerful diesel generator is placed in central Switzerland and can be transported to each of the four NPPs in a short time via helicopter. This is for the case of station blackout, and not especially for SFP accidents.

United States

Following the events at the Fukushima Daiichi nuclear power plant, the U.S. NRC established a senior-level agency task force referred to as the Near-Term Task Force (NTTF). The NTTF was tasked with conducting a systematic and methodical review of the NRC regulations and processes and determining if the agency should make additional improvements to these programs in light of the events at Fukushima Daiichi. As a result of this review, the NTTF developed a comprehensive set of recommendations documented in [267]. This report makes two sets of conclusions and recommendations related to SFP safety, and the NRC has required, through orders, that licensees enhance their ability to respond to beyond-design-basis events. The orders include:

- Order EA-12-049 [268] that requires licensees to develop, implement, and maintain guidance and strategies to maintain or restore core cooling, containment, and SFP cooling capabilities following a beyond-design-basis external event;
- Order EA-12-051 [269] that requires licensees to install reliable means of remotely monitoring wide-range SFP levels to support effective prioritization of event mitigation and recovery actions in the occurrence of a beyond-design-basis external event.

These improvements are intended to increase the likelihood of restoring or maintaining power and mitigation capability during severe accidents. The new SFP level instrumentation required under Order EA-12-051 and the mitigation strategies now required under Order EA-12-049 could significantly enhance the likelihood of successful mitigation beyond that considered under Title 10 of the Code of Federal Regulations (10 CFR) 50.54(hh)(2), which were implemented following the September 11, 2001 attacks in the USA. The new SFP level instrumentation required under Order EA-12-051 ensures a reliable indication of the water level in the SFP.

Table B.1: Extract from the Belgian national action plan (continued on next page) [259].

	Recommendations and suggestions/requirements	Action family	Action
1	Instrumentation and monitoring Enhancement of instrumentation and monitoring	Power supply - Total SBO - SFPs	Additional level measurement
2	Spent fuel pool Improvement of the robustness of the SFP	Operation management - SFPs	SUR[36] procedures in case of SFP accidents
		Power supply - SFPs	Electrical backup for the cooling pumps
			Procedures to manage SFPs
		Water supply[37] - Total SBO	Inadvertent let down of the pools
			Water supply to SFPs in case of aircraft crash[38]
3	Hydrogen in SFP buildings Regardless of the outcome of the assessment of the residual risk of hydrogen generation and accumulation in the SFP buildings, the installation of passive autocatalytic recombiners should be considered	SA management - hydrogen risk	Hydrogen risk management in nuclear auxiliary building
4	Spent fuel pools Two configurations should be evaluated by the licensee for the SFPs: • Configuration with a fuel assembly handled in the reactor pool during a total SBO. The fuel assembly should manually be handled in a safe position. The licensee should investigate the provisions (hardware installations, procedures, lighting, etc.) to be implemented for this configuration.	Power supply - Total SBO	Safe Position Fuel Assembly
	• Configuration with loss of water inventory in the SFPs. The international experience feedback has already pointed out potential problems with the design of the siphon breakers in the SFPs. In case of piping rupture, an insufficient capacity of the siphon breakers may lead to a fast uncovering of spent FAs[39]. The licensee should examine this safety concern.	Water supply - Total SBO	Inadvertent let down of the pools

[36]. Emergency system installed to respond to several accident scenarios of external origin (at Tihange 1).

[37]. Concretely, hard pipes to supply water from the outside of the SFP building with mobile pumps.

[38]. Two pipes on both sides of the SFP building (at Doel 1 and 2).

[39]. Ongoing study, modifications foreseen (size increase for some SFP buildings).

Table B.2: New regulatory requirements for SFPs in Japan [262].

New regulatory requirements		Postulated accident	Requirement details	
A	**Preventive measures against fuel damage in spent fuel pools** [Basic requirements] Licensees must prepare appropriate preventive measures against fuel damage by postulating an accident that may cause severe damage to the fuel stored in SFPs.	(a) Postulated accident 1: Pool water temperature rises and water level drops due to evaporation as the result of a malfunctioning of auxiliary feed-water system causing auxiliary feed failure. (b) Postulated accident 2: A small amount of water is lost due to the siphoning effect, etc., and pool water level decreases.	"To prepare appropriate preventive measures against fuel damage" refers to the fulfilment of following requirements. (i) Top of active fuel is submerged. (ii) A water level that shields radiation is maintained. (iii) Sub-criticality is maintained.	
B	**Measures for cooling, shielding, maintaining the sub-criticality and monitoring of spent fuel pools** [Basic requirements] B-1 Prepare equipment and procedures for cooling of the fuels in SFP, shielding and preventing criticality in the event of loss of SFP cooling function, or cooling water injection function, or leakage of a small amount of pool water.		(i) Install mobile alternative cooling water injection system (Example; injection line, pump trucks etc.) as the alternative water injection system. (ii) Alternative water injection system shall be able to maintain pool water level even in the event of loss of cooling and water injection function and a small-scale leakage.	The monitoring of SFP shall be as below. (i)SFP water level, pool water temperature and air dose rate above the pool shall be measured to the extent possible within the function as a result of severe accident. (ii)This measurement equipment shall be connected to alternative power source if AC or DC power sources are necessary. (iii)Pool status shall be monitored by cameras.
	[Basic requirements] B-2 Prepare equipment and procedures for mitigating fuel damage and preventing criticality in the event that SFP water level cannot be maintained due to the leakage of a large amount of water.	(a) A "leakage of a large amount of water" as mentioned in B-2 refers to the leakage that causes remarkable decrease of pool water level.	(i) Mobile spray equipment shall be prepared as spray equipment (Example; spray headers, spray lines, pump trucks). (ii) Spray equipment shall be able to mitigate the fuel damage by alternative cooling water injection system even in the event that SFP water level cannot be maintained. (iii) Equipment and procedures etc. to reduce the release of radioactive materials to the environment in case of fuel damage as much as possible shall be prepared.	

APPENDIX C: EXAMPLES OF PAST PRECURSOR EVENTS AND ACCIDENTS

This appendix provides brief descriptions of the precursor events and accidents that were listed in Table 3, Section 3.1.2. It also summarizes the results of an assessment of events with loss of SFP cooling or water inventory, made by the U.S. NRC in 1997 [4, 270], as well as the results of a spent fuel uncovery risk assessment of SFPs, made 2006 in France [27].

C.1 Past events with loss of SFP cooling

C.1.1 Loss of shutdown cooling due to station blackout during refuelling outage

On February 9, 2012, during refuelling outage in the Kori-1, Korea, loss of off-site power (LOOP) occurred and emergency diesel generator 'B' failed to start while EDG 'A' was out of service for scheduled maintenance, resulting in a station blackout [271]. Off-site power was restored 12 minutes after the SBO condition began.

The LOOP was caused by a human error during a protective relay test of the main generator. The EDG 'B' failing to start was caused by the failure of the EDG air start system. Further investigation revealed that the utility did not exercise proper control of electrical distribution configuration to ensure the availability of the station auxiliary transformer (SAT) while conducting test on the unit auxiliary transformer (UAT).

After restoring off-site power through the SAT, the operators recovered shutdown cooling by restoring power to a residual heat removal pump. During the loss of shutdown cooling for 19 minutes, the reactor coolant maximum temperature in the hot leg increased by 21.3 °C, and the SFP temperature slightly increased from 21 °C to 21.5 °C.

Causes:

During the test of the protective relays of main generator, the test supervisor ordered not to proceed to next step after the test trouble at channel A. The test personnel continued the test with channel B, while misunderstanding the supervisor's direction, creating the 2 out of 3 logic signals to actuate the circuit breakers in switchyard to open, resulting in loss of 345 kV off-site power grid and concomitant LOOP, since 154 kV off-site powers were unavailable. Although EDG auto-start signal was on, EDG B failed to start caused by solenoid valve of the EDG air start system failure, i.e., mechanical damage, which resulted in SBO.

Additionally, many incorrect responses that present violation of regulatory requirements were identified as follows: (i) The plant manager and other major staffs decided not to record LOOP and SBO in the main control room and did not report the event to regulatory body, NSSC/KINS, (ii) They did not declare emergency action level in accordance with Kori-1 emergency plan, (iii) utility staffs moved fuel while both EDGs were unavailable, which was in violation of technical specification, and (iv) EDG 'B' failure during a performance test subsequent to SBO event was not logged.

Major actions:

From a long-term point of view, for the prevention of reoccurrence and safe operation of the plant, special attention should be paid to the following:

- Reinforce regulatory oversight programme to address safety culture;
- Reinforce reporting requirements;
- Reinforce EDG reliability requirements;
- Reinforce configuration control and risk management during refuelling outage;
- Review test and maintenance procedures in depth;
- Reinforce emergency action level declaration requirements and procedure.

For the prevention of reoccurrence of the event, the following regulatory actions were ordered and/or under implementation:

- Shutdown the plant;
- Opened event to the public;
- Ordered verification of EDGs and alternative AC diesel generators (AAC DG) operability for all nuclear power plants (21 units);
- Reported and transferred investigation to the Government Prosecution Office;
- Planning other enforcement actions.

C.1.2 Dual unit loss of off-site power, resulting from inadequate relay modification

On April 4, 2012, Catawba Unit 1, SC, USA, tripped from 100 % power following a trip of reactor coolant pump 1 D [272]. Shortly after the Unit 1 generator power circuit breakers opened, the Zone G protective relaying system unexpectedly actuated on an instantaneous under-frequency condition, as a result of an error in the relay logic. This opened the switchyard breakers, thereby isolating Unit 1 from the grid and resulting in a LOOP. At the time of the trip, Unit 2 was in Mode 5 during its End-of-Cycle 18, with both of its essential busses aligned to Unit 1 off-site power. Therefore, Unit 2's essential busses lost power as a result of the LOOP, which resulted in loss of residual heat removal and spent fuel cooling on Unit 2. Unit 1 reactor tripped on low reactor coolant system flow.

Both EDGs on each unit automatically started and powered their respective essential busses as designed. Approximately five and one-half hours later, after confirming that the sources of the fault were cleared, off-site power was restored to one essential bus on each unit.

SFP safety assessment:

As a result of this event, residual heat removal and spent fuel cooling were briefly lost. Residual heat removal capability was restored in approximately three minutes following the LOOP. Spent fuel cooling capability was restored in approximately 28 minutes following the LOOP. There was no significant impact to Unit 2 as a result of this event, but anyway, this event is addressing situation where problems on other unit could produce loss of SFP cooling.

Causes:

The LOOP occurred as a result of inadequate design input specification and insufficient control over vendor outsourcing in conjunction with the Zone G relay modification. As a result, a critical design input was not included in the design change package or confirmed by testing. During preparation of the relay setting calculation, the blocking function for the instantaneous generator under-frequency trip was omitted. The vendor calculation check was performed as a high level review and did not identify the missing blocking function. The calculation was subsequently approved and used for relay setting and factory acceptance testing preparation. In addition to the described vendor issue, Catawba engineering personnel did not specify all of the critical design inputs required for proper operation of the Zone G relay scheme. As a result, the design error was not detected during site review or post-modification testing.

Major actions:

- The faulted reactor coolant pump motor cable was replaced;
- The Zone G relay modification error was corrected on both units;
- A modification was implemented to correct the identified breaker coordination issue;
- A formal station process will be developed to direct diagnostic testing of medium voltage cable and connectors on a periodic basis and following identified issues with these components;
- Power cables and Elastimold connectors associated with reactor coolant pump and other critical pump motors will be incorporated into a more rigorous predictive monitoring program;
- Processes associated with modification scope description, specification of critical design inputs, specification of vendor services and oversight, and checker responsibilities will be revised as appropriate.

C.1.3 EDG failed to start after undetected loss of incoming off-site supply

On May 13, 2013, in Forsmark-3, Sweden, during maintenance and testing of relays on the excitation system on the main generator, the 400 kV unit breaker received an unintentional signal to open [273]. However, one phase of the 400 kV breaker did not open. Due to the main and station auxiliary transformers configurations (Y/D resp. D/Y), a substantial line-voltage (> 65 %) was still available for two out of the three line-voltages. The relay protection engineered to sense an undervoltage on the safety-grade auxiliary power busbars was designed to detect only on two out of the three line-voltages. The line-voltages with substantial induced voltage coincided with the line-voltages set up to sense an under-voltage situation. Consequently, none of the safety-grade auxiliary power busbars were disconnected, nor EDG's started.

Safety-grade components with phase imbalance protection were disconnected, at least 146 components, among them components vital for the heat removal from the SFP. Some non-safety components (motors) were overheated and failed.

SFP safety assessment:

The loss of one phase is not analysed in the safety analysis report. The unit has been in an unanalysed condition. A large extent of the core was unloaded with the fuel in the fuel spent pool, gates were open between reactor and SFP. There was no increased temperature in the SFP. In this configuration, the water heat-up rate is approx. 0.7 °C per hour. The temperature was around 35 °C. If manual action had not been implemented, it would have taken around 30 hours before water had started to boil.

Causes and major actions:

The cause of the event is identified to be a loose electrical connection in a cabinet. The equipment that was used during the test had been changed from a one-phase model to a three-phase model, but the test instruction had not been updated correctly. Deeper causes and major recommendations are not yet published in IRS.

C.1.4 Irradiated fuel without forced cooling during refuelling outage

In Almaraz-2, Spain, on November 4, 2007, during core refuelling, component cooling water system (CCWS) pump A had to be shutdown due to the failure of one of its bearings [274]. Forced cooling to the SFP and the reactor core was lost for 7 hours. The temperature in the SFP increased from 34 °C to 46 °C. The temperature increase in the refuelling cavity did not threaten the cooling of the fuel in the vessel either.

Different possibilities to restore the cooling to the SFP were analysed: aligning CCWS common pump with train A, restoring CCWS train B, aligning Almaraz-1 CCWS pump B with Almaraz-2 CCWS train B and aligning Almaraz-1 CCWS pump A with Almaraz-2 CCWS train A. The first option was chosen, since it was the least complicated: only a valve upstream the common pump had to be restored. Availability of different methods to cool the SFP was also verified, in case they were needed: Refuelling water storage tank (RWST), demineralized water system, fire protection system, essential service water system and Almaraz-1 SFP cooling system.

SFP safety assessment:

The loss of the SFP forced cooling increased the temperature of the water in 7 hours from 34 °C to 46 °C, below the high temperature alarm value (57 °C) and the technical specification limit (65 °C). There were alternative methods available to cool the pool at all times.

Causes:

The direct cause of the event was the breakage of the bearing's cage, which caused the bearing to fail and led to the shutdown of the CCWS pump A. This bearing had been installed in July 2007 on detecting an oil leakage through the bearing's cage. Thus, it had been operating 747 hours before it failed. The bearing was sent to the manufacturer to determine the cause of the failure, but it was not possible due to the great damage the bearing had suffered. The root cause analysis established, as the most probable cause, the initial failure of some element of the bearing, which caused its catastrophic failure.

Major actions:

To prevent recurrence of the event, the following corrective actions were defined:

- Implement an additional surveillance programme on the pump;
- Establish a maintenance strategy which takes into account that, when there is only one train operable of the CVCS, CCWS or ESWS, the common pump must be available;
- Carry out a special surveillance when replacing bearings in the CCWS pumps to make sure the pump's performance is adequate;
- Improve the review procedure of CCWS pumps, introducing acceptance criteria for the pumps' shaft.

C.1.5 Disruption of the SFP cooling

On January 23, 2013, Belleville Unit 2, France, while the reactor was in operation, a fire was detected shortly after midnight in the room containing the pumps that cool down the SFP of the unit 2 reactor [23]. EDF's teams and external rescue teams responded quickly after the detection of the fire in the pump room of one of the two SFP cooling system trains. The teams ensured the complete extinction of the fire and the damaged pump was stopped.

During this event, the pump of the second train had been shut down for maintenance on January 10, after vibration problems. After technical analysis during the night, the operator returned to service the pump shut down for maintenance in order to ensure partial cooling of the SFP within the time required by the technical specifications. The pump experienced again abnormal vibrations and EDF stopped it proactively. The French Nuclear Safety Authority (ASN) asked the operator to restore quickly the reliable operation of at least one of the two SFP cooling system trains. EDF started in the afternoon of January 23 to repair both pumps and had spare parts shipped to the site. These new materials were found incompatible with the pumps installed in Belleville. EDF restored the cooling with one of the two SFP cooling system pumps on January 24 at 3:00 in the morning by refurbishing the pump motor that had been concerned by the fire on the night of January 22 to 23, but which was intact. The second train was put into service on January 25 at 6:30, by using a motor that had been dismantled in the Unit-1 reactor in December 2012.

SFP safety assessment:

This event did not have any effect on the staff or the environment. Given the simultaneous failure, for 6 hours and then for 15 hours, of both trains of the SFP cooling, the ASN rated the event at level 1 on the International Nuclear Event Scale.

Major actions:

EDF took the commitment to install before the end of 2012, on at least one SFP cooling system train per reactor, a pump motor ensuring the SFP cooling in case of earthquake. As both motors at that time installed on the Unit 2 reactor of Belleville did not meet these requirements, ASN asked EDF to notify a new event for this deviation and to install quickly compliant motors.

C.1.6 Inoperable SFP cooling pumps results in loss of safety function

On February 13, 2007, San Onofre Nuclear Generating Station (SONGS) Unit 2, CA, USA, was operating at about 98.5 % power with Train A SFP cooling pump removed from service for scheduled maintenance [275]. At about 12:49, the Train B SFP cooling pump tripped on overcurrent. Operators initiated actions in accordance with the Abnormal Operating Instruction (AOI) for loss of SFP cooling. The Train B SFP cooling pump was successfully restarted at 14:07.

SFP safety assessment:

During the period when both SFP cooling pumps were not operating, the temperature in the SFP increased from approximately 21.9 to 22.8 °C. With the SFP cooling pumps off, the time to exceed the maximum allowed temperature of 60 °C was estimated to be 56 hours.

Alternate methods of cooling the SFP were available if required. All Licensee Controlled Specification (LCS) requirements for two SFP cooling pumps inoperable were met and the water level in the SFP was maintained greater than 7 m above the spent fuel.

Major actions:

Initial investigation determined the pump motor had tripped due to actuation of the thermal overload relays; however, the motor was not experiencing an overcurrent condition. Upon further investigation, it was found that thermal overload relays had actuated because of a high temperature in the Motor Control Centre (MCC). The high temperature was a result of a malfunctioning thermostat that failed to turn off a heater strip installed in the MCC to prevent condensation. Strip heaters were permanently disconnected for Units 2 and 3 Class 1 E MCCs, since they are located in areas where normal air conditioning is sufficient to minimize moisture.

C.1.7 Both trains of SFP cooling inoperable results in a loss of safety function

On December 23, 2009, at about 09:57, with SONGS Unit 2 in the steam generator replacement outage and defueled, Train A Salt Water Cooling (SWC) low flow alarm and Component Cooling Water heat exchanger high differential pressure alarm were received in the control room [276]. Since Train B CCWS had been removed from service for scheduled maintenance, operators initiated actions in accordance with the AOI for loss of CCW and SWC.

The reduction in SWC flow was suspected to be caused by debris in the CCW heat exchanger. In accordance with the AOI procedure, actions to clear the debris and restore SWC flow were completed. At approximately 10:14, operators stopped the SWC pump, declared Train A SFP cooling system inoperable, and completed actions required by LCS 3.7.106B when two SFP heat exchangers are inoperable. With the SWC pump off, operators changed the valve line up to reverse SWC flow through the CCW heat exchanger, and at 11:16 restarted the SWC pump.

Prior to stopping the SWC pump to establish reverse flow conditions, the temperature of the SFP was not affected by the reduction in SWC flow. The cooling capacity of the SWC system significantly exceeds the SFP heat load when the plant is defueled. While the SWC pump was off, the SFP temperature increased from about 23.3 to 25.6 °C.

SFP safety assessment:

The maximum SFP temperature during this event was 25.6 °C, which is well below the maximum allowed temperature of 71.1 °C per the LCS. With the SWC pumps off, the time to exceed the maximum allowed temperature was approximately 23 hours. Alternate methods of cooling the SFP were available if required. The water level in the SFP was maintained at least 7 m above the spent fuel, as required by the technical specifications.

Causes and major actions:

Upon investigation, the licensee determined the cause of the SWC low flow alarm was ocean debris (such as kelp), obstructing flow through the CCW heat exchanger. The debris appeared to have entered the system through a damaged SWC pump suction strainer. The SWC pump with the damaged suction strainer was replaced.

C.2 Past events with loss of SFP inventory

C.2.1 Drop in the level of the refuelling pool and flooding of reactor building areas

On 20 May 2002, in the Khmelnitski-1 VVER-1000, Ukraine, a pneumatically actuated 1TG12S06 valve on the coolant pump inlet of the cooling and refuelling pool was shut down for maintenance [277]. Measures were taken to ensure that the work was conducted safely, including closing the adjacent

1TG12S04 valve, and dismantling its control circuitry. 1TG12S04 is located on the pipe between 1TG12S06 and the cooling pool. The compressed air for the lead-in to 1TG12S04 was not shut off. At the same time, testing began on the third train of the safety systems, including the TG12S04 valve.

The staff carrying out the checks did not have information on the status of the equipment. The staff was instructed to assemble the valve circuitry, including 1TG12S04. Immediately after the control circuitry of the 1TG12S04 valve had been assembled, it reset itself (the opening solenoid was spontaneously tripped by a brief failure of the optothyristor in the control circuitry). Water from the cooling pool began to come through the open joint of the 1TG12S06 valve housing into area A327/2.

SFP safety assessment:

The incident had the following consequences:

- A significant drop in the level of the wet refuelling pool (36.1 m to 34.2 m);
- 290 m^3 of borated water with a maximum activity of 3.2×10^{-6} Ci/l leaked out of the wet refuelling pool into the reactor building areas;
- Equipment and areas at levels 4.2 and 6.6 of the reactor building were contaminated with radioactive products (the reference levels were not exceeded, the maximum gamma radiation exposure was 1.1 mR/h; beta contamination was 500 particles/min·cm^2);
- Reactor building areas were flooded, including areas where safety systems equipment is located.

Causes and major actions:

The immediate cause of the leak was unsatisfactory organization and conduct of valve testing. The root cause of the incident was a shortcoming in the procedure for organizing pre-maintenance equipment testing. The corrective measures developed as a result of the investigation into this incident include both organizational measures and measures to eliminate shortcomings in the pre- and post-maintenance testing programme.

C.2.2 Insufficient testing of functionality of siphon breaker valve at SFP

At Borssele NPP, The Netherlands, the supply line of the SFP cooling system lies partially below the bottom level of the pool. This means that, in case of a break at an outside location at a level near the bottom of SFP and before an isolation valve to contain the leakage, drainage of the pool through siphoning could take place leaving the spent fuel elements largely uncovered and uncooled.

Borssele NPP conducted a survey of procedures and safety systems concerning the storage of spent fuel. It was found that the siphon breaker valve, which should prevent draining of the SFP in case of a break of the supply line of the cooling system had never been functionally tested and was not included in the Borssele NPP inspection programme [278]. Moreover, it was established that this spring loaded check valve could not have opened timely to prevent the water level of the SFP from dropping below the top of the stored FAs without operator action to maintain the inventory of the pool. This was due to the fact that the stiffness of the spring of the check valve was not well chosen. It was too large and therefore the siphon drainage effect could not have been interrupted in time.

SFP safety assessment:

In case of a break of the supply line of the SFP cooling system at an outside location and at a level near the bottom of the SFP, and before an isolation valve to contain the leakage, drainage of the pool

through siphoning could take place, leaving the spent FAs largely uncovered and uncooled. This would result in a considerable increase in the level of radiation exposure within the reactor containment.

According to the IAEA [279], the rupture of a low pressure feed line is very unlikely and can be classified as Plant Condition "Beyond Design", with a probability of 10^{-6} to 10^{-4} per year. Also, it is determined that the leakage rate in case of a break of the feed line at the specific location amounts to about 20 m^3/hr, which leaves, considering the overall SFP volume, ample time for operator action to compensate the loss of inventory with the aid of several and diverse systems.

Causes:

Deeper causes for inoperability of the siphon breaker with spring loaded check valve on an aeration line of the supply line of the SFP cooling system includes:

- failure to conduct an adequate initial qualification test after modification and especially the subsequent omission of in-service testing;
- the inoperable siphon breaker with a spring loaded check valve installed and in situ test not provided for; and
- testing and maintenance of an important component of a safety related system not included.

Major actions:

The vacuum breaker check valve was demounted and the spring was replaced by one with considerable less stiffness. A modification was also made to allow an effective in-service testing of the check valve. A positive test was carried out to ascertain the correct functioning of the modified device. Furthermore, actions shall be taken to investigate the proper capacity of the aeration line. The design and modification process should include the systematic assessment of the reliability of the concerned safety related systems. Adequateness and quality of the test and maintenance programme of components that is relevant for of the safe operation of the NPP should be periodically and thoroughly re-evaluated and enhanced.

C.2.3 Siphon breaker missing on SFP cooling system pipes

On January 18, 2012, EDF notified ASN that the absence of a "siphon breaker" orifice on the fuel storage pools of Cattenom reactors 2 and 3 had been detected during an internal inspection [23]. The cooling water is injected at the bottom of the pool by a pipe. In the event of an incident, for example inadvertent operation of certain valves, the injection pipe could extract the water from the pool through a siphon effect, instead of injecting it, which would lead to a drop in the water level. An orifice (siphon-breaker) is drilled in this pipe near the surface of the pool, in order to stop any siphon effect if initiated.

SFP safety assessment:

The described nonconformity is a deviation from the design baseline safety requirements. It had no impact on the workers or the environment, but did compromise defence in depth.

Major actions:

During an inspection carried out as part of the measures taken following the post-Fukushima complementary safety assessments, the licensee found out that these siphon-breakers were indeed present

on the Cattenom NPP reactors 1 and 4, but not on reactors 2 and 3. On January 24, 2012, ASN conducted an inspection on this subject, in particular concerning the steps taken by the licensee. Following this inspection, it asked the licensee to take immediate compensatory measures, to prevent any risk of accidental emptying of the pool.

C.3 Past assessments of risks for SFP accidents

C.3.1 U.S. NRC assessment of events with loss of SFP cooling or water inventory

According to a study performed in 1997 by the U.S. NRC, the loss of SFP coolant inventory in excess of 1 foot had occurred 10 times over the previous 12 years at a rate of about once every 100 reactor-years [4, 270]. Loss of SFP cooling with a temperature increase in excess of 11 °C (20 °F) has occurred 4 times in those 12 years at a rate of approximately 3 times every 1000 reactor-years. The consequences of these actual events have not been severe; however, some events resulted in loss of several feet of SFP coolant level and have continued for more than 24 hours. The primary cause of these events has been human error, most prevalently valve mispositionings.

The U.S. NRC assessment, which included reactors in the USA as well as similar reactors outside the USA, revealed large variations in the designs and capabilities of SFPs and related systems at individual nuclear plants. The assessment identified that the frequency of loss-of-inventory events was relatively high compared to loss-of-cooling events, and prompt off-loads will lead to reduced time to boiling, if cooling is lost. A loss of SFP inventory in combination with higher heat loads reduces the time to respond to SFP events. Thus, the emphasis of the findings was on instrumentation to quickly alert the operators and effective procedures and training to facilitate prompt operator response.

In the conclusion of the U.S. NRC [270], three main areas for possible improvements were emphasized:

- Procedures and training to detect and respond to SFP loss-of-inventory and loss-of-cooling events, including those caused by loss of off-site power are needed and should address configuration controls that can prevent and/or mitigate such events. They should be consistent with the time frames over which SFP events can proceed at the specific plant, recognizing the plant-specific heat load and the possibility of loss of inventory because of cavity seal or gate failures;
- Reliable instrumentation is necessary to monitor SFP temperature and level and SFP area radiation, including periods following a loss of off-site power, in order to detect SFP loss-of-inventory events and loss-of-cooling events in a timely manner;
- Testing, maintenance, and configuration control of plant features such as reactor cavity seals, gate seals, or antisiphon devices need to be examined for those plants where failures could potentially cause loss of SFP coolant inventory sufficient to endanger makeup capability or result in fuel uncovery.

C.3.2 French assessment of the risk of fuel assemblies being uncovered in the SFP

In 2006, French authorities produced a report [27], which summarized findings from the study by Institut de Radioprotection et de Sûreté Nucléaire on fuel storage safety on request by the Electricité de France. Performed studies led to a redefinition of the requirements that are applicable to equipment and whole operation documents involved in SFP cooling safety.

To substantiate its request for relaxing the residual power limits, EDF also demonstrated that an accident situation of total loss of cooling would not result in unacceptable consequences. Various initiating events for total loss of cooling were examined in the investigation:

- loss of two Fuel Pool Cooling and Filtering System trains or loss of common section;
- total loss of electrical supply;
- loss of heat sink;
- internal hazard (fire or flood) causing the two cooling trains to fail.

It also became apparent that numerous rapid drainage scenarios of the SFP could be envisaged, which could lead to dewatering of the suction piping in the cooling system. These scenarios were examined specifically, given that the potential impact of some of them could be more serious than total pool cooling loss.

Loss of cooling functions

During refuelling outages, the residual power of the fuel stored in the SFP could cause the pool to boil in the short term, should cooling be totally lost (between five and eight hours). To prevent this accident, EDF has reinforced the operating specifications and the preventive maintenance programme for the pool cooling function. Modifications have also been incorporated to eliminate pool cooling losses through foreign material being sucked into the cooling system (installation of a strainer on the suction piping), boost monitoring of the pool parameters (temperature and pool level, FPCS flow rate) and more reliable supply of electricity to the FPCS pumps, whilst approving the maintenance of electrical switchboards during this time.

Nevertheless, despite measures provided to increase prevention of loss of cooling, the probability of boiling in the SFP remains high when the reactor is unloaded (probability higher than 10^{-4} for a reactor over this period) considering the various scenarios identified by operating experience examination. The plant operator must therefore be able to cope with an extended cooling loss, which could ultimately result in the uncovering of the fuel stored in the pool, if the evaporated water is not compensated for.

Internal hazard

Some of the reactors currently in service in France are designed without a physical separation between the two cooling trains in the FPCS. In particular, both pumps in this system are located in the same room. An internal hazard (fire, flood, etc.) may cause total loss of cooling of the SFP.

To ensure defence in depth in the event of an internal hazard affecting the cooling circuit of the SFP, equipment modifications are being incorporated on the EDF sites. They guarantee accessibility and operability of the emergency means for making up the pool in the event of fire or flooding in the rooms located in the fuel storage building, and thus, manage the accident transient up to restoration of a train in the cooling system in the SFP.

Accidental drainage of the SFP

Several scenarios (rupture or leak on a drainage pipe in a compartment, drainage of the SFP through the reactor building pool via a rupture or a leak in the piping connected to the reactor coolant system, drainage of the SFP via a residual heat removal pump, gate no longer leak tight, rupture of a steam generator dam during reactor unloading or refuelling, etc.) present a risk of sufficiently rapid kinetics to cause total cooling loss through dewatering of the suction piping on the FPCS system and total or partial

dewatering of an assembly during handling. In addition, it appeared that there was no guarantee that the siphon breaker devices fitted to the piping plunging to the bottom of the pool (especially the discharge pipe of the SFP cooling pump) were dimensioned correctly. Consequently, EDF enlarged the diameter of these siphon breaker devices on all its units.

Provided that the improvements resulting from studies carried out by EDF are considered, operating the SFP with a residual power of the stored FAs higher than the limit power stipulated in the safety analysis report has no real impact on the safety of the installation. French operating experience over 20 years shows that there was no loss of cooling function or support functions lasting long enough for the SFP to boil. For SFP drainage events, two incidents caused drainage in the order of 4 metres from the SFP, the dewatering of the suction piping and the temporary loss of pool cooling. These events did not, nevertheless, cause the temperature to rise dramatically in the pool as cooling was re-established rapidly.

APPENDIX D: OVERVIEW OF SEVERE ACCIDENT COMPUTER CODES

This appendix provides a brief overview of state-of-the-art computer codes applicable to computational analyses of SFP cooling/coolant accidents. The overview includes four internationally recognized codes for analyses of severe reactor accidents, where emphasis is placed on their capability to model phenomena related to SFP accidents. A more general review of these codes can be found elsewhere [280]. A brief description is also given of the French DRACCAR code, which has been successfully applied to SFP accident experiments.

D.1 MELCOR

The MELCOR computer code, which is being developed at Sandia National Laboratories for the U.S. NRC, represents the current state of the art in severe accident analysis. MELCOR is a fully integrated, engineering-level computer code that treats a broad spectrum of severe accident phenomena. It has capabilities to model core heatup and degradation, fission product release and transport within the primary system and containment, core relocation, ex-vessel core concrete interaction, and hydrogen deflagration.

The SFP models in MELCOR have been developed over the past ten years, supported by experimental data. Modelling enhancements include (i) a new rack component, which permits better modelling of the SFP rack and associated heat transfer, (ii) a new air oxidation kinetics model for zirconium-based alloys based on the research sponsored by U.S. NRC [178], (iii) a generalized thermal radiation model (between groups of assemblies modelled as individual rings) to have more flexibility in the modelling of the spent fuel assemblies, and (iv) hydraulic characteristics of both PWR and BWR fuel assemblies [281]. MELCOR provides a best estimate prediction of fuel heat-up, considering all the heat transfer mechanisms, such as radial radiation between assemblies, convective cooling by steam and air, radiation and convective heat transfer to the SFP liner, and heat transfer from the exposed fuel assemblies to an underlying water pool.

The effect of breakaway oxidation in air, see Section 5.4.1, is modelled in MELCOR based on data from ANL tests [178, 179]. The model still assumes a parabolic (protective) behaviour. A new oxidation model, developed at the Paul Scherrer Institut (PSI) [282], includes not only a non-protective linear weight gain in the presence of nitrogen, but also a breakaway model for oxidation in steam atmosphere. This model is now implemented in MELCOR 2.1, and is being assessed by comparison with experimental data.

MELCOR was used in the experiments for BWR assemblies described in Section 6.1.1.1, and the predictions showed good agreement with data for the initiation and propagation of zirconium fire [12]. At each step in the experimental program, MELCOR was used as (i) a tool for the experimental design, (ii) the pre-test results prediction, and (iii) for post-test analysis of the calculated and measured responses. The post-test analysis helped identify important response parameters, which often led to improvements in the conduct of the next phase of testing and improvements in the modelling approach. The experimental and modelling findings and improvements from post-test analysis of the previous experimental programme tests were subsequently used to design and predict the next phase of experiments, and so on. For example, the pressure drops measured in the hydraulic testing did not initially match the MELCOR predictions based on best-estimate hydraulic parameters. When MELCOR was updated with the experimentally derived hydraulic parameters, the MELCOR predictions of the next thermal-hydraulic testing phase were in excellent agreement with the data. The key findings from this integrated experimental and simulation programme are:

- The measured form and friction loss coefficients of a prototypic BWR FA were significantly different from generally accepted values. Use of the measured coefficients was vital for accuracy when calculating (with MELCOR) the naturally induced flow in a heated, prototypic BWR FA;
- Incorporation of “breakaway” Zircaloy oxidation kinetics into MELCOR was vital for accurately capturing the Zircaloy heat-up to ignition and oxygen consumption;
- For the full length ignition test, the MELCOR model predicted the peak cladding temperature of the assembly to within 40 K at all times and the time of ignition to within 5 minutes;
- For the 1×4 ignition experiment, the standard MELCOR model predicted ignition in the centre and peripheral assemblies to within 30 and 15 minutes, respectively. The error in ignition timing between the simulations and experiment is approximately 10 %. The difference in timing is likely due to the inability of the lumped parameter approach used in MELCOR to account for steep radial temperature gradients.

The NRC also conducted an experimental programme to address thermal-hydraulic issues associated with complete loss-of-coolant accidents in pressurized-water reactor SFPs; see Section 6.1.1.2. This experimental program, which is carried out in two phases, is part of an international effort established with the OECD. Figure D.1 compares normalized temperatures as a function of time for the Phase 1 experimental maximum and average temperature and the peak cladding temperature predicted by MELCOR. The MELCOR input model was configured with 12 axial nodes and 1 radial node. The MELCOR post-test prediction was within 1 % of the observed ignition test time. The volumetric flow from the MELCOR predictions captures the experimental trend as the accident progresses and ignition occurs. MELCOR analysis for Phase 2 of the experimental programme is ongoing.

The MELCOR code was also used for NRC’s post-9/11 security assessments and the recent SFP Study (SFPS) [2]. The publication of experimental results in [12], including code-to-code comparisons, as well as the SFPS and review by the Advisory Committee on Reactor Safeguards (ACRS) [283] supports the adequacy of MELCOR’s use for this purpose.

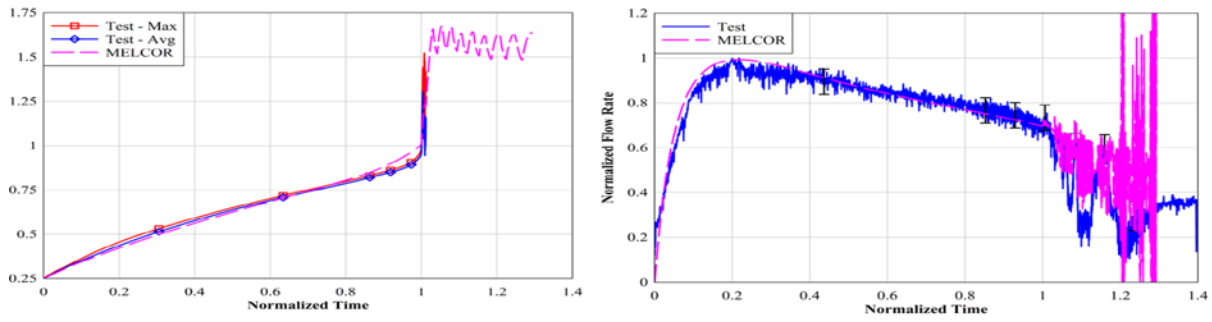

Figure D.1: Comparison of normalized temperatures and flow rates as a function of time between the MELCOR predictions and Phase 1 PWR test data.

D.2 ATHLET-CD

The system code ATHLET-CD (Analysis of THermal-hydraulics of LEaks and Transients with Core Degradation) is designed to describe the reactor coolant system thermal-hydraulic response during severe accidents, including core damage progression as well as fission product and aerosol behaviour, to calculate the source term for containment analyses, and to evaluate accident management measures. It is being developed by Gesellschaft für Anlagen- und Reaktorsicherheit (GRS), Germany, in cooperation with the Institut für Kernenergetik und Energiesysteme (IKE), University of Stuttgart. ATHLET-CD includes also the aerosol and fission product transport code SOPHAEROS, which is being developed by IRSN [284].

The ATHLET-CD structure is highly modular, in order to include a manifold spectrum of models and to offer an optimum basis for further development. ATHLET-CD contains the original ATHLET models for comprehensive simulation of the thermo-fluid-dynamics in the coolant loops and in the core. The ATHLET code comprises a thermo-fluid-dynamic module, a heat transfer and heat conduction module, a neutron kinetics module, a general control simulation module, and a general-purpose solver of differential equation systems called FEBE. The thermo-fluid-dynamic module is based on a six-equation model, with fully separated balance equations for liquid and vapour, complemented by mass conservation equations for up to 5 different non-condensable gases and by a boron tracking model. Alternatively, a five-equation model, with a mixture momentum equation and a full-range drift-flux formulation for the calculation of the relative velocity between phases is also available. Specific models for pumps, valves, separators, mixture level tracking, critical flow etc. are also included in ATHLET.

The rod module ECORE consists of models for fuel rods, absorber rods (AIC and B_4C) and for the fuel assemblies including BWR-canisters and -absorbers. The module describes the mechanical rod behaviour (ballooning), zirconium and boron carbide oxidation (Arrhenius-type rate equations), Zr-UO_2 dissolution as well as melting of metallic and ceramic components. The melt relocation (candling model) is simulated by rivulets with constant velocity and cross section, starting from the node of rod failure. The models allow oxidation, freezing, re-melting, re-freezing and melt accumulation due to blockage formation. The feedback to the thermal-hydraulics considers steam starvation and blockage formation. Besides the convective heat transfer, energy can also be exchanged by radiation between fuel rods and to surrounding core structures.

The release of fission products is modelled by rate equations within the module FIPREM, mostly based on temperature functions taking into account the partial pressure of the material gases. The transport and retention of aerosols and fission products in the coolant system are simulated by the code SOPHAEROS. The nuclide inventories are calculated by a pre-processor (OREST) as a function of power history, fuel enrichment and initial reactor conditions. The release and the transport of nuclides consider the decay heat (α, β, γ) and further decay by means of mother-daughter chains calculated within the module FIPISO.

For the simulation of debris beds, a specific model MEWA was developed with its own thermal-hydraulic equation system, coupled to the ATHLET-thermo-fluid-dynamics on the outer boundaries of the debris bed. The transition of the simulation of the core zones from ECORE to MEWA depends on the degree of degradation in the zone. The current code version comprises also late phase models for core slumping, melt pool behaviour within the reactor pressure vessel lower head (new module AIDA) and vessel failure. The code system ATHLET/ATHLET-CD is coupled to the containment code system COCOSYS, and it is the main process model within the nuclear plant analyser ATLAS. The ATLAS environment allows not only a graphical visualization of the calculated results, but also an interactive control of data processing.

The code validation is based on integral tests and separate effect tests, proposed by the OECD NEA Committee on the Safety of Nuclear Installations validation matrices, and covers thermal-hydraulics, bundle degradation as well as release and transport of fission products and aerosols. Post-test calculations have been performed for the out-of pile bundle experiments in the QUENCH and PARAMETER facility as

well as for the in-pile experiments PHÉBUS FPT2 and FPT3. The TMI-2 accident is used to assess the code for reactor applications. Especially, the recent air ingress benchmark with the calculation of QUENCH-10 and QUENCH-16 tests as well as the post-test calculation of PARAMETER SF4 show the capability of ATHLET-CD to simulate the phenomena during interaction of Zr claddings with air; see Section 6.2.2.3.

The current version ATHLET-CD 3.0A contains a model to consider the oxidation of Zr alloys by oxygen in air and includes also a model to calculate nitride formation. Both reactions are modelled in the module ECORE (rods) as well as in ATHLET (other Zr-containing components, as spacers) and are based on an Arrhenius-type rate equation [285]. This air ingress model was used to predict the ignition in the SFP Phase 2 test (see Section 6.1.1.2), because an explicit model for ignition and fire is not implemented.

D.3 MAAP5

The Modular Accident Analysis Program (MAAP) [286] is a computer code, owned and licensed by EPRI, that can simulate the response of light water reactor power plants, both current designs and Advanced Light Water Reactors (ALWRs), during severe accident sequences, including actions taken as part of accident management. There are two parallel versions of MAAP, one for BWRs and another for PWRs. These versions quantitatively predict the evolution of a severe accident, starting from full power conditions, given a set of system faults and initiating events through events such as core melt, reactor vessel failure, and containment failure. Furthermore, models are included to represent the actions that could stop the accident by in-vessel cooling, external cooling of the RPV, or cooling the debris in containment (ex-vessel cooling). MAAP models thermal-hydraulics and fission product behaviour in the primary system, containment, and reactor/auxiliary buildings (and steam generators for PWRs). Models are included for engineered safeguard system logic and performance. Also, operator actions are simulated by specification of intervention conditions and responses. The SFP model considered in MAAP5 [287] calculates SFP heatup, time to boil and uncover fuel assemblies, Zr-water and Zr-air oxidation, fission product release, and melt progression of FAs during a postulated loss of cooling capability event in the SFP. Tables D.1 and D.2 summarize key features of the MAAP5 SFP model and relevant phenomenological models, respectively.

Three hierarchies are considered in the MAAP5 SFP model: spent fuel assemblies, spent fuel channels (racks) and the whole SFP. Different from the fuel assemblies in the reactor core, which are similar or identical, spent fuel assemblies can be quite different in decay power generation and masses. To simplify the problem, MAAP divides all the spent FAs into a few power groups, assuming that assemblies in a power group are identical in terms of decay power, masses of U, Zr and other materials, and geometries.

Table D.1: Key features of the MAAP5.01 SFP model (continued on next page).

Spent Fuel Storage Pool and Channel	***Spent Fuel Rack and Fuel Assemblies***	***Major Model Inputs***
- A water pool model in MAAP5 containment (reactor building) model, which considers mass and energy transfer to and from a water pool, is used to represent the SFP. - A distributed heat sink model in MAAP5 containment model, which considers heat transfer and potential ablation of a concrete wall with or without steel liner, is used to represent SFP walls and floor. - Model allows up to 40 channels. Each channel can have filled or empty cell, and hot and cold fuel assemblies, but the decay power within a channel is homogenized. - Each channel is homogenized. Thus, in-homogeneity and non-symmetrical nature of the SFP pool must be modelled at the hierarchical level of channel. Users are allowed to use up to 40 channels and each rack can be modelled as multiple channels.	- Spent fuel rack and fuel assemblies are modelled similar to the MAAP5 reactor core model. - The number of spent fuel assemblies in power groups is defined for each spent fuel channel. - The analogy between the core and SFP are listed as the following: ✓ SFP ↔ Reactor Core ✓ SF assemblies ↔ Fuel assemblies ✓ SF channel ↔ Core channels ✓ SF nodes ↔ Core nodes ✓ SF racks ↔ BWR control blade ✓ SF storage pool wall ↔ Core baffle ✓ Area between the SF racks ↔ Core bypass area and the storage pool wall ✓ SFP water level ↔ Core collapsed water level - Spent fuel racks and assemblies are modelled as 2D (channels and axial nodes) objects. There can be one or more channels for each rack. - Up to 20 different types of fuel assemblies can be specified in each channel. - The rack wall (steel with Boraflex plate) is modelled as one of the core components	- Cycle and burn-up history: Cycle length and Accumulated burn-up at the end of cycle - Cooling time, Initial enrichment, Axial power peaking factor, Number of fuel pins and non-fuel rods - Masses of materials: UO_2, Zr, Stainless steel, Ag-In-Cd, and B_4C - Fission Products: Total masses of fission products, Fraction of decay power carried by each fission product group. 25 groups of fission product inputs are sorted into the 18 groups used by MAAP5. - Geometric information ✓ Number of storage cells for each channel (rack) ✓ Number of FAs (filled cells) for each channel (rack) ✓ Centre-to-centre distance between two adjacent channels ✓ Thickness of rack wall and total height of the spent fuel rack

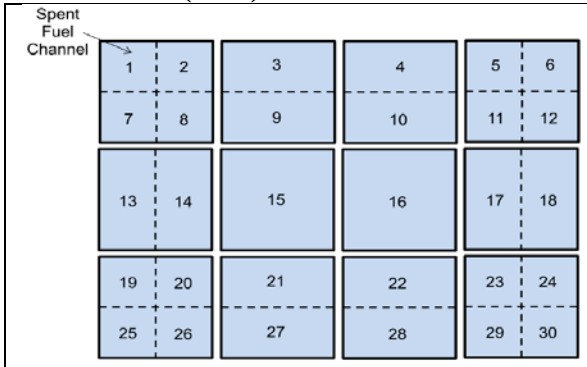

Example of 30 spent fuel channels in 12 spent fuel racks

surrounding each fuel assembly.

- Boiled-up level for each channel is calculated based on the steam generation rate within the channel.

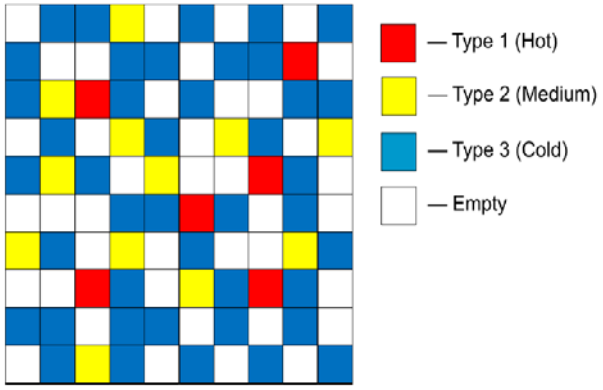

Example of SFP assemblies in 4 power groups in a spent fuel channel

- ✓ Thickness of Boraflex sheet in the rack wall
- ✓ Volumetric fraction of B_4C in the Boraflex plate
- ✓ Height of the top and bottom non-fuel regions in the spent fuel rack
- ✓ Friction factor along the flow channels in the SFP
- ✓ Minimum distance from the outer surface of channel to SFP wall
- ✓ Width, length and depth of SFP

- Heat sink
  - ✓ Thickness of reinforced concrete of the SFP wall
  - ✓ Thickness of steel liner attached to the inner surface
  - ✓ Index of MAAP distributed heat sink materials for the concrete and liner

- Radiation power
  - ✓ Emissivity of the outer surfaces of spent fuel racks and SFP wall
  - ✓ View factor between two spent fuel channels

Table D.2: Phenomenological models employed in the MAAP5.01 SFP model.

SFP Natural Circulation and Zirconium Oxidation Model	*Fuel Relocation Model*	*Radiation Heat Transfer Model*
- **Natural Circulation in SFP:** ✓ Natural circulation from upper space to individual FAs is calculated when the water level is below the bottom of fuel assembly ✓ Natural circulation from upper space through the gap to fuel assembly is calculated once the steel rack wall is melted away. 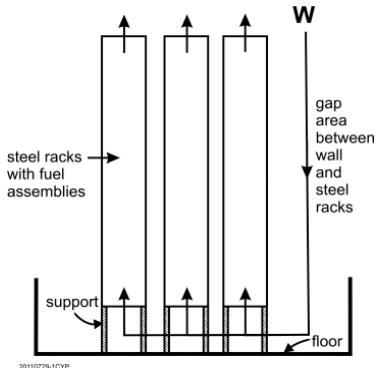 - **Zirconium Oxidation in Air** ✓ $Zr + O_2 \rightarrow ZrO_2 + \triangle H_{zr}$, $\triangle H_{zr} = 1.1\times10^9$ J/kg-mole (78 % higher than that for Zr-steam reaction) ✓ ZrO_2 layer growth rate model, based on [288]: $$\dot{x} = \begin{cases} \frac{10.50}{2\rho_{Zr}^2 x} e^{-15,630/T} & T < 1,333\ K \\ \frac{2.511\times10^5}{2\rho_{Zr}^2 x} e^{-28,485/T} & 1,333\ K \le T \le 1,550\ K \\ \frac{50.40}{2\rho_{Zr}^2 x} e^{-14,634/T} & T > 1,550\ K \end{cases}$$	- Relocation models is similar to the MAAP5 core relocation model except: ✓ Sideward relocation between channels is not allowed. ✓ Molten mass at the bottom node is allowed to relocate into the floor without forming a crust. - Molten steel from steel rack is relocated one axial node at a time - Fuel rod collapse criteria is based on the model used in the core based on the Larson-Miller approach (time at temperature) - Fuel rack collapse is modelled based on the bottom node temperature using the Larson-Miller approach.	- When water level in the SFP is low, radiation power exchange occurs among the spent fuel channels and between the spent fuel channel and spent fuel storage pool wall. - Radiation heat transfer between the racks and storage pool wall is considered by evaluating view factors between the surfaces on rack wall and storage pool wall, which is provided through user's input. 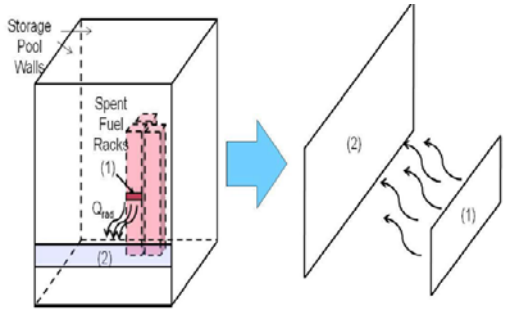 Plate 1 represents the node (i,j) and plate 2 represents the SFP wall

The second level considered in the model is the spent fuel channel, which is similar to the spent fuel rack in concept. In fact, in many situations, a spent fuel rack can be considered as a spent fuel channel. However, MAAP is not restricted to a one-to-one mapping between racks and channels. For example, if users wish to study radiation power from the spent fuel racks to the spent fuel storage pool wall, they may nodalize one rack in the peripheral regions in the pool into a number of channels to acquire more accurate radiation power leaving the rack outer surface. They may also want to combine a number of racks in the central region into one channel to save some computational time.

However, detailed deterministic modelling of the SFP with MAAP5 is at its initial stages, and validation of the relevant models against other detailed codes (such as MELCOR [74]) and experiments is still in progress. Models for further improvement and/or development are listed as follows:

- Model for checkerboard SFP loading: Cooling processes, such as air cooling within the SFP, are expected to be shown to be effective as indicated by Sandia testing and MELCOR calculations, but these are yet to be confirmed for realistic fuel checkerboard SFP loadings;
- Radiation model, natural circulation model, and fission product models to take into account new fission product groups (such as Cs_2MoO_4, Ru, and Pu) and Ru release under air oxidation. The current SFP model does not calculate water natural circulation within fuel racks, and calculates a gas natural circulation once the water level decrease below the bottom of the fuel rack or fuel rack melted away;
- Incorporation of molten core concrete interaction model and models for various engineered safety features (water injection, venting and spray system) into the MAAP5 SFP model;
- Interaction of severe accident progression in the containment and subsequent adverse impacts on the SFP.

D.4 ASTEC

The ASTEC (Accident Source Term Evaluation Code), jointly developed by IRSN, France, and GRS, Germany, aims at describing the behaviour of a water-cooled nuclear power plant in severe accident conditions, including engineered safety systems and procedures used in SA management, from the initiating accidental event until the possible radiological release of radionuclides from the containment building into the atmosphere [289]. The main code applications are source term determination studies, Level 2 Probabilistic Safety Assessment (L2PSA) studies, including the determination of uncertainties, Severe Accident Management (SAM) studies and physical analyses of experiments to improve the understanding of the phenomenology.

ASTEC has progressively reached a larger European dimension through successive projects of the Framework Programmes of Research and Development of the European Commission: EVITA (2000-2004) and especially the SARNET network of excellence project (2004-08 and then 2009-13) [290]. ASTEC has progressively become the reference European SA code through the capitalisation, in terms of models, of the knowledge produced in the network and the assessment by 30 partners.

Applications of ASTEC to SFP accidents were performed in the frame of the Phase 1 and 2 of the OECD/NEA Sandia Fuel Project; see Section 6.1.1.2. The results from Phase 1 were very satisfactory. They particularly stressed the importance of:

- axial radiation in the propagation of the oxidation front and in the maximum temperature reached;
- the necessity to use moderate axial mesh size (5-10 cm) for obtaining accurate peak temperatures and oxygen starvation predictions;
- the limit of oxidation breakaway validation domain.

Regarding Phase 2 of the project, the modelling of radial radiative heat transfer, which plays a key role, was not straightforward due to the non-axisymmetry of the experiment. As a result, it was difficult to capture accurately the behaviour of the peripheral cells, contrary to the DRACCAR code [252], which allows a better geometrical representation of the experiment.

The ASTEC code structure is modular, each of its modules simulating a reactor zone or a set of physical phenomena; see Figure D.2. Two different running modes are possible:

- Stand-alone mode for running each ASTEC module independently, which is useful for module validation and calculation of separate effect tests;
- Coupled mode, where all (or a subset) of the ASTEC modules are run sequentially within a macro-time step. This mode allows explicit feedback between modules.

As illustrated in Figure D.2, ASTEC consists of the following modules:

- **CESAR** simulates the thermal-hydraulics in the primary and secondary circuits and in the reactor vessel. The thermal-hydraulics modelling is based on a 1D 2-fluid 5-equation approach, accounting for both thermal non-equilibrium and momentum non-equilibrium between liquid and gas phases. Up to 5 non-condensable gases (hydrogen, helium, nitrogen, argon, oxygen) are available.
- **ICARE** simulates the core degradation phenomena (both early and late degradation phases). It simulates the early-phase of core degradation with fuel rod heat-up, clad tube ballooning, burst, and oxidation, fuel rod embrittlement or melting, molten mixture candling and relocation, etc. and then the late-phase of fuel degradation with corium accumulation and formation of blockages, corium slump into the lower head and corium behaviour in the lower head until vessel failure.
- **ELSA** calculates the release of fission products, actinides and structural materials (Ag, In, Cd, Sn, Fe, Ni, Cr) from the degraded fuel. The modelling allows description of the release from fuel rods and control rods, followed by the release from debris beds (if any) and, then, the release from the in-core molten pool.
- **SOPHAEROS** computes the aerosol and vapour transport through the reactor cooling circuits via gas flows to the containment. The main vapour-phase and aerosol phenomena are modelled by mechanistic or semi-empirical approaches, using twelve families of species (elements, compounds, gas, volatile, non-volatile…) and five states (suspended aerosols, suspended vapours, vapour condensed on walls, deposited aerosols, sorbed vapours).
- **RUPUICUV** evaluates Direct Containment Heating (DCH), i.e. ex-vessel discharge of hot corium into the cavity after lower head failure (involving vessel blow-down and cavity pressurisation) and potential corium oxidation and entrainment from the cavity to the containment.
- **MEDICIS** simulates the molten-core-concrete interaction by a lumped-parameter 0D approach with averaged melt/crust layers. This module assumes either a well-mixed oxide/metal pool configuration or possible pool stratification into separate oxide and metal layers. It describes concrete ablation, corium oxidation and release of incondensable gases (H_2, CO, CO_2) into the containment.
- **CPA** is used for the simulation of containment thermal-hydraulics and aerosol behaviour. The module is based on a “lumped-parameter” approach, i.e., the containment can be nodalized as several 0D zones, connected by junctions and surrounded by walls, simulating simple or multi-compartment containments (tunnels, pit, dome…) with possible leakages to the environment or to normal buildings, with more or less large openings to the environment.

- **IODE** deals with iodine and ruthenium behaviour in the containment. For iodine, it is composed of around 40 phenomenological models that focus on the predominant chemical reactions in sump, gas phase and at contact with surfaces and the effect of spray on molecular iodide. As for ruthenium, the module is focusing on the three predominant chemical reactions in gas phase.

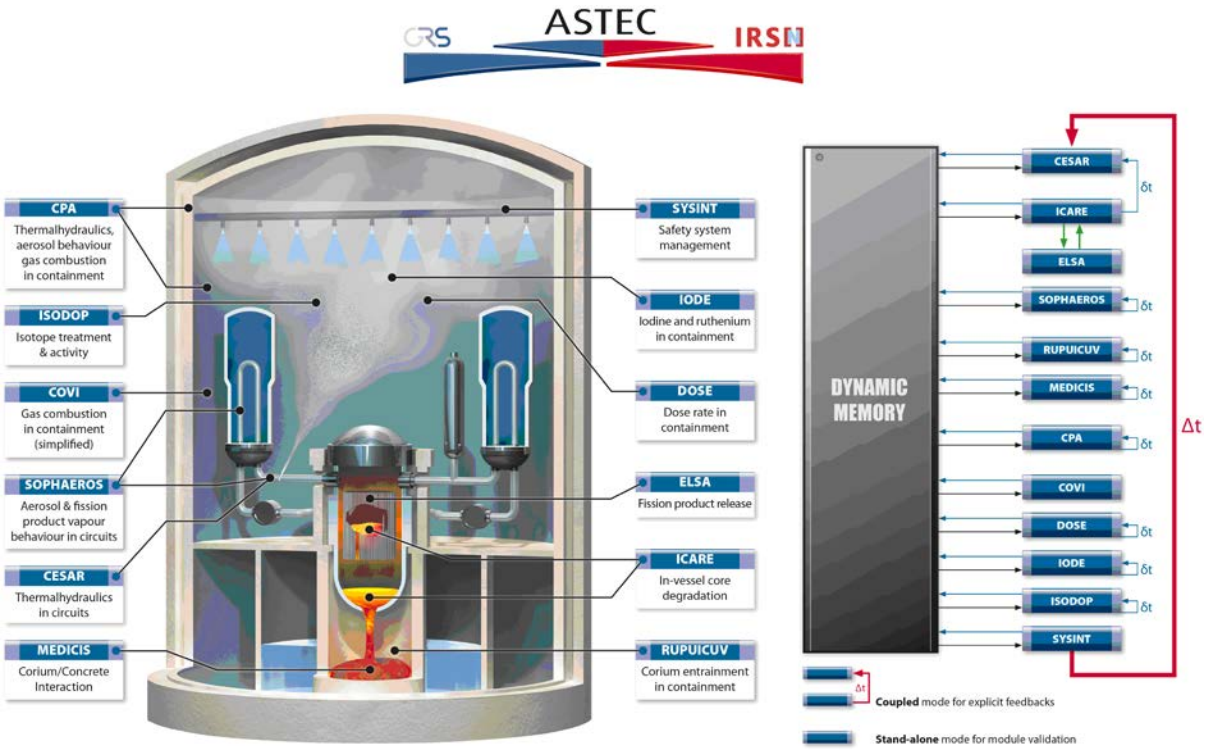

Figure D.2: ASTEC V2.0 modules and code structure.

D.5 The DRACCAR code

The IRSN developed the DRACCAR computer software within the scope of its safety analysis on pressurised water reactors [253, 254]. This software is not a true severe accident code; it is used to study loss-of-coolant accidents, particularly the thermal-mechanical behaviour of the fuel rods, following the loss of coolant in e.g. a reactor core or in a spent fuel storage pool.

The DRACCAR code is based on a 3D non-structured meshing, which enables modelling of a simple fuel rod, a partial or a full fuel assembly, a full core or a SFP. It is based on an axial discretization of the rod, which leads to analyse quasi-independent 2D thermal mechanical problems. Important phenomena, such as fuel pellet eccentricity, heat transfer modes (within the solid and through the fluid) or material property evolution (oxidation, phase transitions, etc.) can thus be taken into account, and the important question of the cladding integrity during a LOCA transient can be addressed even in case of contact between the structural elements. In that case, the geometry is strongly changed (flattened zone contact) as well as the loading nature (mixed stress–displacement loading) and so the rupture is more difficult to model than accomplished by threshold criteria used in most of the multi-rod codes: with DRACCAR, nonlinear geometrical effects are added to non-linear behaviour laws in the modelling.

Also important is the possibility to get a better knowledge on the system's capability to cool structures, whatever are the evolutions of the deformation of the rods and the blockage of the sub-channels. Obviously, these two critical issues, which are essential to treat in modelling LOCA transient effects, can only be dealt with in a realistic manner with a multi-pin code coupled to an efficient 3D thermal–hydraulic code, and that's why DRACCAR is currently coupled to the two phase flow module CESAR of the ASTEC code, able to compute deformed geometry evolutions and thus actualizing the coolant flow passage within the different sub-channels.

The DRACCAR code has been successfully applied to Phase 2 of the OECD/NEA Sandia Fuel Project; see Section 6.1.1.2. For the simulation of Phase 2, the issue is not in the modelling of the heat transfer mechanisms within each cell (as in Phase 1), but rather in the modelling of heat exchange between the central cell and the peripheral ones. The difficulty lies in the fact that the test is typically non-axisymmetric, whereas most of the severe accident codes that participated in the programme were axisymmetric (MELCOR, ASTEC).

A snapshot of the temperature contours throughout the five fuel assemblies after the ignition of the central one illustrates this fact. In Figure D.3a), we can observe that the temperature gradients in the peripheral FAs go from the hot cell wall (close to the central cell) to the cold outer cell wall (in contact with insulation material), and that all the peripheral cells are heated from one face only.

This specific geometry can be modelled using axisymmetric codes, but at the cost of some simplifying hypotheses to reproduce at best average experimental values. However, in order to get some "correct" code results, parametric tunings are necessary to fit the experimental results. A correct calculation can reproduce the central cell temperature up to ignition, but the following events (ignition of the peripheral cells, burn front evolution in the whole FA) could be more difficult to reproduce, because they are linked to the oxidation reactions of the Zircaloy cladding, which is cooled by natural convection. These reactions are very temperature dependent, and the peripheral temperatures calculated with axisymmetric codes are not correct.

With DRACCAR, an exact representation of the geometry can be defined. Each structure has its own thermal-mechanical behaviour, but can also interact with neighbours by thermal radiation or mechanical contact. Applied to the OECD/NEA Sandia Fuel Project Phase 2 geometry, a DRACCAR calculation simulates 1/8 of the central cell with six meshes (and weighted heated rods inside), and 1/2 of a peripheral cell with 15 meshes (and weighted cold rods inside). With this modelling, the temperature gradients in the cells are correct and the exchange surfaces and the geometry also. In this case, no adjustments of the heat transfer coefficients are made necessary, and the code results can be trusted as just as those from the substantial validation matrix.

In Figure D.3b), a snapshot of the calculated temperature in the assemblies at the same time and axial location as in the experiment, Figure D.3a), is shown. The temperature colour code is different, but we can see that the temperature gradients in the cells with DRACCAR are very close to the experimental results. In that case, a more exact calculation of the oxidation front (ignition and propagation) in the peripheral cell can be performed.

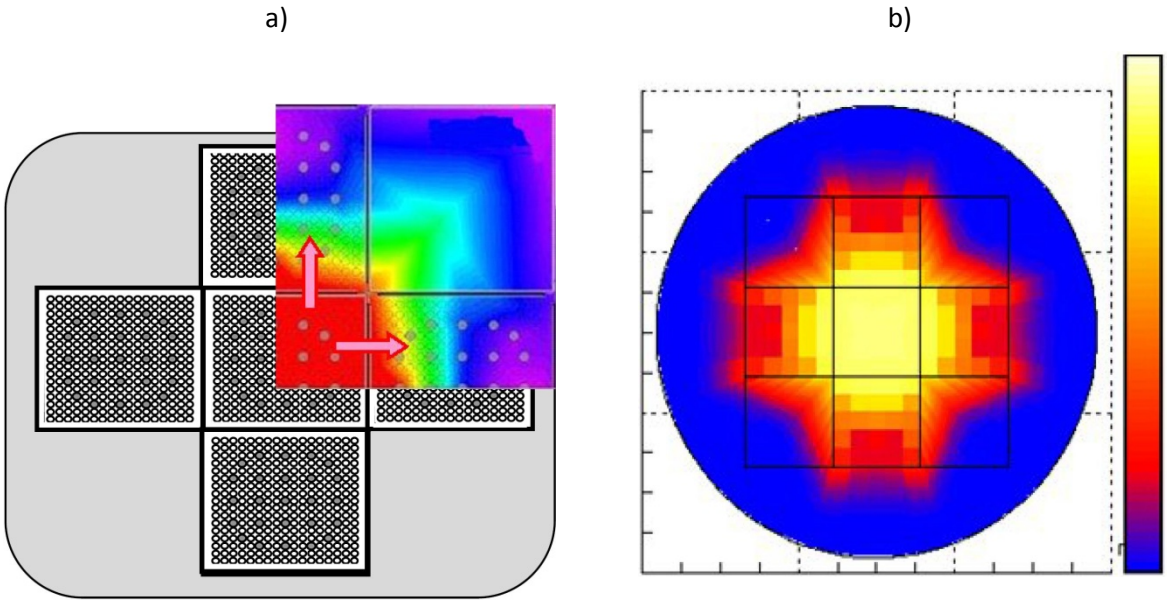

Figure D.3: Temperature distribution across fuel assemblies at a given time and axial level for Phase 2 of the OECD/NEA Sandia Fuel Project. a) Measured results. b) Calculated results from DRACCAR.